Biogeochemical exploration on the Kalahari Copperbelt

N Auret

orcid.org 0000-0002-5488-2921

Dissertation submitted in fulfilment of the requirements for the degree *Master of Science in Environmental Sciences* at the North-West University

Supervisor:	Mr PW van Deventer
Co-supervisor:	Prof SJ Siebert

Graduation May 2018

23702273

DISCLAIMER

Although utmost care was taken to ensure the accuracy of this report, neither the sender and/or the North-West University can be held responsible for any errors or omissions that might have occurred.

ACKNOWLEDGEMENTS

I would like to thank the following persons/organizations for their involvement in and contributions to this project:

- My supervisor, Piet van Deventer, for his mentorship and guidance. For always being helpful and friendly and for sharing his bountiful knowledge.
- My co-supervisor, Prof Stefan Siebert, for his genuine interest and assistance. For his part in structuring the report and interpreting results.
- Cindy Faul, for initiating the project and writing a project proposal.
- Prof Suria Ellis, from the NWU statistics department, who was responsible for all the statistics on the data. For her willingness to always assist and share her knowledge.
- Luan Nel, for assisting me with field work and making it a pleasant experience.
- Stefan Denysschen for helping with sample preparation.
- Eco Analytica Laboratories for completing the ICP-MS analyses.

I would like to thank John Deane and Cathy Knight, from Cupric Africa, for kindly allowing me to collect soil and plant samples from the Khoemacau mining area. For helping to plan sample transects and for providing me with drill core data. I would also like to recognize every personnel member at Khoemacau who helped with sample collection.

I offer thanks to Jaques Janse van Rensburg, from MOD Resources, for allowing me to collect soil and plant samples from Mahumo Deposit.

I would like to express my gratitude to THRIP and Cupric Africa for the financial support that made this project possible.

I would like to thank Sarel and Susan Haasbroek, from Hermansdal, for assisting with the editing of this dissertation.

Finally, I would like to thank my parents for their love and financial support and providing me the opportunity to, in a very small way, make my contribution to the world.

ABSTRACT

Bedrock of the Kalahari Copperbelt (KCB) are covered by thick layers of overburden. A biogeochemical exploration approach on the Ghanzi Ridge, a section of the KCB, was investigated to determine if it can be used as an alternative method to expensive drilling options, in order to detect deep ore bodies. Soil samples as well as leaves from dominant trees and shrubs, such as *Boscia albitrunca*, *Croton gratissimus* and *Grewia bicolor*, were collected. Near-total acid digestion was used to extract trace elements from the soil and plant tissue. Soluble element content in the B horizon was determined by means of ammonium nitrate extraction. All extractions were analysed by ICP-MS. Hierarchical linear modelling (HLM) was applied to compare means and determine correlations. It was applied to the data to identify indicator species, assess which of the A or B horizons reflected underlying mineralisation more accurately, and to determine plant-soil-ore relationships in terms of trace element content.

Trace elements in the B horizon more often reflected underlying mineralisation than did trace elements in the A horizon. Evidence suggests that elevated levels in some leaf tissue might be related to the rooting depth or hyperaccumulating abilities of the tree species. Deep-rooting species may reflect underlying copper mineralisation more accurately than element concentrations in the soil. The elements B, Co, Hg, Mn, Mo, Ni, and Se delivered the most promising results in terms of strong correlations between concentrations in plant tissue and element content in the soil. Strong connections to concentrations of these elements in the underlying ore were also inferred. This study produced evidence of some significant correlations between element concentrations in plants, soil and copper ore. More studies are required to gather enough data to build predictive models that can estimate ore content, based on trace element concentrations in plants and soil.

KEY TERMS

Kalahari Copperbelt, biogeochemical exploration, pathfinder elements, plant-soil-ore relationships.

TABLE OF CONTENTS

TABLE OF TABLES

TABLE OF FIGURES

ABBREVIATIONS

BAC: biological absorption coefficient

CAC: cation absorption coefficient

CEC: cation exchange capacity

DOM: dissolved organic matter

EF: enrichment factor

HLM: hierarchical linear modelling

KCB: Kalahari Copperbelt

MSE: mean square error

PSD: particle size distribution

SOM: soil organic matter

TF: transfer factor

CHAPTER 1: CONCEPTUALIZATION

1.1 Introduction

Thick aeolian and pedogenic calcretes and silcretes cover the bedrock of the Kalahari Copperbelt in Botswana and Namibia (Brown & Cole, 1976; McConnell, 1959, cited by Jones, 1980). In some places within the study region, the depth to Cu/Ag mineralised bedrock was more than 1000 m. Ordinary and conventional geophysical and geochemical exploration methods are not as successful in such areas with thick overburden, compared to shallow ore body exploration. The primary focus of this research is to scrutinise alternative exploration methods to detect deep ore bodies without expensive drilling options. Although the project made use of existing drilling results of known ore bodies, the methods that were applied are unique in the sense that a unique plant-based sampling approach was followed, as well as the specific elements that were analysed and the interpretation of results.

Surface and sub-surface soil samples, as well as leaves from different trees and shrubs that are dominant in the area were taken from three sites, namely Zone 5, Banana Zone and Mahumo deposit. These sites are located over proven ore bodies with prospecting licences, where extensive drilling has taken place in the past.

A near-total acid digestion (according to the EPA 3050B method) was used as extraction method for the soil and leaf samples to determine its trace element content. An ammonium nitrate extraction was also used on the B horizon to quantify the soluble content of elements in the soil. All extractions were then analysed by ICP-MS to determine the trace element concentration of selected ore-associated elements in soil and leaf material. Finally, the pH of the soil was measured to investigate the link between soil pH and plant available elements.

Statistical techniques that were used to establish correlations between data sets include hierarchical linear models (in SPSS and SAS). Statistics were used to determine indicator species, evaluate trace element content in the soil and leaves as a function of ore body depth, compare soil horizons to determine which will more accurately reflect underlying mineralisation and assess the relationship between trace element concentrations in the ore, soil and plant tissue.

1.2 Background

1.2.1 Kalahari Copperbelt

The Kalahari Copperbelt (KCB) is an 800 km stretch of copper mineralisation extending from central Namibia to northern Botswana. The exposed area between Mamuno (near the Namibian border) and Lake Ngami is commonly known as the Ghanzi Ridge - a 250 km long section of the KCB, approximately 50 km wide (Akanyang, *et al.*, 1996; Modie, 2000).

Exploration of the Botswana segment of the belt lead to the discovery of significant Cu-Ag deposits. In the Namibian sector, however, much less exploration has taken place after the 1970s. Copper mineralisation at Klein Aub and in most other sections of the Namibian segment of the copper belt is strata-bound (Maiden & Borg, 2011): some chalcosite occurs in dolomitic siltstone and quartzite strata. Much of the sulphide mineralisation are, however, found in quartz-carbonate veins, lenticles, brittle fractures and tectonic breccias (Maiden & Borg, 2011).

According to Borg and Maiden (2011), economically viable copper accumulations were mainly the result of regionally extensive hydrothermal events that took place after the formation of the dominant cleavage and is controlled locally by structural features like fault intersections and fold zones.

This study focuses mainly on sedimentary rock-hosted stratiform copper deposits of the Ghanzi Ridge, comprised of disseminated to veinlet Cu and Cu-Fe sulphides in the dolomitic or siliclastic sedimentary rocks. Mineral deposits which correlates with the Ghanzi Ridge is distributed over a strike interval of up to 150 km in Botswana only and it also extends into Namibia for another few hundred kilometres. The bulk of the copper occurs within 25 m above the contact between the mudstone and siltstones of the D'Kar Formation and the underlying arkoses and sandstones of the Ngwako Pan Formation (Akanyang, *et al*., 1995).

The mineralisation event is believed to have occurred between diagenesis to basin inversion and metamorphism (Hall, 2007). Sulphide precipitation was typically controlled by stratigraphic redox boundaries consisting of carbonaceous material, mobile hydrocarbons or pre-existing sulphide minerals. Faults provided conduits for ore fluids that escaped during basin compaction, -inversion or both (Hall, 2007). Extreme quantities of Karroo and Cenozoic sediments, up to 200 m thick, cover the bedrock of the Ghanzi Ridge.

Before mining can take place, economically viable mineral resources need to be located with the help of surface geochemical sampling, geophysical assessments and drilling. There are several areas in Southern African countries where neither geochemical nor geophysical analyses can be done successfully due to thick superficial cover materials, such as Kalahari sands, calcretes and other pedogenic deposits.

Alternative prospecting techniques include geobotanical exploration, during which hidden ore deposits can be located by observing morphological changes in plants and mapping the distributions of species (Cannon, 1971), and biogeochemical exploration, which involves the chemical analysis of plant tissue from dominant plant species, can be used for prospecting (Cannon, 1971). Focus is placed on the latter of these technique, since this study adopted a biogeochemical approach.

1.2.2 Biogeochemical exploration

Vascular plants have evolved to survive a wide range of chemical and physical conditions and have developed mechanisms to exclude or absorb and scavenge elements and translocate them to twigs, bark, foliage, flowers and seeds (Dunn, 2007). Hence, plants do not give the same geochemical information as soils (Dunn, 2007). A plant sample may represent an integrated signature of several cubic meters of the soil profile and sometimes bedrock. The roots may also extract elements directly from migrating groundwater and accumulate it in their tissues. In arid and semi-arid environments, roots can obtain several meters in length to reach a permanent water source (Canadell, *et al.*, 1996). In contrast, little or none of that element may be adsorbed by the soil. Using vegetation in interpreting geological phenomena is therefore a valuable tool that can be used to search for ore deposits buried under thick soil covers or layers of unmineralised rock.

Biogeochemistry makes use of plants as sample medium for prospecting specifically when soil samples cannot be taken due to inaccessibility or in the case of transported overburden, due to their root penetration through weathered cover (Anand, *et al.*, 2005; Hill, *et al.*, 2008). It is especially useful in areas of transported cover where the signature indicating the underlying geology is better expressed in the vegetation as opposed to the soils *(*Anand*, et al*., 2005). A geobotanical/biogeochemical study conducted by Cole (1971) on a Ni-Cu ore body in Rhodesia (Zimbabwe) also confirmed that a geobotanical approach was of limited use. Biogeochemistry defined the sub-outcrop of the ore body more accurately than soil geochemistry since it was able to distinguish between anomalies caused by bedrock mineralisation and that which is produced by near-surface oxidized Cu-bearing material.

A case study on PGE-rich komatiites in Australia indicated that biogeochemistry could be an advantageous and sensitive exploration tool. This survey demonstrated, from a multi-element analysis by ICP-MS, that the underlying Ni-rich komatiites were more clearly defined by the Ni signature from the vegetation than the soils (Dunn, 2007). This was also the case in the study by Cole (1971) where the Ni content of the plant material clearly delineated the position of the ore body in a more accurate way than did the soil analyses. Additionally, Pd was not detected in the soils even though it was strongly evident in the vegetation growing over concealed mineralised bedrock (Cole, 1971).

Biogeochemical data can express subtle trends that aid in defining structural tendencies, faults, stratigraphic relationships and lithologies, all of which may be used in combination to indicate a geological setting that is suitable for the emplacement of mineral deposits (Dunn, 2007). The chemical composition of vegetation can be used to determine local and regional geochemical dispersion patterns associated with mineralisation in regolith-dominated terrains (Dunn, *et al*., 2006; Hill & Hulme, 2003). By determining if trace elements within an area are at anomalous or typical background levels, mineral geologists can assess the economic potential of an environment. In personal communication to Dunn (2007), in 1997, Alexander Kovalevsky claimed to have succeeded in predicting both the depth to mineralisation and an estimation of ore grade by using biogeochemical patterns. This concept, however, remains to be tested outside of Siberia.

According to Anand & Cornelius (2004), future discoveries of base metal and gold deposits in deeply weathered sites will probably occur under greater depths of transported overburden where soil and lag geochemical techniques are less effective. This will necessitate exploration geologists to resort to alternative methods to detect concealed mineralisation. Present biogeochemistry results are most encouraging and may lead to a practical method for locating mineralisation where ore deposits are covered by thick overburden. The copper deposits of the Ghanzi Ridge is one such area covered by thick layers of Kalahari sands, calcretes and other pedogenic deposits. Biogeochemistry may therefore prove to be an important and useful exploration tool for prospecting in this area.

1.3 Study area

The KCB stretches discontinuously from central Namibia to northern Botswana. The study area lies within a section of the KCB called the Ghanzi Ridge and includes the Banana Zone, Zone 5 and the Mahumo deposit (Table 1-1; Figure 1-1).

Table 1-1: Sites selected for investigation (MOD Resources Ltd, 2017; Cupric Canyon Capital, 2017)

Deposit site	Company	Resource estimate
Zone 5	Cupric Canyon Capital	100 Mt @ 2% Cu and 20 g/t Ag
Zone 5 North	Cupric Canyon Capital	20 Mt @ 2.6% Cu and 50 g/t Ag
Banana Zone	Cupric Canyon Capital	155 Mt @ 0.85% Cu and 11 g/t Ag
Mahumo deposit	MOD Resources	2.7 Mt @ 2.0% Cu and 50g/t Ag

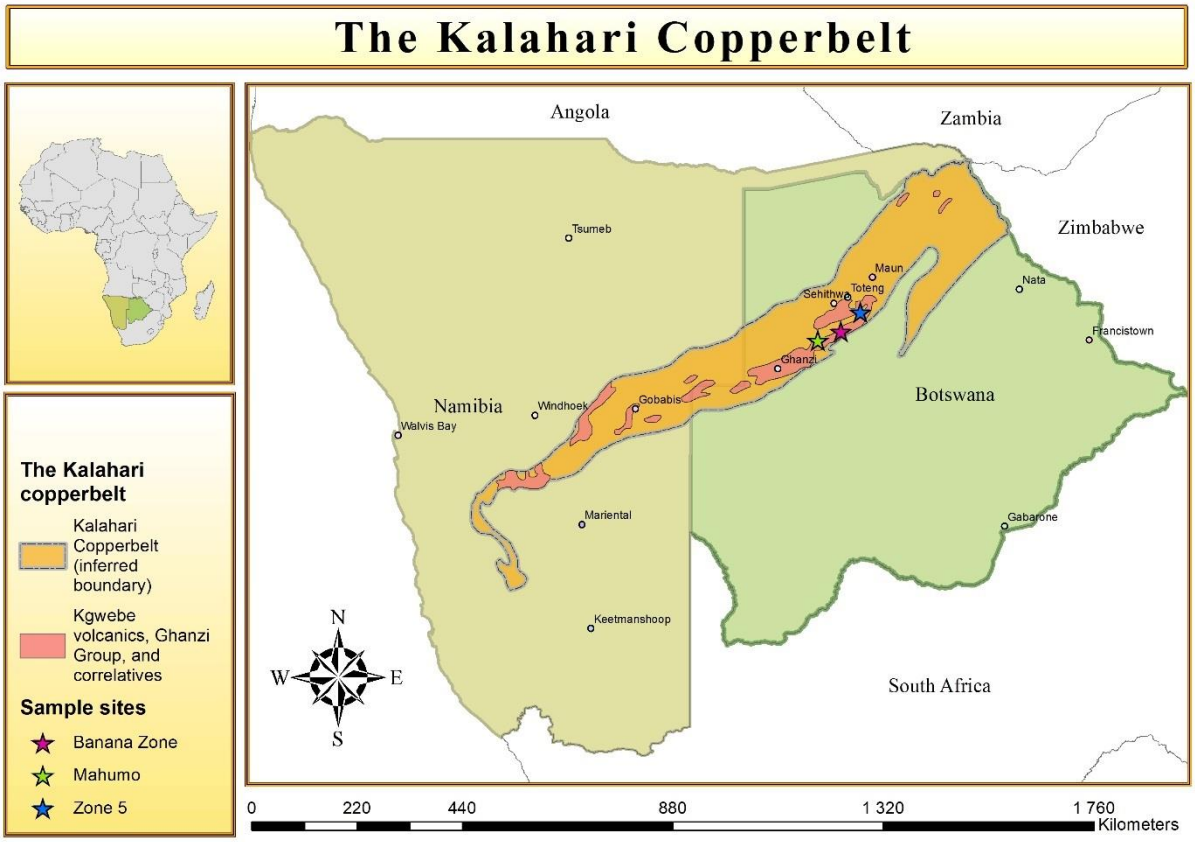

Figure 1-1: Location of the Kalahari Copperbelt and sample sites on the Ghanzi Ridge.

1.4 Research objectives

1.4.1 Problem statement

Transported overburden, i.e. where concealed ores are covered by calcrete and aeolian deposits, are found in large parts of southern Africa. Regions with thick, transported sediment or rock cover present special problems for geochemical exploration methods that use surface samples (Anand, *et al.*, 2010; Bimin, *et al*., 2016). In the KCB study region,

Kalahari overburden Cu/Ag mineralization are intersected at varying depths. The depth of the ore body can range from outcropping or sub-outcropping ore at a depth of only a few metres to much deeper lying ore at over 1000 metres deep.

Due to the depth of mineralized bedrock and the coarse grain nature of the sediments, diffusion and capillary movement of ions to the surface is limited (Ellis & Mellor, 2002; Plaster, 2011). Low rainfall and limited oxidation of the mineralised zone in arid regions result in capillary movement of elements only reaching the capillary fringe layer. Therefore, conventional geochemical surveys cannot be used for prospecting on the Ghanzi Ridge. Geophysical analyses are buffered by the thick sediments and is known to be complicated and expensive.

Mining companies therefore require efficient and effective alternative prospecting methods that can be used in areas of thick surficial cover materials where neither geochemical nor geophysical analyses can be done successfully, and is more environmentally friendly than drilling (Lund, *et al.*, 2005). They also require less expensive prospecting methods before investing in more expensive approaches. A study in Australia (Hill, *et al.*, 2008) confirmed that drilling of surface geophysical and geochemical targets in regions of thick transported overburden are extremely time consuming, expensive and of limited success.

1.4.2 Hypothesis

Transported overburden poses significant challenges to geochemical exploration since the dispersion of indicator elements to the root zone and surface is restricted. Phytoprospecting, by means of biogeochemical exploration, might overcome some of the problems caused by thick overburden, particularly because some plant species develop root systems that can reach great depths and can spread over great distances so that a large volume of soil is sampled by their roots.

The sandy soils of the Kalahari provide an excellent medium to support deep root growth and a rooting depth of at least 68 m has been reported for *Boscia albitrunca* in the central Kalahari, Botswana (Jennings, 1974, cited by Canadell *et al*., 1996). Other trees in the area like *Acacia erioloba, A. fleckii, Dichrostachys cinerea, Terminalia sericea* and *Ziziphus mucronata* all have root depths that can exceed 70 m and reach deep sources of moisture in the water-scarce ecosystem of the Kalahari (Obakeng, 2007). After absorption by plants or trees, the elements migrate to various parts of the organism (Johnson, *et al*., 2002) and by

analysing these parts (specifically the leaves), anomalies indicating possible mineralisation may be found.

Deep-rooted trees growing on overburden that is covering ore bodies, take up and reflect higher than normal concentrations of trace elements in their leaf tissue.

I. If A and B horizons of overburden are situated above copper ore bodies, then copper and other related elements will occur at higher values than the surrounding environment. Element concentrations in the B horizon in specific, will be higher due to illuviation and other soil processes that concentrate elements in the deeper subsoil;
II. If pH decreases in the A and B horizons, then the bio-availability of elements will increase;
III. If tree species grow on overburden above copper ore bodies, then copper and other related elements will be reflected at higher levels in leaf tissue than trees from the surrounding environment;
IV. If higher levels of elements are not reflected in the A and B horizons, then elevated levels in leaf tissue would be related to the rooting depth of the trees species.
V. Trees will accumulate higher levels of trace elements where the ore body is closer to the surface and plant roots can reach it more easily.

1.4.3 Scope of the study

This study is concerned with how trace element concentrations in the ore body are related to the concentrations in the overlying sediment and vegetation growing over the ore deposit. It does not deal with the mechanisms of element translocation (although briefly discussed) and it does not attempt to describe the processes leading to element dispersion and trace element concentrations in specific locations in the soil or plant tissue.

1.4.4 Aims and objectives

The principal aim of this research project is to investigate soil-plant relationships in terms of trace element content and relate it back to the underlying ore body. The accumulation of ore-related trace elements in plant tissue material is investigated for the purpose of prospecting for base metals where the metal deposits are covered with thick superficial deposits. One of the main goals of this study is to identify elements which are not present in the ore body at high quantities, nor of interest to the mining geologist, but are associated with the main ore

body and mineralisation processes. For the remainder of this report, these elements will be referred to as “pathfinder elements”. Hydrothermal enrichment played a role during the mineralisation process and more volatile elements like As, Cd, Hg, Sb, Se and Zn (Kabata-Pendias, 2011; Levinson, 1974) were also incorporated in the ore body. It is in searching for subtle trends in these mobile pathfinder elements and their relationships to the poorly defined signatures of the valuable, but less mobile elements, that successful detection of the ore body may ensue. A further goal of this project is to compare the A and B horizons of the soil overlying the deposit, to establish the best soil sampling medium for soil geochemical surveys. To accomplish these goals, the following objectives need to be achieved:

I. Quantifying total trace element concentrations in the A and B horizons of the soil.
II. Quantifying soluble trace element concentrations in the B horizon of the soil.
III. Quantifying trace element concentrations in the foliage of selected plant species.
IV. Calculating a transfer factor for various plant species, using the elemental concentration in the plant tissue as well as in the soil.
V. Correlating trace element content in the soil and foliage with the depth of the ore body.

The information gathered from the sites along the Ghanzi Ridge can be extrapolated to other upliftment ridges in South Africa, such as the Griqua-Transvaal Ridge in the Northern Cape and North-West, the Soutpansberg Ridge and the contact between the Kaapvaal and Zimbabwe Cratons in Limpopo.

1.5 Chapter overview

- Chapter 2: Literature review

  This chapter deals with the geological setting of the Kalahari Copperbelt. It describes the stratigraphy, lithology, the events that lead to mineralisation as well as the structures controlling element dispersion and deposition. It further describes the vegetation characterizing the study area and discusses the dispersion of elements in the secondary environment and its absorption by plants. The specific pathfinder elements that were investigated, are reviewed, and the calculations for element transfer factors are discussed.

- Chapter 3: Materials and methods

This chapter describes the study design and the gathering of soil and plant samples. It discusses the sampling protocol used for the biogeochemical survey, how sample preparation was carried out and which analytical techniques were used to determine the trace element concentrations of the samples.

- Chapter 4: Indicator plant species

The aim of this chapter is to provide a descriptive report regarding the absorption and accumulation of specific elements by indicator plant species. It attempts to elucidate the connection between the trace element content in the leaves and the depth of the ore body.

- Chapter 5: Soil geochemical comparison of A horizon versus B horizon

This chapter is focused on establishing which of the A or B horizons are more representative of the ore body. It attempts to determine if there is any relationship between the trace element content in the soil and the depth of the ore body.

- Chapter 6: Trace element plant-soil-ore relationships

This chapter considers the relationship between trace element content in the ore body and that of the A horizon, B horizon and leaf tissue of certain tree species. The relationship between concentrations of pathfinder elements in the leaves of dominant plant species (*B. albitrunca*, *C. gratissimus* and *G. bicolor*) and concentrations in the soil are evaluated. The soil pH is also considered when assessing connections between element content in the soil and content in plant tissue. Where the relationship between soil and ore content is investigated, only the principal ore elements (Ag, Cu, Mo, Pb and Zn) are discussed.

- Chapter 7: Conclusion

The main findings and conclusions of this study is reported and recommendations for future research are made.

CHAPTER 2: LITERATURE REVIEW

2.1 Geological setting

2.1.1 Stratigraphy

The Kalahari Copperbelt (stretching from northern Botswana to central Namibia) is an 800 km long by 100 km wide deformed volcano-sedimentary basin comprising the basal Kgwebe volcanic complex and the unconformable overlying Ghanzi-Chobe Supergroup sedimentary successions (Hall, 2007; Modie, 1996). Table 2-1 shows the stratigraphy of the Kalahari Copperbelt. The exposed area between Mamuno (near the Namibian border) and Lake Ngami is commonly known as the Ghanzi Ridge (Modie, 2000). The Ghanzi Ridge is a 250-km long section of the Ghanzi-Chobe Belt and is approximately 50 km wide (Akanyang, *et al.*, 1996). It represents the north-eastern extent of the Damara Orogen, located between the Kalahari and Kongo cratons. The Ghanzi Ridge consists of two main lithostratigraphical subdivisions: an older basal volcanic suite with intercalated sedimentary rocks – the Kgwebe Formation (± 2500 m thick) – and a younger overlying siliclastic sedimentary unit known as the Ghanzi Group (± 5000 m thick) (Akanyang, *et al*., 1996; Modie, 1996). These Proterozoic sediments may be extensions to either the Katanga-Zambia Copperbelt or the Lumagundi System of Zimbabwe (Cole & Le Roex, 1978), both of which carry economically significant copper deposits.

The Ghanzi Ridge section of the Kalahari Copperbelt was targeted in a biogeochemical research study. Figure 2-1 shows some of the important formations within the Ghanzi Group. Thick overburden of Kalahari sand and pedocretes as well as clay layers cover the bedrock. In some places, the overburden can exceed 120 metres. Figure 2-1 also shows the main sample localities and areas of interest on the Ghanzi Ridge. Four suitable sampling localities were identified on the Ghanzi Ridge, namely Zone 5, Zone 5 North, Banana zone and Mahumo Deposit, of which the first three localities are indicated in Figure 2-1.

The Ghanzi Ridge outcrops sporadically along a southwest-northeast trending spine of slightly elevated land (Brown & Cole, 1976). Most of the sedimentary rock in the Ghanzi Group originated locally from the Kgwebe volcanic complex (Hall, 2007). They consist of a series of medium- to fine-grained purple and grey, massive quartzites, grey and green shales, grey and purple siltstones, red mudstones, grey and red limestones and greywackes. In the Ghanzi area, these rocks have been folded into a complex series of synclines and

anticlines with drag folds and several faults. The Ghanzi Beds extends in a south-westerly direction and have been correlated with the Tsumis system in Namibia.

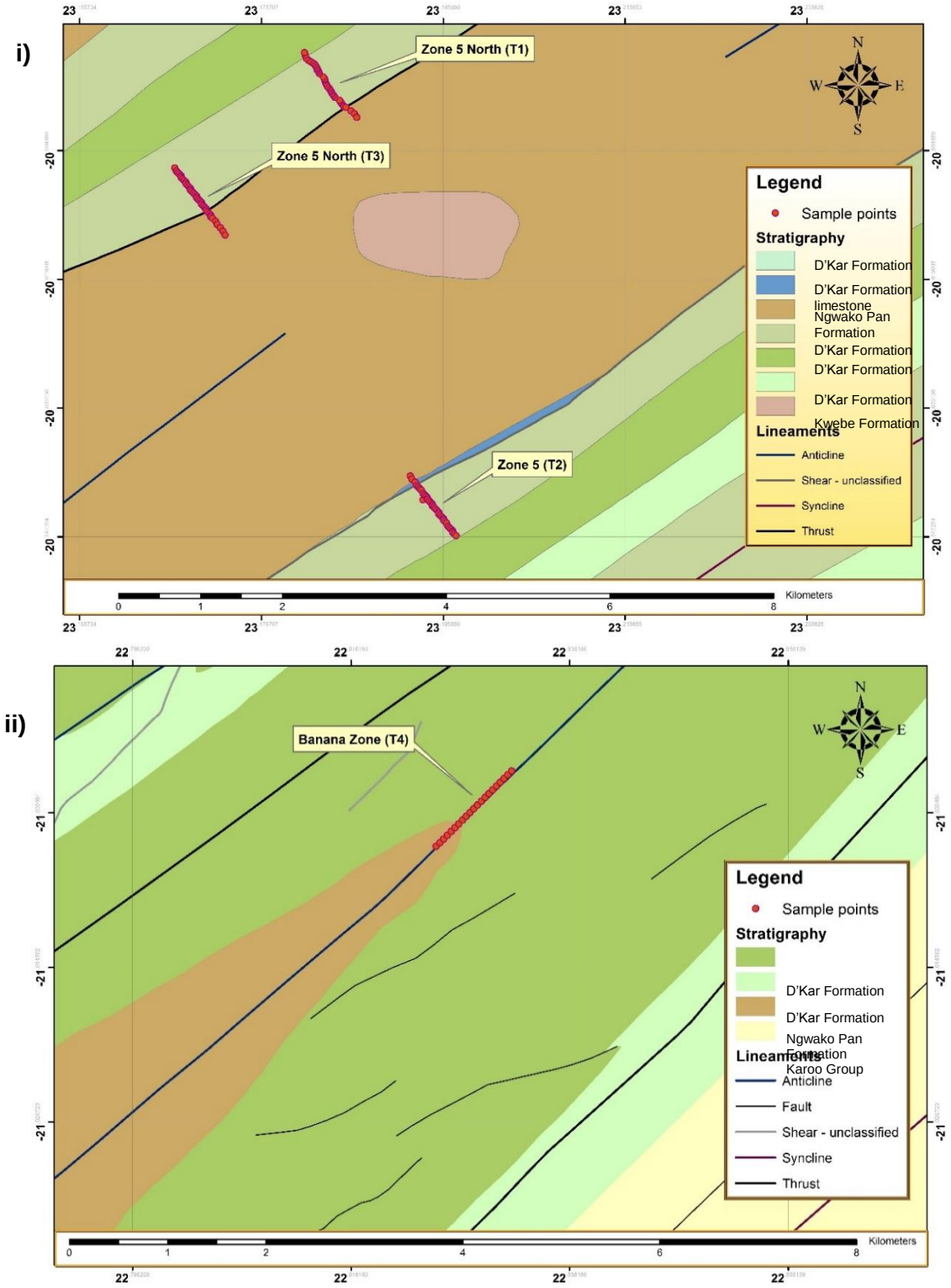

Figure 2-1: Geology of the Ghanzi Ridge with sampling localities i) Zone 5, Zone 5 North; and ii) Banana Zone.

Table 2-1: Stratigraphic column of the KCB, adapted and constructed from Hall (2007), Green (1966, cited by Jones, 1980), Passarge (1904, cited by Jones, 1980), Haddon (2005) and Cole & Le Roex (1978). The red line indicates the stratigraphic position of the KCB deposits.

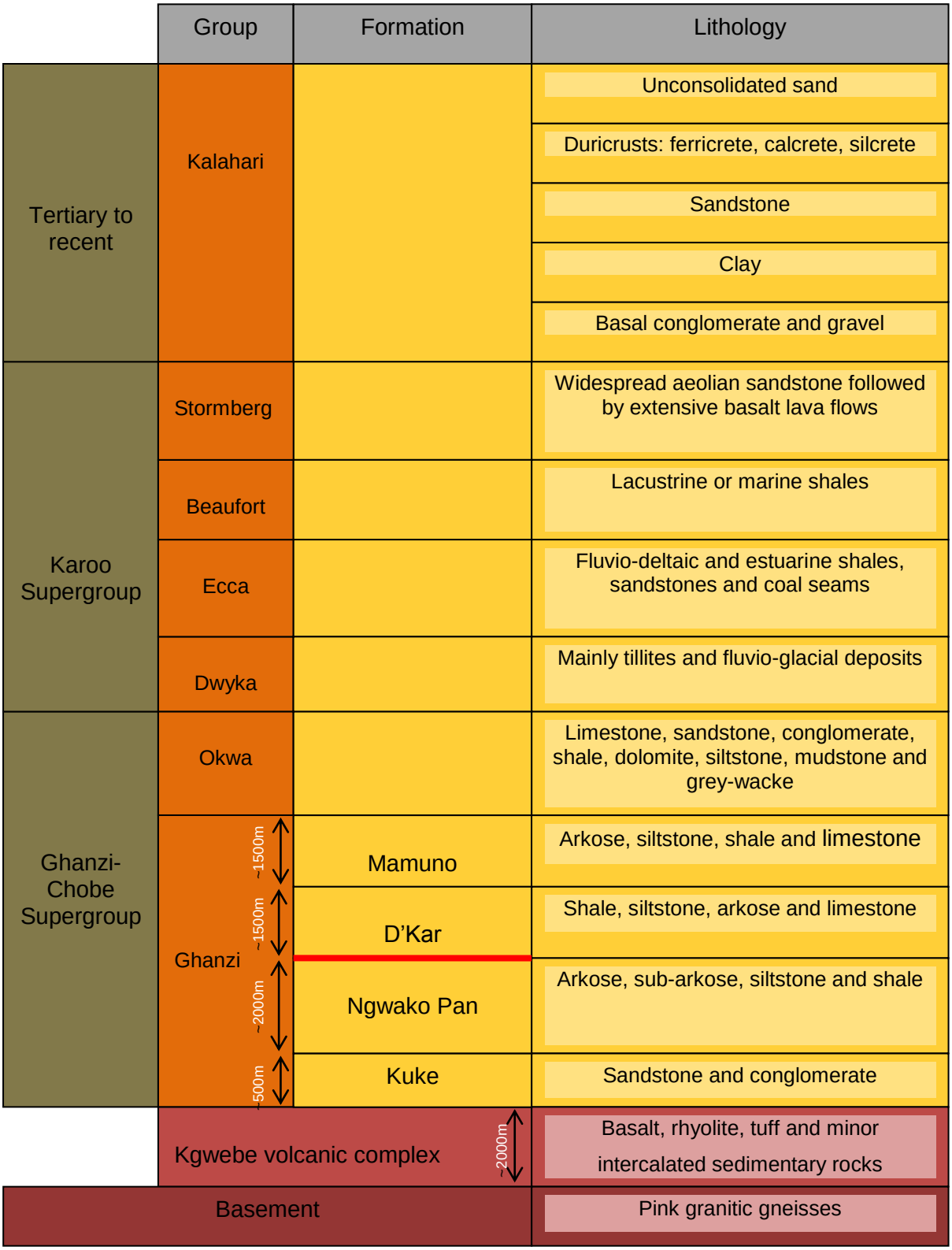

The two Proterozoic sequences (the Kgwebe Formation and Ghanzi Group) are unconformable to and overlain by Phanerozoic sequences of the Karoo Supergroup and Kalahari Group (Modie, 1996). To the southeast it is covered by Cenozoic Kalahari Group sediments and to the north-west by Kalahari Group and Carboniferous to Jurassic Karoo Supergroup sediments (Akanyang, *et al*., 1996). The Kalahari beds cover most of the Ghanzi region. They comprise sands, gravels, silcretes, calcretes, ferricretes, terrace gravels, pan and fluviatile deposits and are usually covered with loose, undisturbed sand. These beds form thin or patchy deposits over the Ghanzi Ridge, but may reach thicknesses of up to 100 m elsewhere (Brown & Cole, 1976).

2.1.2 Surficial cover materials

The Carboniferous to Permian Karoo Supergroup overlies the unconformable contact of the deformed host rock package of the Ghanzi-Chobe Supergroup. Erosion has stripped Paleozoic cover off much of the Ghanzi-Chobe Belt so that Cenozoic calcrete and sandstone of the Kalahari Group unconformably overlies the deformed host rock package in most places (Hall, 2007). According to Passarge (1904, cited by Jones, 1980) the Kalahari beds can be stratigraphically classified in the following succession: underlying Botete beds, followed by Kalahari limestone (calcretes), Kalahari sand and alluvial deposits (Table 2-1).

2.1.3 Mineralisation

Lithological units of the Ghanzi-Chobe Belt can be correlated with similar sequences in Namibia like the Doornpoort, Klein Aub and Eskadron Formations (Modie, 2000). The Goha and Chinamba Hills, which is exposed in northern Botswana forms the north-eastern boundary of the Ghanzi-Chobe Belt. The volcano-sedimentary sequences of the Ghanzi-Chobe belt and their correlatives in Namibia has similar occurrences of stratabound copper sulphide mineralisation. Copper sulphide mineralisation developed at a redox interface within the Ghanzi Group and is also associated with carbonates of the Chinamba Hills Formation (Modie, 2000).

The basal basalts of the Kgwebe Formation, occurring in all the basins, are mineralised with Cu and is the main source for the major stratabound Cu-Ag deposits found in the lower part of the overlying Ghanzi Group sequence (Ayres & Key, 2000; Borg & Maiden, 1987; Ruxton, 1981). The Cu is believed to have been derived through the leaching of underlying basalt (Ayres & Key, 2000; Modie, 1996). Ruxton (1981) therefore proposed a model for ore genesis involving Cu and Ag being released from mineralised basement rocks during semi-

arid to arid weathering, and transport of the elements in solution as copper sulphate. On contact with neutral or alkaline aqueous solutions it was converted to insoluble basic copper carbonate and carried in suspension. These metalliferous waters collected in topographically low areas. The particulate carbonates were deposited with the suspended sediment load and reworked by lacustrine paleocurrents forming placer deposits. Bacterial reduction of groundwater sulphate led to copper being fixed as sulphides in the sediments during diagenesis (Ruxton, 1981).

There is evidence that this diagenetic mineralizing event was followed by local dissolution of sulphides and carbonates during deformation. During the Damaran orogeny, regional metamorphism caused lower greenschist-facies metamorphism. Sulphide recrystallization took place due to this tectonic compression, causing the formation of mineralised calcite and quartz-albite lenses, nodules and veinlets during the early phases and recrystallization along cleavage planes with further compression (Hall, 2007). The sulphides and carbonates were reprecipitated in adjacent veins and shear zones, so that the diagenetic pyrite was replaced by copper sulphides. This process seemingly formed the high-grade structurally controlled ore zones. Sulphide minerals are locally remobilised by fluids, but these events are poorly understood (Hall, 2007).

Through drilling and trenching it has been shown that mineralisation developed in an irregular fashion in a zone extending along the strike of the Ghanzi Group. The main occurrence, south-east of Lake Ngami received widespread coverage in many exploration and academic reports (Modie, 2000).

Cu-Ag mineralisation is largely hosted by the grey-green (chemically reduced), transgressive marine clayey facies of the lower part of the D'Kar Formation (Hall, 2007; Modie, 1996) that overly the continental alluvial red arenite facies of the Ngwako Pan Formation. The mineralised zone can reach a maximum thickness of 20 m with higher grade (~2% Cu) ore bodies having an average thickness of 3-5 m. The major ore minerals, in decreasing order of abundance, are chalcocite, bornite, chalcopyrite and pyrite, with subordinate sphalerite and galena (Hall, 2007; Modie, 2000). Low concentrations (about 0.2%) of secondary Cu minerals include azurite, malachite and chrysocolla (Modie, 2000). Minor amounts of Cu sulphides occur within basaltic flow breccias of the Kgwebe Formation, however it is poorly investigated (Modie, 2000).

Other minerals that may also be present include minor disseminated molybdenite, tennantite (a copper arsenic sulfosalt) that occur sporadically with pyrite or chalcopyrite and trace

amounts of arsenopyrite that is found in most mineralised zones (Hall, 2007). Recent assay results show Ag correlates positive with Pb, indicating that the galena in the ore contains small quantities of Ag. Ag and Pt group elements occur in some mineralised zones in low concentrations. It seems that anomalous Ag concentrations (20-300 ppb or more) are related to bornite-rich zones (Hall, 2007).

The zonation of the sulphide assemblages within the contact zone between the D'Kar and Ngwako Pan Formation is influenced by local changes in the oxidation state, chemical characteristics of the lithologies or the presence of other mobile reductants (Hall, 2007). An example of copper zonation in the Plutus and Zeta deposits are displayed in Figure 2-2 (Hall, 2007). The upper sulphate assemblage largely consists of copper-silver mineralisation, but fractures and veins contain pyrite-sphalerite-galena. The middle sulphate assemblage contains disseminations, cleavages, fractures and veins with bornite and chalcopyrite to chalcopyrite and chalcopyrite-pyrite from the base upwards. The lower zone contains chalcocite or chalcocite-bornite which occurs as coarse sulphides in the veins and aggregates in fractures.

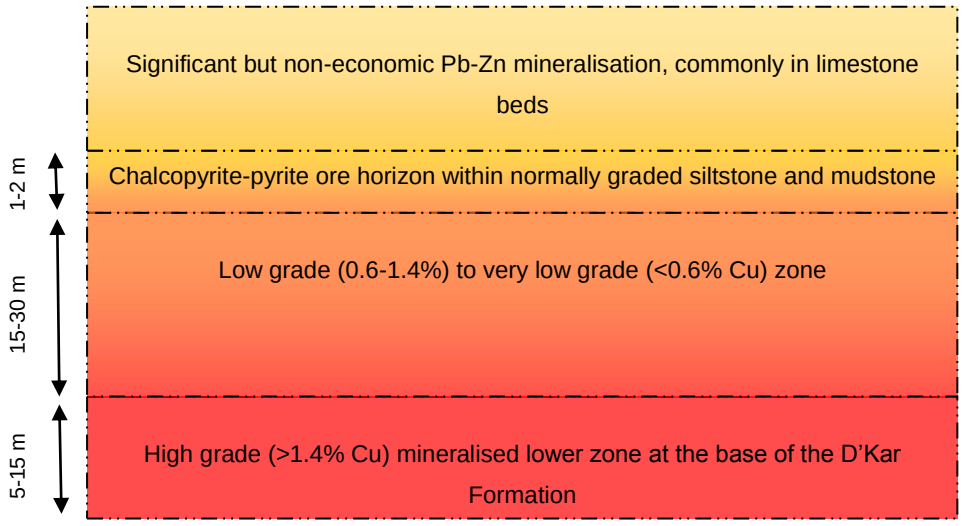

Figure 2-2: Copper occurrences in the Plutus and Zeta deposits, according to Hall (2007).

As opposed to many sedimentary rock-hosted Cu deposits where stratiform mineralisation dominates, the copper sulphides at Boseto are found mainly within veins and structures that formed during deformation and metamorphism (Hall, 2007). The contact between the tougher sandstones of the Ngwako Pan Formation and overlying siltstone-rich D'Kar Formation forms a shear zone. Shear zones parallel to layers are important hosts to Cu mineralisation in the area and are most common at the base of the D'Kar Formation.

Sulphide minerals occur within quartz-calcite veins; sulphides are typically associated with calcite and also have a strong spatial relationship with dolomite and ankerite (Hall, 2007).

According to Hall (2007), disseminated and vein/shear related sulphides have similar sulphide mineral zonation (Figure 2-3). High-grade mineralised zones of chalcocite and bornite occur along a north-east striking zone where accommodation space was created. The vertical and lateral zonation of supposed early disseminated Cu sulphides suggest migration of mineralizing fluids outward from north-east striking transfer faults during diagenesis of the Ghanzi Group (Hall, 2007). North-east to south-west zonation of Cu sulphides is also present at several prospects in the Boseto area. Sulphide assemblages change along strike from chalcosite to bornite to chalcopyrite to pyrite-galena-sphalerite to pyrite-only. So, it appears that ore mineral enriched fluids moved laterally along the D'Kar Formation in a south-west direction, possibly indicating the presence of northwest-southeast trending normal faults. Cu grades are distributed unevenly along strike and down dip due to deep earth processes that tend to form primary minerals and surface processes that usually result in secondary minerals. Hypogene grade are largely controlled by structures. Supergene processes leached primary sulphides from rocks next to steep faults and hematite and goethite minerals replace sulphides in these zones so that Cu oxides like malachite and chrysocolla are then found beneath the leached zones at greater depth. The oxide mineralised zones include minor amounts of the minerals azurite, cuprite, lepidocrocite, tenorite, hemimorphite, covellite, smithsonite, copper and silver (Hall, 2007).

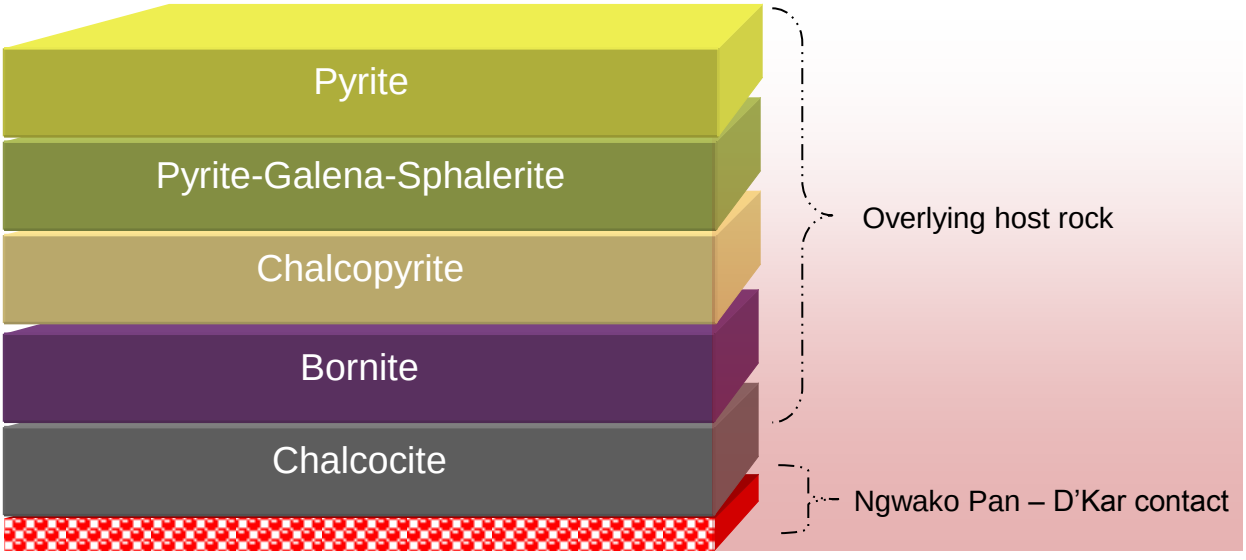

Figure 2-3: Zonation of Cu sulphide minerals in the Boseto area.

The mineralised horizon, at the base of the D'Kar Formation, subcrop below Kalahari sands in the Ghanzi Ridge area in a series of north-east trending folds. Major anticline and syncline

axial surface traces can be found over distances of 10 to 50 km with traces spaced 2 to 8 km apart. A regional cross section of the Ghanzi Ridge area suggests that fold amplitudes are approximately 4-6 km. Fold limbs range in dip from 45˚ to vertical, and fold axial planes strike 220˚ and 235˚ (right-hand-rule format) and dip between 80˚ to the north-west and vertical. Fold asymmetry defines south-east vergence. Many folds in the Ghanzi Ridge have a cuspate shape with an interlimb angle between 50˚ and 20˚, although some folds, including the Plutus anticline, have a box geometry with limb dips abruptly changing from 60˚ to 45˚-30˚ closer to fold crests. Apart from the region to the north-east of (and including) the Boseto copper deposits, anticlines and synclines plunge at shallow angles to both the north-east and south-west between 0˚ and 15˚ creating doubly-plunging folds. Interpretation of the geophysical dataset suggests that the Ghanzi-Chobe region is dissected by several laterally extensive southwest-striking reverse faults with a component of sinistral displacement (Hall, 2007).

Several faults with sinistral strike separation and thrust dip separation of folds cut the D'Kar Formation in the southwestern portion of the study area. This suggests that the thick north-north-east trending quartz veins could be Reidel fractures related to sinistral displacement. As these faults displace folded structures, they must have been developed during a late stage of Damara orogenesis. In addition to the southwest-striking fault system, several north-northeast-striking faults are visible in the aeromagnetic dataset (Hall, 2007).

Satellite imagery and regional aeromagnetic data reveal closely-spaced second-order parasitic folds (short wavelength folds formed within a larger wavelength fold structure – normally associated with differences in bed thickness) within the D'Kar Formation throughout the belt. A syncline to the west of the Plutus-Petra deposit contains several parasitic folds that formed in response to buckling of the D'Kar Formation in the hinge of the syncline and resulted in repetition of magnetostratigraphic units within the D'Kar Formation. Broadly spaced, open parasitic folds in the Ngwako Pan Formation may exist on the limbs of some major folds (Hall, 2007).

The south-western nose of the Plutus anticline is cut by a poorly defined 5 km-wide west-northwest trending graben structure filled with Karoo Supergroup strata. A series of larger grabens occur roughly 40 km west-southwest of the Kgwebe Hills and 10 km north of the Ngunaekau Hills. These grabens are bounded by north-northwest and southwest striking normal faults and filled by basalts of the Stormberg Member of the Karoo Supergroup. A similar graben occurs roughly 20 km north of the Kgwebe Hills near the town of Toteng. The

traces of the southwest-striking faults that bound the Karoo grabens are coincident with the regional southwest-striking faults dissecting the Ghanzi Ridge area (Hall, 2007).

2.2 Vegetation cover

2.2.1 Botswana vegetation

The present-day climate of the Kalahari is semi-arid with dry winters characterised by warm days, cold nights and hot summers during which rainfall occurs. In summer, the mean monthly maximum is 32.2°C and the mean monthly minimum is 18°C, but temperatures may rise well above 43.3°C during the day and fall below 15°C at night (Brown & Cole, 1976). In winter, temperatures may drop below 0°C at night. Throughout the year temperatures are such that evaporation normally exceed precipitation.

Mean annual rainfall of 423 mm has been recorded for Ghanzi (Cooke, 1980); a summer rainfall region, with precipitation confined to the months of October to May. Most of the rain that falls is immediately absorbed by the sandy soils, but in some places, it gathers in small depressions known as pans. Pans form as a result of $CaCO_3$ precipitation during evaporation, because of the precipitate being less permeable than sand.

The vegetation of the Ghanzi area can be categorised as low tree and shrub savanna with numerous associations within this category. The tree and shrub savanna within the Ghanzi area can be divided threefold (Brown & Cole, 1976), each division following closely the patterns of geology and relief (Table 2-2). Table 2-2 also indicates the subdivisions of the Ghanzi Ridge, into four sections (Rains & Yalala, 1970; De Beer, 1962).

The Ghanzi Ridge carries a low tree and shrub savanna characterized by *Boscia albitrunca* trees of about 3-4 m in height and by *Acacia mellifera* subsp. *detinens* shrubs up to 1.5 m high (Brown & Cole, 1976). Scattered *Combretum hereroense, Ziziphus mucronata* subsp. *mucronata* and numerous shrubs like *Grewia flava*, *Tarchonanthus camphoratus* and *Searsia tenuinervis* also forms part of the vegetation composition, with a grass layer usually dominated by *Stipagrostis uniplumis*. The vegetation associations form repetitive sequences that resemble the apparent stratigraphic horizons, drag folds and faults within the major fold structures (Brown & Cole, 1976). The distribution of these associations is determined mainly by differing weathering characteristics of the Ghanzi beds, leading to minor variations of physiography and by different thicknesses of the calcrete and Kalahari sand overlying the Ghanzi beds.

Table 2-2: Vegetation divisions and subdivisions of respectively the Ghanzi area and Ghanzi Ridge.

Vegetation divisions of the Ghanzi area		
1. Kalahari sand plains north and east of the Ghanzi Ridge	2. Ghanzi Ridge	3. Kalahari sand plains south of the Ghanzi Ridge
Open low tree savanna characterized by *Terminalia sericea* and *Philenoptera nelsii*	Variable cover in which *Boscia albitrunca* and *Acacia* species are usually present	Open low tree savanna of *Acacia luederitzii, A. erioloba* and P. *nelsii*

North-east of Ghanzi	In the south-west	Near Kuke	In depressions throughout the area
Low tree shrub savanna characterized by *Combretum imberbe, A. erioloba* and *A. mellifera*	A shrub savanna of *Catophractes alexandrii* and *Rhigozum brevispinosum*	*Combretum apiculatum, C. imberbe* and *P. nelsii* section	*A. leuderitzii* var. *leuderitzii* and *C. imberbe* trees associated with shrub-like forms of *A. mellifera, C. hereroense, Ziziphus mucronata* and *Mundulea sericea*

Calcrete is found as a weathering product over most rock types, but are presumably more developed over limestones and arenites. It outcrops over Ridges and is usually obscured by deposits in the valleys, which are usually only some metres lower than the rises. Therefore, a series of grey calcrete capped ridges (usually with an arenite or quartzite core) alternates with red silt- and gravel-filled valleys, probably underlain by limestone or shale. Each unit has its own characteristic vegetation association, which can be seen on aerial photographs as patterns following the fold structures and bedrock lithology present beneath calcrete and Kalahari sand cover (Brown & Cole, 1976; Cole & Le Roex, 1978).

The calcrete ridges, where groundwater is usually found just beneath the calcrete, typically support a low tree and shrub savanna characterized by *B. albitrunca* and various shrubs (Brown & Cole, 1976). The depressions between the ridges, covered by silt and fine sand, support a savanna grassland, with *B. albitrunca* being characteristically absent. The vegetation associations usually occupy narrow zones, only a few metres wide, but extending

laterally for hundreds of metres, reflecting the patterns of the drag folds and faults (Brown & Cole, 1976).

In thicker sands where the micro-relief is obscured, but where the underlying geology still influences the vegetation, a low tree and shrub savanna of heterogenous composition occurs (Brown & Cole, 1976). *C. hereroense* is the most common tree, occurring with *C. imberbe* and *Acacia. fleckii* north and east of Ghanzi and with *A. mellifera* subsp. *detinens* around D'Kar. *Dichostachys cinerea* is the most common shrub around D'Kar, while *G. flava* and *Petalidium englerianum* are widespread. *Rhigozum brevispinosum*, S. *tenuinervis* and *Ximenia americana* occur less frequently and *Bauhinia macrantha* occur in thicker sand cover.

As the sand cover becomes thicker away from the Ghanzi Ridge, the vegetation associations become more characteristic of the Kalahari sand plain. Away from Ghanzi toward the north-east, the sand gets thicker, rainfall increases and incidence of frost decreases. Trees become larger and occur more frequently and the low tree and shrub savanna characterized by *B. albitrunca* become a low savanna woodland. *Boscia foetida, Combretum albopuctatum, Acacia erubescens* and *Terminalia prunioides* forms part of the association. *Grewia bicolor* will accompany or replace *G. flava* and *Combretum engleri* will do the same with *G. retinervis*. Where there is considerable sand cover, *Commiphora pyracanthoides* subsp. *glangulosa* and *Croton menyhartii* are particularly common even over calcrete, where they are associated with *C. alexandrii.*

North-west of Ghanzi, there is an increased occurrence of deep-rooting species like *Boscia foetida* and *T. prunioides* due to the greater availability of groundwater because of the more widespread calcrete cover and bedrock that is closer to the surface (Brown & Cole, 1976). Species with lateral rooting systems such as *T. sericea* are more abundant south-west of Ghanzi due to increasing sand cover (Brown & Cole, 1976). Trees and shrubs with well-developed tap roots like *B. albitrunca* are a feature of the Ghanzi Ridge, where groundwater is present at depth throughout the year. In contrast, *C. apiculatum* and *T. sericea* (with lateral rooting systems) favour sand-covered areas.

The areas north and south of the Ghanzi Ridge, deeply mantled by Kalahari sand, support a relatively homogenous low tree and shrub savanna. The water table is beyond the reach of plant roots and species depend on the moisture held in the sand after rains. Species with lateral and adventitious root systems favour these sand-covered areas where they can draw on vadose water (in the unsaturated zone above the water table) after rains. The vegetation

of the Kalahari sand plain is therefore characterized by *T. sericea*, together with *Combretum collinum, Philenoptera nelsii* and *Croton gratissimus*, seeing that they have such root systems (Brown & Cole, 1976).

In the Ngwako Pan area, *Terminalia sericea, Dichrostachys cinerea*, *C. gratissimus* and *B. macrantha* shrubs inhabit areas of thick Kalahari sand cover, while scattered *C. gratissimus* and *Philenoptera nelsii* are found on exceptionally deep sand. Low tree and shrub savanna characterized by *C. apiculatum*, with occasional *Markhamia acuminatae* and *Sclerocarya birrea* subsp*. africana* trees grow on outcropping quartz-porphyry rocks. The vegetation assemblage of the sedimentary sequence between Ngwako Pan and the Ngwenalekan Hills consist of woodland, dominated by *T. prunioides* and *A. erubescens* that occur on the dark, brown soils from argillaceous parent material. Red sandy soils from arenites are dominated by *C. apiculatum,* whereas *C. alexandrii* commonly dominate outcropping calcrete. The woodland south of Ngwako Pan contain scattered patches of *Barleria senensis* that is believed to be a possible copper indicator (Cole & Le Roex, 1978).

2.2.2 Plant species selection

Numerous studies in southern Africa have identified certain plant species as potential indicators of concealed mineralisation (Cole & Le Roex, 1978; Kausel, 1991; Lund, *et al*., 2005). *Helichrysum leptolepis*, for instance, is a very reliable indicator of Cu mineralisation. Anomalous plant communities of *H. leptolepis* led to the discovery of copper mineralisation beneath sand and calcrete cover near Witvlei, Namibia (Cole & Le Roex, 1978). Similarly, a geobotanical approach with this plant was used during the 1960's and 1970's to indicate Cu mineralisation and establish the relationship between vegetation associations and concealed bedrock geology in the Ghanzi area (Cole & Le Roex, 1978).

In the Ngwako Pan area deeper rooting indicators like the blue flowering *Ecbolium lugardae* were used to locate Cu mantled by thick layers of calcrete and wind-blown Kalahari sand (Cole & Le Roex, 1978). Recognition of this geobotanical anomaly made it possible to reliably predict the presence of cupriferous argillite and limestone bedrock beneath up to 30 m of calcrete (Cole & Le Roex, 1978). *Ecbolium lugardae* has also been found growing on other Cu deposits in South Africa. Another study by Kausel (1991) found that the occurrence of the blue flowering species *Monechma divaricatum* also correlated well with the occurrence of a Cu bearing ore body in the Ngwako Pan area. Further work by Lund *et al.* (1997) in north-eastern Botswana, identified *Helichrysum candolleanum* and *Blepharis diversispina*, amongst other plants, as possible indicators of Ni and Cu.

Prospecting surveys that include a geobotanical aspect can be very successful in detecting concealed copper mineralisation. Exploration geologists can use certain species of plants as to predict the presence of underlying base metal deposits and further investigation of this prospecting approach is warranted. This study aims to assess the value of selected shrubs and trees as sampling media in prospecting surveys. However, focus is shifted from the geobotanical approach to a biogeochemical one, i.e. plant species with a tendency to accumulate anomalous levels of ore trace elements, and in specific pathfinder elements, which can be detected by analysing the foliage. *Combretum hereroense*, for instance, is known to take up elevated levels of Cu and Ni where they grow over an ore body containing such mineralisation. In a study by Cole (1971), the Ni and Cu content of the plants reflected that of the ore body sub-outcrop more accurately than concentrations in the surface soil. The current study will attempt to identify plants with a similar ability to accumulate ore-related elements in a way that will reflect underlying mineralised areas. The investigated species were selected based on their abundance and anticipated deep root systems. A brief description of each sampled plant species follows.

2.2.2.1 ***Boscia albitrunca* (Capparaceae)**

B. albitrunca (Shepherd's tree; Witgat) is usually a single-stemmed tree, with a rounded, neat crown (Figure 2-4). Its bark is pale, yellowish to almost white (Figure 2-4). Its leaves are oblong-elliptic, leathery, brittle and slightly rough; dark green to grey in colour with a blunt apex and short petiole (Figure 2-4). It has a dominating tap root system and lacks lateral roots (Brown & Cole, 1976) (Figure 2-4).

B. albitrunca grows on sandy or rocky substrates that include granite, schist and calcrete (Curtis & Mannheimer, 2005). A rooting depth of 68 m in the central Kalahari is known for this species (Canadell, *et al*., 1996) and it can possibly be even deeper.

It has been reported by Mshumi (2006) that *B. albitrunca* can absorb significant amounts of gold pathfinders like Ag, Pb, As, W and Hg, indicating its potential suitability during biogeochemical prospecting of other ore deposits.

Figure 2-4: *Boscia albitrunca* with i) pale, yellowish-white bark, ii) single stem and rounded crown, iii) oblong-elliptic; grey to dark green leaves with blunt apex. iv) Root system of *B. albitrunca* in red dune sand to 2 m deep (Brown & Cole, 1976).

2.2.2.2 Boscia foetida subsp. rehmanniana (Capparaceae)

B. foetida subsp. *rehmanniana* (Stink shepherd's tree; Stingwitgat) can be found as a shrub or a tree (Figure 2-5). Its bark is whitish with fissures exposing a rough, dark bark. Its leaves are oblong, small, with a very short petiole; has an olive-green colour and are spirally arranged or clustered on dwarf shoots (Figure 2-5). Its flowers have a characteristic unpleasant, foetid odour.

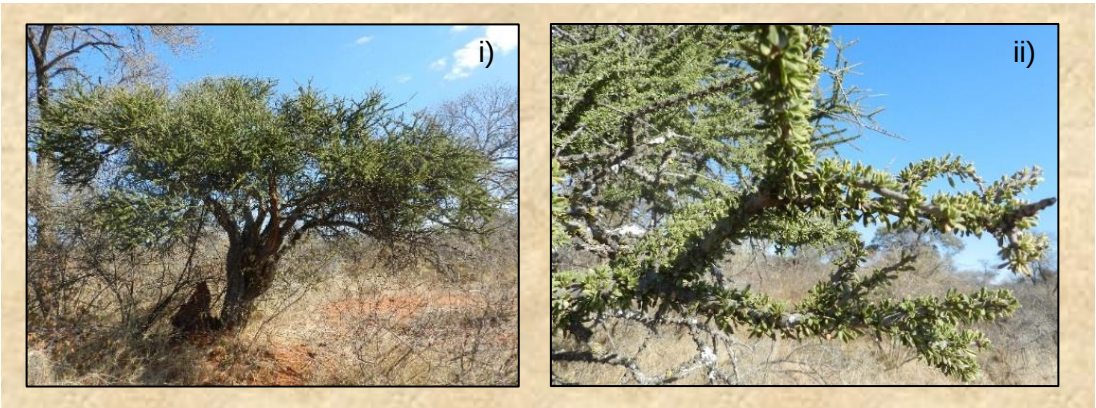

Figure 2-5: *Boscia foetida* subsp. *rehmanniana* is a i) tree or shrub with ii) small, oblong, olive-green leaves.

B. foetida subsp. r*ehmanniana* is only found on gravel, stony or rocky substrates and on sand only if there is underlying rock (Curtis & Mannheimer, 2005). It is mostly a shrub up to 3

m high with a deep rooting system and it retains its foliage throughout the year (Cole & Le Roex, 1978; Curtis & Mannheimer, 2005).

2.2.2.3 *Combretum apiculatum* (Combretaceae)

C. apiculatum (Red bushwillow; Rooibos) is usually a shrub or shrubby tree up to 8 m in height (Figure 2-6). Its leaves are broadly elliptic, leathery, with an undulate margin; the apex is abruptly pointed and often twisted (Figure 2-6).

Figure 2-6: *Combretum apiculatum* i) habit ii) broadly elliptic leaves with abruptly pointed, twisted apex. iii) Root system of *C. apiculatum* in dark, brown, cracking, clay loam soil with calcrete at 60 cm (Brown & Cole, 1976).

C. apiculatum grows on various substrates, including granite, dolomite, calcrete, basalt, schist, mica, gravel and sand (Curtis & Mannheimer, 2005). It develops extensive lateral root systems (Figure 2-6) that can draw on vadose water held in the soil and sand after rains. According to Cole and Brown (1976) this species may develop a tap root in heavy soils (Figure 2-6).

2.2.2.4 *Croton gratissimus* (Euphorbiaceae)

C. gratissimus (Lavender Fever-berry; Laventelkoorsbessie) is mostly a shrub and sometimes a tree, up to 3 m high; less often up to 8 m high. It has simple, elliptic to lanceolate leaves that are dark green above (Figure 2-7) and silvery with scattered red-brown scales below; the petiole is 6-25 mm long. The young branchlets are covered by dense, silvery hairs and rust-brown scales. It is found mostly on plains, rocky outcrops and hill slopes, and grows on sand, rock and calcrete substrates (Curtis & Mannheimer, 2005).

Figure 2-7: *Croton gratissimus* has elliptic to lanceolate leaves that are dark green above and silvery below.

2.2.2.5 *Grewia bicolor* (Tiliaceae)

G. bicolor (White raisin; Witrosyntjie) is usually a shrub up to 3 m in height (Figure 2-8). Its leaves are held horizontally in one plane or drooping; the leaves are dark green above and greyish-white and densely woolly below (Figure 2-8); the base is asymmetrically blunt. It produces yellow flowers (2-3 per stalk) and carries orange to red-brown fruit, as 2-3 lobed berries, on a branched stalk.

Figure 2-8: *Grewia bicolor* is a i) slender shrub or small tree with ii) leaves often drooping, dark green above, grey to white below. iii) Root system of *G. bicolor* in dark, brown, cracking clay loam soil to 0.5 m (Brown & Cole, 1976).

G. bicolor grows on substrates such as sand, calcrete, stones and rock (Curtis & Mannheimer, 2005). It develops extensive lateral root systems (Figure 2-8) that can draw on vadose water held in the soil and sand after rains (Brown & Cole, 1976).

2.2.2.6 *Grewia flavescens* (Tiliaceae)

G. flavescens (Sandpaper raisin; Skurwerosyntjie) is generally a slender shrub up to 3 m in height (Figure 2-9). It has characteristically square, longitudinally grooved stems. Its leaves are held horizontally, both surfaces are rough, and it has a light green colour (Figure 2-9). It carries yellow-brown fruit that is round to bilobed (seldom four-lobed) and up to 15 mm in diameter. *G. flavescens* is found on sandy and rocky substrates, including calcrete, granite and schist (Curtis & Mannheimer, 2005).

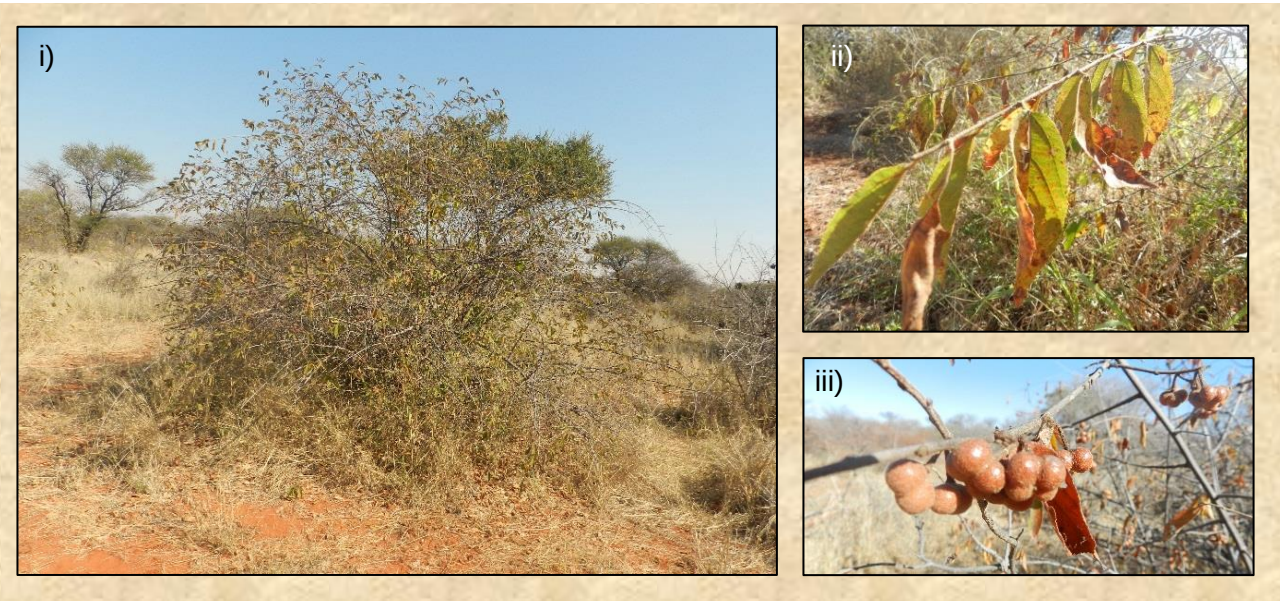

Figure 2-9: *Grewia flavescens* is a i) slender shrub with ii) light green leaves held horizontally, and iii) round to bilobed fruit that are shiny when ripe.

2.2.2.7 *Gymnosporia buxifolia* (Celastraceae)

G. buxifolia (Common spikethorn; Gewone pendoring) is a very spiny shrub up to 3 m high and occasionally a tree of over 3 m (Curtis & Mannheimer, 2005). Leaves are smooth, papery to parchment-like and clustered on branch tips (Figure 2-10). It has a broadly tapered to rounded apex (Palgrave, 1984) (Figure 2-10). Flowers have a strong, unpleasant scent. Its fruit has a rough-textured capsule which usually splits into three parts. *G. buxifolia* is found in various habitats, and often on calcareous soils (Curtis & Mannheimer, 2005) and on termite mounds (Palgrave, 1984).

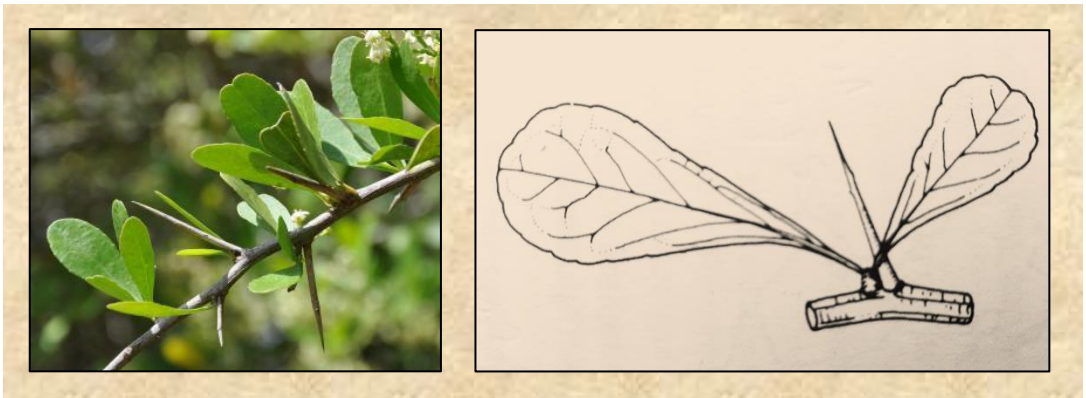

Figure 2-10: *Gymnosporia buxifolia* with i) smooth, pale-green papery leaves and spines up to 100 mm long; and ii) leaves with a broadly tapering to rounded apex (Palgrave, 1984).

2.2.2.8 *Philenoptera nelsii* (Fabaceae)

P. nelsii (Kalahari apple-leaf; Kalahari-appleblaar) is mostly a tree of 3-8 m, but sometimes smaller; the younger plants are more shrub-like. Its leaves are apparently simple, dark green, large, leathery and puckered (Figure 2-11). Its flowers are white to purple.

It is found in various habitats, but mostly on plains where it usually grows on deep sand, but occasionally on calcrete or dolomite (Curtis & Mannheimer, 2005).

Figure 2-11: *Philenoptera nelsii* with large, leathery, dark green leaves.

2.2.2.9 *Terminalia prunioides* (Combretaceae)

T. prunioides (Lowveld cluster-leaf; Sterkbos) is either a tree of 3-8 m in height or a shrub of 1-3 m (Figure 2-12). Its bark is vertically striated and fibrous and the young branchlets are plum-coloured, often long and entangled with each other. The leaves are obovate-elliptic, clustered on dwarf branchlets, dark green above and paler below, with the base running into the petiole (Figure 2-12). Its fruit are up to 60 mm long and has a bright purple to plum-red wing (Figure 2-12). *T. prunioides* is a deep-rooting species (Brown & Cole, 1976; Cole & Le Roex, 1978). Preferred substrates include gravel, sand, calcrete and different rock types such as basalt, granite and calcrete (Curtis & Mannheimer, 2005).

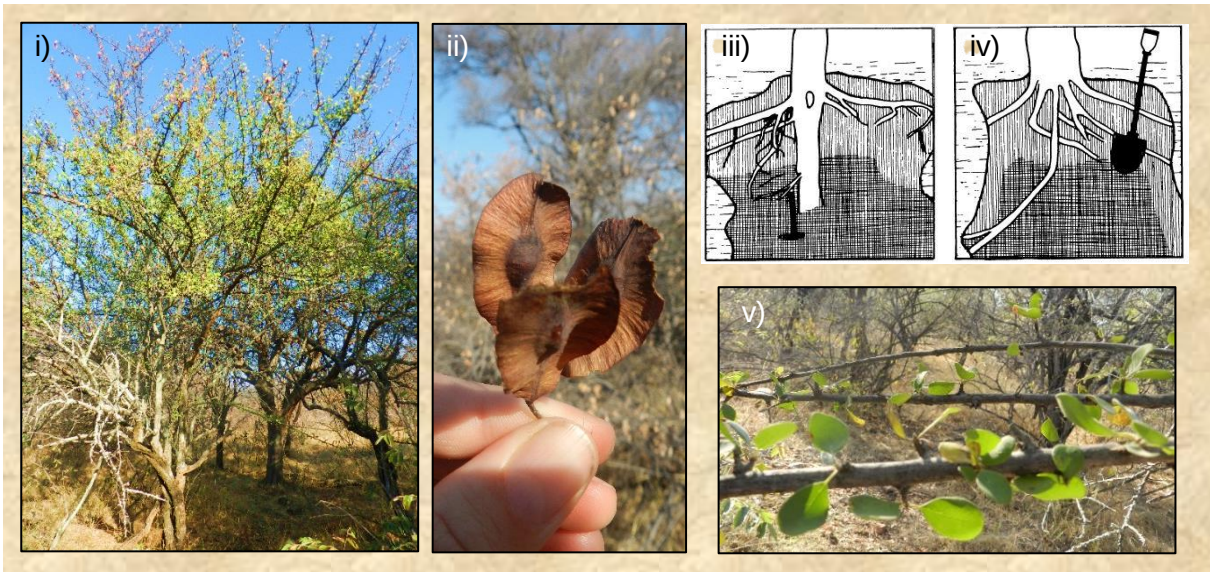

Figure 2-12: *Terminalia prunioides* is a i) shrub or tree with ii) fruit that is often a bright plum-red colour. iii) Root system of *T. prunioides* in dark, brown, cracking clay loam soil with calcrete at 1 m and iv) in red, sandy soil over calcrete to 1 m (Brown & Cole, 1976). v) Leaves are dark green above, paler below and clustered on dwarf branchlets.

2.2.2.10 *Terminalia sericea* (Combretaceae)

T. sericea (Silver cluster-leaf; Vaalboom) is usually a tree of up to 8 m with branches growing horizontally, giving a layered appearance to the crown (Figure 2-13).

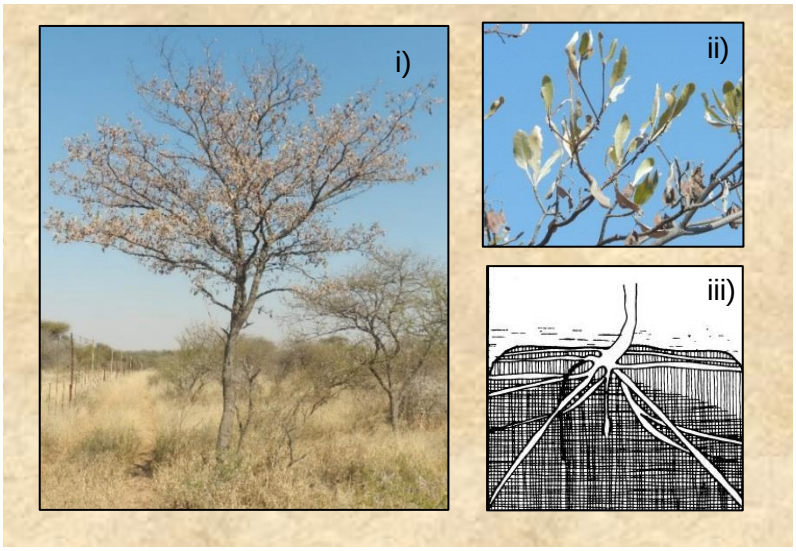

Figure 2-13: *Terminalia sericea* is a ii) medium-sized tree with ii) pale silvery-green, silky leaves. iii) Root system of *T. sericea* in red dune sandy soil to 3 m (Brown & Cole, 1976).

The bark peels and flakes in rings to expose dark underbark. Its leaves are obovate-elliptic, pale green with silky hairs, 3-4 times longer than wide and are clustered towards the ends of the branchlets (Figure 2-13). Its fruit are pink to rose-red and turns brown upon drying. *T. sericea* is found in various habitats, but always on sand (Curtis & Mannheimer, 2005). It has adventitious roots extending outwards in all directions from a central rootstock (Figure 2-13). In some cases, it can penetrate as deeply as species with tap roots (Brown & Cole, 1976)

2.3 Element dispersion and plant absorption

2.3.1 Dispersion patterns in overburden

The transport and fixation of elements in the near-surface environment are used by geochemists to determine element distribution patterns and detect mineral deposits at depth. High concentrations of elements in ore deposits will disperse with time and can be recorded as anomalies against 'normal' background concentrations (Barr, *et al*., 2015). An ore body's footprint is increased by primary dispersion as well as secondary dispersion.

Primary dispersion includes alteration and dispersion of primary elements associated with ore emplacement. It describes the process of components in the mineralising fluids moving into country rock and altering primary minerals so that the concentrations of the pathfinder elements are elevated (Barr, *et al.*, 2015). Secondary dispersion includes element migration from alteration and ore zones after emplacement. An understanding of secondary dispersion patterns will enable the exploration geologist to trace element migration in the near-surface environment and into the biosphere (Barr, *et al.*, 2015). The secondary dispersion of ore elements or alteration minerals are reflected in surface media such as tills, stream sediments, groundwater and vegetation.

Secondary minerals, formed by weathering of ores, include Fe-oxides as well as other secondary metalliferous minerals. The stability of secondary ore minerals is controlled mainly by pH, Eh and the abundance of reacting ions it comes into contact with (Hawkes, 1957). Many secondary metalliferous minerals are only stable in the presence of metal-rich solutions. A sizable portion of these elements will leave the site of oxidation in soluble form with the entry of groundwater circulation. Bedding, foliation and vein structures can often be followed from bedrock to the disintegrated residual cover.

Groundwater (or water below the water table) generally move under the influence of gravity from an area of higher to an area of lower hydrostatic pressure (Hawkes, 1957). The water,

and its dissolved salts, can move against the force of gravity by diffusion, capillary rise and the migration of ions on the surface of soil particles (Hawkes, 1957). These processes mostly take place in the unsaturated fringe zone of vadose water between the water table and land surface. The movement against a force of gravity commonly results in dispersion of dissolved constituents both upwards and laterally in the direction of decreasing concentration (Hawkes, 1957). The overall effect of this action is a spreading of dispersion patterns upward from the source in the bedrock. Elements with high mobility (like Zn and Co) will move more readily in groundwater and soil moisture. As solutions containing ore-derived elements encounter permeable, unconsolidated sediments or residual soils, exchange reactions will take place and the element content of the sediment or soil is increased. As an equilibrium is reached, the pattern of dissolved ions will spread farther from the source into fresh material. Mechanisms of trace element transport to the surface include groundwater flow, capillary action, ionic diffusion, self-potential effect, vaporization, organisms, as components of gases and transportation by gases.

Distribution of mobile elements is smoothed since it goes into solution in element-rich areas and is re-deposited in depleted areas. This leads to a more homogenous pattern. An anomaly defined by a mobile element can therefore be located and mapped with fewer samples than an immobile element anomaly (Hawkes, 1957).

Microbes can mobilise elements during secondary dispersion and cause them to migrate to the surface by means of fractures and faults. They are then adsorbed on Fe-Mn-oxides and clay and are incorporated into the biosphere (Barr, *et al.*, 2015). These complexes have certain element and isotope signatures that resemble the deposit at depth and are especially of interest in the areas of thicker or transported overburden where surface geochemistry is well known to be unreliable (Barr, *et al*., 2015). While direct drilling through overburden to sample bedrock is more effective, drilling is an expensive undertaking, so anything reliable and cheaper is generally desired.

According to Hoffman (1986, cited by Ackay *et al*., 1998) trace element distribution in soil profiles is affected by various geochemical factors. These factors include organic matter content, soil texture, contents of Fe/Mn-oxides, clay content, proximity to bedrock, bedrock composition, pH of the soil and site drainage. Some of these factors remain constant where the same soil horizon is sampled (Levinson, 1974), but may also vary between different horizons. One should also keep in mind that single geochemical anomalies of an element may be related to transport of that element along structural discontinuities, followed by their precipitation upon reaching Fe and Mn-oxides in the soil profile (Gatehouse, *et al.*, 1977).

Elements are mobilised by either groundwater related-, gas streaming- or biotic processes. Groundwater related processes such as density or thermally induced advection, lateral advective flow, capillary rise, electrochemical transport or dilatancy pumping are the most effective. Other mechanisms such as biotic processes where deep-rooted vegetation transport elements by hydraulic pumping, bioturbation by termites and ants, and biomethylation of organometallic compounds also play a key role (Gee, 2005). In arid to semi-arid environments, where the water table is quite deep, it is difficult to establish the mechanisms responsible for the effective rise of ions through transported sediment above the water table. Deep-rooted plants are possibly the main mechanism of element transfer, while bioturbation and gas-streaming may also contribute to an unknown extent (Gee, 2005).

Hawkes (1957) conducted a study to describe the mechanisms of element migration. He stated that the mobility of an element is strongly dependent on its tendency to remain stable in aqueous solutions or suspension. Capillarity can move solutions through the fine pore spaces of soils against the force of gravity and diffusion can move ions in the direction of decreasing concentration through an aqueous system.

The most important characteristics of ionic solutions that have to be considered to understand the formation of secondary geochemical anomalies include (Hawkes, 1957):

- Solubility of salts;
- H^+ concentration;
- Coprecipitation;
- Oxidation potential;
- Sorption;
- Formation of complex ions and organic compounds.

Each of these factors are briefly described in the following section, based on suppositions by Hawkes (1957).

2.3.1.1 Solubility of salts

The ability of ions to remain in aqueous form is limited by the solubility of the salts it forms with ions of opposite charge in the same solution. In the environment of an oxidizing sulphide deposit, where the concentrations of the component ions (produced by the oxidation of sulphide minerals) is relatively high, various ore-related elements are precipitated as secondary minerals, for example, the oxidation of galena and other sulphides

produce an abundance of Pb and sulphate ions, leading to the formation of anglesite ($PbSO_4$). Many secondary compounds are stable in the acidic, metal- and sulphate-rich solutions of an oxidizing sulphide deposit, but will dissolve when it encounters normal solutions closer to the surface.

2.3.1.2 H^+ concentration

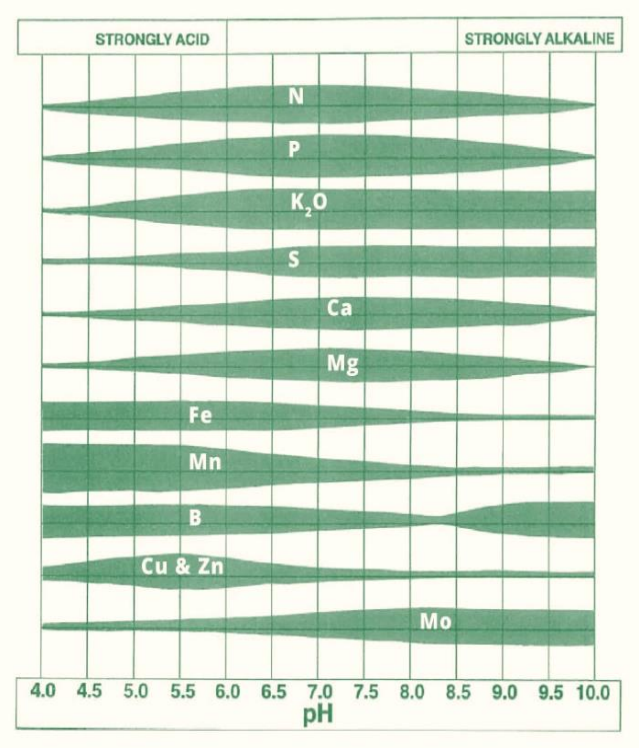

The solubility and stability of compounds are very sensitive to the pH of the aqueous environment. Most elements are soluble in acid solutions, but are precipitated as salts or hydroxides with increasing pH.

pH may be important in plant tolerance, primarily through its relationship to the availability of Ca, as well as some important nutrients in the soil. For instance, Fe, Al, Mg, Mn, Zn, Cu and P are relatively unavailable in alkaline soils, but may be available in toxic quantities in highly acidic soils (Cannon, 1971).

Figure 2-14: Effect of soil pH on bio-availability of elements (JJ Agriservice, 2013).

Availability of an element depends on its solubility, which in turn is related to pH (JJ Agriservice, 2013) (Figure 2-14). Many elements are more soluble and available in the soil at low pH (pH < 5.5), including Cu, Cd, Hg, Pb, Ni and Zn (Freitas & Prasad, 2003). At lower pH levels, Cu is present in the soil solution as the copper ion, Cu^{2+}. At higher pH values (from pH 7.5 up to pH 12.3, Cu is precipitated and copper hydroxide, $Cu(OH)_2$, becomes the dominant species (Addai-Mensah, *et al.*, 2011).

2.3.1.3 Coprecipitation

Precipitating minerals commonly incorporate traces of certain elements into their crystal lattice, for instance, As, Co and Cu is precipitated with limonite, while Mn-oxides may host Co, Ba and various other minor elements (Hawkes, 1957).

2.3.1.4 Adsorption

Where ionic solutions encounter solid particles, the ions are bound to the surface of the particle. The exchange capacities of the particles determine the number of ions that will be held by adsorption (Hawkes, 1957). The root tips of plants have high exchange capacity, assisting in the absorption of mineral nutrients (Coleman & Williams, 1950). The adsorbed ions are still part of the aqueous system, since a change in ionic content of the solution will affect the ratios of the adsorbed ions (Hawkes, 1957).

2.3.1.5 Oxidation potential

Many minerals that are stable under deep-seated conditions will break down in the presence of atmospheric oxygen (Hawkes, 1957). Sulphides will form sulphates and ferrous iron (Fe^{2+}) will form ferric iron (Fe^{3+}). Mn, Cu, V, U and other elements may undergo similar reactions. Where oxygen has been consumed and carbonaceous matter has accumulated because of organic activity, sulphates will again be reduced to sulphides and Fe^{3+} converted to Fe^{2+} (Hawkes, 1957).

2.3.1.6 Inorganic complexes

Complexing agents like H_2O, NH_3, CN^-, Cl^-, OH^- and S^{2-} are important in keeping certain elements in soluble form (Hawkes, 1957).

2.3.1.7 Organic compounds

Simple ions, formed from a single atom, can combine with organic compounds to form metallo-organic complexes. Organic acids can solubilize otherwise insoluble mineral constituents or prevent their precipitation from solution, so that they play a vital role in the movement of elements in the surficial environment (Hawkes, 1957).

2.3.1.8 Assimilation of elements

Micro-organisms can remove certain elements from the nutrient solution (Hawkes, 1957). They can immobilise elements to such an extent that they become unavailable to plants.

2.3.2 Effect of calcretes on element dispersion

Calcretes form chemical and physical barriers to the expression of sub-cropping mineralisation on the surface (Krug, 1995). Consequently, they hide potential mineral deposits from detection by geochemical means.

According to Butt (1992, cited by Krug, 1995), some of the negative impacts of calcretes include:

- Lower concentrations of mobile ore-elements due to leaching of the pre-existing soil profile;
- Further dilution and suppression of the anomaly contrast due to the addition of $CaCO_3$ – the replacement of primary and secondary minerals by carbonates may cause the mobilization and loss of some elements such as Zn and Pb; and
- Reduction of chemical mobility of many elements due to high pH in the regolith, so that the development of epigenetic anomalies is restricted.

Some of the positive impacts of calcrete on exploration include (Butt, 1992, cited by Krug, 1995):

- Precipitation and accumulation of leached elements from the underlying neutral to acid regolith, upon contact with the alkali environment of the calcrete;
- Enrichment of Au in calcareous horizons of soils, so that a near-surface expression of concealed mineralisation is created or enhanced; and
- Transport and deposition of economic concentrations of U with calcretes being the host rock and aquifer that facilitates this process.

Clay in calcrete (like montmorillonite) has a high CEC and may therefore carry ore-related elements (Krug, 1995). The calcrete environment is especially favourable to higher cation exchange capacity (CEC), since montmorillonite has the ability to absorb cations as pH increases (Levinson, 1974).

Calcretes form in the drier parts of the world, in warm regions with limited precipitation. Under conditions of poor drainage, $MgCO_3$ and other soluble salts may coprecipitate with $CaCO_3$ (Krug, 1995). After $CaCO_3$ the second most abundant constituent of calcrete is silica. High pH favours calcite precipitation and silica solution so that silicates are replace by calcite as calcrete formation proceeds (Krug, 1995).

$CaCO_3$ precipitation is controlled by pressure, pH, temperature and concentration, according to the equilibrium reaction: $CaCO_3 + H_2O \leftrightarrow Ca^{2+} + OH^- + HCO_3^-$.

There are several factors affecting element mobility in the geochemical environment, so that there will always be discrepancies between theoretical estimations of relative mobility and observed mobilities (Krug, 1995). Andrews-Jones (1968, cited by Levinson, 1974) categorized elements according to their relative mobility in the secondary environment (Table 2-3).

Table 2-3: Relative mobility of some trace elements in the secondary environment (Andrews-Jones, 1968, cited by Levinson, 1974). For the purpose of this study, only elements included in analyses are referred to.

Relative mobility	ENVIRONMENTAL CONDITIONS			
	Oxidizing	Acid	Neutral to alkaline	Reducing
Very high	B	B	Mo, V, Se	
High	Mo, V, Zn	Mo, V, Se, Zn, Cu, Co, Ni, Hg, Ag, Au		
Medium	Cu, Co, Ni, Hg, Ag, Au, As, Cd	As, Cd	As, Cd	
Low	Pb, Bi, Sb	Pb, Bi, Sb, Fe, Mn	Pb, Bi, Sb, Fe, Mn	Fe, Mn
Very low to immobile	Fe, Mn, Sn, Cr	Sn, Cr	Sn, Cr, Zn, Cu, Co, Ni, Hg, Ag, Au	Sn, Cr, B, Mo, V, Se, Zn, Co, Cu, Ni, Hg, Ag, Au, As, Cd, Pb, Bi, Sb

Dispersion haloes are seldom found at the surface, where transported overburden is present above the weathering profile. The thicker the calcrete profile, or the more mature it is (higher $CaCO_3$ concentration), the more difficult it is for element anomalies to attain a surface expression (Krug, 1995). Exceptions may be found where deep-rooted plants tap anomalous elements at depth and deposit them as leaf litter at surface, or where biological activity carried material through the transported overburden (Krug, 1995). Biogeochemical anomalies have been detected in the Witvlei area of Namibia and the Ngwako Pan (100 km south-west of Maun) of Botswana through 30 m of calcrete (Krug, 1995).

There is much contradiction concerning the relative mobilities of elements in the calcrete environment. Expected relative mobilities of some elements in a carbonate environment is as follows:

Mobile Ni > Ca, Ba > Zn, Co > Pb > Cd Immobile

Mn does not precipitate as readily in calcareous environment, leading to some extent of MnO-enrichment in the soil relative to the calcrete (Krug, 1995). Cu, Ni and Co usually display upward depletion in calcrete due to the diluting effect of pedogenic calcrete formation, while Pb and Zn are often enriched in the soils relative to the calcrete.

One element that does appear to be relatively immobile is Cd and it may be useful for pinpointing mineralisation at the follow-up stage. However, regardless of the relative mobility of elements, calcrete, with its high pH environment, will restrict dispersion by causing the precipitation of elements usually carried in acid solutions (Krug, 1995). Not only can calcrete trap ore-related elements chemically, but also mechanically and so reduce dispersion even further (Krug, 1995).

2.3.3 Plant absorption of elements

Many species in arid or semi-arid environments have deep penetrating roots of up to 100 m, because they rely on the saturation zone of the water table for their moisture (Canadell, *et al*., 1996; Mshumi, 2006; Stanton, 1988). This is the case for most of the plants occupying the Ghanzi Ridge. They have tap roots which can reach the water table (Brown & Cole, 1976). Plants with these types of root systems can penetrate through thick overburden to sample at much greater depths and detect deep-seated deposits (Brooks, 1972 cited by Mshumi, 2006).

Except for Ca, the levels of major and minor nutrients are low in most soils. The concentrations of nutrients vary with the nature of the overburden. Soils over the Ghanzi Ridge and areas floored by calcrete and shallow water limestone have higher levels of Ca, P, Fe and K when compared to areas mantled by Kalahari sand (Brown & Cole, 1976). The presence of shallow calcrete will influence the Ca levels in the soil, which in return may determine the presence or absence of certain species at that site. Along the Ghanzi Ridge, the soils of the calcrete ridges have higher Ca, but lower K and Fe concentrations compared to the sporadic sand and silt-filled valleys (Brown & Cole, 1976).

The plant available pools of nutrients in deeper soil layers are comparable to those in shallow soil horizons (Jackson, *et al*., 2004). Phosphorus weathering, for instance, is usually greater in deep soil layers as opposed to top soil. In addition, hydraulic lift (i.e. the nocturnal transfer of water by roots from moist to dry regions in the soil) could mobilise nutrients in the soil through mass flow or diffusion. It can also indirectly influence the availability of some nutrients (Maeght, *et al.*, 2013). Roots can affect the concentration of ions and are also involved in other interactions due to the root exudates in the rhizosphere (Hinsinger, 1998).

The ability of plants to access nutrients is influenced by spatial distribution and morphology of the roots, root physiology and symbiotic interactions (Maeght, *et al.*, 2013). Element absorption takes place via the roots by means of cation exchange or diffusion at the surface of clay minerals (Brooks, 1972 cited by Mshumi, 2006). The surface of the root tip and the immediate surrounding solution are characterized by elevated levels of H^+ ions. It is a local effect probably caused by hydrolysis of CO_2 escaping the roots. The abundant H^+ ions will cause active cation-exchange reactions between the clay minerals and the surface of the roots. H^+ ions exchange for ions on the surface of clay minerals, after which the elements move through the soil to the roots (Hawkes, 1957). The elements are then transported to the above-ground parts of the plant. Non-essential elements are absorbed along with the essential elements and are accumulated in the more extreme parts of the plant like the twigs, tree tops and outer bark. Plants growing over ore deposits can accumulate ore-related elements in vast amounts, thereby reflecting the underlying substrate (Brooks, 1972 cited by Mshumi, 2006).

The plant's nutritional requirements will determine the distribution of salts throughout the plant structure. Plants require small amounts of elements like B, Cu, Fe, Mn, Mo and Zn (Bohn, *et al*., 2015; Hawkes, 1957). Nutritional requirements differ between species. The absorption of one element may be stimulated or suppressed by the presence of other elements in the solution (Hawkes, 1957).

According to Baker (1981), metal-tolerant plants deal with elevated levels of elements in the soil either by exclusion or accumulation. He suggested two types of plant-soil relationships: excluders or accumulators. Excluders are defined by a differential uptake and transport of elements, while accumulators tend to translocate and accumulate high levels of elements in the above-ground parts of the plant (Baker, 1981). Indicators exhibit an intermediate response to element concentrations in soil and the elements in the plant reflect some measure of the bio-available concentrations in soil. In other words, proportional relationships exist between element levels in the soil, uptake and accumulation in plant tissue (Baker,

1981). Movement of cations into the plant is controlled by a selective restraining effect of cell membranes, e.g. Pb is largely immobilised by precipitation in the cell walls and nuclei of the roots of some plants. U and V are apparently precipitated in the roots in the same way (Hawkes, 1957).

2.3.4 Transfer factor

The enrichment factor (EF), biological absorption coefficient (BAC) or transfer factor (TF) are terms that can be used to describe the relationship of element content in the biosphere to content in the lithosphere. It is also defined as the ratio between leaf element concentration and soil concentration (Baker, 1981) and it represents the degree of element translocation from soil to plant. In the past, elements with a high transfer factor were targeted for prospecting by means of plant analysis (Hawkes, 1957).

TF is an index for evaluating the potential transfer of an element from soil to plant. It reflects on the ability or tendency of a plant to absorb and accumulate a certain element with respect to its concentration in the soil substrate (Adamo, *et al.*, 2014; Lund, *et al.*, 2005; Osman, *et al.*, 2013). The transfer factor is calculated by dividing the element concentration in the plant over its concentration in the soil and is represented by the following equation:

$$\mathrm{TFi} = \frac{[\mathrm{Xi}]\mathrm{plant}}{[\mathrm{Xi}]\mathrm{soil}}$$

where TFi is the transfer factor of element i and Xi is the concentration of element i.

The absorption of elements by plants depends on the concentration of available elements as well as the type of soil. The solubility, absorption and retention of elements in soil should be considered when determining the degree of accumulation of a plant (Penuelas & Sardans, 2005, cited by Osman *et al.,* 2013). TF will therefore not necessarily be linear to the concentration of elements in the soil, but is also dependent on soil properties.

According to Nan and Zhao (2000, cited by Kalavrouziotis *et al*., 2012) the transfer of elements is affected by SOM, pH, CEC and plant species characteristics such as age. Research by Osman *et al*. (2013) indicated that element absorption by plants in sandy soil is higher than clay soil - low transfer factor may be caused by soil alkalinity that reduces the mobility of ions - and organic matter can chelate with positive ions so that the ions become unavailable to plants. TF quantifies the differences in the bio-availability of an element for

plant absorption and is regarded an indicator of element mobility in the soil (Kachenko & Singh, 2006, cited by Kalavrouziotis *et al*., 2012).

TF represents the degree of element translocation from soil to plant, therefore the higher its value, the more intensive the element transfer will be. Elements accumulate primarily in the root system of a plant and to a more limited extent in the leaves (Kalavrouziotis, *et al*., 2012). It seems that the roots and stems have a physiological mechanism that prevents the accumulation of some elements like Cd and Zn in the leaves and seeds of plants (Kalavrouziotis, *et al.*, 2012).

In a study by Adamo *et al.* (2014), TF of the studied elements decreased with increasing total soil concentrations, indicating that the proportion of elements taken up by the plants did not increase with increasing concentration in the soil. The degree of accumulation remained under the control of the plant's metabolism, regardless of higher total element concentration.

Plants are classified as either excluders or accumulators based on whether the TF values are respectively low or high (Gauthier, *et al*., 2017). Hyperaccumulators are defined as plants that accumulate a hundred times more of an element in their leaves than normal plants (Lund, *et al.*, 2005). For Cu, Cr, Ni, Co or Pb this concentration is more than 1000 ppm and for Zn and Mn it is more than 10 000 ppm in their leaf dry matter (Baker & Brooks, 1989). It should, however, be considered that highly enriched elements do not necessarily best reflect the relative abundance of that element in the soil (Hawkes, 1957).

The following chapter describes the study design, gathering of soil and plant samples, sample preparation and analyses that took place to determine the trace element content so that the relationship between element levels in plant tissue, soil and ore could be evaluated.

2.3.5 Elements identified for analysis

Cu and Ag are the principal focus of mining operations along the Ghanzi Ridge, but other base metals like Mo, Pb and Zn are also of economic importance. Mineralisation anomalies are often better expressed by pathfinder elements, not necessarily targeted for exploitation, but useful as indicators for the deposit. According to Maghsoudi, *et al*. (2016), the elements Ag, As, Au, Cu, Mo, Pb, Sb and Zn are among the best-known indicators of copper deposits and have been used to prospect for this type of deposit in various areas. Other elements that can be used as pathfinders include Ba, Bi, Cd, Co, Hg, Mn and rarely Ge, Se, U and V Ge (Causey, *et al.*, 2013; Chaffee, 1977).

If a deposit is enriched in more than one element, it is more effective to test for the most mobile element in the reconnaissance work and the least mobile elements in the detailed survey (Hawkes, 1957). According to Bonnett *et al*. (2016), the elements Cd, Co, Cu, Fe, Hg, Mn, Mo, Ni, Sb and Zn are more mobile, while Ag, As, Au, Bi, Cr, Pb and V are more immobile. Therefore, in the event where an ore body contains equal amounts of Pb and Zn, the residual soil may contain many times as much Pb as Zn, since Pb is relatively immobile and is retained, whereas Zn will be leached out (Hawkes, 1957; Lovering, 1934). Generally, Pb, Sn, As and Sb are immobile and held in the residual soil, while Zn ad Co is usually impoverished, and Cu and Mo is intermediate (Hawkes, 1957). The mobile elements may be transported in solution and reprecipitated locally, leading to a lateral and downhill spread of the dispersion pattern outward from the bedrock source. The higher mobility of Cu and Zn may therefore render these elements to be more valuable as trace elements in regional surveys to lead to zones of potential mineralisation. Elements like Pb can then be used to pinpoint the mineralisation due to its relatively less mobile character *(*Akcay*, et al*., 1998). However, in the case of the Ghanzi Ridge, it might be difficult to trace Pb in the surface soil and plant tissue due to the thick overburden and the fact that the soil is not residual, but rather transported (wind-blown) or of a pedogenic origin.

A description of the elements identified for analysis are given in the following section. Selective elements were identified based on preselected criteria, namely their association with Cu ore deposits, solubility in the soil, absorbability by plants and translocation from roots to leaves. The elements As, Cd, Co, Cu, Pb, Hg, Mo, Ni, Se, Ag and Zn are discussed:

2.3.5.1 Arsenic

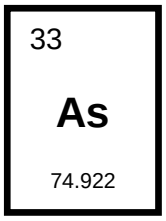

Arsenic is associated with deposits of several elements and metalloids and therefore is known as a good indicator in geochemical prospecting surveys (Kabata-Pendias, 2011). According to Chen *et al*. (2016), As is not ideal to be analysed for the detection of copper anomalies, but Dunn (2007) reported that As can be of great value as a pathfinder element for various types of deposits, including base metals, gold and platinum-group metals. According to Hawkes (1957), arsenic, will delineate mineralised areas more sharply than elements such as Co, since it has a lower mobility (Hawkes, 1957). Arsenic values below 1 ppm are subject to analytical interferences that make accurate measurement by ICP-MS difficult, but for higher As concentrations, reproducibility during ICP-MS analysis, can be remarkably good (Dunn, 2007).

According to Lazo *et al*. (2007), As enrichment in soil is mainly associated with Fe–S, Cu–S and Ni–S mineralisation (Causey, *et al.*, 2013; Chaffee, *et al*., 1995; Kabata-Pendias, 2011). Arsenic minerals and compounds are readily soluble, and arsenopyrite may be easily oxidized by both O_2 and Fe^{3+}. However, the mobility of As is largely restricted by the great stability of the Fe arsenates that form as secondary minerals (Hawkes, 1957). Strong sorption by Fe as well as Al hydroxides, clays, P and Ca compounds and soil organic matter (SOM) greatly limits the mobility of As in soil (Kabata-Pendias, 2011). According to Kabata-Pendias (2011) the most important parameter controlling the As sorption, is the Eh–pH regime of soil.

Due to the sorption effect of Fe and Al oxides, 80% of the total As in soil is strongly associated with these oxides. Only a limited fraction of As is then easily mobile and available to plants (Kabata-Pendias, 2011). General trends in As absorption in plants can be expressed by a plant/soil transfer factor of 0.01, which indicates a medium degree of accumulation in plants (Kabata-Pendias, 2011). Several reports on the linear relationship between As contents of vegetation and concentrations in soils of both total and soluble species suggest that plants take up As passively with the water flow (Kabata-Pendias, 2011). With increasing soil As, high As concentrations were recorded in both old leaves and roots, but at a low content of As, a higher accumulation in leaves than in roots was reported (Kabata-Pendias, 2011).

2.3.5.2 Cadmium

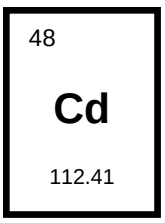

Cadmium is related to copper deposits (Chaffee, *et al.*, 1995). It is usually also associated with Zn, but because Cd is not an essential element it can be passively taken up by the roots, and elevated concentrations in plant tissue usually reflect zones of Zn enrichment better than Zn itself (Dunn, 2007; Dunn & Thompson, 2009). According to Dunn (2007), the precision determination of Cd by ICP-MS is accurate. Close to detection (0.01 ppm) precision is not that good, but it improves dramatically at concentrations of just 0.05 ppm.

During weathering, Cd forms simple compounds that are easily mobile and has a distribution pattern similar to that of Zn. Cd-Zn interactions in soil are common; both antagonistic and enhancing effects have been reported, but in most cases, Zn reduces the absorption of Cd (Kabata-Pendias, 2011). Cd-Cu interactions are also complex, but the inhibitory effect of Cu on Cd is most often reported. Cd-Mn/Ni interactions involves Cd replacing the other elements (Kabata-Pendias, 2011). Cu-Se mutual antagonistic effects have been reported

and Cd absorption by plants may also be inhibited by an excess of Ca (Kabata-Pendias, 2011).

According to Kabata-Pendias (2011), Eh-pH controls the Cd mobility in soils and an increase in pH results in increased adsorption of Cd by SOM. Cd is the most mobile in acidic soils (pH 4.5-5.5), but it is rather immobile in alkaline soil. Other important processes controlling the fixation of Cd, include adsorption by clays and the presence of large quantities carbonate in the soil solution. According to Isenbeck *et al.* (1987, cited by Kabata-Pendias, 2011), no other soil factors are so active in the immobilization of Cd as elevated carbonate concentrations in the soil. Although all the top soil of the Ghanzi Ridge is not carbonate rich, it is very common due to various calcrete layers in the overburden.

According to Taylor and Percival (2001, cited by Kabata-Pendias, 2011), 55-90% of Cd in soil solution is present as free Cd^{2+} and is readily available to plants. Although Cd is a non-essential element, it is still effectively absorbed by both root and leaf systems. Various parameters of rhizospheres might significantly alter Cd availability due to root exudates. Interactions with Zn and SOM may also lower Cd bio-availability. However, it is often reported that a linear relationship exists between Cd in plant tissue and its concentration in growth media (Kabata-Pendias, 2011). A great proportion of the Cd is accumulated in the roots, but it can be rapidly translocated from roots to shoots and leaves in the form of metallo-organic complexes (Kabata-Pendias, 2011).

2.3.5.3 Cobalt

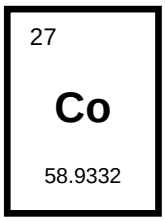

Cobalt is associated with copper ore and can be used as pathfinder element for Cu deposits (Causey, *et al.*, 2013; Chaffee, *et al*., 1995). Despite greater Cu concentrations and availability in the soil, Co may exceed Cu levels in the plant, presumably due to the need of plants to more closely regulate the absorption of an essential element, like Cu, as opposed to a non-essential element, like Co (Morrison, 1980). It may therefore prove to be more useful as pathfinder element for Cu deposits than Cu itself. Occasionally, there is also a spatial relationship between Co and Au deposits, with a zone of Co enrichment peripheral to the central zone of Au anomalies. Precision detection of Co by ICP-MS analysis is usually good (Dunn, 2007).

Co becomes relatively mobile under surficial conditions, with a mobility similar to that of Zn (Hawkes, 1957). Co behaviour in soil seems to be strongly influenced mainly by the Mn-oxide phase formation, since the adsorption capacity of Co by Mn-oxides is very high

(Kabata-Pendias, 2011). Also, quantities of Co are always higher in the B horizons of soil, where Fe is concentrated (Kabata-Pendias, 2011). Adsorbed or precipitated Co may be solubilized by both a reduction of soil Eh and a decrease in soil pH.

Co in nutrient or soil solution is easily available to plants, and enrichment of soil with Co increases its levels in plants (Kabata-Pendias, 2011). Co content in plants are highly controlled by both soil factors and the ability of plants to absorb this element (Kabata-Pendias, 2011). General trends in Co absorption in plants can be expressed by a plant/soil transfer factor of 0.1 (Kabata-Pendias, 2011), therefore exhibiting a medium degree of accumulation in plants. Co appears to be strongly bound in root cells, but when Co is taken up in excess by roots, it principally follows the transpiration stream, resulting in an enrichment of Co at the leaf margins and tips (Kabata-Pendias, 2011). Foliar concentrations of stable cobalt increase uniformly until senescence (Dunn, 2007). Where the absorption of other elements in the soil are concerned, it has been reported that antagonistic interactions exist between Co and Ni, Cu, Zn, Ca, and Fe (Kabata-Pendias, 2011). For instance, elevated levels of Co induce Fe deficiency in plants and suppress absorption of Cd by roots. In contrast, Co interacts synergistically with Zn, Cr, and Sn. The most significant relationship observed, were between Co and Mn or Fe in plants. Geochemical as well as biochemical antagonisms between these elements have arisen from their affinity to occupy the same sites in crystalline structures and from the similarity of their metallo-organic compounds.

2.3.5.4 Copper

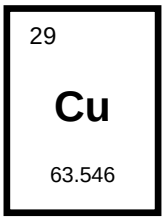

Copper is often associated with sphalerite (ZnS), pyrite (FeS_2) and galena (PbS). The ores are commonly found in acid igneous rocks and various sedimentary deposits (Kabata-Pendias, 2011). Chen *et al.* (2016) considers Cu a well-fit element to be analysed for the detection of copper anomalies. Cu concentrations are usually well above the detection limit of 0.01 ppm by ICP-MS, with excellent precision (Dunn, 2007).

Cu is a rather immobile element in soil and shows relatively minor variation in total content. A common characteristic of Cu distribution in soil profiles is its tendency to accumulate in the top horizons or upper few centimetres of soils. This phenomenon is caused by numerous factors, but above all, Cu concentration in surface soils reflects its bioaccumulation. However, due to its tendency to be adsorbed by SOM, carbonates, clay minerals, and oxyhydroxides of Mn and Fe, it may be also accumulated in deeper soil layers (Kabata-Pendias, 2011). Other variables affecting Cu mobility include pH and Cu soil content

(Pnizovsky, *et al*., 2006, cited by Kabata-Pendias, 2011). Overall solubility of both cationic and anionic forms of Cu decreases at a soil pH of about 7-8. In the presence of calcareous soils, precipitation of $CuCO_3$ strongly affects the Cu activity in soil solution (Kabata-Pendias, 2011).

Cu seems to be quite mobile in soil solution and readily taken up by plants. It exhibits a medium degree of accumulation in plants and general trends in Cu absorption in plants can be expressed by a plant/soil transfer factor of 0.1 (Kabata-Pendias, 2011). The concentration of Cu in plant tissues seems to be a function of its level in the nutrient solution or in soils (Kabata-Pendias, 2011). Cu concentrations in plants is generally in the range of 5-25 ppm and concentrations above 100 ppm are rare even when the soil Cu concentrations are high (Reeves & Baker, 2000, cited by Ghaderian & Ravandi, 2012). Cu mobility within plant tissue strongly depends on the level of Cu supply, being the highest with high Cu levels in the soil (Kabata-Pendias, 2011). However, Cu has low mobility relative to other elements in plants and most of the Cu appears to remain in root and leaf tissues until they senesce; only minor amounts may move to young organs (Kabata-Pendias, 2011).

In terms of the relationship between Cu absorption and absorption of other elements in the soil, Cu–Zn interactions are commonly observed. Each element may competitively inhibit root absorption of the other (Kabata-Pendias, 2011). Cu–Fe antagonism is also indicated, so that high levels of Cu in a plant decrease the Fe content and Fe, in turn, reduces Cu absorption from soil solutions (Kabata-Pendias, 2011). Cu–Mo antagonistic interactions, where Cu aggravates the Mo deficiency in plants, also take place (Kabata-Pendias, 2011). Cu–Cd interactions are both antagonistic and synergistic in element absorption by roots (Kabata-Pendias, 2011). Cu–Se interactions are observed mainly as inhibited Cu absorption with increased Se level (Kabata-Pendias, 2011). Cu–Mn interactions are reported to be both synergistic and antagonistic in the absorption processes under defined conditions and at high concentrations of both elements. Cu–Ni synergism is observed in similar conditions as Cu–Mn relationships (Kabata-Pendias, 2011). Antagonistic reactions between Cu and Cr may also occur within plant tissues, as well as in external root media (Kabata-Pendias, 2011).

2.3.5.5 Lead

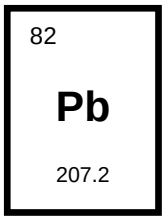

Lead has highly chalcophilic properties and its primary form in the natural state is therefore galena (PbS) (Kabata-Pendias, 2011). The Pb content of plants grown in mineralised areas is, in general, highly correlated with the Pb

concentration in soil, although this relationship varies among different plant tissues. Nevertheless, Pb is described as a very useful element for geochemical prospecting (Kabata-Pendias, 2011). Chen *et al*. (2016) also considers Pb a well-fit element to be analysed for the detection of copper anomalies. Precision for Pb is very good at levels greater than 1 ppm. False anomalies are very rare and confidence can be taken that the values are the true composition of the samples (Dunn, 2007).

During weathering, Pb sulphides slowly oxidize and have an ability to form carbonates and to be fixed by clay minerals, hydroxides, and SOM. According to Hawkes (1957), the immobility of Pb may be attributed to the relatively stable galena as compared to other sulphides (Hawkes, 1957). The Pb distribution within soil profiles is not uniform and reveals a great association with hydroxides, especially of Fe and Mn (Kabata-Pendias, 2011). High soil pH may precipitate Pb as hydroxides, phosphates, or carbonates, as well as promote the formation of Pb-organic complexes that are rather stable. Pb also tend to accumulate near the soil surface, mainly due to its adsorption by SOM (Kabata-Pendias, 2011).

Pb is very strongly bound in almost all types of soil, causing its phytoextraction to be rather limited (Kabata-Pendias, 2011). It is not known how much soil-Pb might be available to plants, but when Pb is present in soluble forms, plant roots can absorb great amounts (Kabata-Pendias, 2011). The rate of absorption increases with increasing Pb concentration in the soil solutions and with time. There is much evidence that Pb is taken up from soils by roots, at both low and high Pb concentrations, and that this process is strongly governed by soil and plant factors (Kabata-Pendias, 2011). General trends in Pb absorption in plants can be expressed by a plant/soil transfer factor of 0.1 (Kabata-Pendias, 2011). Pb therefore exhibits a medium degree of accumulation in plants. The mode of its absorption is passive, and the rate of absorption is reduced by the presence of $CaCO_3$ and by low temperature. When Pb is absorbed by plants, its translocation to above-ground parts is very poor and a large proportion of Pb remains concentrated in root tissues (Kabata-Pendias, 2011). According to Ghaderian and Ravandi (2012), Pb is not essential or beneficial to plants and is usually present at 1-10 ppm in plant tissue. The strong Pb adsorption in soils may mean that Pb additions to soil are permanent and irreversible (Kabata-Pendias, 2011). However, the Pb content of roots is correlated to the Pb content of soil, which indicates its absorption by plants (Kabata-Pendias, 2011). Certain soil and plant factors, such as SOM, are known to promote both Pb absorption by roots and Pb translocation to plant tops (Kabata-Pendias, 2011).

Airborne Pb, a major source of Pb pollution, is also readily absorbed by plants through foliage. However, the KCB is generally located far from sources of industrial pollution, so that its absorbance by plant foliage is extremely unlikely. The interference of Pb with trace element uptake by plant roots has been reported only for Zn and Cd; Pb has a stimulating effect on Cd absorption. The Zn–Pb antagonism adversely affects the translocation of each element from roots to tops.

2.3.5.6 Mercury

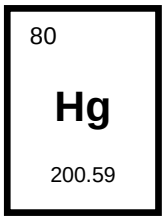

Mercury is a common element in hydrothermal deposits. It is associated with Cu deposits (Causey, *et al*., 2013; Chaffee, *et al.*, 1995) and as a chalcophile element, it shows affinity to other elements, such as Ag, Cd, and Zn (Kabata-Pendias, 2011). Trends in Hg levels may be linked to bedrock structure such as faults, fractures or breccias, acting as conduits through which Hg emanations can migrate. According to Dunn (2007), Hg acts as a pathfinder element for Au and other elements. Foliage tends to have higher concentrations of Hg than twigs (Dunn, 2007). There is usually a very high correlation between Hg in twigs and Hg in foliage, but the expression of anomalies for Hg in twigs is subdued because levels are close to the limit of detection. Consideration should be given to the possibility that Hg concentrations may be derived from airborne particles near mining areas and that this might lead to false anomalies (Dunn, 2007). However, it has been suggested that ore-bodies at depths of 200-2000 m can generate Hg haloes that can be reflected in plants (Dunn, 2007). In dry plant tissue Hg is rarely present at concentrations lower than 1-2 ppb as reported with ICP-MS (Dunn, 2007). Concentrations are usually ≥ 10 ppb and when above 10 ppb, the analytical precision becomes excellent; Hg data shows very good reproducibility (Dunn, 2007).

Hg accumulation is related to organic C and S levels in soils and is concentrated in surface soils at several times the concentration in subsoils (Kabata-Pendias, 2011). Its concentrations in soil solution are very low and are controlled mainly by precipitation and the formation of organic complexes (Kabata-Pendias, 2011). Hg mobility therefore requires dissolution processes, and biological and chemical degradation of organomercury compounds (Kabata-Pendias, 2011). In contrast to other trace elements, the amount of mobilised Hg decreases at pH < 3 and at pH > 12, due to the extremely high buffering capacity of SOM, in both acidic and alkaline states (Kabata-Pendias, 2011).

Mercury is easily absorbed by root systems and is also relatively easily translocated within plants (Kabata-Pendias, 2011). In general, Hg content in plants are high when the Hg

content of soils are also high, but this relationship does not always hold (Kabata-Pendias, 2011). General trends in Hg absorption in plants can be expressed by a plant/soil transfer factor of 0.1 (Kabata-Pendias, 2011), thereby exhibiting a medium degree of Hg accumulation in plants. Plants are also known to directly absorb Hg vapour. Hence, soil Hg is not only directly absorbed by plants, but also indirectly absorbed from Hg vapour that is gradually released in soils. Methylated Hg (Me–Hg) is readily mobile and easily absorbed by some higher plants. There might be some Hg losses by volatilization from soils, which will increase with higher soil temperature and with higher soil alkalinity (Kabata-Pendias, 2011). Studies also showed that plants took up several times more Hg from calcareous soil than from acidic soil (Kabata-Pendias, 2011).

2.3.5.7 Molybdenum

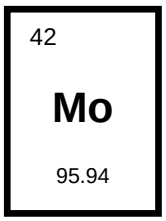

Molybdenum is associated with Cu deposits (Chaffee, *et al.*, 1995). It is a significant pathfinder for Cu-Mo, Cu-Au-Mo and other Mo-bearing deposits. Cu-Mo porphyries are usually better defined from the Mo content of the vegetation than by the Cu content (Dunn, 2007). According to Dunn (2007), reproducibility of Mo analyses is excellent at the levels typically found in vegetation. Mo is also one of the few elements for which studies claim to be successful in quantifying the depth through overburden to ore. Kovalevsky (1987, cited by Dunn, 2007), investigated the exploration characteristics with respect to Mo of 506 species. He stated that very few plant tissues establish significant barriers to Mo absorption, and most parts of most species will therefore be suitable for biogeochemical surveys. In terms of quantifying depth through overburden to ore, he reported that it was possible to predict the depth to mineralisation, estimated from sampling different tissues in a non-barrier plant. He defined this concept as ‘biogeochemical logging’. Dunn (2007) declared this quantification of ore body depth an exciting concept, but it apparently has not been tested outside of Siberia.

Easily mobile Mo anions are readily co-precipitated by SOM, $CaCO_3$, and by several cations like Cu^{2+}, Pb^{2+}, Zn^{2+}, Mn^{2+}, and Ca^{2+}. Differential adsorption of Mo by Fe, Al, and Mn hydrous oxides contributes to the retention of Mo in surface soils (Kabata-Pendias, 2011). In contrast to other micronutrients Mo is least soluble in acidic soils and readily mobilised in alkaline soils (Kabata-Pendias, 2011).

The bio-availability of Mo is highly governed by soil pH and drainage conditions. Mo from wet alkaline soils is most easily absorbed. In acidic soils (pH < 5.5), low in Mo, and especially in soils with a high Fe-oxide level, Mo is hardly available to plants (Hawkes, 1957; Kabata-

Pendias, 2011). General trends in Mo absorption in plants can be expressed by a plant/soil transfer factor of 0.1 (Kabata-Pendias, 2011). Mo exhibits a medium degree of accumulation in plants and is one of the most mobile elements in plants (Kabata-Pendias, 2011). Its relative enrichment in different plant tissues vary by species, but it is easily transported from the roots to above-ground parts (Kabata-Pendias, 2011).

In terms of its interaction with other elements in the soil, Mo and Cu exhibits antagonism in plants. Soil factors that increase the availability of Mo to plants usually have inhibitory effects on the Cu absorption by plants (Kabata-Pendias, 2011). The Mo–S relations may have antagonistic or stimulating effects on Mo absorption by plants. Mo–Mn antagonism resulting from soil acidity influences the availability of these elements. Mo–Fe interactions are demonstrated as low Mo availability in Fe-rich soils, whereas increased Mo levels may induce Fe deficiency. A Mo–P interaction is often demonstrated as an enhancing effect of P on Mo availability in acid soils. The Mo concentrations in plants closely reflect the mobile Mo pool, for Mo seems to be very readily absorbed by plants when present in soluble forms (Kabata-Pendias, 2011).

2.3.5.8 Nickel

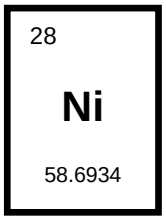

The great affinity of Ni for S accounts for its frequent association with segregates of sulphur-rich ore deposits (Chaffee, *et al.*, 1995; Kabata-Pendias, 2011). It often forms sulphides and sulph-arsenides together with Fe and Co, and is associated with several Fe minerals. The analytical precision for Ni by ICP-MS is very good and levels in plants are often more than the detection limit of 0.1 ppm (Dunn, 2007).

Ni is easily mobilised during weathering, and unlike Mn^{2+} and Fe^{2+}, Ni^{2+} is relatively stable in aqueous solutions and is capable of migration within soil profiles (Kabata-Pendias, 2011). Several soil properties, particularly clay fraction, SOM, and pH control Ni behaviour and plant-availability (Kabata-Pendias, 2011). Mn-oxides in soil accumulate Ni. However, less than 15 to 30% of the total Ni is extracted with the Mn-oxides and the fraction of soil Ni carried in the oxides of Fe and Mn seems to be readily available to plants (Kabata-Pendias, 2011). The secretion of organic anions, and modification of soil pH by roots and fungi in the rhizosphere may decrease Ni adsorption to soil particles, and thus increase its plant-availability.

Ni is easily extracted from soil by plants and its content in plant tissues are simple functions of Ni forms in the soil (Kabata-Pendias, 2011). Ni exhibits a slight degree of accumulation in plants and is moderately mobile when transported from the roots to above-ground parts. Ni is likely to be accumulated in both leaves and seeds. However, in most plants Ni is accumulated mainly in roots. General trends in Ni absorption in plants can be expressed by a plant/soil transfer factor of 0.01 (Kabata-Pendias, 2011).

Studies of inter-elemental relationships, involving Ni in leaves, displayed few significant associations. According to Lee (1977, cited by Freitas & Prasad, 2003) this is attributed to the probability that the absorption mechanism for Ni is different than the mechanism for other elements.

2.3.5.9 Selenium

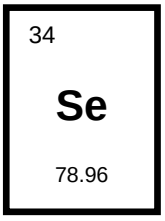

The association of Se with host minerals, such as pyrite, chalcopyrite, and sphalerite, is relatively common and it is therefore associated with Cu deposits (Chaffee, *et al.*, 1995). The easy methylation of Se, mainly due to biological processes, yields the formation of volatile Se forms and has a significant role in the biogeochemical cycling of this element (Kabata-Pendias, 2011). Some laboratories declare that low levels of Se cannot be accurately measured by ICP-MS (Dunn, 2007). Geochemically Se follows S and relatively high concentrations in plants can be a good indication of sulphide-bearing minerals. S/Se ratios can be used to assist in focusing in on drill targets. However, it should be considered that the precision of the data for Se as well as S is not 100% accurate (Dunn, 2007).

The behaviour of Se in highly calcareous soil is of special concern since Se becomes easily water-soluble in soils that are low in sesqui-oxides (Kabata-Pendias, 2011). Mobile and easily plant-available Se occurs in well-aerated, alkaline soils of arid and semi-arid regions. SOM has a strong tendency to form organometallic complexes, thereby removing Se from soil solution (Kabata-Pendias, 2011).

Phyto-availability of Se in soil varies significantly, depending on soil parameters. During chemical weathering of rocks, Se is easily oxidized and its oxidation state, as well as its solubility, is controlled by the pH–Eh soil system (Kabata-Pendias, 2011). High Se mobility can be expected in soils of high pH and Eh. Controversially, low mobility occurs in soils with high contents of hydroxides, clay granulometric fractions, and SOM (Kabata-Pendias, 2011). Selenates occur in soluble forms in the soil of arid and semiarid regions. The Se solubility of

most soils is rather low. Phosphates and sulphates reduce the Se adsorption, especially on Fe-oxides, and are effective in releasing and mobilising up to 90% of the soil-adsorbed selenites and selenates (Kabata-Pendias, 2011).

Se is rarely accumulated by plants. However, some plants have the ability to accumulate Se and they may concentrate Se to extremely high levels (Kabata-Pendias, 2011). When absorbed, it is easily transported from the roots to above-ground parts of the plant. General trends in Se absorption in plants can be expressed by a plant/soil transfer factor of 0.001 (Kabata-Pendias, 2011). The absorption of Se by plants depend on several factors, in particular pH, but when Se is present in soluble forms, it is readily absorbed by plants. The amount of water-soluble Se (the fraction of soil Se considered available to plants) varies considerably and does not correlate with the total soil Se (Kabata-Pendias, 2011). The total Se level is, therefore, a poor predictor of the phyto-availability of the element, but Kabata-Pendias (2011) reported that in most cases, there is a positive linear correlation between Se in plant tissues and Se content in soil. Some research indicates that the total soil Se gives a better measure of plant response than do its soluble fractions (Kabata-Pendias, 2011).

An antagonistic interaction of Se–Hg was reported for several plants. High Se concentrations inhibit the absorption of elements, mainly Mn, Zn, Cu, and Cd (Kabata-Pendias, 2011). These relationships depend on the ratio between the elements, and therefore stimulating effects of high Se levels on absorption of some trace elements may sometimes be expected (Kabata-Pendias, 2011).

2.3.5.10 Silver

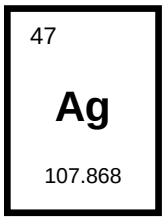

Silver is often associated with Cu and Zn ores (Causey, *et al.*, 2013; Chaffee, *et al.*, 1995). Ag occur mainly as sulphides in soil, that are associated with Fe and Pb. MnO_2 also has a strong affinity for Ag, and appears to be the most significant sorbant of this element (Kabata-Pendias, 2011). Values of Ag in dry plant tissue by ICP-MS are common in the low tens of ppb, at which level precision is very good, and at higher concentrations, the precision is excellent (Dunn, 2007). Chen *et al*. (2016) considers Ag a well-fit element to be analysed for the detection of copper anomalies.

Ag behaviour in soil is controlled mainly by pH–Eh conditions and SOM and despite several mobile complexes, Ag is apparently immobile in soils with pH above 4 (Kabata-Pendias, 2011). The amount of Ag absorbed by plants seems to be related to soil content (Kabata-

Pendias, 2011). Therefore, Ag can be accumulated in plants growing in Ag-mineralised areas. General trends in Ag absorption in plants can be expressed by a plant/soil transfer factor of 0.1 (Kabata-Pendias, 2011). Ag seems to be slightly soluble in soil solution and not easily taken up by plants. It generally exhibits a medium degree of accumulation in plants, but is easily transported from the roots to the above-ground parts (Kabata-Pendias, 2011).

2.3.5.11 Zinc

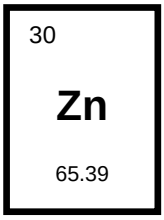

Zinc occurs in most base-metal ores and some precious-metal deposits (Hawkes, 1957). Zn is very mobile during weathering processes and its easily soluble compounds are readily precipitated by reactions with carbonates. It can also be absorbed by minerals and organic compounds, especially in the presence of sulfur anions (Kabata-Pendias, 2011). Elevated concentrations of the element are often observed in calcareous and organic soils.

Key factors controlling the mobility of Zn in soils are very similar to those listed for Cu, but Zn appears to occur in more readily soluble forms. Zn is soluble as a chloride or sulphate and may be transported to the surface by groundwater (Rankama & Sahuma, 1950, cited by Freedman, 1972). Zn is only immobilised when it is well beyond the acidic environment of oxidizing sulphides and reaches fine particles in the soil (Hawkes, 1957).

Although Zn is very mobile in most soils, clay fractions and SOM can bind Zn quite strongly, especially in neutral and alkaline pH regimes (Kabata-Pendias, 2011). However, dissolved organic matter (DOM) is a key factor affecting Zn mobility in soils with alkaline pH range of 7–7.5. Oxides and hydroxides of Al, Fe, and Mn appear to be of importance in binding Zn in some soils. The Zn fractions associated with the Fe and Mn-oxides are likely to be the most available to plants (Kabata-Pendias, 2011).

Soluble forms of Zn are readily available to plants, and the absorption of Zn has been reported to be linear with element concentrations in the nutrient solution and in soils. The composition of the nutrient solution, particularly the presence of Ca, is significant (Kabata-Pendias, 2011). Some authors regard Zn in plants as highly mobile, whereas others consider Zn to have intermediate mobility (Collins, 1981; Whitehead, 2000). Zn is likely to be concentrated in mature leaves (Kabata-Pendias, 2011). Plants usually reflect changes in the Zn content of growth media and therefore are good indicators in biogeochemical investigations (Kabata-Pendias, 2011).

Zn is an essential element for plant metabolism and can be expected to commonly reach quite high levels in plant tissue (Dunn & Thompson, 2009). It is usually found in concentrations of 20-200 ppm in plants. Zn is readily precipitated as insoluble sulphate in the rhizosphere, thereby minimizing absorption and transport to the leaves, so that hyperaccumulation of Zn is exceedingly rare (Ghaderian & Ravandi, 2012).

There are reports of both antagonism and synergism regarding Zn-Cd interaction in the absorption–transport processes. Zn–Cu antagonistic interactions were observed, in which the absorption of one element was competitively inhibited by the other (Kabata-Pendias, 2011). Zn–Fe antagonism is widely known. An excess of Zn leads to a marked reduction in Fe concentration in plants (Kabata-Pendias, 2011). Zn–As interaction was reported as possibly antagonistic. Similar interaction between Zn and Hg was also mentioned. Plants grown in Zn-contaminated soils accumulate a great proportion of the element in roots (Kabata-Pendias, 2011). General trends in Zn absorption in plants can be expressed by a plant/soil transfer factor of 0.1 (Kabata-Pendias, 2011).

Zinc is very mobile and easily bio-accumulated. It exhibits a medium degree of accumulation in plants and is moderately mobile in its translocation from the roots to above-ground parts of the plant (Kabata-Pendias, 2011). The variation of Zn in most plants is sensitive to factors unrelated to mineralisation, so that the response to different soil compositions may be largely masked. Toxic elements like U and Pb may more accurately reflect soil composition, even though the absolute quantities in plants are very small (Hawkes, 1957). However, Chen *et al.* (2016) considers Zn a well-fit element to be analysed for the detection of copper anomalies. Zn is present at levels well above its detection limit of 0.1 ppm and analytical precision is extremely good (Dunn, 2007). To delineate areas of Zn mineralisation it is necessary to look for quite substantial changes in Zn concentrations, since variability of Zn data may be related to the health of the tree rather than subtle changes in substrate chemistry (Dunn, 2007).

CHAPTER 3: MATERIALS AND METHODS

3.1 General methodology

The Ghanzi Ridge was targeted because it contains a relatively large mineral deposit that has been defined by drilling and geophysics but has very minor surface outcrops or surface mineralisation. Thick overburden of Kalahari sand and pedocretes, as well as clay layers, cover the bedrock. In some places, the overburden can exceed 120 metres. Taking the geology and objectives of the project into perspective, a surface soil and plant sampling program was compiled. Drilling and geophysical exploration have not disturbed the surface to an extent where it would have any effect on the surface assessments. Figure 3-1 shows the main sample localities and areas of interest on the Ghanzi Ridge.

Sampling took place along transects laid out along the dip of the ore body in locations with different ore grades and dip angles. Four suitable sampling localities were identified on the Ghanzi Ridge, namely Zone 5, Zone 5 North, Banana zone and Mahumo Deposit (Figure 3-1). A total of five transects were sampled. One transect was sampled at each of Zone 5, Banana Zone and Mahumo Deposit. Two transects were sampled at Zone 5 North. Soil samples were collected from both the A and B horizons and plant tissue samples were taken of 10 woody species (*Boscia albitrunca*, *Boscia foetida* subsp. *rehmanniana*, *Combretum apiculatum*, *Croton gratissimus*, *Grewia bicolor*, *Grewia flavescens*, *Gymnosporia buxifolia, Philenoptera nelsii*, *Terminalia prunioides* and *Terminalia sericea*).

3.2 Sample collection

3.2.1 Transect design

Sites for placing the transects were based on recommendations made by geologists from exploration companies. Sites were located where drilling has been done in the past and therefore borehole data of the underlying geology was available. For each transect, samples were collected at surface level above the ore body at 25-metre intervals. Background samples (beyond the sub-outcrop of the ore body) were spaced further apart (50 m). The length of transects were also advised by the local geologist (Deane, 2016). Sample positions were predetermined in ArcGIS (version 10.2), by plotting transects perpendicular to the north-easterly bedrock strike of the sampling areas. Sub-outcrops of the ore body formed the start of each transect and the transect extended in the direction of increasing depth of the

ore. After sampling the mineralised area, further sampling was continued beyond the sub-cropping ore body into the background (scientific control) area. Composite samples of the A and B soil horizons as well as tissue from the dominant plant species were collected at each transect. Layout of transects at each locality are illustrated (Table 3-1 to Table 3-5).

3.2.2 Soil sampling

Soil samples from the A and B horizons were collected separately, at a spacing of 25 m, along transects running across the mineralised zone to the geochemical background. A hand auger was used to gather the samples, which were then placed in ziploc bags. Soil from the first extraction of the auger was collected to represent the A horizon. The B horizon was collected from deeper within the soil profile and varied between sites, but it was generally about 40-60 cm deep. The B horizon was distinguished from the A horizon, based on textural and colour differences in the soil. The first extraction of soil from the auger following the appearance of the transition zone between soil horizons represented the B horizon.

3.2.3 Plant tissue sampling

Plants are widespread, and its tissue are easy and cheap to collect, with a lower environmental impact than more invasive sampling techniques (Intertek, n.d.). Dunn *et al*. (2006) suggested that the most frequently occurring species with deep root systems are selected for sampling. Foliage and bark often give the strongest geochemical signature (Dunn, *et al.*, 2006), and since leaf tissue is much easier to sample and gave the best result in previous investigations, it was used as sampling medium. Plant tissues exhibit seasonal variation and therefore field work was completed within the span of two weeks during June. At each point per transect, at least 20 g of leaf tissue were collected. Sampling took place evenly from the circumference of each tree or shrub since element concentrations may be distributed unevenly on different sides of a plant. Fresh samples were placed in paper bags to minimize the amount of sample sweating and decomposition.

Plant samples were collected across the mineralised zone and the adjacent background. Samples were collected at a spacing of 25 m to match the soil sampling strategy. Some species that were targeted for sampling did, however, not occur at every sampling point and were therefore collected only where present.

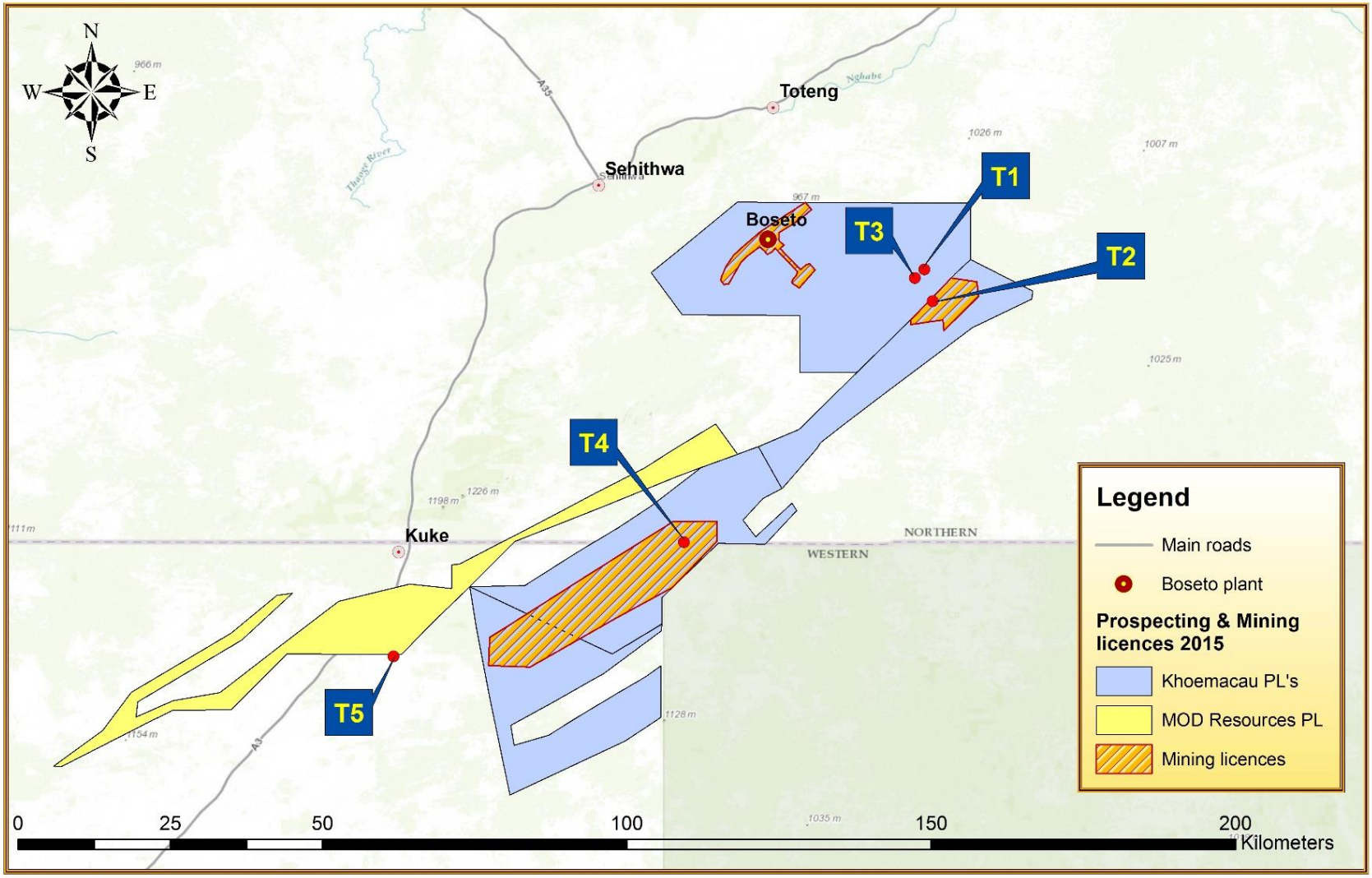

Figure 3-1: Location of sample transects: T1 and T3 at Zone 5 North, T2 at Zone 5, T4 at Banana Zone and T5 at Mahumo deposit.

Table 3-1: Schematics and details of the first transect with soil horizons and plant species sampled.

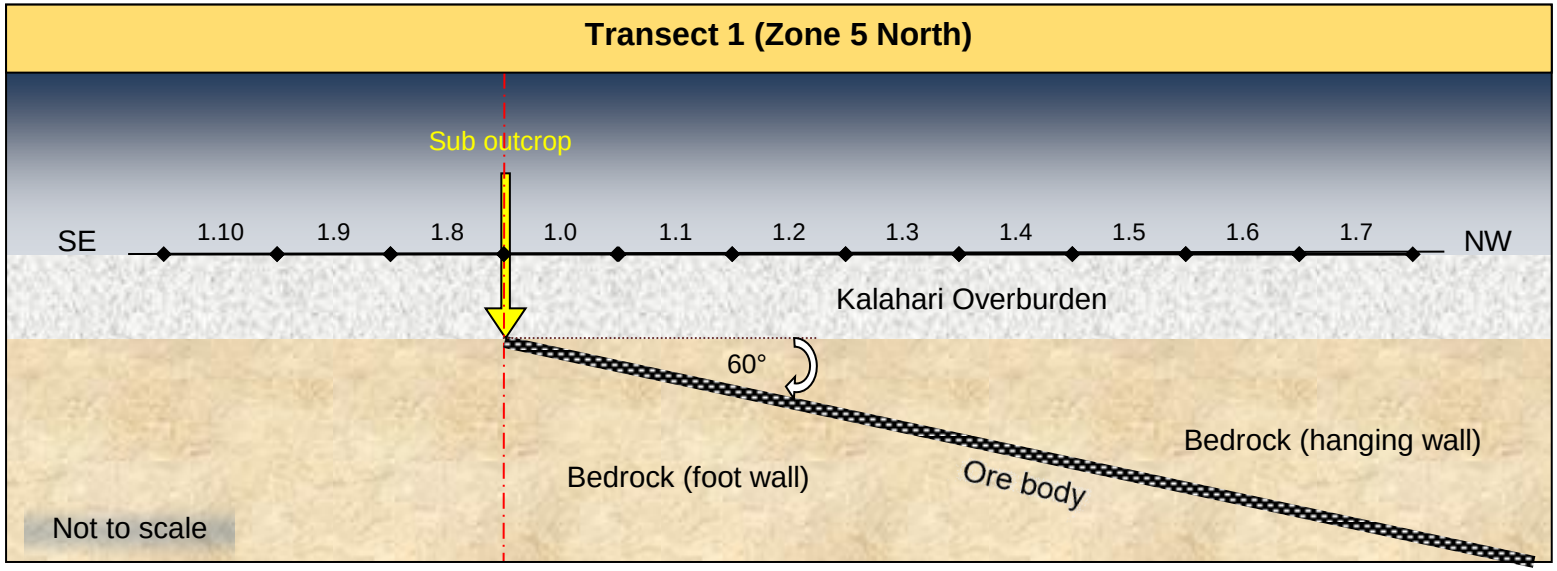

Transect info
Transect length: 1000 m \# soil samples: 58 \# vegetation samples: 114

Sub-outcrop info
Intersecting mineralisation at 90-100 m; 3.5% Cu over 7 m thickness; 30-35 m overburden above sub-outcrop; Ore body dip: 60° NW.

A horizon	B horizon	*Croton gratissimus*	*Boscia albitrunca*	*Grewia bicolor*	*Terminalia sericea*
1.0 A	1.0 B	1.0 Cg	1.0 Ba	1.0 Gb	1.0 Ts
1.1 A	1.1 B	1.1 Cg	1.1 Ba	1.1 Gb	1.1 Ts
1.2 A	1.2 B	1.2 Cg	1.2 Ba	1.2 Gb	1.2 Ts
1.3 A	1.3 B	1.3 Cg	1.3 Ba	1.3 Gb	1.3 Ts
1.4 A	1.4 B	1.4 Cg	1.4 Ba	1.4 Gb	1.4 Ts
1.5 A	1.5 B	1.5 Cg	1.5 Ba	1.5 Gb	1.5 Ts
1.6 A	1.6 B	1.6 Cg	1.6 Ba	1.6 Gb	-
1.7 A	1.7 B	1.7 Cg	1.7 Ba	1.7 Gb	-
1.8 A*	1.8 B*	1.8 Cg*	1.8 Ba*	1.8 Gb*	1.8 Ts*
1.9 A*	1.9 B*	1.9 Cg*	1.9 Ba*	1.9 Gb*	1.9 Ts*
1.10 A*	1.10 B*	1.10 Cg*	1.10 Ba*	1.10 Gb*	1.10 Ts*

* Background samples

Table 3-2: Schematics and details of the second transect with soil horizons and plant species sampled.

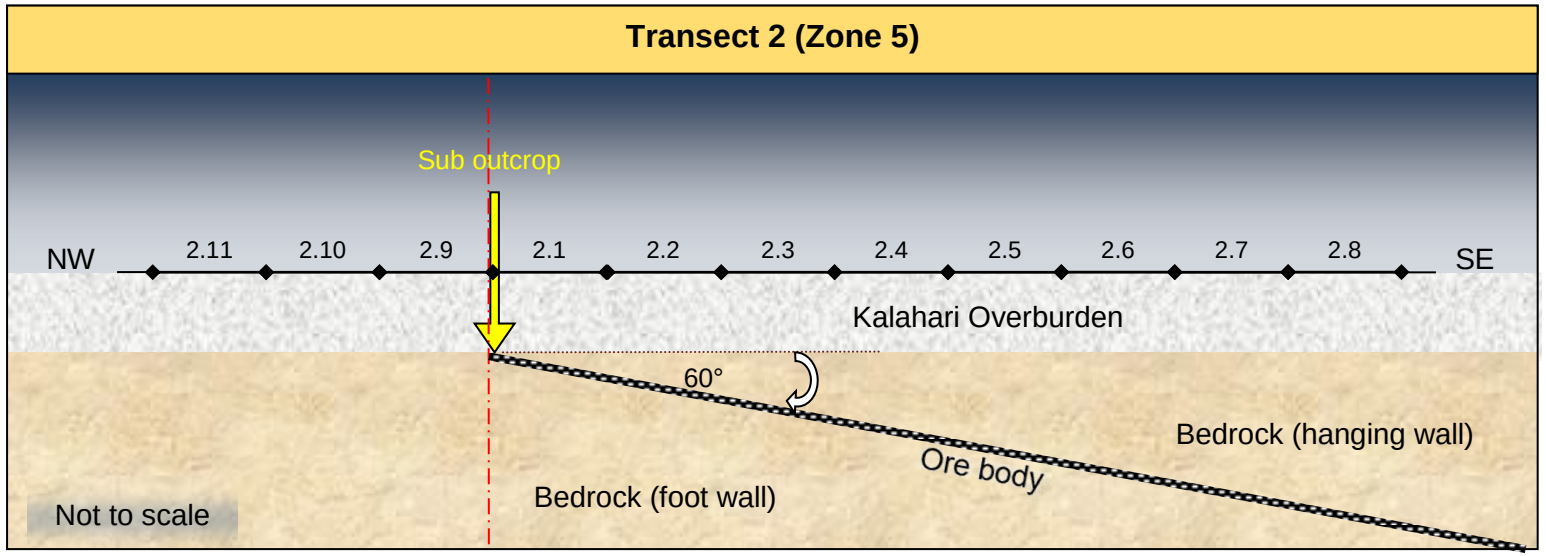

Transect info

Transect length: 890 m

soil samples: 70

vegetation samples: 58

Sub-outcrop info

Intersecting mineralisation at 75 m;

1.2% Cu over 9.4 m thickness;

40-45 m overburden above sub-outcrop;

Ore body dip: 60° SE.

A horizon	B horizon	*Boscia albitrunca*	*Grewia bicolor*	*Terminalia prunioides*
2.1 A	2.1 B	2.1 Ba	2.1 Gb	2.1 Tp
2.2 A	2.2 B	2.2 Ba	2.2 Gb	2.2 Tp
2.3 A	2.3 B	2.3 Ba	2.3 Gb	-
2.4 A	2.4 B	2.4 Ba	2.4 Gb	2.4 Tp
2.5 A	2.5 B	2.5 Ba	-	-
2.6 A	2.6 B	2.6 Ba	2.6 Gb	-
2.7 A	2.7 B	2.7 Ba	-	-
2.8 A	2.8 B	2.8 Ba	2.8 Gb	-
2.9 A*	2.9 B*	2.9 Ba*	2.9 Gb*	2.9 Tp*
2.10 A*	2.10 B*	2.10 Ba*	2.10 Gb*	2.10 Tp*
2.11 A*	2.11 B*	2.11 Ba*	2.11 Gb*	2.11 Tp*

* Background samples

Table 3-3: Schematics and details of the third transect with soil horizons and plant species sampled.

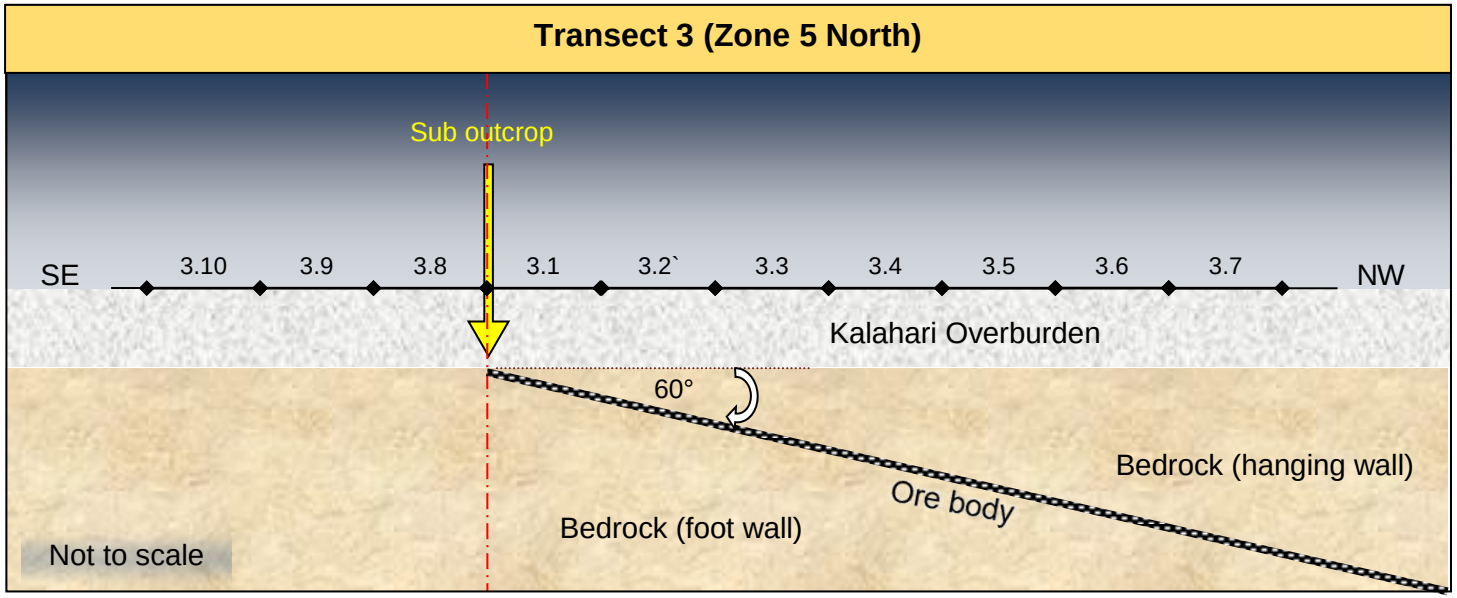

Transect info

Transect length: 1000 m

soil samples: 66

vegetation samples: 63

Sub-outcrop info

Intersecting mineralisation at 70 m;

1.3% Cu over 16 m thickness;

30-35 m overburden above sub-outcrop;

Ore body dip: 60° NW.

A horizon	B horizon	*Croton gratissimus*	*Boscia albitrunca*	*Grewia bicolor*
3.1 A	3.1 B	3.1 Cg	-	3.1 Gb
3.2 A	3.2 B	3.2 Cg	3.2 Ba	3.2 Gb
3.3 A	3.3 B	3.3 Cg	-	3.3 Gb
3.4 A	3.4 B	3.4 Cg	3.4 Ba	3.4 Gb
3.5 A	3.5 B	-	3.5 Ba	3.5 Gb
3.6 A	3.6 B	-	3.6 Ba	-
3.7 A	3.7 B	-	3.7 Ba	-
3.8 A*	3.8 B*	3.8 Cg*	-	3.8 Gb*
3.9 A*	3.9 B*	3.9 Cg*	3.9 Ba*	3.9 Gb*
3.10 A*	3.10 B*	3.10 Cg*	3.10 Ba*	-

* Background samples

Table 3-4: Schematics and details of the fourth transect with soil horizons and plant species sampled.

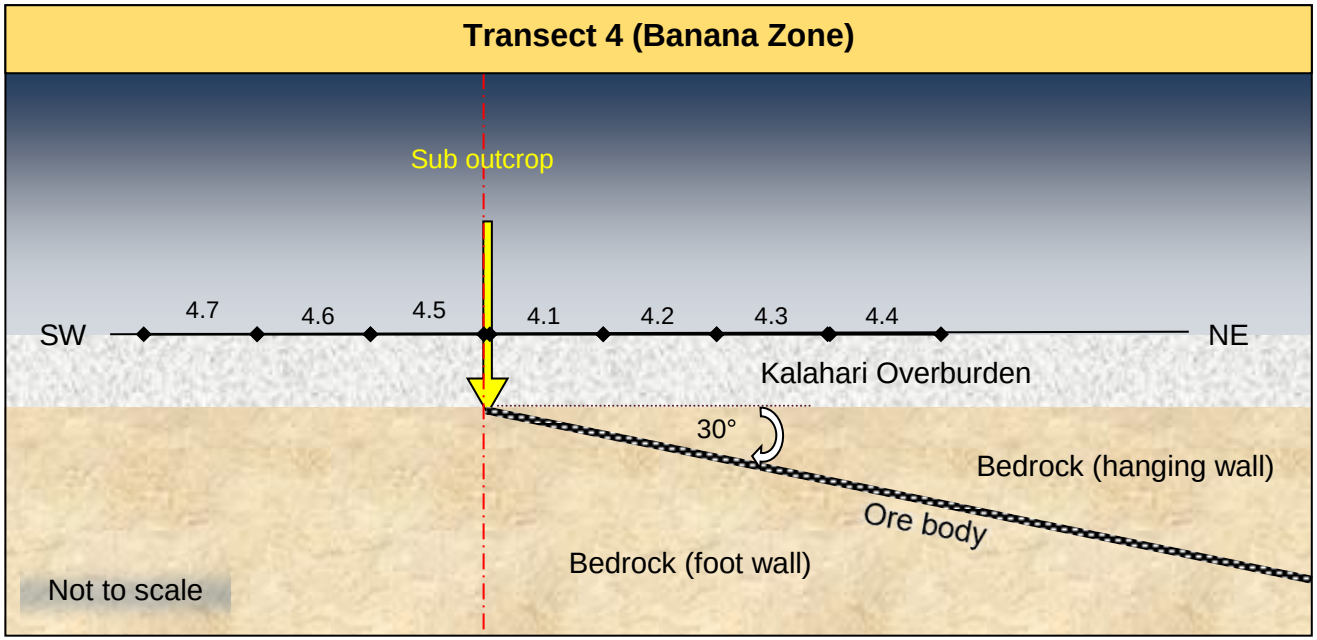

Transect info
Transect length: 1050 m \# soil samples: 40 \# vegetation samples: 54

Sub-outcrop info
Intersecting mineralisation at 37 m; 2% Cu over 6.5 m thickness; 30 m overburden above sub-outcrop; Ore body dip: 30° NE.

A horizon	B horizon	*Croton gratissimus*	*Boscia albitrunca*	*Grewia bicolor*
4.1 A	4.1 B	4.1 Cg	4.1 Ba	4.1 Gb
4.2 A	4.2 B	4.2 Cg	4.2 Ba	4.2 Gb
4.3 A	4.3 B	4.3 Cg	4.3 Ba	4.3 Gb
4.4 A	4.4 B	4.4 Cg	-	4.4 Gb
4.5 A*	4.5 B*	4.5 Cg*	4.5 Ba*	-
4.6 A*	4.6 B*	4.6 Cg*	-	4.6 Gb*
4.7 A*	4.7 B*	4.7 Cg*	4.7 Ba*	4.7 Gb*

* Background samples

Table 3-5: Schematics and details of the fifth transect with soil horizons and plant species sampled.

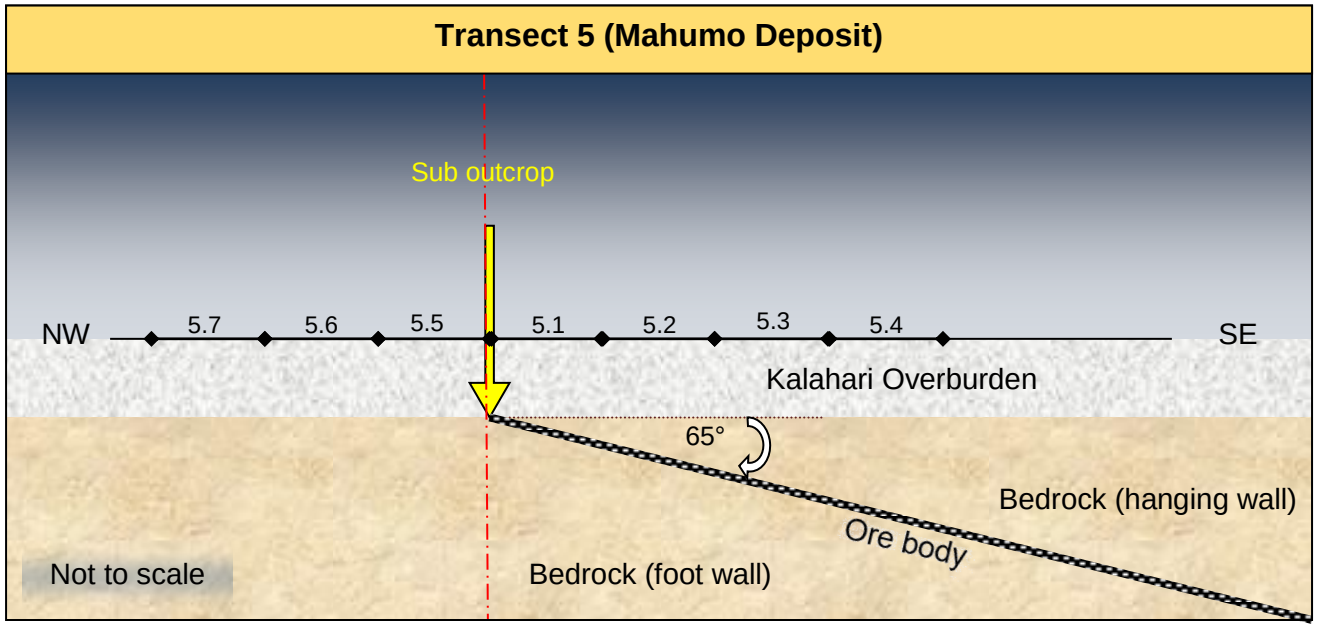

Transect info

Transect length: 350 m

soil samples: 22

vegetation samples: 34

Sub-outcrop info

Intersecting mineralisation at 29 m;

1.8% Cu over 1.2 m thickness;

Ore body dip: 65° SE.

A horizon	B horizon	*Croton gratissimus*	*Boscia albitrunca*	*Grewia bicolor*
5.1 A	5.1 B	5.1 Cg	5.1 Ba	5.1 Gb
5.2 A	5.2 B	5.2 Cg	5.2 Ba	5.2 Gb
5.3 A	5.3 B	-	5.3 Ba	5.3 Gb
5.4 A	5.4 B	5.4 Cg	5.4 Ba	5.4 Gb
5.5 A*	5.5 B*	-	-	5.5 Gb*
5.6 A*	-	5.6 Cg*	5.6 Ba*	5.6 Gb*
5.7 A*	-	5.7 Cg*	-	5.7 Gb*

* Background samples

3.3 Sample preparation

Sample preparation of plant tissue took place concurrent to field work. At the end of each sampling day, the leaves were removed from the brown paper bags and separated from the twigs and fruit. Samples were gently rinsed with distilled water and then placed in bags fashioned out of shade cloth. The leaves were rinsed before drying since airborne dust must be considered as a possible source of contamination to plant samples. The bags with the leaves were then suspended on a strung rope in a location sheltered from dust. It was left for a few days to air-dry and packaged into new paper bags with the same sample name. Dried leaf samples were milled to a powder in a coffee grinder. Utmost care was taken during procedures to prevent any cross contamination, by properly rinsing the coffee grinder before milling each sample.

After fieldwork was completed, soil samples were air-dried to remove soil moisture. Each soil sample was slightly ground by using a mortar and pestle to break down the aggregates, after which it was screened with a 2-mm sieve to remove the gravel fraction and any organic material. The samples were then ground in a carbide ring mill into a fine powder (< 75 micron).

The samples (plant tissue and soils) from four consecutive sampling points were mixed to make-up composites - composite samples minimize spikes in data due caused by localized variations in element concentrations. Samples of individuals of the same species or of the same soil horizon were mixed. The composites included samples from four points that were 25 m apart, and each composite therefore represents a 100-m section of the transect. For background samples, less samples were mixed together since less samples were taken there. The background samples were grouped together in a way that ensured at least three repetitions for each transect. Each composite sample was homogenised before sub-samples were analysed by ICP-MS to determine the trace element content.

3.4 Analytical methods

3.4.1 pH

The soil pH for both the A and B horizons were determined. Using the < 2 mm fraction of the soil of each composite sample, 20 g was weighed, and 50 ml of distilled water was added. Each mixture was stirred and left to settle for 50 min, after which it was again stirred and left

for 10 min. A calibrated handheld pH meter was then used to determine the pH values. The pH meter was calibrated after every 20 measurements.

3.4.2 EPA 3050B acid digestion

The soil samples and plant tissue were digested according to the EPA 3050B method (EPA, 1996). This method is a strong acid digestion that will dissolve almost all elements that could become available to the environment, but it is not a total digestion technique. Elements bound in silicate structures will usually not be dissolved.

The samples were digested by repeatedly adding volumes of nitric acid (HNO_3) and hydrogen peroxide (H_2O_2) to 1-2 gram of representative sample material. The digestate was then reduced in volume while heating and diluted to a final volume of 50 ml and the samples were analysed by Agilent 7500 ICP-MS. ICP-MS has an advantage over other analytical methods in the sense that accurate and precise determinations can be made on dry tissue at ultra-trace levels for more than 60 elements (Dunn, 2007).

3.4.3 Ammonium nitrate extraction

Ammonium nitrate extractions were completed for the B horizon soil samples to determine the soluble trace element content, which will give a better indication of the elements available for plant absorption. A subsample of 20 g from each composite soil sample was placed in a shaking bottle (100-150 ml). 50 ml ammonium nitrate solution (1 M) was added, and the mixture was shaken for 2 hours at 20 rpm at room temperature. The solid particles were allowed to settle for 15 min and the supernatant solution was then decanted and filtered (0.45 μm). The first 5 ml of the filtrate was disposed of and the remaining solution was collected for ICP-MS analysis.

3.4.4 ICP-MS analysis

The soil samples and plant tissue were analysed using Agilent 7500 CE ICP-MS fitted with a Micromist-type nebulizer (reducing matrix interferences and for a more robust plasma) and standard quarts spray chamber. The instrument was optimized using a solution containing Li, Y, Ce and Tl (1 ppb) for standard low-oxide/low-interference levels (≤ 1.5%) while maintaining high sensitivity across the mass range. Typical instrumental conditions are displayed in Table 3-6.

For quantitative results, the instrument was calibrated using a certified mixed multi-element stock standard solution containing all the elements of interest. Analysts also employed Quality Control Standards from another independent supplier to assure the correct QC criteria were met. Detection limits for each analysed element are displayed in Table 3-7.

Table 3-6: Instrument conditions

Parameter	Value
Forward Power	1550 W
Plasma Gas Flow	15 L/min
Nebulizer gas Flow	1.2 L/min
Sampling Depth	8 mm
Spray Camber Temp	2 °C

Table 3-7: Lower limits of detection for selected elements.

Element	Mass	DL (ppm)	DL (ppb)
B	11	1.32E-03	1.318
Mn	55	1.92E-05	0.019
Fe	57	1.19E-03	1.192
Co	59	1.57E-06	0.002
Ni	60	1.36E-05	0.014
Cu	63	2.85E-05	0.029
Zn	66	2.25E-04	0.225
As	75	6.26E-06	0.006
Se	82	2.26E-04	0.226
Mo	95	2.06E-05	0.021
Ag	107	2.23E-05	0.022
Cd	111	1.20E-04	0.120
Sb	121	3.04E-06	0.003
Hg	202	1.29E-05	0.013
Pb	208	5.83E-06	0.006

3.5 Statistical methods

Standard statistical analysis techniques such as linear regression or analysis of variance do not take into account the dependencies of data from the same site transect, which is necessary since element concentration share variance according to their common mineralisation unit and common transect (sampling area). Therefore, when traditional statistical analyses (that assume independence) are applied to clustered data, incorrect

standard errors are produced (McCoach, 2010). Multilevel (or hierarchical linear) models were used instead, since the degree of relatedness of observations within the same cluster is estimated and modelled so that standard error estimates are correctly calculated (McCoach, 2010). Hierarchical linear modelling (HLM) simultaneously investigates relationships within and between hierarchical levels of clustered data, thereby making it more effective at accounting for variance among variables at different levels *(*Feldstain*, et al*., 2012). Predictors at both the lowest (individual) level and higher (organisational) level can be used to explain the variance in the dependent variable. HLM is used to analyse variance in the dependant variable (element concentration) when the predictor variables are at varying hierarchical levels (Feldstain, *et al*., 2012).

Element concentration data for leaves of each sampled plant species were clustered into the following organisational units:

- species sampled over shallow ore (labelled ‘min1’);
- species sampled over deeper ore (labelled ‘min2’);
- species sampled on background (labelled ‘back’);
- species sampled on mineralisation, but independent of ore depth and transect (labelled ‘min’).

For species occurring less frequently, it was not possible to collect a series of samples at various depths on a single transect. In such cases, ore depth and transect site were disregarded and samples for the species were grouped together as ‘min’.

Element concentration data for soil were clustered into similar organisational units:

- soils sampled over shallow ore (labelled ‘min1’);
- soils sampled over deeper ore (labelled ‘min2’);
- soils sampled on background (labelled ‘back’).

HLM was used to evaluate the dependence of data in the same transect. The goal was to determine the difference for ‘back’, ‘min’, ‘min1’ and ‘min2’, by taking into account the dependence of data within an organisational unit.

The responses of element concentrations from the same cluster (‘min1’, ‘min2’, ‘back’) will likely exhibit some degree of relatedness with each other, given that they were sampled from the same organisational unit. According to McCoach (2010), HLM allows for adjusting and modelling this dependence of data.

HLM was used to obtain the results generated in Chapters 4 to 6. An SPSS statistical package (version 24) was used for comparison of means from different groups. In Chapter 4, SPSS was used to compare mean trace element content in the leaves of plant species growing on different mineralisation units to identify potential indicator species. In Chapter 5, SPSS was used to compare mean trace element concentrations in soil from different mineralisation units to determine which soil horizon gave a more accurate indication of underlying mineralisation.

Regression analysis with SAS software (version 9.4), was used for correlations where dependence of data was taken into account. Regression analysis creates output results that include t-values, p-values and R^2 values. The t-values and p-values are used to test whether the coefficients (regression coefficient and intercept) are significant. The p-value indicates the level of confidence that each individual variable has some correlation with the dependent variable. A p-value of < 0.05 is considered statistically significant. With a p-value of 0.05 (or 5%), there is only a 5% chance that the generated results would have come up in a random distribution (Princeton University, 2007). It can therefore be said, with a 95% probability of being correct, that the variable is having some effect (Princeton University, 2007). The t statistic is the coefficient divided by its standard error (Princeton University, 2007). The t-value measures the size of the difference between population means relative to the variation in the sample data and it is determined by calculating the difference and representing it in units of standard error (Runkel, 2016). The larger a t-value, the greater the evidence against the null hypothesis that there is no significant difference (Runkel, 2016). The closer T is to 0, the more likely that the difference is significant (Runkel, 2016). The R-squared of the regression is the fraction of the variation in the dependent variable that is accounted for (or predicted by) the independent variables (Princeton University, 2007). It is generally of secondary importance, unless the objective is to make accurate predictions from the regression equation. The p-value gives an indication of the confidence with which each variable can be correlated with the dependent variable, which is the important thing to consider (Princeton University, 2007).

Regression analysis was used in Chapter 4 to determine the correlation between ore depth and trace element content of plant tissue. In Chapter 5 it was used to determine the correlation between ore depth and trace element content of soil. And in Chapter 6, regression analysis was applied to determine the relationship between concentrations of the main trace elements in the ore body and concentrations in the sampling media. Regression analysis was also used to establish a connection between element concentrations in the A and B soil horizons and element concentrations in plant tissue.

CHAPTER 4: INDICATOR PLANT SPECIES

4.1 Introduction

Thick surficial cover material that mantle the Kalahari Copperbelt, poses a major challenge to exploration companies. Biogeochemical exploration is a method employed to detect sub-surface mineral deposits by quantifying absorption of trace elements in plant tissue material (Lund, *et al*., 2005). It is suspected that anomalies will be better expressed in plant tissue than in soils in such areas where mineralisation lies as deep as 1160 m and its expression at surface level is buffered by thick overlying sediments. A biogeochemical approach provides reproducible results for striking anomalies in transported sediment, like wind-blown sands in the case of the Kalahari, where no other sampling techniques work (Dunn, *et al*., 2006; Gee, 2005; Hill & Hulme, 2003).

The semi-arid climate of the Kalahari led to the development of plant communities where most of the species have extensive root systems with major laterals and deep tap roots. Different geological features may promote the development of specific deep-rooted trees along underlying mineralised bedrock and their very presence as well as their element content may then provide definitive and useful anomalies (Cole & Le Roex, 1978). Research by Cole and Le Roex (1978) in the Ghanzi area concluded that the vegetation patterns reflected the thickness of the Kalahari sand cover. Distribution of the plant communities and minor relief features reflected the presence of calcretes or superficial sand. Mineralised beds tend to form slight topographic highs on the sub-outcropping bedrock surface and calcretes will develop less strongly over mineralised beds as opposed to the adjoining country rock. Where thicker accumulations of calcrete occur, a larger volume of water can be retained, which might be responsible for different vegetation associations over different thicknesses of calcrete. Calcrete is a common occurrence in the semi-arid environment of the Kalahari and where present, it is more likely that leaf analysis of deeply rooted trees and shrubs will detect bedrock mineralisation as opposed to analysing surface soils (Cole & Le Roex, 1978). Although interpretation is less definitive where thick layers of Kalahari sand and calcrete mantle the bedrock, vegetation is still indicative of lithology, geological structures and depth and nature of overburden, especially in areas of shallow overburden.

Numerous plant species have historically been used in the Ghanzi and Ngwako Pan areas to indicate copper mineralisation. In the Ghanzi area *Helicrysum leptolepis* was used in areas of shallow overburden, and in Ngwako Pan indicators like *Ecbolium lugardae* were used in

thick aeolian sand (Cole & Le Roex, 1978). Other species found in Ngwako Pan and north-eastern Botswana, like *Monechma divaricantum, Helichrysum candolleanum* and *Blepharis diversispina,* also exhibited correlations with Cu-bearing ore (Kausel, 1991; Lund, *et al*., 1997). Cole and Le Roex (1978) have detected Cu anomalies in both the leaves and stems of *Grewia flava, Combretum hereroense, Catophractes alexandrii* and *Acacia mellifera*. Although *G. flava* and *A. mellifera* showed anomalies, their extensive lateral roots only reflected on the near surface Cu content.

There is very little information available regarding the ability of plants in Botswana to act as indicators for trace elements in underlying base metal deposits. This study sets out to test whether any woody species are suitable indicators for detecting copper ore bodies. The first part of this chapter deals with the tendency of selected plant species to reflect certain levels of trace elements in the leaves, which can be related to the presence or absence of an underlying ore body. The aim is only to report in a descriptive manner, the extent to which these plants will absorb and possibly accumulate specific elements.

The second part of the chapter focuses on identifying correlations between the trace element content in plant tissue and the depth of the ore body. Plants would probably accumulate higher levels of trace elements where the ore body is closer to the surface and plant roots can reach it more easily. Understanding the relationship between leaf element concentrations and ore depth, can contribute to the development of statistical prediction models aimed at detecting concealed ore bodies. Plant species that can absorb and even accumulate ore-related trace elements in a manner that accurately delineates the location and depth of the ore body are considered indicators of such ore deposits and can be used to detect these deposits elsewhere in similar environments.

4.2 Method

4.2.1 Absorption of trace elements on and off the ore body

According to Dunn (2007), the spatial relationships of element concentrations rather than absolute concentrations, are important for biogeochemical exploration. Dominant species were targeted in this biogeochemical survey to develop spatially explicit models. Species were qualified as indicators by evaluating their ability to take up and accumulate pathfinder elements in a way that can be related back to soil element content and underlying mineralisation.

Data for each composite sample was grouped into background data ('back': away from the ore body) and mineralisation data (for species growing on the ore body). This was done for every species per each of the five transects. The mineralisation data were again divided into two groups, with one group containing the data from the first part of the transect where the ore body is shallower ('min1'), and the second group containing the data from the second part where the ore body lies deeper ('min2'). This division was necessary to ensure that the expression of anomalies by plant species were not subdued in the second part of the transect where overburden is too thick ('depth'). In cases where the signature is diluted by thicker overburden, the data group for the shallower ore body could still reflect the mineralisation. Some species occurred sporadically and only a limited number of individuals could be sampled. No comparison with ore depth was made for these species, in other words collected data were not divided into two mineralisation groups ('min1' and 'min2'). Instead, ore depth was disregarded, and data were grouped together as 'min'.

It is hypothesised that individuals of species found on 'min1' would contain significantly higher concentrations of selected trace elements than at least 'back', which is located away from the ore body. If so, then it can be said that individuals above the shallow ore body are indicators of the ore due to mineralisation and plant absorption. It can also be hypothesised that individuals of species found on 'min1' could contain significantly higher concentrations of selected trace elements than 'min2'. If so, it would indicate that the depth of the ore is important in terms of mineralisation and plant absorption.

A two-way ANOVA type of hierarchical linear modelling (HLM) was used to statistically analyse a data structure where mineralisation within plant species groups were compared, taking into account the different transects. The relationship between element concentration (outcome variable) and both the mineralisation unit (predictor variable) and the plant species (predictor variable) were of specific interest. The difference of leaf element content data was modelled for 'back', 'min', 'min1' and 'min2' (the mineralisation units) and difference were also determined between different plant species, taking into account the dependence of transects.

4.2.2 Trace element absorption as a function of ore body depth

Trace element data for all the composite plant samples on the ore body, over all five transects, were used to test whether there are any correlations between the content of plant tissue and the depth of the ore body. Data for plant species *B. albitrunca*, *B. foetida* subsp. *rehmanniana*, *C. apiculatum*, *C. gratissimus*, *G. bicolor*, *G. flavescens*, *G. buxifolia*, *T.*

prunioides and *T. sericea* were included in the analysis. Only data for the individuals growing over the ore body ('min1' and 'min2') were used and background data were omitted.

The depth of the ore was determined by using borehole logs from the exploration companies Cupric Canyon Capital (Deane, 2016) and MOD Resources (MOD Resources Ltd, 2015). For each species sampled on a transect, concentrations of trace elements in the leaves were correlated with approximate depth to mineralisation ('depth') to determine whether higher concentrations of the ore body's trace elements were absorbed at shallower depths. It is hypothesised that concentrations of trace elements will increase as the depth to the ore body decreases. If a significant negative correlation is detected, then leaf content of target trace elements can be used to predict where ore bodies are near the surface. It would further support that ore depth is important in terms of mineralisation and plant absorption.

Regression analysis was carried out using SAS software (version 9.4) to determine whether the depth of the ore body had an effect on the element concentrations found in plant tissue. Data from all plant species growing over underlying mineralisation were used in this model.

4.3 Results and discussion

4.3.1 Absorption of trace elements by plants

Table 4-1 contains the mean trace element content in plants for the different mineralisation units. The mean square error (MSE) and transect variance for leaf element concentrations are also indicated. The MSE gives the unexplained variance within the mineralisation groups ('back', 'min', 'min1', 'min2'), while the transect variance gives the variance between different transects.

The statistical test resulted in a statistical significance ('sig') value in SPSS, commonly known as the p-value. The p-value gives the probability that the obtained value could be acquired under the assumption that the null hypothesis (the statement that there is 'nothing different/new/interesting' e.g. there is no difference between the mean concentration values) is true (Colm McGuinness, 2015; Ellis & Steyn, 2003). The p-values for the mean element concentrations between mineralisation units are displayed in Table 4-1. A small p-value (selected to be $p < 0.05$ for this study) indicates that the probability of the actual statistic (the mean values) is low if the null is true, so the evidence does not support the null hypothesis for some statistic derived from the data. The null hypothesis is therefore rejected, and it is accepted that there is a statistical significance between the means of the different

mineralisation units. A small p-value was calculated for the mean leaf content of the elements Ag, As, B, Cd, Co, Cu, Mn and Zn ($p < 0.05$) (Table 4-1), indicating statistical significance between the mineralisation units. This means that for plant species growing in differently mineralised areas, these elements were accumulated in significantly different amounts. They may therefore be of value as indicator elements since they are absorbed in contrasting quantities by plants growing on different mineralisation units. Take Cu for instance (Table 4-1); there was a statistical significant difference between trace element content in the plants on background (5.72^{b}) and 'min2' (3.88^{a}), as indicated by the superscripts "a" and "b". 'Min1' (4.8^{b}) also differed significantly from 'min2', but there was no statistical significance between 'back' and 'min1'. 'Min' (4.46^{ab}) exhibited no statistical significance to 'back', 'min1' or 'min2'. As expected, the highest levels of Cu were found in plants collected from 'min1', where the ore body is closer to the surface and the plant roots can reach and absorb higher quantities of Cu. The same applies to B and As.

Table 4-1: Relationship between mean leaf element content (ppm) of different mineralisation units ('back', 'min', 'min1' and 'min2').

	Mean leaf element concentrations						
	Back	min	min1	min2	**Mean square error**	**Transect variance**	**p-value**
B	124.52^{b}	94.5^{ab}	126.46^{b}	86.94^{a}	1463.26	579.99	0.002
Mn	124.2^{b}	140.9^{ab}	84.13^{a}	146.33^{b}	423.34	276.27	<0.001
Fe	85.91^{a}	99.94^{a}	82.75^{a}	96.69^{a}	1303.29	108.25	0.181
Co	1.27^{b}	3.09^{a}	0.31^{c}	0.22^{c}	0.06	0.02	0.006
Ni	2.34^{ab}	2.74^{ab}	2.03^{b}	2.6^{a}	0.49	0.22	0.397
Cu	5.72^{b}	4.46^{ab}	4.8^{b}	3.88^{a}	2.91	0.09	<0.001
Zn	11.52^{a}	13.33^{a}	11.45^{a}	10.52^{a}	5.80	0.42	0.026
As	0.12^{ab}	0.09^{ab}	0.14^{b}	0.09^{a}	<0.01	0.01	0.005
Se	0.49^{a}	0.06^{a}	0.54^{a}	0.56^{a}	0.23	0.08	0.216
Mo	388.44^{a}	3626.15^{a}	0.2^{a}	11.59^{a}	45451231.70	<0.01	0.562
Ag	0.08^{b}	0.56^{a}	0.09^{b}	0.17^{b}	0.24	<0.01	0.038
Cd	0.04^{a}	0.01^{a}	0.07^{a}	0.06^{a}	0.01	<0.01	0.031
Sb	0.02^{a}	0^{a}	0.02^{a}	0.01^{a}	<0.01	<0.01	0.232
Hg	0^{a}	0.01^{a}	0.02^{a}	0.06^{a}	0.03	<0.01	0.204
Pb	0.03^{a}	0.05^{a}	0.06^{a}	0.13^{a}	0.04	0.01	0.099

^{a,b,c} Means with different superscripts differed statistically significant.

A large p-value was calculated for the mean leaf content of the elements Fe, Hg, Mo, Pb, Se and Sb ($p>0.05$), indicating that there was no statistically significant difference between the mineralisation units. They will not be useful as indicator elements since they were not

absorbed in contrasting quantities by plants sampled from different units. Mo exhibited an extremely high MSE resulting from a very high 'min' concentration. This was possibly caused by species specific tendencies to absorb and accumulate Mo (the group of plant species involved in the calculation of 'min', differed from the plant species used to calculate 'min1' and 'min2').

A p-value < 0.05 was calculated for the mean leaf content of As, B, Cd, Co, Cu, Fe, Mn, Ni, Pb, Se and Zn between different plant species (Table 4-2). This means that a statistically significant difference exists between the various plant species for these elements. In other words, different species will absorb/exclude the elements to a different extent. Elevated Mo values are indicated for G. bicolor and P. nelsii (Table 4-2), resulting in a very high MSE. This may again be attributed to distinct plant species with different tendencies to absorb and accumulate Mo in their tissue. Mo, Ag and Hg had p-values > 0.05, indicating no statistically significant difference between the tendency of different species to absorb and accumulate these elements. The fact that species did not tend to absorb some of the elements to different extents, do not necessarily mean that it cannot be used as an indicator species. It only means that the plants absorb and accumulate the elements in a similar manner. However, Mo and Hg did not exhibit significant differences in terms of its accumulation in plants growing on different mineralisation units. It can therefore be inferred that these elements might be less useful as pathfinder elements of copper ore.

Statistical significance does not automatically suggest that the result is meaningful in practice, since these tests tend to deliver small p-values (that indicate significance) as the size of the data set increases (Ellis & Steyn, 2003). However, the standardised difference between the means of two populations can be used to remark on practical significance. A measure called the effect size was used to establish the relationship between trace element content in each plant species and the mineralisation units they were sampled on (Table 4-3:). The effect size not only makes the difference between two means independent of units and sample size, but also connects it with the spread of the data (Ellis & Steyn, 2003). The effect sizes were calculated with the following formula:

$$d = \frac{\overline{x_1} - \overline{x_2}}{Smax}$$

- x_1 is the mean element concentration of a specific plant species growing on the ore body (min/min1/min2).
- x_2 is the mean element concentration of a specific plant species growing on background (back).

- S_{max} is the maximum of S_1 and S_2 (the sample standard deviations). Division by S_{max} results in a conservative effect size, so that a practically significant result is not too easily concluded.

The effect size was interpreted as follows (Cohen, 1988, cited by Ellis & Steyn, 2003): d = 0.2 (small effect); d = 0.5 (medium effect) and d = 0.8 (large effect). Data with d ≥ 0.8 is considered practically significant, because it resulted from a difference having a large effect.

A large effect (d ≥ 0.8) was reported for *B. albitrunca* (Figure 4-1) for the elements Mn, Zn, Cd and Sb, indicating the difference in element absorption between mineralised areas and background had a large effect and accumulation of these elements by *B. albitrunca* is of practical significance. *B. foetida* subsp. *rehmanniana* had large effect sizes for many of the analysed elements, including B, Mn, Fe, Cu, Zn, As and Se (Figure 4-1). This species may therefore be particularly valuable as indicator species in biogeochemical surveys. *C. apiculatum* had large effect sizes for the elements B, Mn, Fe, Co, Zn and Ag (Figure 4-1). Elements with large effect sizes for *C. gratissimus* included only Cu and Zn (Figure 4-1). *G bicolor* exhibited large effect sizes for elements Fe, Cu, Sb, Hg and Pb (Figure 4-1). *G. flavescens* had large effect sizes only for Co and Ni (Figure 4-1). *G. buxifolia* displayed large effect sizes for none of the analysed elements (Figure 4-1). *P. nelsii* had large effect sizes for the elements B, Mn, Cu, Zn, As and Mo (Figure 4-1). *T. prunioides* had large effect sizes for only B, Zn and As (Figure 4-1). *T. sericea* displayed large effect sizes for only Ni, As and Pb (Figure 4-1).

Elements that were detected most frequently in practically significant quantities in plant species, include B, Mn, Cu, Zn and As. These elements more often displayed large effect sizes, as opposed to other analysed elements, indicating that the difference in element absorption between mineralised areas and background were significant. They might therefore be a better choice to analyse for when attempting to detect buried mineralisation during a biogeochemical survey. Plant species that exhibited large effect sizes for a wider array of elements include *B. albitrunca*, *B. foetida* subsp. *rehmanniana*, *C. apiculatum*, *G. bicolor* and *P. nelsii*. These species may therefore be more useful as indicators of buried Cu mineralisation. However, it should also be considered that the frequency of plant species occurrence will affect its potential as indicator species of an ore deposit. *B. albitrunca* and *G. bicolor* were more dominant in the area sampling took place, so that they might be more useful in biogeochemical surveys conducted in this region, provided they also absorb and accumulate ore-related elements in anomalous quantities.

Table 4-2: Relationship between mean leaf element content of different plant species. Ba – *Boscia albitrunca*; Bf – *Boscia foetida* subsp. *rehmanniana*; Ca – *Combretum apiculatum*; Cg – *Croton gratissimus*; Gb – *Grewia bicolor*; Gf – *Grewia flavescens*; Gs – *Gymnosporia buxifolia*; Pn – *Philenoptera nelsii*; Tp – *Terminalia prunioides*; Ts – *Terminalia sericea.*

	Mean leaf element concentrations (ppm)												
	Ba	Bf	Ca	Cg	Gb	Gf	Gs	Pn	Tp	Ts	**MSE**	**Transect variance**	**p-value**
B	129.64^{a}	498.82^{b}	79.22^{acde}	58.97^{c}	89.33^{d}	78.6^{acde}	0^{e}	70.57^{acde}	143.6^{a}	70.22^{cd}	1463.26	579.99	<0.001
Mn	74.53^{ad}	202.58^{ceg}	138.72^{abcfi}	99.81^{bg}	59.39^{fh}	153.94^{abcfi}	26.19^{dhj}	217.39^{g}	26.72^{ij}	340.33^{k}	423.34	276.27	<0.001
Fe	75.76^{a}	84.04^{ab}	88.01^{ab}	73.73^{a}	137.82^{b}	103.28^{ab}	37.82^{a}	83.14^{ab}	88.82^{a}	79.22^{ab}	1303.29	108.25	<0.001
Co	0.7^{a}	0.64^{ac}	2.56^{d}	0.03^{b}	0.1^{b}	7.04^{e}	0.17^{bc}	0.15^{ab}	0.46^{ac}	0.16^{bc}	0.06	0.02	<0.001
Ni	3.21^{ad}	3.63^{acd}	1.02^{abe}	1.2^{b}	1.01^{b}	5.24^{cd}	1.04^{be}	1.62^{abef}	0.08^{e}	4.92^{cf}	0.49	0.22	<0.001
Cu	2.06^{a}	8.25^{b}	4.17^{acd}	6.41^{bc}	6.62^{bc}	4.24^{acd}	2.91^{ad}	5.17^{bcd}	6.47^{bc}	4.01^{d}	2.91	0.09	<0.001
Zn	8.1^{a}	6.92^{ac}	15.43^{bd}	12.58^{be}	12.2^{be}	10.04^{ae}	10.24^{ae}	15.32^{bd}	13.99^{be}	11.65^{cde}	5.80	0.42	<0.001
As	0.11^{ad}	0.4^{b}	0.06^{abcd}	0.07^{c}	0.12^{ad}	0.05^{abcd}	0.12^{acd}	0.07^{abcd}	0.17^{d}	0.07^{ac}	<0.01	0.01	<0.001
Se	1.26^{ac}	2.11^{a}	0.07^{bc}	0.19^{b}	0.09^{b}	0.02^{bc}	0.41^{b}	0.07^{bc}	0.01^{b}	0.37^{b}	0.23	0.08	<0.001
Mo	15.69^{a}	0.75^{a}	0.1^{a}	0.17^{a}	1294.23^{a}	0.25^{a}	0^{a}	5439.09^{a}	0^{a}	0^{a}	45451231.70	<0.01	0.775
Ag	0.03^{a}	0.25^{ab}	0.79^{b}	0.12^{a}	0.06^{a}	0.05^{ab}	0.05^{ab}	0.06^{ab}	0.01^{a}	0.25^{ab}	0.24	<0.01	0.070
Cd	0.27^{a}	0.02^{b}	0.01^{b}	0.01^{b}	0^{b}	0.01^{b}	0.07^{b}	0.01^{b}	0^{b}	0.02^{b}	0.01	<0.01	<0.001
Sb	0.02^{a}	0.02^{ab}	0.01^{abc}	0.02^{ab}	0.03^{b}	0^{abc}	0.02^{ab}	0.01^{abc}	0.02^{ab}	0^{c}	<0.01	<0.01	<0.001
Hg	0.02^{a}	0.03^{a}	0^{a}	0.01^{a}	0.09^{a}	0^{a}	0.01^{a}	0.01^{a}	0.03^{a}	0^{a}	0.03	<0.01	0.240
Pb	0.05^{ab}	0.09^{ab}	0.03^{ab}	0^{a}	0.15^{b}	0^{ab}	0^{ab}	0.04^{ab}	0.1^{ab}	0.1^{ab}	0.04	0.01	0.023

^{a,b,c,d,e,f,g,h,i,j} Means with different superscripts differed statistically significant.

Table 4-3: Relationship between trace element content in plant tissue samples from different mineralisation units. The listed values are effect sizes calculated with reference to background values. Large effect sizes (d ≥ 0.8) are indicated in red. Ba – *Boscia albitrunca*; Bf – *Boscia foetida* subsp. *rehmanniana*; Ca – *Combretum apiculatum*; Cg – *Croton gratissimus*; Gb – *Grewia bicolor*; Gf – *Grewia flavescens*; Gs – *Gymnosporia buxifolia*; Pn – *Philenoptera nelsii*; Tp – *Terminalia prunioides*; Ts – *Terminalia sericea.*

	Effect sizes for leaf element concentrations																
	Ba		Bf	Ca	Cg		Gb		Gf	Gs	Pn	Tp	Ts				
	min1	min2	min1	min	min1	min2	min1	min2	min	min1	min	min1	min1	min2	**MSE**	**Transect variance**	**p-value**
B	0.46	0.47	**2.12**	**1.30**	0.05	0.01	0.04	0.18	0.27	0.05	**1.40**	**1.65**	0.16	0.13	1463.26	579.99	0.042
Mn	0.07	**0.87**	**2.83**	**2.62**	0.21	0.27	0.26	0.10	0.69	-	**4.68**	0.08	-	-	423.34	276.27	<0.001
Fe	0.27	0.16	**0.86**	**0.97**	0.04	0.67	**1.06**	0.40	0.25	-	0.13	0.32	-	-	1303.29	108.25	0.241
Co	0.34	0.38	0.23	**8.51**	0.10	0.38	0.15	0.30	**5.10**	0.02	0.05	0.18	0.40	0.12	0.06	0.02	<0.001
Ni	0.54	0.69	0.62	0.59	0.05	0.33	0.14	0.20	**1.05**	0.06	0.34	0.19	**1.59**	0.60	0.49	0.22	0.008
Cu	0.28	0.44	**2.83**	0.72	0.44	**1.53**	**0.94**	**2.03**	0.57	0.79	**1.07**	0.04	0.33	0.08	2.91	0.09	0.001
Zn	**0.81**	0.24	**2.18**	**2.14**	0.22	**0.85**	0.37	0.53	0.40	0.12	**1.88**	**0.87**	0.68	0.15	5.80	0.42	<0.001
As	0.01	0.09	**2.37**	0.46	0.12	0.39	0.11	0.12	0.30	0.56	**1.12**	**1.35**	**0.95**	0.01	<0.01	0.01	<0.001
Se	0.45	0.12	**1.59**	0.02	0.27	0.45	0.10	0.29	0.05	0.06	0.06	0.23	0.05	0.01	0.23	0.08	0.733
Mo	<0.01	0.01	<0.01	<0.01	<0.01	<0.01	0.58	0.58	<0.01	<0.01	**1.61**	<0.01	<0.01	<0.01	45451231.70	<0.01	0.826
Ag	0.04	0.04	0.08	**3.10**	0.08	0.08	0.01	0.11	0.01	0.01	0.07	<0.01	0.07	0.64	0.24	<0.01	0.182
Cd	**1.26**	0.62	0.14	0.15	0.02	0.21	0.03	0.12	0.09	0.16	0.08	0.14	0.28	0.04	0.01	<0.01	0.001
Sb	**1.15**	0.44	0.24	0.14	0.77	0.72	0.05	**1.89**	0.03	-	0.20	0.39	-	-	<0.01	<0.01	<0.001
Hg	0.14	0.01	0.17	<0.01	0.01	0.06	<0.01	**1.42**	<0.01	0.05	0.08	<0.01	0.39	0.06	0.03	<0.01	0.011
Pb	0.05	0.27	<0.01	0.28	0.15	0.28	0.54	**0.86**	<0.01	0.30	0.39	0.12	0.11	**0.96**	0.04	0.01	0.587

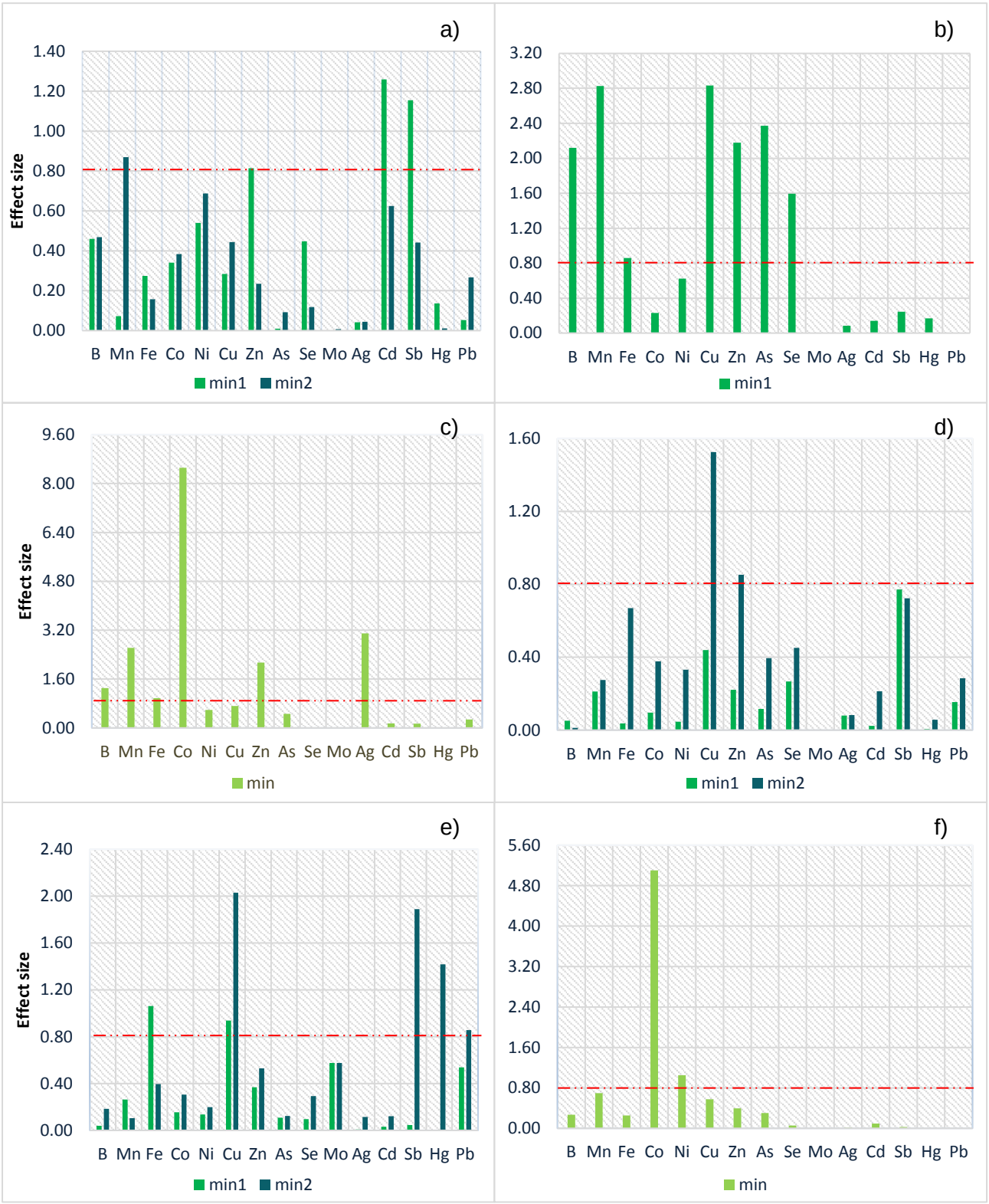

Figure 4-1: Effect sizes of leaf element concentrations for trees in mineralised areas: a) *B. albitrunca* (min1; min2); b) *B. foetida* (min1); c) *C. apiculatum* (min); d) *C. gratissimus* (min1; min2); e) *G. bicolor* (min1; min2); f) *G. flavescens* (min). > 0.8 is a large effect size relative to background concentrations.

Figure 4-1 (continued): Effect sizes of leaf element concentrations for trees in mineralised areas: g) *G. buxifolia* (min1); h) *Philenoptera nelsii* (min); i) *Terminalia prunioides* (min1); j) *Terminalia sericea* (min1; min2). > 0.8 is a large effect size relative to background concentrations.

4.3.2 Trace element absorption as a function of ore body depth

Regression analysis with SAS software (version 9.4), was used for correlations where dependence of data was taken into account. Output results that include t-values, p-values and R^2 values were generated. The p-value indicates the level of confidence that each individual variable (ore depth in this case) has some correlation with the dependent variable (element concentration in the plant). A p-value of < 0.05 is considered statistically significant. With a p-value of 0.05 (or 5%), there is only a 5% chance that the generated results would have come up in a random distribution (Princeton University, 2007). It can therefore be said, with a 95% probability of being correct, that the variable is having some effect (Princeton

University, 2007). The t-value measures the size of the difference between population means relative to the variation in the sample data and it is determined by calculating the difference and representing it in units of standard error (Runkel, 2016). The larger a t-value, the greater the evidence against the null hypothesis that there is no significant difference (Runkel, 2016). The closer T is to 0, the more likely that the difference is significant (Runkel, 2016). The R-squared of the regression is the fraction of the variation in the dependent variable that is accounted for (or predicted by) the independent variables (Princeton University, 2007). It is generally of secondary importance, unless the objective is to make accurate predictions from the regression equation. The p-value gives an indication of the confidence with which each variable can be correlated with the dependent variable, which is the important thing to consider (Princeton University, 2007).

Regression analysis (Table 4-4) shows each element and how its concentration in plant tissue relates to the depth of the copper mineralisation. Element observations used in the regression model to generate the values for each element ranged between 179 and 220. The parameter estimates, namely the regression coefficient and intercept (Table 4-4) are the values for the regression equation to determine the extent to which the dependent variable (element concentration in plant tissue) is predicted by the independent variable (ore body depth). The regression is presented by the following equation:

$$Y = a + bX$$

where ‘a’ represents the intercept and ‘b’ represents the regression coefficient. ‘Y’ represents the dependent (predicted) variable, which is element concentration and ‘X’ represents the independent variable, namely ore body depth. Expressed in terms of the variables for Cu for instance, the regression equation is

$$[Cu] = 5.71 – 0.0031 \text{ (ore depth)}$$

These estimates indicate a relationship between the independent variable (ore body depth) and the dependent variable (element concentration in leaf tissue). The estimates in the equation above indicates the amount of increase in Cu concentration that would be predicted by a 1-unit increase in ore depth. The regression coefficient is -0.0031. So, for every unit increase in ore depth, a -0.0031 unit decrease in Cu concentration is predicted. It is important to note that if an independent variable is not significant, the parameter estimate is not significantly different from 0, which should be taken into consideration when interpreting the parameter estimate. The t-values and p-values (Table 4-4) are used to test whether the coefficients are significant.

A preselected p-value of < 0.05 was chosen to indicate that parameter estimates would be statistically significant (i.e. the null hypothesis can be rejected and it can be said that the coefficient is significantly different from 0). In the case of Cu (Table 4-4; $p < 0.001$), the coefficient for ore depth is significant at the 0.05 level. Other elements that have a p-value of < 0.05 and therefore a significant coefficient, include As, Co, Hg, Mn, Mo, Ni, Sb, Se and Zn. Elements with a large p-value (> 0.05), include Ag, B, Cd, Fe, and Pb.

R^2 (Table 4-4) gives the proportion of variance in the dependent variable (element concentration) which can be predicted from the independent variable (ore depth). In the case of Cu (Table 4-4), the R^2 indicates that 11% of the variance in Cu concentration in plant tissue can be predicted from the ore depth. The R^2 values for all analysed elements are indicated in Figure 4-2. The R^2 is interpreted as follows: $R^2 = 0.01$ (small); $R^2 = 0.1$ (medium) and $R^2 = 0.25$ (large). A large R^2 was not reported for any of the elements, but Cu, Zn and Hg exhibited a medium R^2, and Ag, As, Co, Mn, Mo, Ni, Sb and Se had small R^2 values (Figure 4-2). When analysing trace element content of leaves it should therefore be considered that especially Cu, Zn and Hg concentrations are influenced by the depth of the ore body and the effect of depth should therefore be accounted for when interpreting analysis results for these elements.

Table 4-4: Correlation between ore body depth and trace element content in plant tissue. Medium R^2 values are listed in red.

	Mean	Sum	Intercept	Regression coefficient	t-value	p-value	R^2
B	90.95	20008.80	95.795	-0.0123	-1.02	0.310	<0.01
Mn	87.79	10886.40	74.496	0.0398	2.12	0.036	0.02
Fe	88.09	10922.60	83.200	0.0146	1.2	0.231	0.01
Co	0.33	72.48	0.253	0.0002	2.8	0.006	0.02
Ni	2.29	503.84	1.935	0.0009	2.76	0.006	0.02
Cu	4.48	986.46	5.706	-0.0031	-5.66	<0.001	**0.11**
Zn	10.86	2388.40	12.385	-0.0039	-5.25	<0.001	**0.11**
As	0.14	30.40	0.099	0.0001	5.29	<0.001	0.09
Se	0.48	105.79	0.295	0.0005	2.14	0.033	0.03
Mo	8.65	1547.70	-0.275	0.0254	3.45	0.001	0.04
Ag	0.08	16.93	0.056	0.0001	1.89	0.060	0.01
Cd	0.10	21.91	0.095	<0.0001	0.39	0.694	<0.01
Sb	0.02	2.15	0.009	<0.0001	3.37	0.001	0.07
Hg	0.06	12.62	-0.046	0.0003	3.49	0.001	**0.13**
Pb	0.13	28.19	0.125	<0.0001	0.16	0.873	<0.01

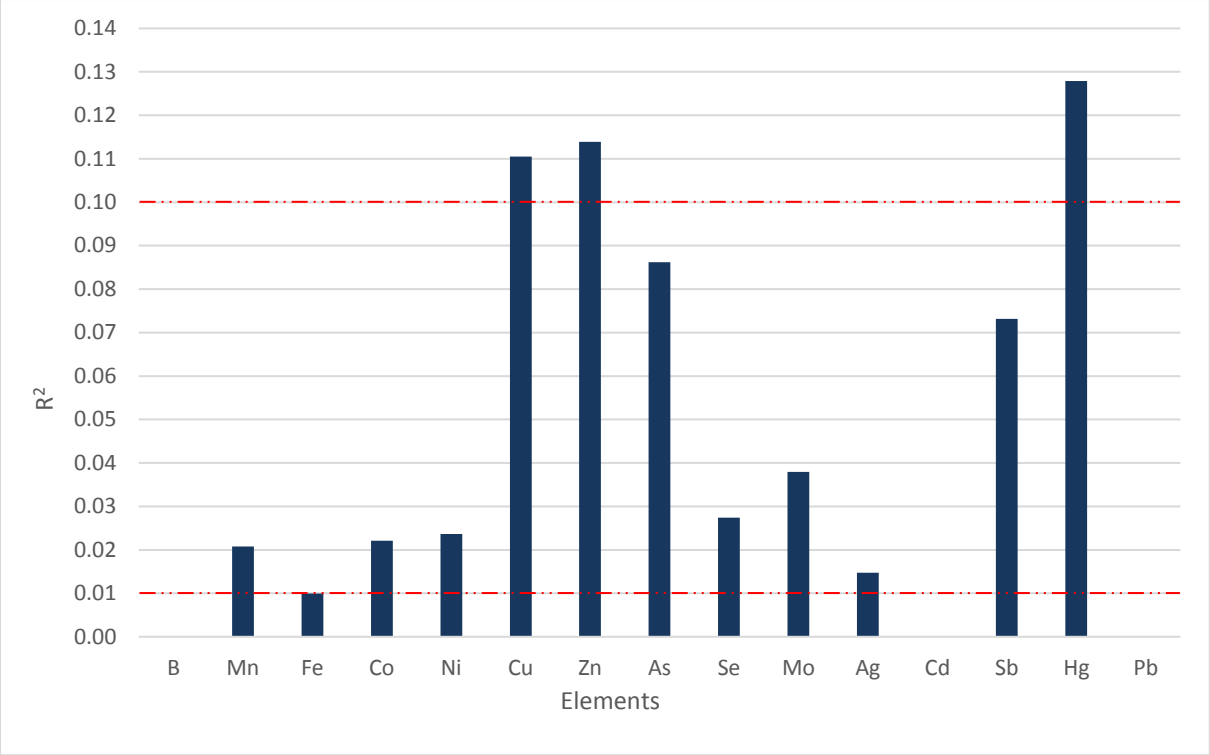

Figure 4-2: R^2 values for element concentrations in plant tissue, as it relates to ore depth. Red lines indicate the R^2 categories. R^2 = 0.01 (small) and R^2 = 0.1 (medium).

Cu and Zn have negative regression coefficients, indicating that an increase in ore depth will result in lower concentrations of these elements in plant tissue; and although Hg has a medium R^2, the regression coefficient is positive, indicating that an increase in ore body depth is accompanied by an increase in Hg concentration in the leaves.

Effect sizes (Table 4-5) were calculated for dominant species to give an indication of the effect of ore depth on the accumulation of trace elements in tissues of distinct species. The difference in leaf element concentrations of samples between 'min2', where the ore body is deeper, and 'min1', where the ore body is shallower, were used to calculate the effect sizes. The values in Table 4-5 therefore reflect leaf element concentrations evaluated in terms of their practical significance, while the effect of ore body depth was accounted for.

A large effect ($d \geq 0.8$) was reported for *B. albitrunca* (Table 4-5) for the elements Mn, Cu, Mo, Cd and Pb (Table 4-5), indicating that the difference in element absorption between mineralised areas 'min1' and 'min2' still had a large effect, also when the effect of ore depth has been considered. Accumulation of these elements by *B. albitrunca* is therefore of practical significance. For *C. gratissimus*, only Fe had a large effect. *G. bicolor* had large

effect sizes for the elements Fe and Pb and *T. sericea* had large effect sizes for elements Ni, Cu, Zn, As, Ag, Hg and Pb.

Table 4-5: Relationship between trace element content in plant tissue samples from different mineralisation units, with ore depth taken into account. The listed values are effect sizes calculated for mineralisation unit 'min2' relative to 'min1'. Large effect sizes (d ≥ 0.8) are indicated in red. Ba – *Boscia albitrunca*; Cg – *Croton gratissimus*; Gb – *Grewia bicolor*; Ts – *Terminalia sericea*.

	Ba	*Cg*	*Gb*	*Ts*	Depth at which covariates are evaluated (m)	MSE	Transect variance	p-value
B	0.50	0.42	0.33	0.35	395.48	1332.15	756.40	0.002
Mn	**1.04**	0.12	0.06	-	334.23	460.75	370.15	0.248
Fe	0.08	**1.23**	**1.19**	-	395.48	312.75	183.23	0.280
Co	0.57	0.29	0.43	0.75	395.48	0.05	0.02	0.003
Ni	0.55	0.06	0.36	**1.21**	395.48	0.46	0.36	0.003
Cu	**0.93**	0.04	0.09	**1.00**	395.48	2.06	0.98	<0.001
Zn	0.47	0.09	0.32	**0.85**	395.48	5.27	0.79	0.006
As	0.42	0.03	0.28	**1.19**	395.48	<0.01	0.01	0.006
Se	0.22	0.09	0.13	0.26	395.48	0.22	0.10	0.053
Mo	**2.51**	0.32	0.49	0.26	350.61	296.02	180.49	0.026
Ag	0.30	0.46	0.09	**3.61**	395.48	0.01	<0.01	0.006
Cd	**1.68**	0.20	0.23	0.03	395.48	<0.01	<0.01	0.013
Sb	0.52	0.09	0.78	-	334.23	<0.01	<0.01	0.285
Hg	0.67	0.74	0.56	**0.81**	399.84	0.03	<0.01	<0.001
Pb	**1.04**	0.68	**0.95**	**1.32**	395.48	0.05	0.03	<0.001

In cases where significant differences exist between element content in plants sampled on different parts of the transect overlying the ore body, while accounting for the effect of ore depth, some other factor must be responsible for differences in element concentrations. Localized factors related to soil characteristics, such as the pH-Eh regime, the concentrations of elements present in that section of the ore body, or some other contributing factor, such as root development, may have played a role in the different element concentrations found in the plant tissue.

4.4 Conclusion

A summary of the results from Chapter 4 is displayed in Table 4-6. Elements that were generally accumulated in practically significant amounts in plant tissue of species growing over concealed copper mineralisation, include As, B, Cu, Mn and Zn. It is therefore

recommended that focus is placed on these five elements during biogechemical exploration for copper ore bodies, since they produced the most accurate indication of the underlying ore body.

Plant species that accumulated a wide range of trace elements in practically significant amounts include *B. foetida* subsp*. rehmanniana, C. apiculatum, G. bicolor* and *P. nelsii.* Sampling and analysis of these species will produce the most promising results in a bio-exploration program. However, when conducting a biogeochemical survey, trace element analysis can be adapted to each sampled plant species, according to the elements that delivered the most practical significant results (Table 4-6). The previously mentioned species (apart from *G. bicolor*) were not the most dominant species in the sampling region and may be absent from a selected sampling site. In this case it may be better to include more frequently occurring species, such as *B. albitrunca* and *C. gratissimus* in the sampling design.

Some trace elements exhibited some degree of correlation with depth of ore body, namely Cu, Zn and Hg (Table 4-6). It should therefore be considered that mineralisation depth will influence the concentrations of these elements in plant tissue. The effect of ore depth should therefore be considered when interpreting results for these elements.

Table 4-6: Summary of results.

		B	Mn	Fe	Co	Ni	Cu	Zn	As	Se	Mo	Ag	Cd	Sb	Hg	Pb
Statistically significant differences ($p < 0.05$) between mean leaf element concentrations of plants growing on different mineralisation units ('min', 'min1', 'min2' and 'back')		x	x		x		x	x	x			x	x			
Practically significant differences between leaf element content of plants on the ore body and plants growing on background (large effect d ≥ 0.8 in red; medium effect d = 0.5 in orange)	*B. albitrunca*		x			x		x					x	x		
	B. foetida subsp. *rehmanniana*	x	x	x		x	x	x	x	x						
	C. apiculatum	x	x	x	x	x	x	x				x				
	C. gratissimus			x			x	x						x		
	G. bicolor			x			x	x			x			x	x	x
	G. flavescens			x	x	x										
	G. buxifolia						x		x							
	P. nelsii	x	x				x	x	x		x					
	T. prunioides	x						x	x							
	T. sericea					x		x	x			x				x
Significant ($p<0.05$) reduction/increase in leaf element concentration with every unit increase in ore depth			x		x	x	x	x	x	x	x			x	x	
Proportion of variance in element concentration that can be predicted from ore depth (medium $R^2 = 0.1$, in red; small $R^2 = 0.01$, in orange)			x		x	x	x	x	x	x	x	x		x	x	

CHAPTER 5: SOIL GEOCHEMICAL COMPARISON OF A HORIZON VERSUS B HORIZON

5.1 Introduction

Traditional geochemical sampling programs target a depth of 20-30 cm below surface which is approximately in the 'A' horizon of soils, for sampling and analysis (Cannon, *et al*., 2013; Heberlein, 2010). Trees absorb elements from deeper in the surficial cover and return it to the upper soil upon shedding of their leaves. The A horizon is more dynamic than the B horizon in terms of accumulation of fresh organic carbon derived from the recycling process of plant tissue material and also due to remobilization of elements (Shaw, 1990).

Particle size distribution (PSD) and texture of the B horizon have in most cases a higher clay content due to downwards illuviation of fine particles by means of water infiltration. The significance of this is that the cation adsorption capacity (CAC) of the B horizon are higher than that of the A horizon (Boguslavsky, 2000; Giltrap, *et al.*, 1995). Accumulation of cations in the A horizon is mostly associated with carbon concentration and recycling of the plant tissue material (more specifically the leaves), even where the leave tissue is still in undecomposed form. The higher clay fraction with higher CAC in the B horizon is therefore, from a theoretical point, much more reliable with respect to accumulation of trace elements in upper parts of the soil profile. A slight increase in CAC in the A horizon is caused by the organic carbon which is in transitional form and which will eventually be illuviated downwards and accumulate in the B horizon. The A horizon is characterized by a leaching of specific elements which move downward to be precipitated in the B horizon (Hawkes, 1957). The potential downward movement of these elements may contribute to the trace element content of the B horizon and conceal to some extent the subtle additions from oxidizing mineralisation to the B horizon (Fedikow & Ziehlke, 2005). In cases where the immediate source for element enrichment in the subsoil is the decaying plant matter overhead, it is common to find that anomalies in the B horizon of transported soils over ore deposits do not extend downward into the immediately underlying parent material (Hawkes, 1957). However, the effect of trace elements being added to the soil by organic matter remains greater in the A horizon and it is therefore presumed that although absolute element concentrations may be higher in the A horizon, the B horizon will more accurately reflect bedrock mineralisation.

Soil particles within the B horizon tend to be coated with a film of hygroscopic water and amorphous Mn dioxide (Hawkes, 1957). Fe and Al also tend to be enriched in the subsoil

due to soil-forming processes (Hawkes, 1957). It is well known that some Mn-oxide species have an extremely high CEC value which contributes to the accumulation of adsorbed elements. Fe, Mn, Al and also other trace elements form amorphous compounds in the soil that is generally a locus of stable accumulation of elements (Boguslavsky, 2000; Hawkes, 1957). The amorphous materials are an effective chemical trap for ions and polar molecules due to its large surface area and the positive and negative charges on the surface of the clay particles. Ore-related elements move upwards driven by capillary forces (to a minor extent) but mainly by diffusion, which is driven by various gradients such as temperature, concentration, vapour pressure and others. It moves through the permeable bedrock and overburden as well as fractures and joints, mainly as element and metal-enriched volatiles (halides, halogens and Hg-vapour) and are adsorbed on the Mn-oxides (Barr, *et al.*, 2015; Fedikow & Ziehlke, 2005) and clay fraction. These elements presumably represent the chemical signatures of oxidizing mineralisation at depth.

Certain processes in the secondary environment can influence the dispersion of ore-related elements. Soil-forming processes may modify anomalies that formed in residual or transported cover. In arid climates, Ca that leaches and reprecipitates in the soil profile is a key factor. Specific elements, such as Zn and Cu, that are concentrated in Fe and Mn-oxides at redox fronts may be derived from overlying sediments by leaching and be unrelated to any basement mineralisation. These anomalies may be identified as false by regression analysis or by the absence of a multi-element signature (Anand, 2016). Another consideration is that the surficial Kalahari sediments covering the deposit is composed mainly of sand and gravel fractions and excessively low silt and clay contents. Under these conditions it can be expected that only low-order trace element values will be detected, since the elements are normally adsorbed by clay colloids (Cole & Le Roex, 1978)

Hawkes (1957) described a study during which a Zn anomaly in the residual soil were more clearly defined by the B horizon, while the A horizon had an inhomogeneous and erratic pattern of Zn distribution. He also reported for a case study on forest soils at a Cu mine that the B horizon proved to be more reliable for geochemical sampling than the A horizon. However, it should be noted that this might not be the case in other types of soils in other climatic regions, where there may be no indication of variation in the distribution of elements in the soil profile and samples taken from any part of the profile may be used equally well in geochemical soil surveys (Hawkes, 1957).

The A and B horizons were sampled in this study to determine which soil horizon will be better suited as sampling medium to detect mineralisation at depth. Geochemical anomalies

can be recognized only by their contrast with non-mineralised areas (Hawkes, 1957). Therefore, this chapter focuses on quantifying the element content for the A and B horizons sampled over buried mineralisation and compares it to background concentrations. The trace element content of each horizon is then correlated with the depth of the ore body (Figure 5-1). It will then be possible to establish which of the A or B horizon is more representative of the underlying mineralisation.

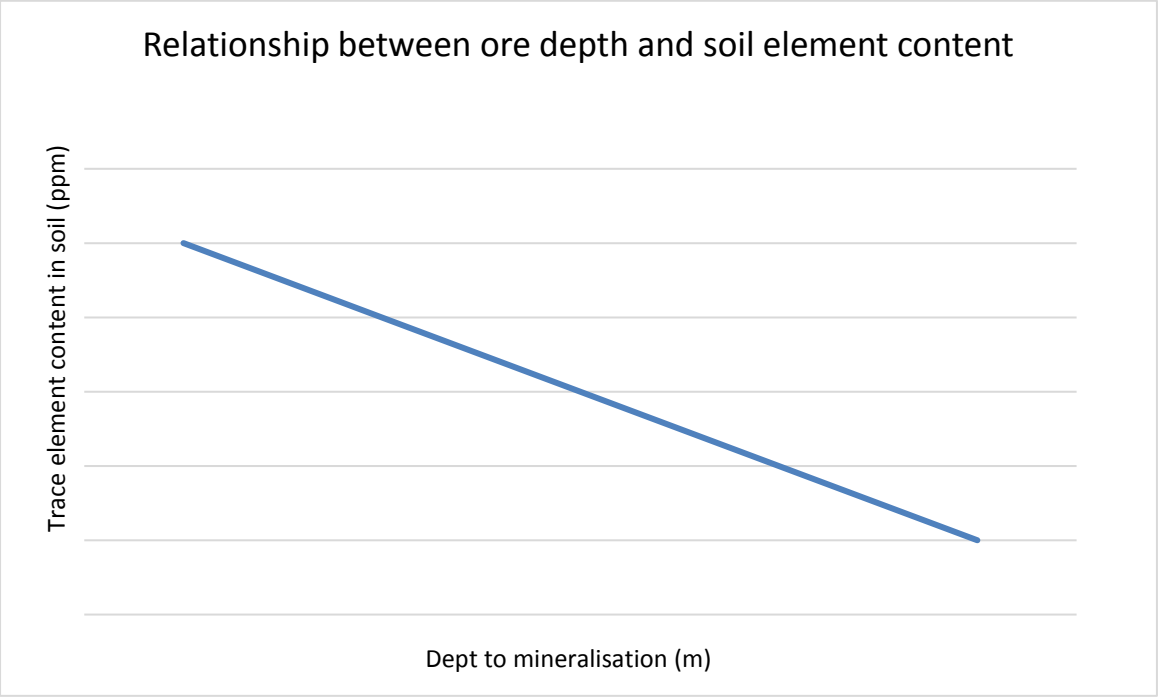

Figure 5-1: Expected correlation trend between trace element content in the soil and the depth of underlying ore.

5.2 Method

5.2.1 Trace element content in soil on and off the ore body

Trace element content of each soil horizon, sampled over mineralised bedrock, were compared to the background concentrations. To achieve this objective, data for all the transects were grouped together into mineralised units (‘min1’ and ‘min2’) which were then compared to background content (‘back’). This was done for both the A and B soil horizons.

A hierarchical linear modelling (HLM) approach, that is similar to a two-way ANOVA analysis, was applied to analyse a data structure where mineralisation within soil horizon groups were compared, taking into account the different transects. Of specific interest was

the relationship between element concentration (outcome variable) and the mineralisation unit (predictor variable). The difference of soil element content data was modelled for ‘back’, ‘min1’ and ‘min2’ (the mineralisation units) and difference were also determined between the two soil horizons, taking into account the dependence of transects.

5.2.2 Trace element content in soil as a function of ore body depth

Trace element data for the A and B soil horizons, sampled along the five transects, were used to establish if there was a correlation between content in the soil and depth of the ore body. Regression analysis with SAS software (version 9.4) were used to determine if the depth of the ore body influenced the element concentrations found in the soil. Only data from soils sampled over underlying mineralisation were used in this model. As in Chapter 4, the depth of the ore was established by using borehole logs from Cupric Canyon Capital (Deane, 2016) and MOD Resources (MOD Resources Ltd, 2015).

5.3 Results and discussion

5.3.1 Accumulation of trace elements in soil horizons

Table 5-1 and Table 5-2 shows the mean trace element content in A and B soil horizons for the different mineralisation units. The mean square error (MSE) and transect variance for soil element concentrations are also indicated. The MSE gives the unexplained variance within the mineralisation groups (‘back’, ‘min1’, ‘min2’), while the transect variance gives the variance between different transects.

Significant differences of the mean element concentrations between mineralisation units were based on p-values (Table 5-1 and Table 5-2). A small p-value (selected as $p < 0.05$ for this study) indicated a statistically significant difference between the means of mineralisation units. In terms of the A horizon, a p-value < 0.05 was calculated for the mean soil concentrations of the elements B, Co, Cu, Hg, Mn, Ni, and Zn, indicating statistical significance. This means that for A horizon soils in different mineralisation areas, these elements were accumulated in significantly different amounts. They may therefore be valuable as indicator elements when sampling the A horizon, since they are accumulated in contrasting quantities on different mineralisation units. In the case of Cu (Table 5-1), different superscripts (“a” and “b”) were used to indicate significance differences between trace

element content for 'back' (6.92[b]) and 'min2' (4.85[a]). 'Min1' (5.67[b]) also differed significantly from 'min2', but there was no statistical significance between 'back' and 'min1'.

A large p-value (> 0.05) was calculated for the mean A horizon content of the elements Ag, As, Cd, Fe, Mo, Pb, Sb and Se (Table 5-1), indicating that there was no significant difference between the mineralisation units. This means that for A horizon soils in different mineralisation areas (of specific interest, soils on background versus soils sampled on the ore body), these elements were not accumulated in significantly different amounts. They may therefore not be as useful as indicator elements when using the A horizon as sampling medium.

In terms of the B horizon, a p-value < 0.05 was calculated for the mean leaf content of the elements Ag, As, B, Cu, Mn, Mo, Ni, Se and Zn, indicating significant differences. This means that for B horizon soils in different mineralisation areas, these elements were accumulated in significantly different amounts. They may therefore be of value as indicator elements when using the B horizon as sampling medium.

Table 5-1: Relationship between mean soil element content (ppm) of different mineralisation units (back, min1 and min2) for the A horizon.

	Back	min1	min2	MSE	Transect variance	p-value
B	32.09[ab]	43.18[b]	28.26[a]	460.24	54.70	0.003
Mn	47.34[b]	40.69[a]	47.13[b]	109.02	1116.39	0.005
Fe	3239.86	3059.02	3168.65	698390.17	1357208.60	0.658
Co	294.99[ab]	248.89[b]	356.91[a]	20339.36	1126.32	0.001
Ni	874.85[ab]	1221.55[b]	736.58[a]	481849.02	38166.07	0.002
Cu	6.92[b]	5.67[b]	4.85[a]	3.15	6.01	<0.001
Zn	4.52[b]	4.35[b]	5.39[a]	1.16	5.00	<0.001
As	0.45	0.49	0.48	0.01	0.08	0.383
Se	0.03	0.04	0.03	<0.01	<0.01	0.277
Mo	1.1	1.66	1.55	4.44	0.10	0.558
Ag	0.04	0.07	0.06	0.01	<0.01	0.429
Cd	0.01	0.01	0.01	<0.01	<0.01	0.071
Sb	0.04	0.04	0.03	<0.01	<0.01	0.654
Hg	0.55[b]	1.62[a]	1.41[a]	1.06	0.35	<0.001
Pb	2.03	1.92	1.82	0.21	0.46	0.173

[a,b] Means with different superscripts differed significantly.

A large p-value (> 0.05) was calculated for the mean B horizon content of the elements Cd, Co, Fe, Hg, Pb and Sb (Table 5-2), indicating that there was no significant differences between the mineralisation units. This means that for B horizon soils in different mineralisation areas (of specific interest, soils on background versus soils sampled on the ore body), these elements were not accumulated in significantly different amounts. Therefore, they have limited use as indicator elements when using the B horizon as sampling medium, since they are not absorbed in contrasting quantities by soils on different mineralisation units.

When reviewing the mean element concentrations of mineralisation units for the different soil horizons (Table 5-1 and Table 5-2), it shows that, compared to the B horizon, mean concentrations of Mn and Co were higher in the A horizon. On the other hand, mean concentrations of B, Fe, Ni and Mo were higher in the B horizon when compared to the A horizon. This indicates an accumulation of the elements in the B horizon.

Table 5-2: Relationship between mean soil element content of different mineralisation units (back, min1 and min2) for the B horizon.

	Back	min1	min2	MSE	Transect variance	p-value
B	43.16[b]	46.48[b]	64.86[a]	624.38	54.41	<0.001
Mn	39.18[ab]	37.66[b]	44.18[a]	100.01	687.08	0.007
Fe	3734.94	3750.67	4157.13	904799.93	752793.69	0.084
Co	204.92	179.71	135.89	19750.99	4241.77	0.126
Ni	1219.32[b]	1339.59[b]	1892.13[a]	644791.75	38032.33	0.001
Cu	7.44[b]	5.35[a]	5.98[a]	3.50	3.06	<0.001
Zn	4.6[ab]	4.27[b]	5.41[a]	1.64	3.32	<0.001
As	0.42[b]	0.44[b]	0.54[a]	0.02	0.07	<0.001
Se	0.03[ab]	0.02[b]	0.04[a]	<0.01	<0.01	<0.001
Mo	2.16[ab]	2.11[b]	3.46[a]	5.59	0.75	0.013
Ag	0.04	0.04	0.06	<0.01	<0.01	0.039
Cd	0.01	0.01	0.01	<0.01	<0.01	0.453
Sb	0.04	0.04	0.03	<0.01	<0.01	0.197
Hg	0.72	0.45	0.82	0.95	0.12	0.171
Pb	2	1.97	2	0.23	0.38	0.951

[a,b] Means with different superscripts differed statistically significant.

Statistical significance does not necessarily suggest that the result is meaningful in practice, therefore the standardised difference between the means of two populations were used to remark on practical significance. Effect sizes (Table 5-3) were used to evaluate the

relationship between trace element content in each soil horizon and the mineralisation units they were sampled on.

A large effect (d ≥ 0.8) was reported only for Hg in the A horizon (Figure 5-2). In the B horizon, the elements B, Ni and Cu had large effect sizes (Figure 5-2). This means that for these elements, the difference in accumulation in the soil horizons between mineralised areas and background had a large effect and accumulation of these elements is of practical significance. These elements may therefore be the most useful in geochemical prospecting surveys where soil is used as sampling medium.

Table 5-3: Relationship between the trace element content of the A and B soil horizons and mineralisation units. The listed values are effect sizes calculated with reference to background values. Large effect sizes (d ≥ 0.8) are indicated in red.

	A horizon					B horizon				
	min1	min2	MSE	Transect variance	p-value	min1	min2	MSE	Transect variance	p-value
B	0.49	0.17	460.24	54.70	0.003	0.13	**0.83**	624.38	54.41	<0.001
Mn	0.19	0.01	109.02	1116.39	0.005	0.05	0.23	100.01	687.08	0.007
Fe	0.13	0.05	698390.17	1357208.60	0.658	0.01	0.33	904799.93	752793.69	0.084
Co	0.31	0.42	20339.36	1126.32	0.001	0.16	0.45	19750.99	4241.77	0.126
Ni	0.48	0.19	481849.02	38166.07	0.002	0.15	**0.81**	644791.75	38032.33	0.001
Cu	0.41	0.68	3.15	6.01	<0.001	**0.82**	0.57	3.50	3.06	<0.001
Zn	0.07	0.35	1.16	5.00	<0.001	0.15	0.36	1.64	3.32	<0.001
As	0.13	0.11	0.01	0.08	0.383	0.05	0.40	0.02	0.07	<0.001
Se	0.05	0.25	0.00	<0.01	0.277	0.25	0.35	<0.01	<0.01	<0.001
Mo	0.26	0.21	4.44	0.10	0.558	0.02	0.52	5.59	0.75	0.013
Ag	0.29	0.21	0.01	<0.01	0.429	0.02	0.44	<0.01	<0.01	0.039
Cd	0.29	0.08	<0.01	<0.01	0.071	0.04	0.22	<0.01	<0.01	0.453
Sb	0.01	0.05	<0.01	<0.01	0.654	0.10	0.21	<0.01	<0.01	0.197
Hg	**0.90**	0.72	1.06	0.35	<0.001	0.26	0.09	0.95	0.12	0.171
Pb	0.13	0.26	0.21	0.46	0.173	0.03	0.00	0.23	0.38	0.951

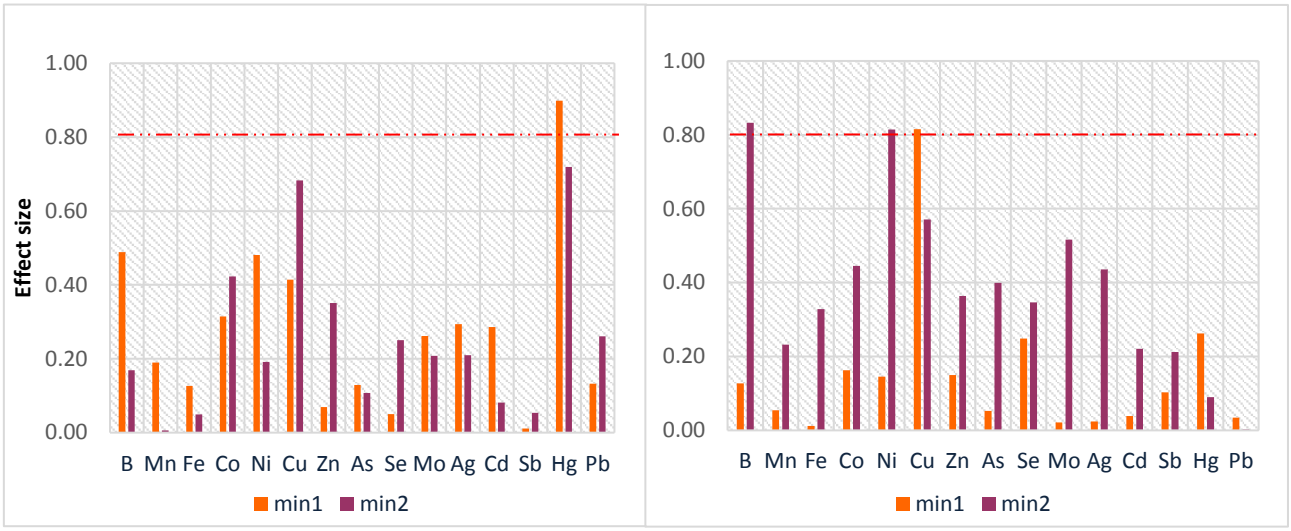

Figure 5-2: Effect sizes of soil element concentrations for soils in mineralised areas: a) A horizon (min1; min2); b) B horizon (min1; min2). > 0.8 is a large effect size relative to background concentrations.

5.3.2 Trace element content in soil as a function of ore body depth

Regression analysis, with SAS software, shows each element and how its concentration in the soil relates to the depth of the copper mineralisation. Between 103 and 109 observations were used to determine the tabled values for each element. The regression coefficient and intercept (Table 5-4) predicts the dependent variable (element concentration in soil) from the independent variable (ore body depth). As discussed in Chapter 4, the regression equation is presented by the following equation:

$$Y = a + bX$$

where 'a' represents the intercept and 'b' represents the regression coefficient. 'Y' represents the dependent (predicted) variable, which is element concentration and 'X' represents the independent variable, namely ore body depth. Expressed in terms of the variables for Cu for instance, the regression equation for the A horizon is

$$[Cu] = 5.97 – 0.0035 \text{ (ore depth)};$$

and the regression equation for the B horizon is

$$[Cu] = 5.72 – 0.0014 \text{ (ore depth)}.$$

The parameter estimates in these equations estimate the relationship between the independent variable (ore body depth) and the dependent variable (element concentration).

The estimates indicate the amount of increase in Cu concentration that would be predicted by a 1-unit increase in ore depth. For the A horizon, the regression coefficient is -0.0035. Therefore, for every unit increase in ore depth, a -0.0035 unit decrease in Cu concentration is predicted. The t-values and p-values (Table 5-4) are used to test whether the coefficients are significant.

A preselected p-value of < 0.05 was chosen to indicate that parameter estimates with a p-value of 0.05 or lower would be statistically significant (i.e. the null hypothesis can be rejected, and it can be said that the coefficient is significantly different from 0. Element concentrations in the A horizon with a p-value < 0.05, and therefore significant coefficient, include Ag, As, B, Cd, Cu, Hg, Mn, Ni, Pb and Sb. Elements with a large p-value (> 0.05), include Fe, Co, Zn, Se and Mo.

The R-square (Table 5-4) is the proportion of variance in the dependent variable (element concentration) which can be predicted from the independent variable (ore depth). An R^2 of 0.01 is considered small, an R^2 of 0.1 is medium and an R^2 of 0.25 is large. Using Cu content in the A horizon as example, the R^2 indicates that 20% of the variance in Cu concentration in the A horizon can be predicted from the ore depth. The R^2 for each analysed element in the A horizon is indicated in Figure 5-3.

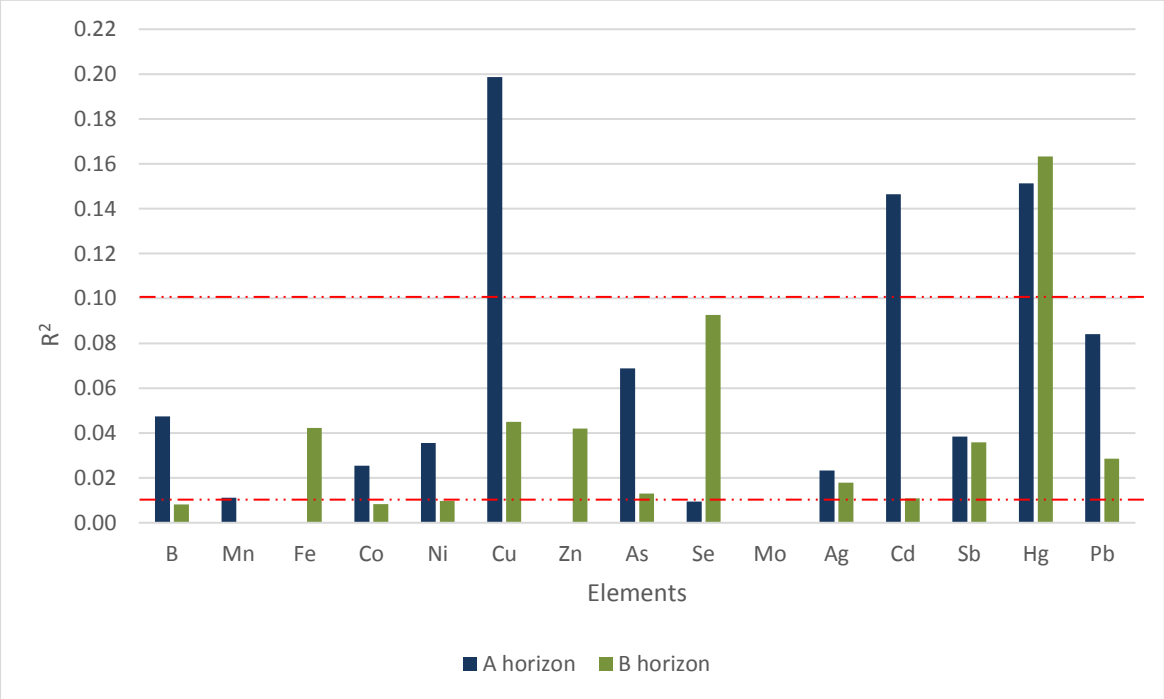

Figure 5-3: R^2 values for element concentrations in the soil horizons, as it relates to depth of ore. Red lines indicate the R^2 categories. R^2 = 0.01 (small); R^2 = 0.1 (medium) and R^2 = 0.25 (large).

A large R^2 was not reported for any of the elements in the A horizon, however Cu, Cd and Hg exhibited a medium R^2, and B, Mn, Co, Ni, As, Ag, Sb and Pb had a small R^2 (Figure 5-3). When analysing trace element content of the A horizon it should therefore be considered that especially Cu, Cd and Hg concentrations are influenced by the depth of the ore body and the effect of depth should therefore be considered when interpreting analysis results for these elements. Cu and Cd have negative regression coefficients, indicating that an increase in ore depth, will result in lower concentrations of these elements in the A horizon. Hg has a medium R^2, but the regression coefficient is positive, indicating that an increase of Hg content in the A horizon is accompanied by an increase in ore depth.

In the B horizon, none of the elements exhibited a large R^2 value, however Hg exhibited a medium R^2, and Fe, Ni, Cu, Zn, As, Se, Ag, Cd, Sb and Pb had small R^2 values (Figure 5-3). When analysing trace element content of the B horizon, it should therefore be considered that especially Hg concentrations are influenced by the depth of the ore body and it should be considered when interpreting analysis results for this element. Hg has a positive regression coefficient (Table 5-4), indicating that an increase in ore body depth is accompanied by an increase in Hg concentration in the B horizon.

Table 5-4: Correlation between ore body depth and trace element content in the soil horizons.

	A horizon							B horizon						
	Mean	Sum	Intercept	Regression coefficient	t-value	p-value	R^2	Mean	Sum	Intercept	Regression coefficient	t-value	p-value	R^2
B	35.05	3785.90	42.348	-0.0165	-2.53	**0.013**	0.047	55.86	5809.70	52.302	0.0083	1.07	0.289	0.008
Mn	35.85	3871.90	39.403	-0.0080	-2.11	**0.037**	0.011	33.89	3524.40	33.395	0.0012	0.27	0.784	<0.001
Fe	2901.90	313404.80	2838.363	0.1438	0.57	0.572	0.002	3863.00	401756.50	3507.840	0.8321	2.50	**0.014**	0.042
Co	312.37	33735.40	277.217	0.0796	1.67	0.099	0.025	158.51	16484.80	176.027	-0.0410	-1.08	0.283	0.008
Ni	956.40	103291.30	1158.032	-0.4565	-2.15	**0.034**	0.036	1626.40	169143.90	1506.019	0.2820	1.16	0.247	0.010
Cu	4.44	479.73	5.966	-0.0034	-5.56	**<0.001**	0.199	5.12	532.36	5.722	-0.0014	-2.34	**0.021**	0.045
Zn	4.35	469.42	4.292	0.0001	0.34	0.734	<0.001	4.32	449.27	3.783	0.0013	2.56	**0.012**	0.042
As	0.41	44.26	0.498	-0.0002	-7.13	**<0.001**	0.069	0.41	42.45	0.443	-0.0001	-2.36	**0.020**	0.013
Se	0.03	3.12	0.033	<0.0001	-1.05	0.297	0.009	0.02	2.31	0.011	<0.0001	3.85	**<0.001**	0.093
Mo	1.58	170.87	1.672	-0.0002	-0.45	0.653	0.001	2.72	283.39	2.636	0.0002	0.34	0.735	0.001
Ag	0.06	6.70	0.087	-0.0001	-3.88	**<0.001**	0.023	0.05	5.25	0.060	<0.0001	-1.70	0.093	0.018
Cd	0.01	0.93	0.011	<0.0001	-5.93	**<0.001**	0.147	0.01	0.82	0.009	<0.0001	-1.27	0.207	0.011
Sb	0.03	3.16	0.035	<0.0001	-4.48	**<0.001**	0.038	0.03	3.07	0.035	<0.0001	-3.20	**0.002**	0.036
Hg	1.60	173.13	0.900	0.0016	4.83	**<0.001**	0.151	0.67	69.49	0.109	0.0013	3.07	**0.003**	0.163
Pb	1.70	183.94	1.954	-0.0006	-5.68	**<0.001**	0.084	1.82	189.42	1.970	-0.0003	-2.93	**0.004**	0.029

5.4 Conclusion

A summary of the results from Chapter 5 are shown in Table 5-5. Elements that were generally accumulated in practically significant amounts in soil sampled over concealed copper mineralisation, include B, Cu, Ni and Hg.

When analysing soils, it is therefore recommended that focus is placed on these four elements. However, when conducting a soil geochemical survey, trace element analysis can be adapted to each soil horizon, according to the elements that delivered the most practical significant results. This implies that for the A horizon, analyses will target Hg and Cu concentrations and for the B horizon the analyses will target B, Ni, Cu and Mo.

Some trace elements exhibited a degree of correlation with depth of ore body. A medium R^2 (R^2 = 0.1) was reported for Cu, Cd and Hg in the A horizon and for Hg in the B horizon (Table 5-5). It should therefore be considered that mineralisation depth will influence the concentrations of these elements in soil. The effect of ore depth should therefore be considered when interpreting results for these elements.

Table 5-5: Summary of results: A vs B horizon as sampling medium.

		B	Mn	Fe	Co	Ni	Cu	Zn	As	Se	Mo	Ag	Cd	Sb	Hg	Pb
Statistically significant differences ($p<0.05$) between mean soil element concentrations on different mineralisation units ('min', 'min1', 'min2' and 'back')	A horizon	x	x		x	x	x	x							x	
	B horizon	x	x			x	x	x	x	x	x	x				
Practically significant differences (large effect, d≥0.8 in red; medium effect, d=0.5 in orange) between element content in soil over mineralisation and soil on background	A horizon						x								x	
	B horizon	x				x	x				x					
Significant ($p<0.05$) reduction/increase in soil element concentration with every unit increase in ore depth	A horizon	x	x			x	x		x			x	x	x	x	x
	B horizon			x			x	x	x	x				x	x	x
Proportion of variance in element concentration that can be predicted from ore depth (medium $R^2 = 0.1$, in red; small $R^2 = 0.01$, in orange)	A horizon	x	x		x	x	x		x			x	x	x	x	x
	B horizon			x		x	x	x	x	x		x	x	x	x	x

CHAPTER 6: TRACE ELEMENTS PLANT-SOIL-ORE RELATIONSHIPS

6.1 Introduction

Thick layers of overburden pose significant challenges to geochemical exploration since the migration of indicator elements to the surface is restricted. For successful exploration, it is necessary to understand the mechanisms of element migration and to identify the elements or compounds that truly reflect dispersion from deeply buried ore deposits. Most of the ore discoveries that is yet to occur, will be at depth, so these deposits will have to be detected from the surface with geochemistry and geophysics (Barr, *et al*., 2015). Biogeochemistry offers an innovative approach by which elements can be traced from the geosphere to the biosphere (Dunn, 2007).

Phytoprospecting is of interest, particularly since some plant species develop root systems that can reach depths of more than 300 m (Levinson, 1974). The roots of a large tree can extract elements from a large volume of soil, overburden, groundwater and occasionally, bedrock. During chemical weathering, mobilised elements are concentrated in the form of dissolved ions in the soil moisture and these elements then become available for plant absorption by complex mechanisms (Levinson, 1974). After absorption by plants or trees, the elements migrate to the above-ground parts of the plant where they may become accumulated. Distinct species display different requirements for and tolerance to various chemical elements, therefore partitioning of elements and selective absorption and transference into the plants take place (Dunn & Hastings, 1998). By analysing plant tissues, anomalies indicating possible mineralisation, may be found (Levinson, 1974).

The relationship between element concentrations in the soil and those in the underlying ore, are affected by element mobility. Chemical reactions dominating the mobility of elements near the oxidizing sulphide deposit may vary significantly from those associated with normal environments (Hawkes, 1957). For instance, in the zone of secondary enrichment, where chloride is absent, Ag is more mobile than Pb or Au.

In addition to their total concentrations, the dispersion of elements in soil depend also on their chemical form, the type and strength of the chemical bonds, the solutions in contact with the sample, the mineralogical and physical properties of the solid phase, environmental

factors like climate and the bio-availability of the chemical form (Alonso-Azcarate, *et al*., 2016).

The concentrations of elements in plants are significantly lower than in the soil (Akcay, *et al*., 1998). Leaf element concentration depends on the bio-available levels in the soil, which is only a small fraction of the total concentration that can be absorbed by plants through the roots and translocated to the leaves (Alonso-Azcarate, *et al*., 2016). Elements available for absorption by plants include ions either dissolved in the soil moisture or adsorbed on the clay minerals of the soil. Soil pH, cation exchange capacity, oxidation potential and presence of complexing agents will influence the availability of elements (Hawkes, 1957). The binding properties between the soil particles and elements as well as the synergistic and antagonistic interactions between the elements will complicate the process of element absorption by plants (Hill & Hulme, 2003). The root tips of plants have a weak atomic charge and are slightly acidic so that hydrogen ions are exchanged for cations such as Cu, Ni, Zn and others related to it. The elements must first be solubilized by the plants and then transferred to the aerial parts (Hill, *et al*., 2008). Element absorption may also be affected by biomass, soil mineralogy (elemental species) and the physiology of the plant (Stanton, 1988).

According to Brooks (1998, cited in Lund *et al*., 2005), good biogeochemical indicator species have an “approximately linear relationship between elemental content in the plants and the concentration of the same element in the soil”. The total concentration of a trace element in the soil and its chemical form will affect its bio-availability. A combination of high element concentration and low pH will lead to high plant absorption of elements (Thornton, 1999, cited in Ghaderian & Ravandi, 2012).

Due to the numerous factors affecting element absorption, the total soil element content does not always accurately reflect the level of elements available to plants. It is suggested that the soluble trace element content will correlate better with the trace element content in the leaves. This chapter sets out to find a connection between concentrations of key ore-related elements and soil- and plant element concentrations. The total and soluble trace element content of the soil are then compared to content in plant tissue.

Objectives for this chapter, involve identifying correlations between trace element content in the leaves of dominant plant species (*B. albitrunca*, *C. gratissimus* and *G. bicolor*) and

1. Total element concentration in the A horizon;
2. Total element concentration in the B horizon;

3. Soluble element concentration in the B horizon; and
4. Element content in the ore.

6.2 Method

Soil and plant samples were analysed by ICP-MS to determine the trace element content. Subsamples of the soils were also used to determine soil pH for both the A and B horizons using the < 2 mm fraction of the soil of each composite sample.

Composite soil and plant tissue samples were digested according to the EPA 3050B method: a strong acid digestion that will dissolve almost all elements that could become available to the environment. Ammonium nitrate extractions were completed for the B horizon soil samples to determine the soluble trace element content, which will give a better indication of the elements available for plant uptake. The soil samples and plant tissue were analysed using Agilent 7500 CE ICP-MS.

Regression analysis with SAS software (version 9.4) was applied to establish the relationship between concentrations of the key trace elements in the ore body and concentrations in the sampling media. It was also used to evaluate the connection between element concentrations in the A and B soil horizons and element concentrations in plant tissue. To summarise, the objectives were to test for the relationships between

i) key trace elements (Ag, Cu, Mo, Pb and Zn) of the ore body;
ii) total element concentration of 17 selected elements (Ag, As, B, Ba, Cd, Co, Cr, Cu, Fe, Hg, Mn, Mo, Ni, Pb, Sb, Se, and Zn) in the A horizon;
iii) total element concentration of the 17 selected elements in the B horizon;
iv) soluble element concentration of the 17 selected elements in the B horizon;

and element concentrations in the plant tissue of three dominant species.

The correlations between trace element content in the soil and content in plant tissue were quantified by calculating transfer factors. If an increase in soil element content is accompanied by an increase of the same or higher quantities of the element in plant tissue, the transfer factor is defined as TF>1. This applies to all the results discussed in the remainder of this chapter.

6.3 Results and discussion

6.3.1 Trace element content in plant tissue as a function of content in soil and ore.

Regression analysis results for elements Sb, As, Ba, B, Cd, Cr, Co, Cu, Fe, Pb, Mn, Hg, Mo, Ni, Se, Ag and Zn are displayed in Appendix A (Table A-1 to Table A-18). In each case, model 1 evaluates the relationship between the dependent variable (trace element content in plant tissue) and the independent variable (trace element content in soil). Model 2 evaluates the relationship between leaf content and soil content, with the effect of pH accounted for. pH is included in the model as a co-variable, since it influences the bio-availability of elements and therefore the degree of element absorption plants. Regression fit plots for elements displaying significant and large correlations between plant tissue and soil elemental content, are also included in Appendix A (Figure A-1 to Figure A-18).

Relationships between concentrations of the key elements in the ore body and concentrations of these elements in the plant tissue of the most frequently occurring species was investigated with regression analysis and are displayed in Appendix B (Table B-1 to Table B-3). Species that were evaluated include *B. albitrunca*, *C. gratissimus* and *G. bicolor.* The concentrations of elements in the ore, were calculated as a factor of the ore thickness, to give an indication of the quantity of elements available for migration into upper overburden layers and absorption by plants. Element concentrations in the ore are therefore indicated in units of ppm/m. Regression fit plots for elements displaying significant and large correlations between plant tissue and ore elemental content are also included in Appendix B (Figure B-1 to Figure B-2).

6.3.2 Summary of findings on trace element correlations between plants, soil and ore.

R^2 values expressing the extent of the correlation between trace element levels in plant tissue and trace element levels in the underlying substrates and ore, are summarised in Table 6-1. Values are displayed only in cases where the regression models are statistically significant. Included in the table, are counts for each element of each plant species, to indicate the number and strength of significant correlations the element exhibited in terms of the connection between concentrations of the element in plant tissue and the concentrations in the soil. Regression models that produced large R^2-values, can predict a large proportion of the variance in leaf element concentrations. These are therefore the models which will be

the most successful when it comes to making predictions from element concentrations in the soil and ore body.

In *B. albitrunca*, Ni and Ba proved to be elements with the highest count for significant correlations between soil and plant tissue content. Large proportions of the variance in Ni and Ba leaf content can be predicted from several of the regression models. In *C. gratissimus*, Mn proved to be the element with the highest count for significant correlations between soil and plant tissue content. Large proportions of the variance in Mn leaf content can be predicted from several of the regression models. Cr, Co, Mo, Ni and Se also exhibited some strong correlation in several of the regression models. In *G. bicolor*, Ba and Mn proved to be elements with the highest count for significant correlations between soil and plant tissue content. Large proportions of the variance in Ba and Mn leaf content can be predicted from several of the regression models.

Table 6-1: R^2 values for *B. albitrunca, C. gratissimus* and *G. bicolor* (expressed as percentages). R^2 values are only indicated in cases where models produced statistically significant results. The size of R^2 is indicated as follow: red (large R^2); orange (medium R^2); green (small R^2).

B. albitrunca

Model	Variable	Sb	As	Ba	B	Cd	Cr	Co	Cu	Fe	Pb	Mn	Hg	Mo	Ni	Se	Ag	V	Zn
1	Ore content								35.0										3.0
1	A horizon (total)			20.4	18.6			19.2				34.9				16.3			
2	A horizon (total); pH			26.6	35.5			40.8			14.4	36.9		27.4	21.3	46.5			
1	B horizon (total)		13.9	17.7		44.0						18.1			34.9		15.4		
2	B horizon (total); pH		14.0	25.0	23.4	48.7		37.1			15.3	19.2		27.6	42.5	45.4	16.0		
1	B horizon (soluble)		10.3	22.9	8.5									0.9	31.4				
2	B horizon (soluble); pH		10.8	28.4	22.5			36.5						25.6	37.2				
Large R^2				2	1	2		3	1			2		3	4	2			
Medium R^2			4	4	3			1			2	2			1	1	2		
Small R^2					1														1

C. gratissimus

Model	Variable	Sb	As	Ba	B	Cd	Cr	Co	Cu	Fe	Pb	Mn	Hg	Mo	Ni	Se	Ag	V	Zn
1	Ore content																31.9		
1	A horizon (total)		3.8						12.4		6.5	31.0				34.5			20.2
2	A horizon (total); pH	13.3	36.7			20.4	35.3	34.0			27.9	46.8	25.1	18.0	52.1	65.1	5.6	24.5	
1	B horizon (total)											41.5							
2	B horizon (total); pH		35.2			20.5	38.5	34.0			25.4	47.9	23.9	21.2	47.2	54.3		37.9	
1	B horizon (soluble)												4.4	13.8					
2	B horizon (soluble); pH		38.6			18.6	35.8	29.8				48.0	19.0	24.1	47.4				
Large R^2			3				3	3			2	5	1		3	3	1	1	
Medium R^2		1				3			1				2	4				1	1
Small R^2			1								1		1				1		

Table 6-1 (continued): R^2 values for *B. albitrunca, C. gratissimus* and *G. bicolor* (expressed as percentages). R^2 values are only indicated in cases where models produced statistically significant results. The size of R^2 is indicated as follow: red (large R^2); orange (medium R^2); green (small R^2).

G. bicolor

Model	Variable	Sb	As	Ba	B	Cd	Cr	Co	Cu	Fe	Pb	Mn	Hg	Mo	Ni	Se	Ag	V	Zn
1	Ore content													25.7					
1	A horizon (total)	13.1		14.0	16.5			17.4				28.8				10.9	10.9		13.6
2	A horizon (total); pH	17.7	22.7		16.8	16.0	17.2	33.9	14.0		10.0	43.1			47.8	21.1			19.0
1	B horizon (total)	5.2		29.9								20.2							
2	B horizon (total); pH		20.5	37.2		14.7	26.4	24.7	15.1		9.8	42.5			45.9				17.7
1	B horizon (soluble)			42.8											12.0				
2	B horizon (soluble); pH		14.5	61.4		13.1	21.3	27.0				47.0			43.6		7.3		19.0
Large R^2				4			1	2				4		1	3				
Medium R^2		2	3	1	2	3	2	2	2			1			1	2	1		4
Small R^2		1									2						1		

6.4 Conclusion

Although promising results for a wider variety of plant species were generated in Chapter 4, only a limited number of samples could be gathered for most species. Therefore, regression analyses were completed only for three of the most frequently occurring species.

Large correlations were reported for several models predicting trace element content in leaves of *B. albitrunca, C. gratissimus* and *G. bicolor.* Models that exhibited a strong correlation to trace element concentrations in *B. albitrunca* plant tissue include:

I. Total Mn content in the A horizon (model 1);
II. Total Ba, B, Co, Mn, Mo and Se content in the A horizon (model 2);
III. Total Cd and Ni content in the B horizon (model 1);
IV. Total Cd, Co, Mo, Ni and Se content in the B horizon (model 2);
V. Soluble Ni content in the B horizon (model 1);
VI. Soluble Ba, Co, Mo and Ni content in the B horizon (model 2).

Models that exhibited a strong correlation to trace element concentrations in *C. gratissimus* plant tissue include:

I. Total Mn and Se content in the A horizon (model 1);
II. Total As, Cr, Co, Pb, Mn, Hg, Ni and Se content in the A horizon (model 2);
III. Total Mn content in the B horizon (model 1);
IV. Total As, Cr, Co, Pb, Mn, Ni, Se and V content in the B horizon (model 2);
V. Soluble As, Cr, Co, Mn and Ni content in the B horizon (model 2).

Models that exhibited a strong correlation to trace element concentrations in *G. bicolor* plant tissue include:

I. Total Mn content in the A horizon (model 1);
II. Total Co, Mn, and Ni content in the A horizon (model 2);
III. Total Ba content in the B horizon (model 1);
IV. Total Ba, Cr, Mn and Ni content in the B horizon (model 2);
V. Soluble Ba content in the B horizon (model 1);
VI. Soluble Ba, Co, Mn and Ni content in the B horizon (model 2).

CHAPTER 7: CONCLUSION

7.1 Summary of findings

In Chapter 4, plant species were evaluated in terms of significant differences between leaf element concentrations for plants growing over the ore body compared to plants growing in the surrounding area/background. Chapter 5 compared the element concentrations for soil above copper ore to element concentrations for soil in the surrounding environment. Significant differences were obtained for three elements in the B horizon (B, Ni and Cu), and a single element in the A horizon (Hg). When the results from Chapter 4 are considered with results from Chapter 5, it shows that significant differences were calculated more often for element concentrations in plant species, than for element concentrations in soils. For instance, *B. foetida* subsp. *rehmanniana* delivered large effect sizes for seven elements (B, Mn, Fe, Cu, Zn, As and Se), while large effect sizes were calculated for a maximum of three elements in a specific soil horizon. Several plant species expressed anomalous quantities of certain elements in their plant tissue, whereas concentrations of these elements did not occur in higher than normal levels in the soil. This might be indicative of elevated levels in leaf tissue being related to the rooting depth of the tree species or the ability of the plant to hyperaccumulate certain elements. In these instances, element concentrations in the plants will reflect the trace element content of the underlying copper ore more accurately than element concentrations in the soil.

In Chapter 5, it was reported that copper and other related elements occurred at higher values in the A and B horizon of overburden situated above copper ore, as opposed to the surrounding environment. As mentioned previously, significant differences were calculated for more elements in the B horizon than for elements in the A horizon, when comparing element concentrations in soils of different mineralisation units. It was originally hypothesized that element concentrations in the B horizon specifically, will be higher due to illuviation and other soil processes that concentrate elements in the deeper subsoil. However, even though absolute concentrations in the B horizon were not always higher than the concentrations in the A horizon, it exhibited spatial relationships that were more accurate in terms of reflecting underlying mineralisation. It was found that trace elements in the B horizon more often gave an indication of underlying mineralisation than did trace elements in the A horizon.

Regression, discussed in Chapter 6 delivered outcomes expressing the correlation between trace element concentrations in soil and the concentrations of elements in plant tissue. Where available, as in the case of the key ore-related elements, element concentration data for the ore body was used to create models predicting ore element content from concentrations in plant tissue. Cu content in the leaves of *B. albitrunca* exhibited a strong correlation to Cu content in the ore body. Ag content in the leaves of *C. gratissimus* also exhibited a strong correlation to Ag content in the ore body. Furthermore, a strong correlation between Mo content in the leaves of *G. bicolor* and Mo content in the ore body was reported. This makes it possible to predict a large proportion of the variance in ore element content from the levels of these elements in plant tissue.

Although the concentrations of the main ore elements were known, no such data was available for other pathfinder elements. Therefore, only models evaluating the relationship between trace element content in soil and trace element content in plant tissue could be created for pathfinder elements. Only a limited indication of the connection between leaf element content and element concentrations in the underlying ore could be inferred. Since ore data were not available for many of the elements discussed in this report, models predicting ore content from leaf content could not be generated for various elements. To overcome this information gap, the findings of Chapter 5 are considered here. In Chapter 5, the A and B soil horizons were evaluated in terms of significant differences between soil element concentrations for overburden above copper ore relative to soil element concentrations in the surrounding environment/background. Certain elements accumulated in significantly different quantities in soils from different mineralisation units. Provided that there is a strong correlation between concentrations of any given element in plant tissue and soil, and provided the element was accumulated in significantly different concentrations in the soils of different mineralisation units, it can be deduced that the element concentrations in plant tissue are probably related to concentrations of the element in the underlying copper ore.

B. albitrunca exhibited various strong correlations between element content in leaves and content in the soil, for a number of elements (see Chapter 6). Many of these elements were also accumulated in significantly different quantities in soils of different mineralisation units. Such elements include Mn, B, Co, Ni and Se. Ba were not discussed in Chapter 4 and therefore no further conclusions can be drawn for this element in terms of its ore content prediction value. It is suggested that the following prediction models will be the most useful for estimating ore element concentrations from soil and *B. albitrunca* leaf content:

I. Total Mn in the A horizon (model 1);
II. Total B, Co and Mn in the A horizon (model 2);
III. Total Ni in the B horizon (model 1);
IV. Total Mo, Ni and Se in the B horizon (model 2);
V. Soluble Ni in the B horizon (model 1) and
VI. Soluble Mo and Ni in the B horizon (model 2).

C. gratissimus exhibited various strong correlations between leaf element content and soil content for a number of elements (see Chapter 6). Many of these elements were also accumulated in significantly different quantities in soils of different mineralisation units. Such elements include Mn, Co, Hg, Ni, As and Se. Cr and V were not discussed in Chapter 4 and therefore no conclusion can be drawn for these elements in terms of their ore content prediction value. From the available data, it is suggested that the following prediction models will be the most useful to estimate ore element concentrations from soil and *C. gratissimus* leaf content:

I. Total Mn in the A horizon (model 1);
II. Total Co, Mn, Hg and Ni in the A horizon (model 2);
III. Total Mn in the B horizon (model 1);
IV. Total As, Mn, Ni and Se in the B horizon (model 2);
V. Soluble As, Mn and Ni in the B horizon (model 2).

G. bicolor exhibited various strong correlations between leaf element content and soil content for a number of elements (see Chapter 6). Many of these elements were also accumulated in significantly different quantities in soils of different mineralisation units. Such elements include Mn, Ba, Co, Cr and Ni. Ba and Cr were not discussed in Chapter 4 and therefore no conclusion can be drawn for these elements in terms of their ore content prediction value. It is suggested that the following prediction models will be the most useful to estimate ore element concentrations from soil and *G. bicolor* leaf content:

I. Total Mn in the A horizon (model 1);
II. Total Co, Mn and Ni in the A horizon (model 2);
III. Total Mn and Ni in the B horizon (model 2);
IV. Soluble Mn and Ni in the B horizon (model 2).

7.2 Major conclusions

This section describes the conclusions made regarding the indicator potential of woody plant species, as well as the degree of element accumulation in different soil horizons. It also concludes on element concentrations in the ore and how it relates to concentrations in soil and in the plant tissue of selected species.

I. Evidence suggests that elevated levels in some leaf tissue might be related to the rooting depth or hyperaccumulating abilities of tree species. Certain elements in specific plant species will therefore reflect underlying copper mineralisation more accurately than element concentrations in the soil.

II. The specific trace elements in soil that reflected underlying copper ore differed between different soil horizons. Trace elements in the B horizon more often reflected underlying mineralisation than did trace elements in the A horizon.

III. *B. albitrunca, C. gratissimus* and *G. bicolor* exhibited various strong correlations between soil and leaf element content for several elements. Many of these elements were also accumulated in significantly different quantities in soils of different mineralisation units. It was therefore surmised that for many elements, concentrations in plant tissue were also related to concentrations in the underlying copper ore.

IV. The correlations between trace element content in the soil and content in plant tissue were quantified by calculating transfer factors. In numerous cases, an increase in soil element content was accompanied by an increase of the same or higher quantities of the element in plant tissue, the transfer factor in these instances defined as TF>1. Species with large transfer factor exhibited hyperaccumulating abilities.

7.3 Recommendations for future research

- Some of the plant species discussed in Chapter 4 (such as *B. foetida* subsp. *rehmanniana*, *C. apiculatum* and *T. prunioides*), only occurred sporadically at sampling sites. Therefore, a limited number of individuals were available for sampling. For HLM and regression analysis, it is ideal to include 50 observations when running any given model, so that a higher level of confidence can be associated with results. The author recommends that future studies determining correlations between element concentrations in plant tissue and concentrations in the

underlying substrates, should design a sampling protocol which meets these requirements.

- The sampling design for this project, entailed transects running along the dip of the ore body, with samples being collected at regular intervals along the transect. The implications of this type of design are that borehole data cannot be associated with each specific sample point. It is suggested for similar future studies, that sample points are located at borehole sites and soil and plant samples should then be collected in an appointed radius around the borehole (see Figure 7-1). The effect of the dipping ore body can still be investigated, with the added advantage that each sample point can be connected to a specific borehole. More borehole data can then be included in regression analysis, making it possible to create more effective prediction models to estimate trace element content in the ore body.

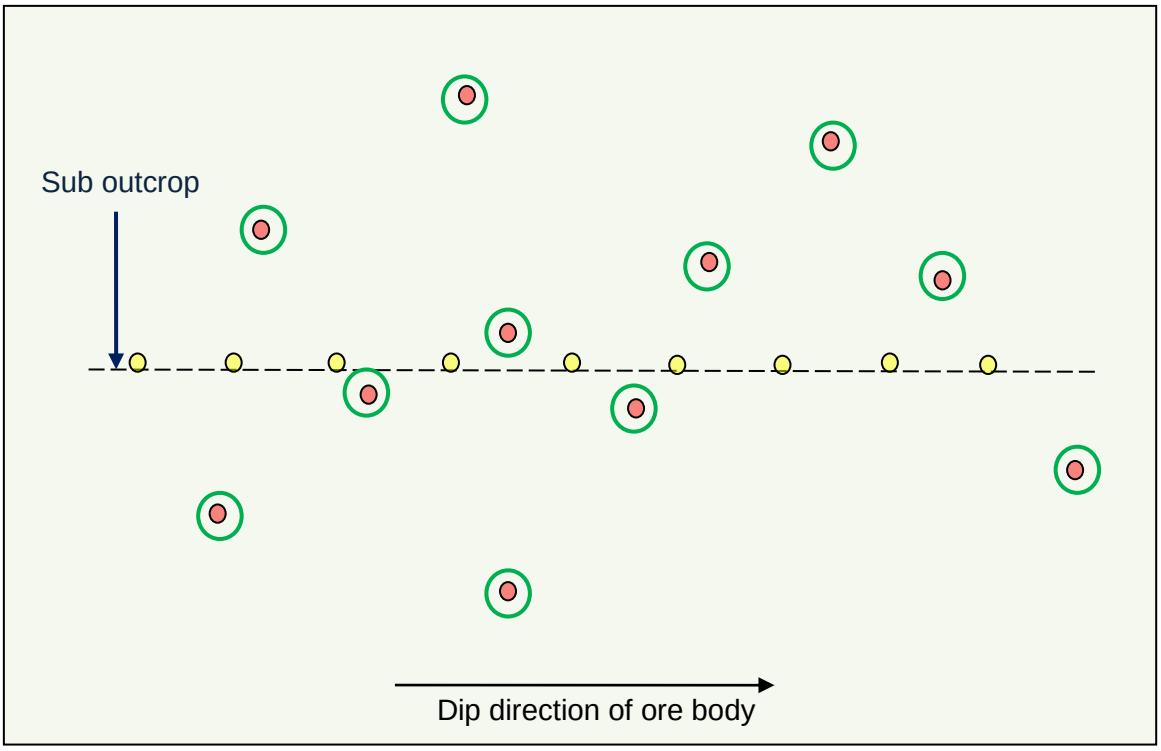

Figure 7-1: Scenario illustrating proposed sample sites for similar future investigations into plant-soil-ore trace element correlations.

- In this study, assay results for drill core included only the main elements associated with copper ore (Cu, Zn, Pb, Mo and Ag). These are essentially the elements that will be exploited during mining. However, concentrations of these elements in the overlying overburden do not always give the most accurate delineation of the ore body. It is therefore necessary to target other ore-related elements (such as Co, Cd, Hg, As and others) that can act as pathfinders of copper ore. One of the objectives of this study was to target these pathfinder elements. However, the concentrations of these elements in the ore body were not known. Therefore, any given pathfinder element could only be evaluated in terms of the relationship between its concentrations in plant tissue and its concentrations in the soil. For future studies, it is recommended that drill core is assayed for a wider range of elements, so that predictions models can be created not only for the main ore elements, but also for pathfinder elements that might give a more accurate reflection of underlying copper mineralisation.
- There is still a lot of research that needs to be done in terms of plant-soil-ore trace element correlations, in order to develop predictions models that can be used to detect concealed copper ore. Once drill core data is available for the main ore elements as well as pathfinder elements, the concentrations of these elements in soil and plant tissue might be used to predict (to a certain extent) the concentrations that will be present in the underlying ore. It is suggested that prediction models are created in such a way that ore content is defined as the dependent variable; and soil content, plant tissue content and pH is included in the model as independent variables. For instance, consider the following finding: Co content in *B. albitrunca* leaves related strongly to total Co concentrations in the soil A horizon (in model 2 where pH is also considered). If drill core data for Co becomes available and the relationship between Co content in the ore and Co content in the overlying soil and plat tissue is determined, the following prediction model can be created:

  Ore [Co] = x (total [Co] in the A horizon) + y (pH) + z ([Co] in leaves of *B. albitrunca*),

  where x, y and z are regression coefficient for the different regression parameters. This model can then be used to predict Co concentrations in the ore by using its concentrations in the soil and *B. albitrunca* leaves and also the pH of the soil.

REFERENCES

Aaron, D.S. & Anand, R.R. 2012. Source of anomalous gold concentrations in termite nests, Moolart Well, Western Australia: implications for exploration. *Geochemistry: Exploration, Environment, Analysis,* 12(4): 327-337.

Adamo, P.A., Agrelli, D., Albanese, S., De Vivo, B., Iavazzo, P. & Lima, A. 2014. Bioavailability and soil-to-plant transfer factors as indicators of potentially toxic element contamination in agricultural soils. *Science of the Total Environment:* 11-22.

Addai-Mensah, J., Albrecht, T.W.J. & Fornasiero, D. 2011. Effects of pH, concentration and temperature on copper and zinc formation/ precipitation in solution. Paper presented at the conference Chemeca 2011: Engineering a Better World, Hilton Sydney, New South Wales, Australia, 18-21 September. http://www.conference.net.au/chemeca2011/papers/477.pdf Date of access: 5 Mar. 2018.

Akanyang, P., Davis, D.W., Kwok, Y.Y. & Schwartz, M.O. 1996. Geology, geochronolgy and regional correlation of the Ghanzi Ridge, Botswana. *South African Journal of Geology,* 99(3): 245-250.

Akanyang, P., Ngwisanyi, T.H. & Schwartz, M.O. 1995. The sediment-hosted Ngwako Pan copper deposit, Botswana. *Economic Geology,* (90)*:* 1118-1147.

Akcay, M., Lermi, A. & Van, A. 1998. Biogeochemical exploration for massive sulphide deposits in areas of dense vegetation: an orientation survey around the Kankoy Deposit (Trabzon, NE Turkey). *Journal of Geochemical exploration,* (63): 173-187.

Alonso-Azcarate, J., Esbri, J.M., Garcia-Noguero, E.M., Garcia-Ordiales, E., Higueras, P., Gonzales-Corrochano, B., Lopez-Berdonces, M.A. & Martinez-Coronado, A. 2016. Potentially harmful elements in soils and holm-oak trees (Quercus ilex L.) growing in mining sites at the Valle de Alcudia Pb-Zn district (Spain) - some clues on plant metal uptake. *Journal of Geochemical Exploration,* (182):166-179.

Anand, R., Cohen, D.R., Coker, W.B. & Kelley, D.L. 2010. Major advances in exploration geochemistry, 1998-2007. *Geochemistry: Exploration, Environment, Analysis,* 10(1): 3-16.

Anand, R.R. 2016. Regolith-landform processes and geochemical exploration for base metal deposits in regolith-dominated terrains of the Mt Isa region, northwest Queensland, Australia. *Ore Geology Reviews,* (73): 451-474.

Anand, R.R. & Cornelius, M. 2004. Vegetation and soil expression of the Jaguar base metal deposit, Yilgarn craton. *Regolith:* 7-8.

Ayres, N. & Key, R.M. 2000. The 1998 edition of the National Geological Map of Botswana. *Journal of African Earth Sciences,* 30(3): 427-451.

Baker, A.J.M. 1981. Accumulators and excluders - strategies in the response of plants to heavy metals. *Journal of Plant Nutrition,* 3(1-4): 643-654.

Baker, A.J.M. & Brooks, R.R. 1988. Botanical exploration for minerals in the humid tropics. *Journal of Biogeography,* (15): 221-229.

Baker, A.J.M. & Brooks, R.R. 1989. Terrestrial higher plants which hyperaccumulate metallic elements - a review of their distribution, ecology and phytochemistry. *Biorecovery,* (1): 81-126.

Barr, J., Ihlenfeld, C. & Kyser, K. 2015. Applied geochemistry in mineral exploration and mining. *Elements,* (11): 241-246.

Bimin, Z., Rong, Y., Shanfa, X., Wensheng, Y. & Xueqiu, W. 2016. Geochemical challenges of diverse regolith-covered terrains for mineral exploration in China. *Ore Geology Reviews,* (73): 417-431.

Bohn, H.L., O'Connor, G.A. & Strawn, D.G., 2015. Soil chemistry. 4th ed. Chichester, UK: John Wiley & Sons, Ltd.

Bonnett, L.C., Gazley, M.F. & Salama, W. 2016. Geochemical exploration for supergene copper oxide deposits, Mount Isa inlier, NW Queensland, Australia. *Journal of Geochemical Exploration,* (168): 72-102.

Boocock, C. & Van Straten, O.J. 1962. Notes on the geology and hydrogeology of the central Kalahari region, Bechuanaland Protectorate. *South African Journal of Geology,* 65(1): 125-176.

Borg, G. & Maiden, K.J. 1987. Alteration of late Middle Proterozoic volcanics and its relation to stratabound copper-silver mineralisation along the margin of the Kalahari Craton in SWA/Namibia and Botswana. *Geological Society Special Publication,* (33): 347-354.

Brown, R.C. & Cole, M.M. 1976. The vegetation of the Ghanzi area of western Botswana. *Journal of Biogeography,* (3): 169-196.

Canadell, J., Ehleringer, J.R., Jackson, R.B., Mooney, H.A., Sala, O.E. & Schulze, E.D. 1996. Maximum rooting depth of vegetation types at the global scale. *Oecologia,* (108): 583-595.

Cannon, H. L. 1971. The use of plant indicators in groundwater surveys, geologic mapping, and mineral prospecting. *Taxon,* 20(2-3): 227-256.

Cannon, W.F., Federico, S., Fey, D.L., Kilburn, J.E., Smith, D.B. & Woodruff, W.F. 2013. Geochemical and mineralogical data for soils of the conterminous United States: Appendix 1. U.S. Geological survey soil sampling manual for the North American soil geochemical landscapes project. Virginia, US: United States Geological Survey.

Causey, J.D., Denning, P.D., Hammarstrom, J.M., Hayes, T.S., Horton, J.D., Kirschbaum, M.J., Parks, H.L., Taylor, S.D., Wilson, A.B., Wintzer, N.E. & Zientek, M.L. 2013. Descriptive models, grade-tonnage relations, and databases for the assessment of sediment-hosted copper deposits - with emphasis on deposits in the central African copperbelt, Democratic Republic of the Congo and Zambia. Virginia, US: United States Geological Survey.

Chaffee, M.A. 1977. Geochemical exploration techniques based on distribution of selected elements in rocks, soils and plants, Vekol porhyry copper deposit area, Pinal County, Arizona. Washington, D.C.: United States Government Printing Office .

Chaffee, M.A., Cox, D.P., Cox, L.J. & Douglas, P.K. 1995. Porphyry Cu deposits. Virginia, US: United States Geological Survey.

Chen, J., Chen, Z., Tian, S. & Xu, B. 2016. Application of fractal content-gradient method for delineating geochemical anomalies associated with copper occurences in the Yangla ore field, China. *Geoscience Frontiers:* 1-9.

Coleman, N.T. & Williams, D.E. 1950. Cation exchange properties of plant root surfaces. *Plant and Soil,* 2(2): 243-256.

Cole, M.M. 1971. Biogeographical/geobotanical and biogeochemical investigations connected with exploration for nickel-copper ores in the hot, wet summer/dry winter savanna woodland environment. *Journal of the South African Institute of Mining and Metallurgy:* 199-209.

Cole, M.M. & Le Roex, H.D. 1978. The role of geobotany, biogeochemistry and geochemistry in mineral exploration in South West Africa and Botswana - a case history. *Transactions of the Geological Society of South Africa,* (81): 277-317.

Collins, J.C. 1981. Zinc. (*In* Lepp, N.W., *ed*. Effect of heavy metal pollution on plants. Liverpool,UK: Applied Science Publishers. p. 145-170.

Colm McGuinness. 2015. Statistical significance, p-values and confidence intervals: a brief guide for non-statisticians using SPSS statistics. http://bbm.colmmcguinness.org/live/Advanced/Statistical%20Significance.pdf Date of access: 5 Oct. 2017.

Cooke, H.J. 1980. Landform evolution in the context of climatic change and neo-tectonism in the Middle Kalahari of north-central Botswana. *Transactions of the Institute of British Geographers,* 5(1): 80-99.

CTAHR. 2007. Soil nutrient management for Maui County. https://www.ctahr.hawaii.edu/mauisoil/a_comp03.aspx Date of access: 14 Nov. 2017.

Cupric Canyon Capital. 2017. Khoemacau/Boseto exploration. https://www.cupriccanyon.com/development-exploration/exploration Date of access: 2 Nov. 2017.

Curtis, B.A. & Mannheimer, C.A. 2005. Tree atlas of Namibia. Windhoek, Namibia: National Botanical Research Institute.

De Beer, J.S. 1962. Provisional vegetation map of the Bachuanaland Protectorate. Botswana*:* Department of Agriculture.

Deane, J. 2016. Drill core logs [corr]. 19Jun., Toteng.

Deane, J. 2016. Planning sample transects [corr]. 19 Jun., Toteng.

Dunn, C.E. 2007. Biogeochemistry in mineral exploration. 9th ed. Amsterdam: Elsevier.

Dunn, C.E. & Hastings, N.L. 1998. Biogeochemical survey of the Ootsa-François lakes area using outer bark of Lodgepole Pine (NTS 93F/13, 14, and part of 12), mafic suite of elements with thorium and lanthanum, north central British Columbia. British Columbia: Geological Survey of Canada.

Dunn, C.E., Hulme, K.A. & Hill, S.M. 2006. Biogeochemistry for mineral exploration in Canada & Australia: a comparison based on international collaboration. (*In* Fitzpatrick, R.W. & Shand, P., *ed*. Regolith 2006: Consolidation and dipersion of ideas. Hahndorf Resort, South Australia: CRC Leme p. 161-165.

Dunn, C.E. & Thompson, R.I. 2009. Biogeochemical signatures of the area around the MAX molybdenum mine, southern British Columbia, Ottawa: Geological Survey of Canada.

Ellis, S. & Mellor, A. 2002. Soils and environment. Abingdon, UK: Routledge.

Ellis, S.M. & Steyn, H.S. 2003. Practical significance (effect sizes) versus or in combination with statistical significance (p-values). *Management Dynamics,* 12(4): 51-53.

Emmons, W.H. 1913. The enrichment of sulphide ores. Washington, D.C.: Washington Governemnt Printing Office.

EPA, 1996. Method 3050B: Acid digestion of sediments, sludges and soils. https://www.epa.gov/homeland-security-research/epa-method-3050b-acid-digestion-sediments-sludges-and-soils Date of access: 16 Jun. 2017.

Fedikow, M.A. & Ziehlke, D.V. 2005. Multimedia geochemical signatures of a REE-enriched britholite-allanite zone in the Eden Lake aegirine-augite syenite, Lynn Lake area, Northwestern Manitoba (NTS 64C/9). Manitoba: Manitoba Industry, Trade and Mines.

Feldstain, A., MacKay, C., Rocchi, M. & Woltman, H. 2012. An introduction to hierarchical linear modeling. *Tutorials in Quantitative Methods for Psychology,* 8(1): 52-69.

Freedman, J. 1972. Geochemical prospecting for zinc, lead, copper, silver, Lancaster Valley, Southeastern Pennsylvania. Washington, D.C.: United States Government Printing Office.

Freitas, H.M.D. & Prasad, M.N.V. 2003. Metal hyperaccumulation in plants - biodiversity prospecting for phytoremediation technology. *Electronic Journal of Biotechnology,* 6(3): 285-321.

Gatehouse, S., Russell, D.W. & Van Moort, J.C. 1977. Sequential soil analysis in exploration geochemistry. *Journal of Geochemical Exploration,* (8): 483-494.

Gauthier, A., Kozovits, A.R., Leite, M.G.P., Li, H., Messias, M.C.T. & Schettini, A.T. 2017. Exploring Al, Mn and Fe phytoextraction in 27 ferruginous rocky outcrops plant species. *Flora: 175-182.*

Gee, R.D. 2005. Geochemical anomalies in transported overburden. Hunter Valley NSW: AMIRA International 6th Biennial Exploration Managers Conference.

Ghaderian, S.M. & Ravandi, A.A.G. 2012. Accumulation of copper and other heavy metals by plants growing on Sarcheshmeh copper mining area, Iran. *Journal of Geochemical Exploration,* (123): 25-32.

Giltrap, D.J., Parfitt, R.L. & Whitton, J.S. 1995. Contribution of organic matter and clay minerals to the cation exchange capacity of soils. *Communications in soil science and plant analysis,* 26(9-10): 1343-1355.

Haddon, I.G. 2005. The sub-Kalahari geology and tectonic evolution of the Kalahari basin, Southern Africa. Johannesburg: University of Witwatersrand.

Hall, W.S. 2007. Geology and paragenesis of the Boseto copper deposits, Kalahari copperbelt, Northwest Botswana. Golden: Department of Geology and Geological Engineering.

Hartig, J. 2005. Analysis of hierarchical data. Nicosia: EARLI JuRe preconference.

Hawkes, H.E. 1957. Principles of geochemical prospecting. Washington, D.C.: United States Government Printing Office.

Heberlein, D.R. 2010. An assessment of soil geochemical methods for detecting copper-gold porphyry mineralisation through Quaternary galciofluvial sediments at the WBX-MBX and 66 Zones, Mt. Milligan, north-central British Columbia. Vancouver, Canada: Geoscience BC.

Hill, S.M. & Hulme, K.A. 2003. River bed gums as a biogeochemical sampling medium in mineral exploration and environmental chemistry programs in the Curnamona craton and adjacent regions of NSW and SA. *Advances in Regolith:* 205-210.

Hill, S.M., Lewis, D.M. & Reid, N. 2008. Spinifex biogeochemical expressions of buried gold mineralisation: The great mineral exploration penetrator of transported regolith.. *Applied Geochemistry,* (23): 76-84.

Hinsinger, P. 1998. How do plant roots aquire mineral nutrients? Chemical processes involved in the rhizozphere. *Advances in Agronomy,* (64): 225-265.

Jackson, R.B., Jobbagy, E.G., McCulley, R.L. & Pockman, W.T. 2004. Nutrient uptake as a contributing explanation for deep rooting in arid and semi-arid ecosystems. *Oecologia,* (141): 620-628.

Johnson, G.B., Losos, J.B., Raven, P.H. & Singer, S.R. 2002. Biology. 6th ed. Boston: McGraw-Hill.

Jones, C.R. 1980. The geology of the Kalahari. *Botswana Notes and Records,* (12): 1-14.

Kabata-Pendias, A. 2011. Trace elements in soils and plants. 4th ed. Florida, USA: Taylor and Francis Group.

Kalavrouziotis, I.K., Kostakioti, E. & Koukoulakis, P. 2012. Assessment of metal transfer factor under irrigation with treated municipal wastewater. *Agricultural Water Management,* (103): 114-119.

Kausel, G. 1991. Study of heavy metal tolerant flora in Botswana. *Botswana Notes and Records,* (23): 159-174.

Krug, M.A. 1995. Geochemical exploration in calcrete terrains. Grahamstown: Rhodes University (Thesis – PhD).

Levinson, A.A. 1974. Introduction to exploration geochemistry. Calgary: Applied publishing Ltd.

Lovering, T.S. 1934. Geology and ore deposits of the Breckenridge mining district, Colorado. Washington: United States Government Printing Office.

Lund, W., Nkoane, B.B.M., Sawula, G.M. & Wibetoe, G. 2005. Identification of Cu and Ni indicator plants from mineralised locations in Botswana. *Journal of Geochemical Exploration,* (86): 130-142.

Lund, W., Sawula, G., Takuwa, D.T. & Wibetoe, G. 1997. Determination of cobalt, nickel and copper in flowers, leaves, stem and roots of plants using ultrasonic slurry sampling electrothermal atomic absorption spectrometry. *Journal of Analytical Atomic Spectrometry,* (12): 849-854.

Maeght, J., Pierret, A. & Rewald, B. 2013. How to study deep roots - and why it matters. *Frontiers in Plant Science,* (4): *1*-14.

Maghsoudi, A., Parsa, M., Sadeghi, M. & Yousefi, M. 2016. Prospectivity modeling of porphyry-Cu deposits by identification and integration of efficient mono-elemental geochemical signatures. *Journal of African Earth Sciences,* (114): 228-241.

Maiden, K.J. & Borg, G. 2011. The Kalahari copperbelt in central Namibia: controls on copper mineralisation. *Society of Economic Geologists newsletter*, October: 1-48.

McCoach, D.B. 2010. Hierarchical linear modeling. (*In* Hancock, G.R. Mueller, R.O. *ed*. The reviewer's guide to quantitative methods in the social sciences. New York: Routledge. p. 432.

MOD Resources Ltd.. 2015. Mod Resources: Quarterly activities report - March 2015. http://www.4-traders.com/MOD-RESOURCES-LTD-10353071/news/Mod-Resources-Quarterly-Activities-Report-March-2015-20250048/ Date of access: 30 Oct. 2017.

MOD Resources Ltd.. 2017. Botswana copper project. http://www.modresources.com.au/botswana-copper Date of access: 2 Sept. 2017.

Modie, B.N. 2000. Geology and mineralisation in the Meso- to Neoproterozoic Ghanzi-Chobe Belt of nortwest Botswana. *Journal of African Earth Sciences,* 30(3): 467-474.

Modie, B.N.J. 1996. Depositional environments of the Meso- to Neoproterozoic Ghanzi-Chobe belt, northwest Botswana. *Journal of African Earth Sciences,* 22(3); 255-268.

Morrison, R.S. 1980. Aspects of the accumulation of cobalt, copper and nickel by plants, Palmerston North, New Zealand: Massey University (Thesis – PhD).

Mshumi, U. 2006. Can Acacia karroo and Boscia albitrunca spp. be used in the biogeochemical prospecting for gold: a case study at the Blue Dot Mine, Amalia, Northwest Province, South Africa. Cape Town: University of the Western Cape.

Obakeng, O.T. 2007. Soil moisture dynamics and evapotranspiration at the fringe of the Botswana Kalahari, with emphasis on deep rooting vegetation. Enschede: ITC International Institute for Geo-Information science and earth observation.

Osman, M.H., Shayoub, M.H., Shmou, M.I. & Taha, K.K. 2013. Soil-plant transfer and accummulation factors for trace elements at the Blue and White Niles. *Journal of Applied and Industrial Sciences,* 1(2): 97-102.

Plaster, E.J. 2011. Soil science & management. 5th ed. New-York: Cengage Learning.

Princeton University. 2007. Interpreting regression output. http://dss.princeton.edu/online_help/analysis/interpreting_regression.htm Date of access: 1 Nov. 2017.

Rains, A.B. & Yalala, A.M. 1970. The central and southern state lands, Botswana. Tolsworth, UK: Ministry of Overseas Development.

Runkel, P. 2016. What are t values and p values in statistics? http://blog.minitab.com/blog/statistics-and-quality-data-analysis/what-are-t-values-and-p-values-in-statistics Date of access: 4 Nov. 2017.

Ruxton, P. 1981. The sedimentology and diagenesis of copper-bearing rocks of the Southern margin of the Damaran Orogenic Belt, Namibia and Botswana. West Yorkshire, England.

Shaw, A.J. 1990. Heavy metal tolerance inplants: evolutionary aspects. Florida: CRC Press.

Stanton, N.L. 1988. The underground in grasslands. *Annual Review of Ecology and Systematics,* (19): 573-589.

Stony Brook State University of New York. 2000. Organic sorption and cation exchange capacity of glacial sand, Long Island. New York: Stony Brook University.

Whitehead, D.C. 2000. Nutrient elements in grassland: soil-plant-animal relationships. Devon: CABI Publishing.

APPENDIX A

A-1 Antimony

Regression analysis results for Sb are displayed in Table A-1.1 to Table A-1.3. Regression analysis was used to predict the dependent variable, [Sb] in *B. albitrunca* tissue, from the independent variables, soil concentrations and soil pH (Table A-1.1).

The regression coefficient of pH in model 2, for total A horizon content, indicated a statistically significant relationship (Table A-1.1; $p < 0.05$). However, model 2 had a p-value > 0.05, indicating that no statistically significant predictions in terms of [Sb] in the leaves of *B. albitrunca* can be made.

The regression coefficient of soluble B horizon content indicated a statistically significant relationship in model 1 as well as model 2 (Table A-1.1; $p < 0.005$ and $p < 0.05$). However, Sb concentrations for most of the soil samples were below the lowest detectable limit for ICP-MS and the correlation between soil content and concentrations in plant tissue was caused by only two samples with detectable levels of Sb. Therefore, unreliable results were produced.

Table A-1.1: Regression analysis for Sb content in the leaves of *B. albitrunca*. Significant at $p < 0.05$; highly significant at $p < 0.005$.

Model	Independent variable	Intercept	Regression coefficient	t-value	p-value	R^2 (contributing)	Total R^2
1	A horizon (total)	0.017	-0.128	-0.97	0.344	0.023	0.023
2	A horizon (total)	0.071	-0.031	-0.27	0.788	0.023	0.105
	pH		-0.008	-2.45	**0.025**	0.083	
1	B horizon (total)	0.014	-0.006	-0.08	0.934	<0.001	<0.001
2	B horizon (total)	0.075	-0.030	-0.81	0.430	<0.001	0.106
	pH		-0.009	-2.08	0.052	0.106	
1	B horizon (soluble)	0.013	8.734	4.63	**<0.001**	0.025	0.025
2	B horizon (soluble)	0.070	6.478	2.35	**0.030**	0.025	0.118
	pH		-0.008	-1.96	0.066	0.093	

Regression analysis was used to predict the dependent variable, [Sb] in *C. gratissimus* tissue, from the independent variables, soil concentrations and soil pH (Table A-1.2).

The regression coefficient of pH in model 2, for total A horizon content, indicated a statistically significant relationship (Table A-1.2; $p < 0.05$). Every unit increase in pH will result in a 0.004 decrease in leaf Sb content. The contributing R^2 value (Table A-1.2),

indicates that 1% of the variance in leaf content can be predicted from soil pH. Even though the unique contribution of total A horizon content was not significant, model 2 exhibited statistical significance and it can be used to predict 13.3% of the variance in [Sb] for *C. gratissimus*.

The regression coefficient of soluble B horizon content indicated a statistically significant relationship in model 1 (Table A-1.2; $p < 0.05$). However, Sb concentrations for most soil samples were below the lowest detectable limit for ICP-MS and the correlation between soil content and concentrations in the leaves of *C. gratissimus* was caused by only a few samples with detectable levels of Sb. Therefore, unreliable results were produced.

Table A-1.2: Regression analysis for Sb content in the leaves of *C. gratissimus*. Significant at $p < 0.05$; highly significant at $p < 0.005$.

Model	Independent variable	Intercept	Regression coefficient	t-value	p-value	R^2 (contributing)	Total R^2
1	A horizon (total)	0.021	-0.176	-2.09	0.055	0.123	0.123
2	A horizon (total)	0.045	-0.124	-1.26	0.226	0.123	0.133
	pH		-0.004	-2.29	**0.037**	0.010	
1	B horizon (total)	0.023	-0.274	-1.67	0.119	0.109	0.109
2	B horizon (total)	0.043	-0.196	-0.75	0.468	0.109	0.115
	pH		-0.003	-0.74	0.471	0.006	
1	B horizon (soluble)	0.017	-6.383	-2.24	**0.043**	0.096	0.096
2	B horizon (soluble)	0.044	-3.799	-1.17	0.263	0.096	0.103
	pH		-0.004	-1.50	0.158	0.007	

Regression analysis was used to predict the dependent variable, [Sb] in *G. bicolor* tissue, from the independent variables, soil concentrations and soil pH (Table A-1.3).

The regression coefficient of total A horizon content indicated a statistically significant relationship in model 1 (Table A-1.3; $p < 0.05$). Every 1 ppm increase in total [Sb] in the soil will result in a 0.243 ppm decrease in [Sb] in the leaves of *G. bicolor* (Figure A-1.1). The decreasing concentrations in leaf content is an unexpected trend. Some other factor, such as pH, plant physiology or antagonistic interactions with other elements, may have caused this tendency. Model 1 can be used to predict 13.1% of the variance in leaf content. The unique contributions of each independent variable in model 2 were not statistically significant. However, model 2 exhibited statistical significance and it can therefore be used to predict 17.7% of the variance in leaf Sb content.

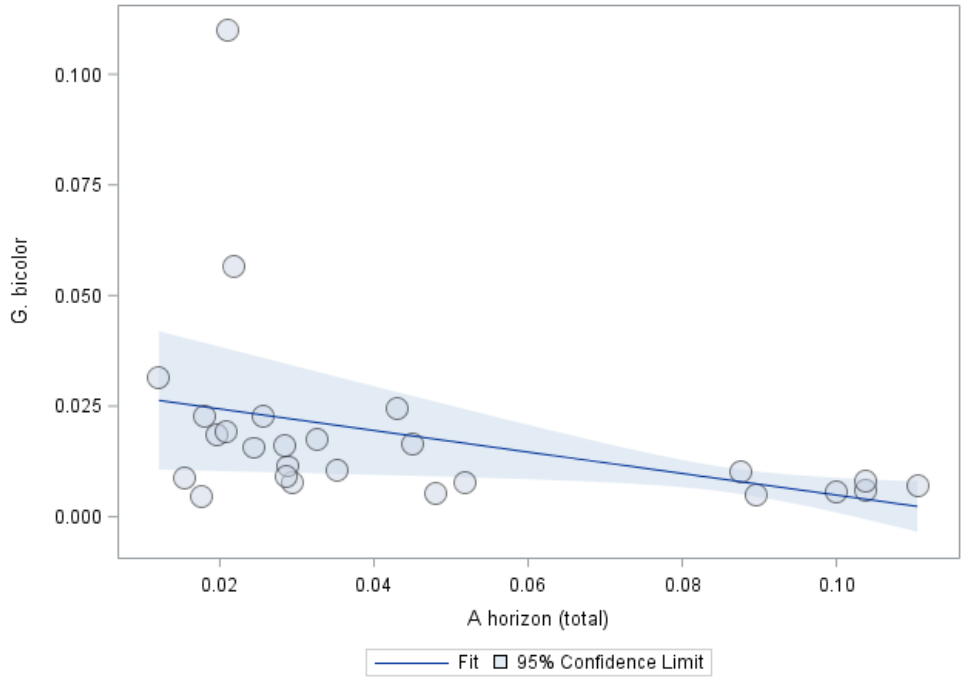

Figure A-1.1: Total Sb content in the A horizon versus Sb content in leaves of *G. bicolor*.

The regression coefficient of total B horizon content indicated a statistically significant relationship in model 1 (Table A-1.3; $p < 0.005$). Every 1 ppm increase in soluble [Sb] in the soil will result in a 0.208 ppm decrease in [Sb] in the leaves of *G. bicolor* (Figure A-1.2).

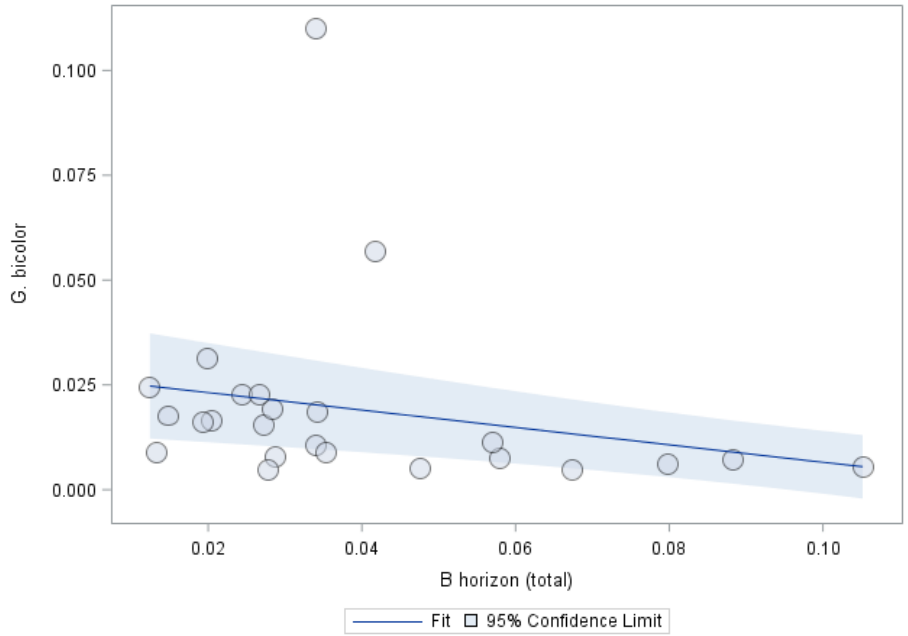

Figure A-1.2: Total Sb content in the B horizon versus Sb content in leaves of *G. bicolor*.

The same unexpected trend as for the A horizon is exhibited. The same factors may also have played a role. The R^2 indicates that 5.2% of the variance in Sb leaf content can be predicted with model 1. Regression parameters of model 2 are not statistically significant.

The regression coefficient of soluble B horizon content indicated a statistically significant relationship in model 1 (Table A-1.3; $p < 0.05$). However, Sb concentrations for most soil samples were below the lowest detectable limit for ICP-MS and the correlation between soil content and concentrations in plant tissue was caused by only a few samples with detectable levels of Sb. Therefore, unreliable results were produced. Model 2 is not statistically significant.

Table A-1.3: Regression analysis for Sb content in the leaves of *G. bicolor*. Significant at p < 0.05; highly significant at p < 0.005.

Model	Independent variable	Intercept	Regression coefficient	t-value	p-value	R^2 (contributing)	Total R^2
1	A horizon (total)	0.029	-0.243	-2.44	**0.023**	0.131	0.131
2	A horizon (total)	0.099	-0.103	-1.90	0.071	0.131	0.177
	pH		-0.011	-1.29	0.211	0.047	
1	B horizon (total)	0.027	-0.208	-3.58	**0.002**	0.052	0.052
2	B horizon (total)	0.131	0.044	0.25	0.802	0.052	0.167
	pH		-0.016	-1.35	0.194	0.115	
1	B horizon (soluble)	0.022	-6.801	-2.24	**0.037**	0.056	0.056
2	B horizon (soluble)	0.178	7.758	0.89	0.385	0.056	0.189
	pH		-0.023	-1.35	0.192	0.132	

A-2 Arsenic

Regression analysis results for As are displayed in Table A-2.1 to Table A-2.3. Regression analysis was used to predict the dependent variable, [As] in *B. albitrunca* tissue, from the independent variables, soil concentrations and soil pH (Table A-2.1).

The regression coefficient of total B horizon content indicated a statistically significant relationship in model 1 (Table A-2.1; $p < 0.05$). Every 1 ppm increase in total [As] in the soil will result in a 0.628 ppm increase in [As] in the leaves of *B. albitrunca* (Figure A-2.1). The R^2 indicates that 13.9% of the variance in As leaf content can be predicted with model 1. In model 2, the unique contribution of total B horizon content is also statistically significant. The total R^2 (Table A-2.1) indicates that 14% of the variance in leaf content can be predicted with model 2.

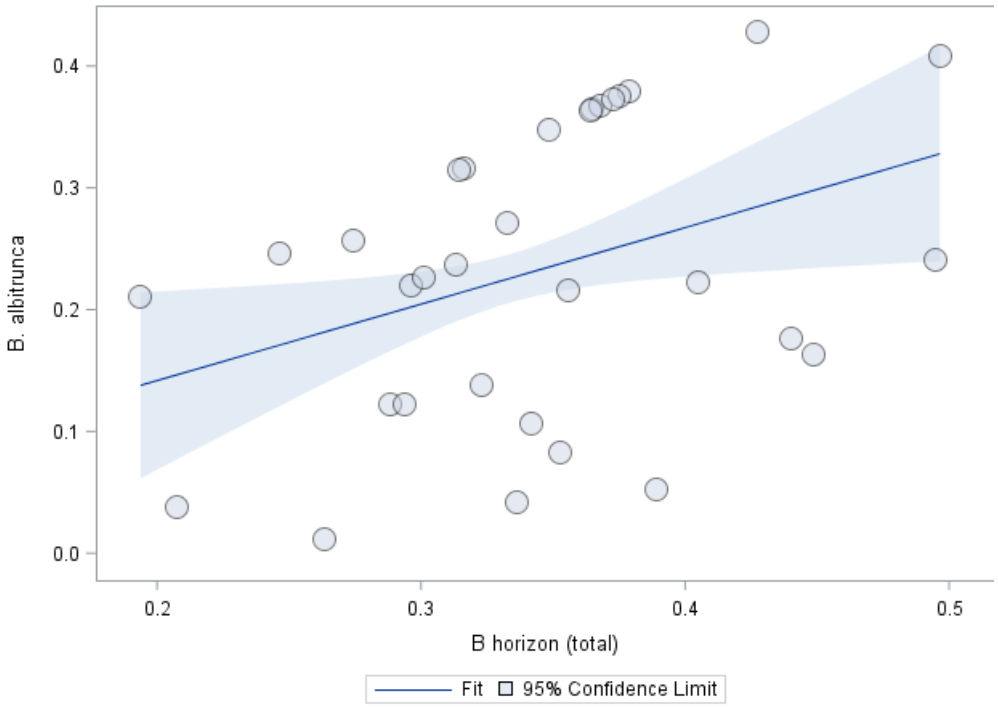

Figure A-2.1: Total As content in the B horizon versus As content in leaves of *B. albitrunca*.

The regression coefficient of soluble B horizon content indicated a statistically significant relationship in model 1 (Table A-2.1; $p < 0.05$). Every 1 ppm increase in soluble [As] in the soil will result in a 4.677 ppm decrease in leaf As content (Figure A-2.2).

Table A-2.1: Regression analysis for As content in the leaves of *B. albitrunca*. Significant at $p < 0.05$; highly significant at $p < 0.005$.

Model	Independent variable	Intercept	Regression coefficient	t-value	p-value	R^2 (contributing)	Total R^2
1	A horizon (total)	0.120	0.324	1.94	0.063	0.077	0.077
2	A horizon (total)	0.141	0.325	1.97	0.059	0.077	0.077
	pH		-0.003	-0.05	0.960	<0.001	
1	B horizon (total)	0.016	0.628	2.44	**0.021**	0.139	0.139
2	B horizon (total)	-0.042	0.629	2.43	**0.022**	0.139	0.140
	pH		0.009	0.13	0.894	0.001	
1	B horizon (soluble)	0.263	-4.677	-2.51	**0.018**	0.103	0.103
2	B horizon (soluble)	0.424	-4.907	-2.29	**0.030**	0.103	0.108
	pH		-0.024	-0.32	0.751	0.004	

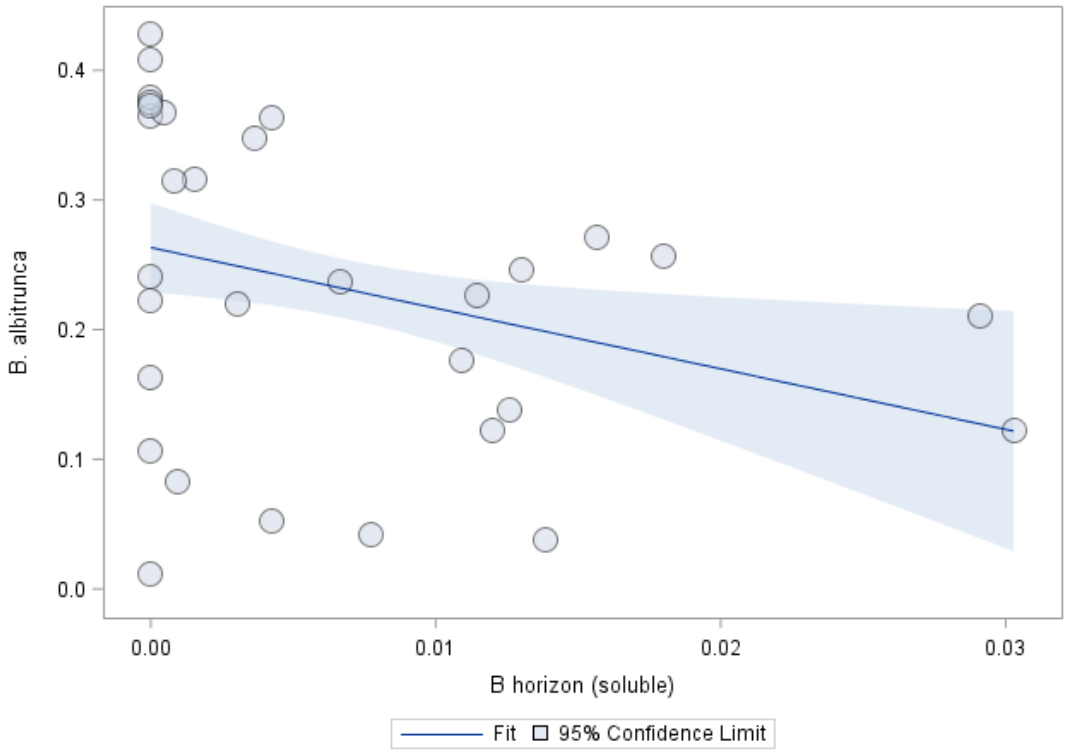

Figure A-2.2: Soluble As content in the B horizon versus As content in leaves of *B. albitrunca*.

The decreasing concentrations in leaf content is an unexpected trend. It is suspected that some other factor, such as pH, plant physiology or antagonistic interactions with other elements, may have caused this tendency. The R^2 indicates that 10.3% of the variance in As leaf content can be predicted with model 1. In model 2, the unique contribution of soluble B horizon content is also statistically significant. The total R^2 (Table A-2.1) indicates that 10.8% of the variance in leaf content can be predicted with model 2.

Regression analysis was used to predict the dependent variable, [As] in *C. gratissimus* tissue, from the independent variables, soil concentrations and soil pH (Table A-2.2).

The regression coefficient of total A horizon content indicated a statistically significant relationship in model 1 (Table A-2.2; $p < 0.05$). Every 1 ppm increase in total [As] in the soil will result in a 0.058 ppm decrease in leaf As content. The negative correlation is unexpected. However, a positive correlation was calculated in model 2, indicating that pH may have played a role in producing the negative regression coefficient in model 1. The R^2 indicates that 3.8% of the variance in As leaf content can be predicted with model 1. In model 2, the unique contribution of total A horizon content is not statistically significant. However, pH makes a statistically significant contribution and model 2 exhibits statistical

significance. According to the total R^2 (Table A-2.2), model 2 can therefore be used to predict 36.7% of the variance in leaf As content.

The regression coefficient of pH in model 2, for total B horizon content, indicated a statistically significant relationship (Table A-2.2; $p < 0.005$). Every unit increase in pH will result in a 0.104 ppm decrease in [As] in the leaves of *C. gratissimus*. The large contributing R^2 (Table A-2.2) indicates that 34.9% of the variance in leaf content can be predicted from soil pH. Even though the unique contribution of total B horizon content was not significant, model 2 exhibited statistical significance and it can be used to predict 35.2% of the variance in leaf As content.

The regression coefficient of soluble B horizon content indicated a statistically significant relationship in model 2 (Table A-2.2; $p < 0.05$). Every 1 ppm increase in soluble [As] in the soil will result in a 3.132 ppm decrease in leaf As content. The same unexpected trend as for the A horizon is displayed. The decreasing concentrations in leaf content is an unexpected trend. It is surmised that some other factor, such as pH, plant physiology or antagonistic interactions with other elements, may have caused this tendency. The regression coefficient for pH also indicated a statistically significant relationship (Table A-2.2; $p < 0.005$). Every unit increase in pH will result in a 0.083 ppm decrease in [As] in the leaves of *C. gratissimus*. The contributing R^2 values indicate that 7.1% of the variance in leaf content can be predicted from total [As] in the soil and 31.5% of the variance is attributed to the effect of pH. Model 2 can therefore be used to predict 38.6% of the variance in As leaf content.

Table A-2.2: Regression analysis for As content in the leaves of *C. gratissimus*. Significant at $p < 0.05$; highly significant at $p < 0.005$.

Model	Independent variable	Intercept	Regression coefficient	t-value	p-value	R^2 (contributing)	Total R^2
1	A horizon (total)	0.120	-0.058	-2.39	**0.025**	0.038	0.038
2	A horizon (total)	0.844	0.107	1.42	0.170	0.038	**0.367**
	pH		-0.117	-4.01	**0.001**	0.329	
1	B horizon (total)	0.107	-0.022	-0.69	0.495	0.003	0.003
2	B horizon (total)	0.757	0.113	1.18	0.250	0.003	**0.352**
	pH		-0.104	-4.31	**<0.001**	0.349	
1	B horizon (soluble)	-2.428	-2.428	-1.95	0.065	0.071	0.071
2	B horizon (soluble)	0.690	-3.132	-2.53	**0.020**	0.071	**0.386**
	pH		-0.083	-7.26	**<0.001**	0.315	

Regression analysis was used to predict the dependent variable, [As] in *G. bicolor* tissue, from the independent variables, soil concentrations and soil pH (Table A-2.3).

The regression coefficient of pH in model 2, for total A horizon content, indicated a statistically significant relationship (Table A-2.3; $p < 0.005$). Every unit increase in pH will result in a 0.105 ppm decrease in [As] in the leaves of *G. bicolor*. The R^2 indicates that 21.6% of the variance in leaf As content can be predicted by soil pH. Even though the unique contribution of total A horizon content was not significant, model 2 exhibited statistical significance and it can be used to predict 22.7% of the variance in leaf As content.

The regression coefficient of total B horizon content indicated a statistically significant relationship in model 2 (Table A-2.3; $p < 0.05$). Every 1 ppm increase in total [As] in the soil will result in a 0.088 ppm increase in leaf As content. The regression coefficient for pH also indicated a statistically significant relationship (Table A-2.3; $p < 0.005$). Every unit increase in pH will result in a 0.09 ppm decrease in [As] in the leaves of *G. bicolor*. The contributing R^2 indicates that 0.4% of the variance in leaf content can be predicted from total [As] in the soil and 20.1% of the variance is attributed to the effect of pH. Model 2 van therefore be used to predict 20.5% of the variance in As leaf content.

The regression coefficient of pH in model 2, for soluble B horizon content, indicated a statistically significant relationship (Table A-2.3; $p < 0.005$). Every unit increase in pH will result in a 0.059 ppm decrease in [As] in the leaves of *G. bicolor*. The contributing R^2 (Table A-2.3) indicates that 13.2% of the variance in leaf content can be predicted from soil pH. Even though the unique contribution of soluble B horizon content was not significant, model 2 exhibited statistical significance and it can be used to predict 14.5% of the variance in leaf As content.

Table A-2.3: Regression analysis for As content in the leaves of *G. bicolor*. Significant at $p < 0.05$; highly significant at $p < 0.005$.

Model	Independent variable	Intercept	Regression coefficient	t-value	p-value	R^2 (contributing)	Total R^2
1	A horizon (total)	0.128	-0.032	-1.13	0.265	0.011	0.011
2	A horizon (total)	0.783	0.108	1.61	0.117	0.011	0.227
	pH		-0.105	-4.06	**<0.001**	0.216	
1	B horizon (total)	0.126	-0.023	-0.72	0.480	0.004	0.004
2	B horizon (total)	0.694	0.088	2.34	**0.026**	0.004	0.205
	pH		-0.090	-5.93	**<0.001**	0.201	
1	B horizon (soluble)	0.106	1.186	0.61	0.544	0.013	0.013
2	B horizon (soluble)	0.514	0.599	0.33	0.743	0.013	0.145
	pH		-0.059	-3.38	**0.002**	0.132	

A-3 Barium

Regression analysis results for Ba are displayed in Table A-3.1 to Table A-3.3. Regression analysis was used to predict the dependent variable, [Ba] in *B. albitrunca* tissue, from the independent variables, soil concentrations and soil pH (Table A-3.1).

The regression coefficient of total A horizon content indicated a statistically significant relationship in model 1 (Table A-3.1; $p < 0.05$). Every 1 ppm increase in total [Ba] in the soil will result in a 0.13 ppm increase in leaf Ba content (Figure A-3.1). The R^2 indicates that 20.4% of the variance in leaf Ba content can be predicted by model 1. Model 2 also exhibited statistical significance, even though the unique contribution of pH was not significant. Therefore, model 2 can be used to predict 26.6% of the variance in leaf Ba content.

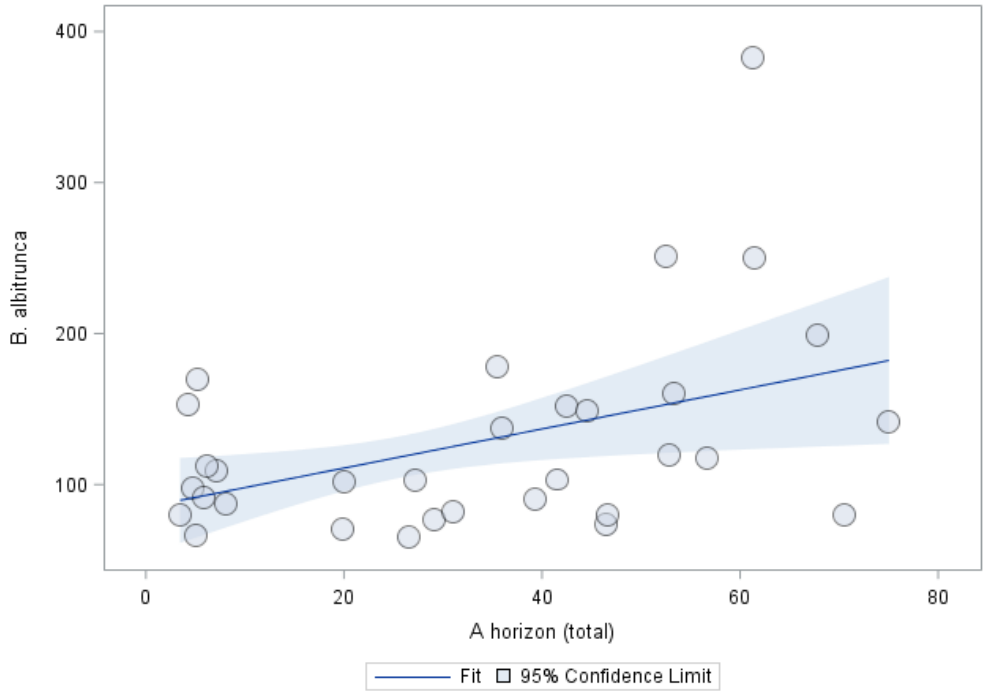

Figure A-3.1: Total Ba content in the A horizon versus Ba content in leaves of *B. albitrunca*.

The regression coefficient of total B horizon content indicated a statistically significant relationship in model 1 (Table A-3.1; $p < 0.005$). Every 1 ppm increase in total [Ba] in the soil will result in a 0.092 ppm increase in [Ba] in the leaves of *B. albitrunca* (Figure A-3.2). The R^2 indicates that 17.7% of the variance in leaf Ba content can be predicted by model 1. The unique contributions of each independent variable in model 2 were not statistically significant. However, model 2 did exhibit statistical significance and it can therefore be used to predict 25% of the variance in leaf Ba content.

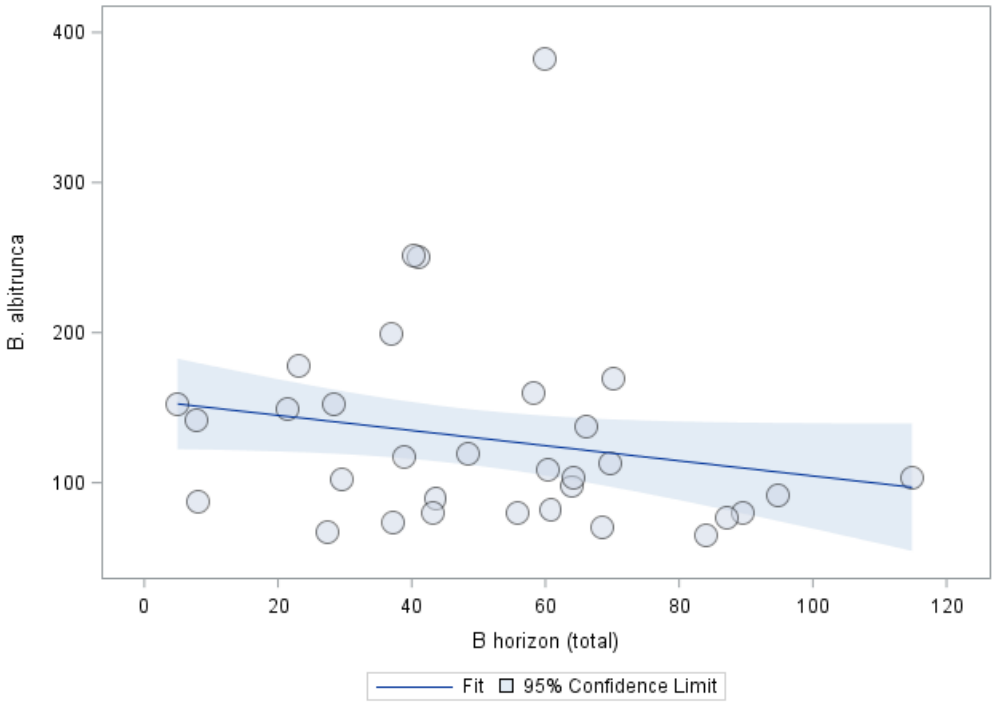

Figure A-3.2: Total Ba content in the B horizon versus Ba content in leaves of *B. albitrunca*.

The regression coefficient of soluble B horizon content indicated a statistically significant relationship in model 1 (Table A-3.1; $p < 0.05$). Every 1 ppm increase in soluble [Ba] in the soil will result in a 0.241 ppm increase in leaf Ba content (Figure A-3.3). The R^2 indicates that 22.9% of the variance in leaf Ba content can be predicted by model 1. Model 2 also exhibited statistical significance, even though the unique contribution of pH was not significant. Model 2 can be used to predict 28.4% of the variance in leaf Ba content.

Table A-3.1: Regression analysis for Ba content in the leaves of *B. albitrunca*. Significant at p<0.05; highly significant at p<0.005.

Model	Independent variable	Intercept	Regression coefficient	t-value	p-value	R^2 (contributing)	Total R^2
1	A horizon (total)	0.903	0.130	2.73	**0.014**	0.204	0.204
2	A horizon (total)	-14.900	0.083	2.67	**0.016**	0.204	**0.266**
	pH		2.550	1.45	0.163	0.063	
1	B horizon (total)	1.950	0.092	3.66	**0.002**	0.177	0.177
2	B horizon (total)	-15.381	0.053	1.91	0.073	0.177	**0.250**
	pH		2.747	1.20	0.244	0.072	
1	B horizon (soluble)	1.626	0.241	2.93	**0.009**	0.229	0.229
2	B horizon (soluble)	-13.416	0.165	2.99	**0.008**	0.229	**0.284**
	pH		2.376	1.39	0.181	0.055	

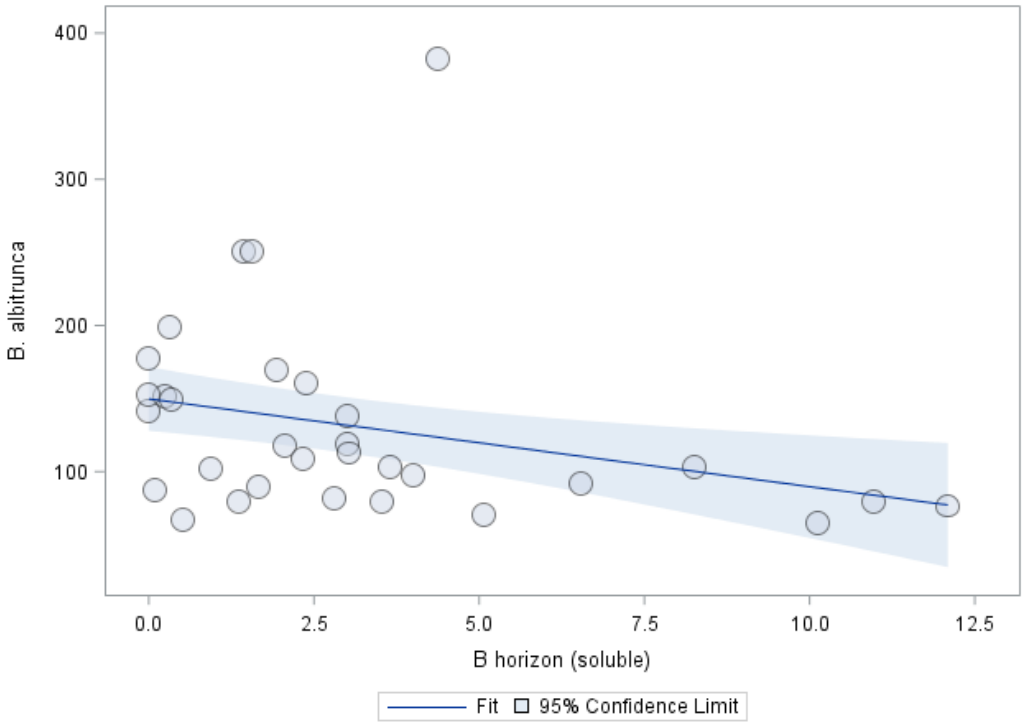

Figure A-3.3: Soluble Ba content in the B horizon versus Ba content in leaves of *B. albitrunca*.

Regression analysis was used to predict the dependent variable, [Ba] in *C. gratissimus* tissue, from the independent variables, soil concentrations and soil pH (Table A-3.2).

None of the independent variables displayed a statistically significant correlation with Ba content in the leaves of *C. gratissimus*.

Table A-3.2: Regression analysis for Ba content in the leaves of *C. gratissimus*. Significant at p < 0.05; highly significant at p < 0.005.

Model	Independent variable	Intercept	Regression coefficient	t-value	p-value	R^2 (contributing)	Total R^2
1	A horizon (total)	10.069	-0.031	-0.67	0.514	0.040	0.040
2	A horizon (total)	9.895	-0.031	-0.52	0.609	0.040	0.040
	pH		0.028	0.02	0.988	<0.001	
1	B horizon (total)	10.628	-0.055	-0.94	0.362	0.076	0.076
2	B horizon (total)	0.739	-0.107	-1.77	0.101	0.076	0.117
	pH		1.631	1.13	0.280	0.041	
1	B horizon (soluble)	9.976	-0.070	-0.72	0.483	0.040	0.040
2	B horizon (soluble)	4.618	-0.119	-1.07	0.306	0.040	0.052
	pH		0.860	0.49	0.630	0.011	

Regression analysis was used to predict the dependent variable, [Ba] in *G. bicolor* tissue, from the independent variables, soil concentrations and soil pH (Table A-3.3).

The regression coefficient of total A horizon content indicated a statistically significant contribution in model 2 (Table A-3.3; $p < 0.05$). However, model 2 did not exhibit statistical significance and can therefore not be used to predict Ba concentrations in *G. bicolor* tissue.

The regression coefficient of total B horizon content indicated a statistically significant relationship in model 1 (Table A-3.3; $p < 0.005$). Every 1 ppm increase in total [Ba] in the soil will result in a 0.34 ppm increase in leaf Ba content (Figure A-3.4). The R^2 indicates that 29.9% of the variance in leaf Ba content can be predicted by model 1. Model 2 also exhibited statistical significance, even though the unique contribution of pH was not significant. Model 2 can be used to predict 37.2% of the variance in leaf Ba content.

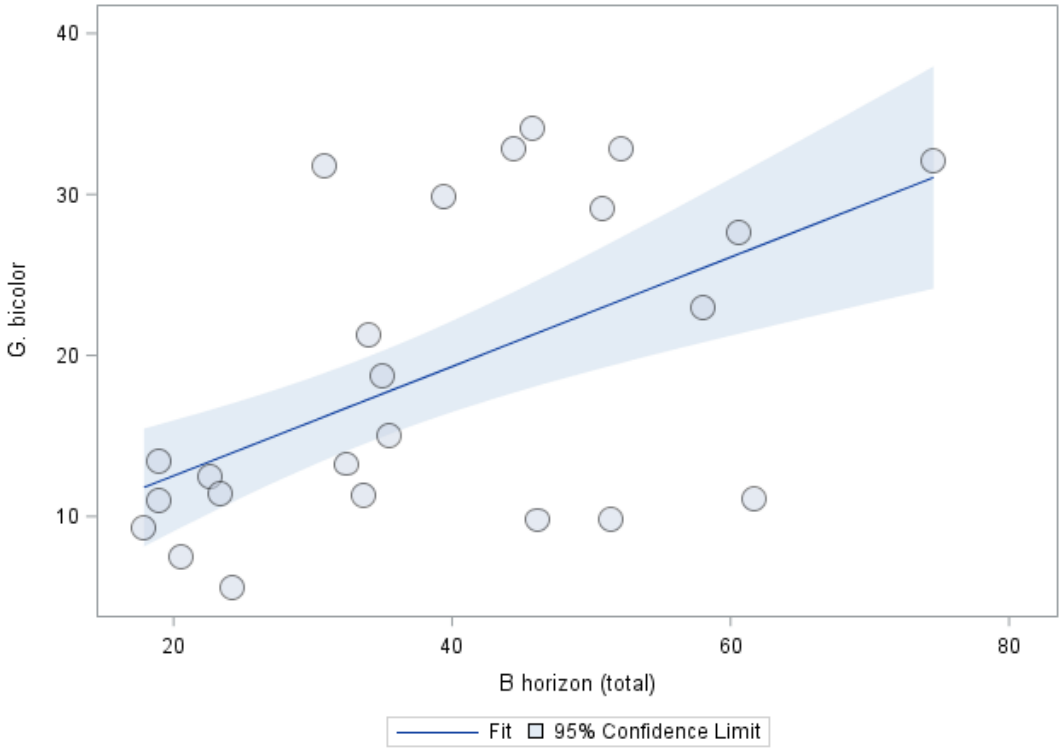

Figure A-3.4: Total Ba content in the B horizon versus Ba content in leaves of *G. bicolor*.

The regression coefficient of soluble B horizon content indicated a statistically significant relationship in model 1 (Table A-3.3; $p < 0.005$). Every 1 ppm increase in soluble [Ba] in the soil will result in a 0.806 ppm increase in leaf Ba content (Figure A-3.5). A statistically significant relationship is also indicated in model 2, by the regression coefficients of soluble B horizon content as well as pH (Table A-3.3; $p < 0.005$).

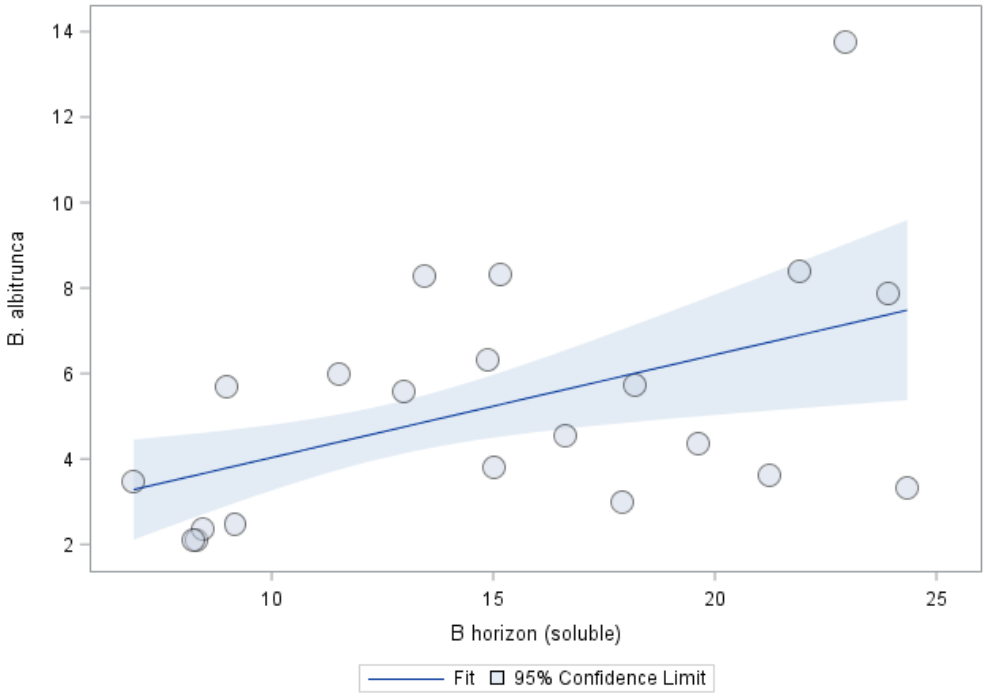

Figure A-3.5: Soluble Ba content in the B horizon versus Ba content in leaves of *G. bicolor*.

Every 1 ppm increase in soluble [Ba] in the soil will result in a 1.275 ppm increase in leaf Ba content. Every unit increase in pH will result in a 9.209 ppm decrease in [Ba] in the leaves of *G. bicolor*. The contributing R^2 values (Table A-3.3) indicates that 42.8% of the variance in leaf content can be predicted from soluble [Ba] in the soil and 18.6% of the variance is attributed to the effect of pH. Therefore, model 2 can be used to predict 61.4% of the variance in Ba leaf content.

Table A-3.3: Regression analysis for Ba content in the leaves of *G. bicolor*. Significant at p < 0.05; highly significant at p < 0.005.

Model	Independent variable	Intercept	Regression coefficient	t-value	p-value	R^2 (contributing)	Total R^2
1	A horizon (total)	11.366	0.177	1.85	0.077	0.092	0.092
2	A horizon (total)	40.114	0.293	2.13	**0.045**	0.092	0.140
	pH		-4.751	-1.21	0.240	0.048	
1	B horizon (total)	5.733	0.340	4.52	**<0.001**	0.299	**0.299**
2	B horizon (total)	38.731	0.460	3.28	**0.004**	0.299	**0.372**
	pH		-5.393	-1.82	0.083	0.073	
1	B horizon (soluble)	5.904	0.806	6.41	**<0.001**	0.428	**0.428**
2	B horizon (soluble)	62.412	1.275	6.99	**<0.001**	0.428	**0.614**
	pH		-9.209	-4.51	**<0.001**	0.186	

A-4 Boron

Regression analysis results for B are displayed in Table A-4.1 to Table A-4.3. Regression analysis was used to predict the dependent variable, [B] in *B. albitrunca* tissue, from the independent variables, soil concentrations and soil pH (Table A-4.1).

The regression coefficient of total A horizon content indicated a statistically significant relationship in model 1 (Table A-4.1; $p < 0.05$). Every 1 ppm increase in total [B] in the soil will result in a 1.294 ppm increase in leaf B content (Figure A-4.1). The R^2 indicates that 18.6% of the variance in B leaf content can be predicted by model 1. A statistically significant relationship is also indicated in model 2, by regression coefficients of soluble B horizon content as well as pH (Table A-4.1; $p < 0.05$ and $p < 0.005$). Every 1 ppm increase in total [B] in the soil will result in a 1.073 ppm increase in leaf B content. Every unit increase in pH will result in an 82.279 ppm increase in [B] in the leaves of *B. albitrunca*. The contributing R^2 values (Table A-4.1) indicate that 18.6% of the variance in leaf content can be predicted from the [B] in the soil and 16.9% of the variance is attributed to the effect of pH. Therefore, model 2 can be used to predict 35.5% of the variance in B leaf content.

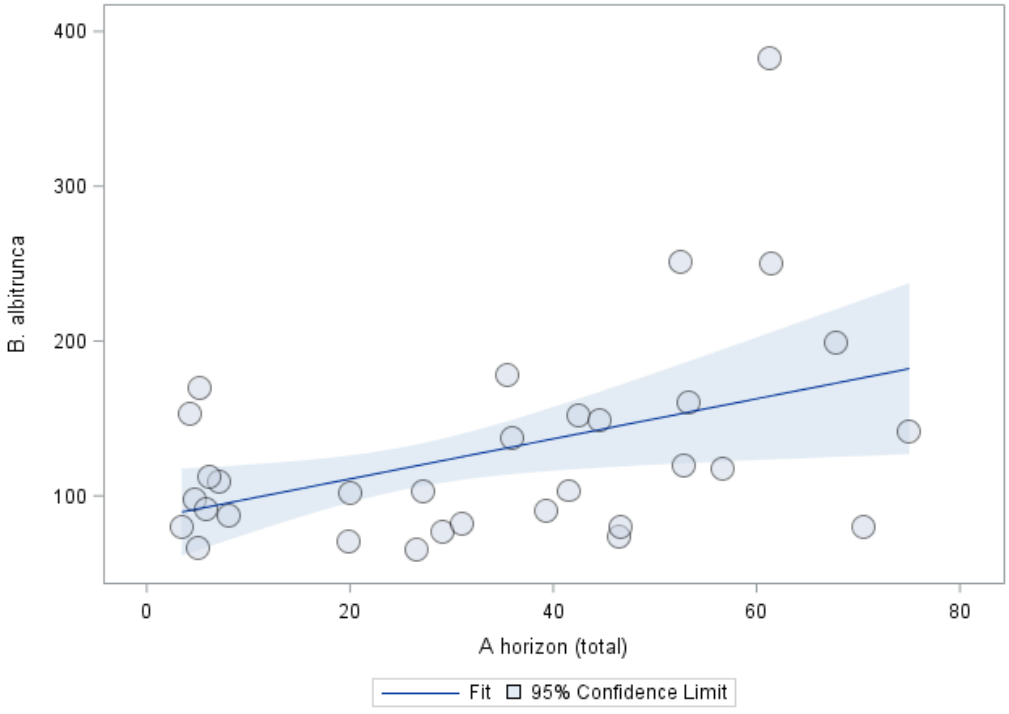

Figure A-4.1: Total B content in the A horizon versus B content in leaves of *B. albitrunca*.

The regression coefficient of pH in model 2, for total B horizon content, indicated a statistically significant relationship (Table A-4.1; $p < 0.005$). Every unit increase in pH will result in a 91.249 ppm increase in [B] in the leaves of *B. albitrunca*. Even though the unique contribution of total B horizon content was not significant, model 2 exhibited statistical significance and it can be used to predict 23.4% of the variance leaf B content.

The regression coefficient of soluble B horizon content indicated a statistically significant relationship in model 1 (Table A-4.1; $p < 0.05$). Every 1 ppm increase in soluble [B] in the soil will result in a 6.003 ppm decrease in leaf B content (Figure A-4.2).

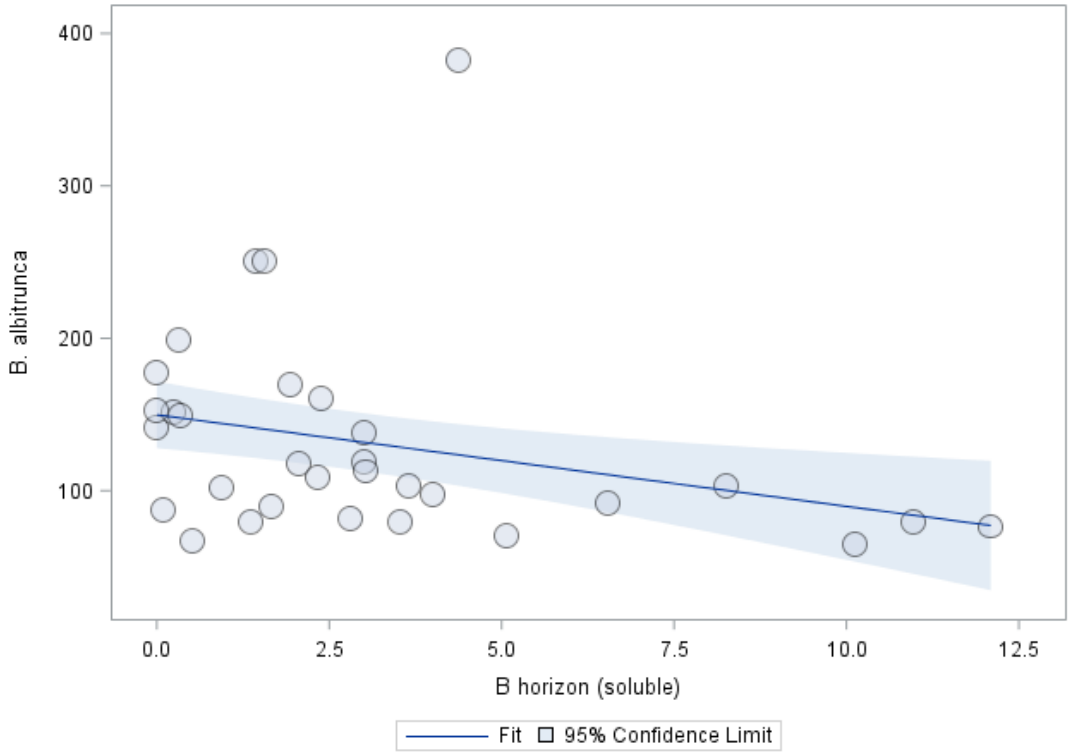

Figure A-4.2: Soluble B content in the B horizon versus B content in leaves of *B. albitrunca*.

The decreasing concentrations in leaf content is an unexpected trend. It is surmised that some other factor, such as pH, plant physiology or antagonistic interactions with other elements, may have caused this tendency. In model 2, the unique contribution of soluble B horizon content is no longer statistically significant. However, pH makes a statistically significant contribution and model 2 exhibits statistical significance. According to the total R^2 (Table A-4.1), model 2 can therefore be used to predict 22.5% of the variance in leaf B content.

Table A-4.1: Regression analysis for B content in the leaves of *B. albitrunca*. Significant at p < 0.05; highly significant at p < 0.005.

Model	Independent variable	Intercept	Regression coefficient	t-value	p-value	R^2 (contributing)	Total R^2
1	A horizon (total)	85.062	1.294	2.43	**0.022**	0.186	0.186
2	A horizon (total)	-458.105	1.073	2.12	**0.043**	0.186	**0.355**
	pH		82.279	4.20	**<0.001**	0.169	
1	B horizon (total)	155.039	-0.505	-1.83	0.077	0.039	0.039
2	B horizon (total)	-474.005	-0.149	-0.66	0.517	0.039	0.234
	pH		91.249	4.06	**<0.001**	0.195	
1	B horizon (soluble)	149.742	-6.003	-3.06	**0.005**	0.085	0.085
2	B horizon (soluble)	-422.242	-2.019	-0.89	0.381	0.085	0.225
	pH		83.451	3.45	**0.002**	0.140	

Regression analysis was used to predict the dependent variable, [B] in *C. gratissimus* tissue, from the independent variables, soil concentrations and soil pH (Table A-4.2).

None of the independent variables displayed a statistically significant correlation with B content in the leaves of *C. gratissimus*.

Table A-4.2: Regression analysis for B content in the leaves of *C. gratissimus*. Significant at p < 0.05; highly significant at p < 0.005.

Model	Independent variable	Intercept	Regression coefficient	t-value	p-value	R^2 (contributing)	Total R^2
1	A horizon (total)	61.174	0.039	0.17	0.867	0.001	0.001
2	A horizon (total)	-83.883	0.062	0.30	0.764	0.001	0.184
	pH		21.075	1.93	0.066	0.183	
1	B horizon (total)	58.086	-0.004	-0.03	0.976	<0.001	<0.001
2	B horizon (total)	-77.207	0.061	0.44	0.668	<0.001	0.224
	pH		19.395	1.48	0.154	0.224	
1	B horizon (soluble)	59.036	-0.225	-0.21	0.837	0.002	0.002
2	B horizon (soluble)	-84.826	0.632	0.84	0.414	0.002	0.229
	pH		20.611	1.52	0.144	0.227	

Regression analysis was used to predict the dependent variable, [B] in *G. bicolor* tissue, from the independent variables, soil concentrations and soil pH (Table A-4.3).

The regression coefficient of total A horizon content indicated a statistically significant relationship in model 1 (Table A-4.3; $p < 0.005$). Every 1 ppm increase in total [B] in the soil will result in a 0.282 ppm increase in leaf B content (Figure A-4.3). The R^2 indicates that 16.5% of the variance in leaf B content can be predicted by model 1. Model 2 also exhibited

statistical significance, even though the unique contribution of pH was not significant. Model 2 can be used to predict 16.8% of the variance in leaf Ba content.

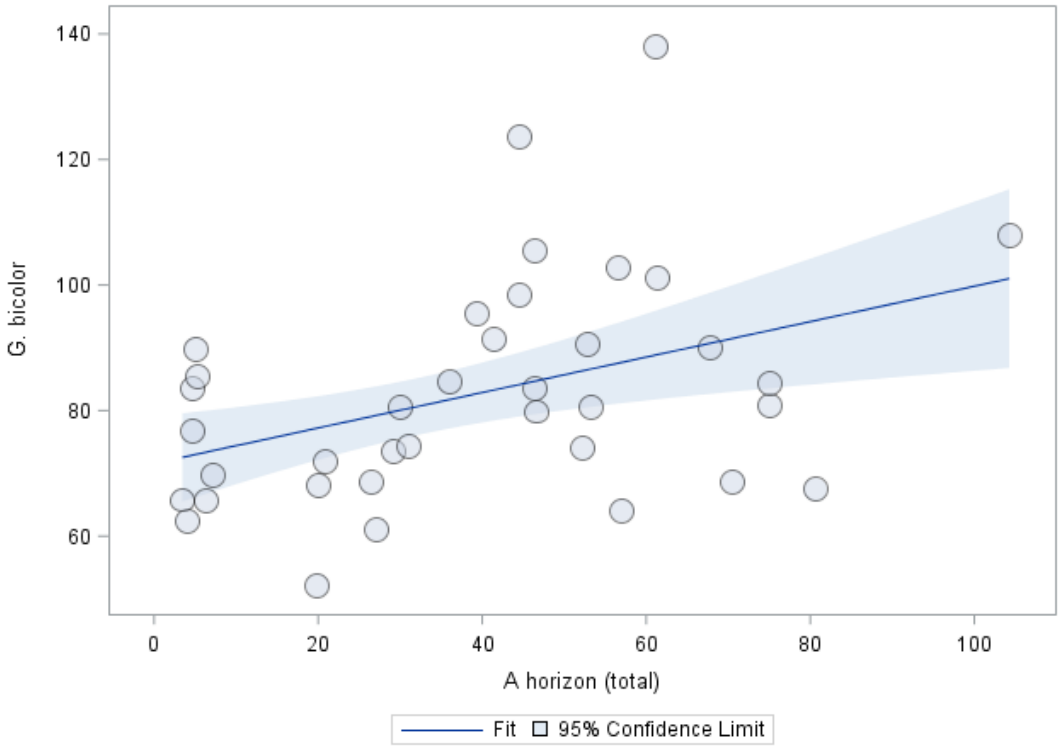

Figure A-4.3: Total B content in the A horizon versus B content in leaves of *G. bicolor*.

Table A-4.3: Regression analysis for B content in the leaves of *G. bicolor*. Significant at p < 0.05; highly significant at p < 0.005.

Model	Independent variable	Intercept	Regression coefficient	t-value	p-value	R^2 (contributing)	Total R^2
1	A horizon (total)	71.587	0.282	3.08	**0.004**	0.165	0.165
2	A horizon (total)	59.212	0.284	3.02	**0.005**	0.165	0.168
	pH		1.795	0.40	0.693	0.003	
1	B horizon (total)	79.001	0.078	0.75	0.461	0.015	0.015
2	B horizon (total)	64.471	0.084	0.79	0.434	0.015	0.019
	pH		2.075	0.39	0.702	0.004	
1	B horizon (soluble)	82.757	0.190	0.25	0.807	0.002	0.002
2	B horizon (soluble)	65.477	0.301	0.39	0.700	0.002	0.007
	pH		2.469	0.42	0.680	0.005	

A-5 Cadmium

Regression analysis results for Cd are displayed in Table A-5.1 to Table A-5.3. Regression analysis was used to predict the dependent variable, [Cd] in *B. albitrunca* tissue, from the independent variables, soil concentrations and soil pH (Table A-5.1).

The regression coefficient of pH in model 2, for total A horizon content, indicated a statistically significant contribution (Table A-5.1; $p < 0.05$). However, model 2 did not exhibit statistical significance and can therefore not be used to predict Cd concentrations in *B. albitrunca* tissue.

The regression coefficient of total B horizon content indicated a statistically significant relationship in model 1 (Table A-5.1; $p < 0.005$). Every 1 ppm increase in total [Cd] in the soil will result in a 21.5 ppm increase in leaf Cd content (Figure A-5.1).

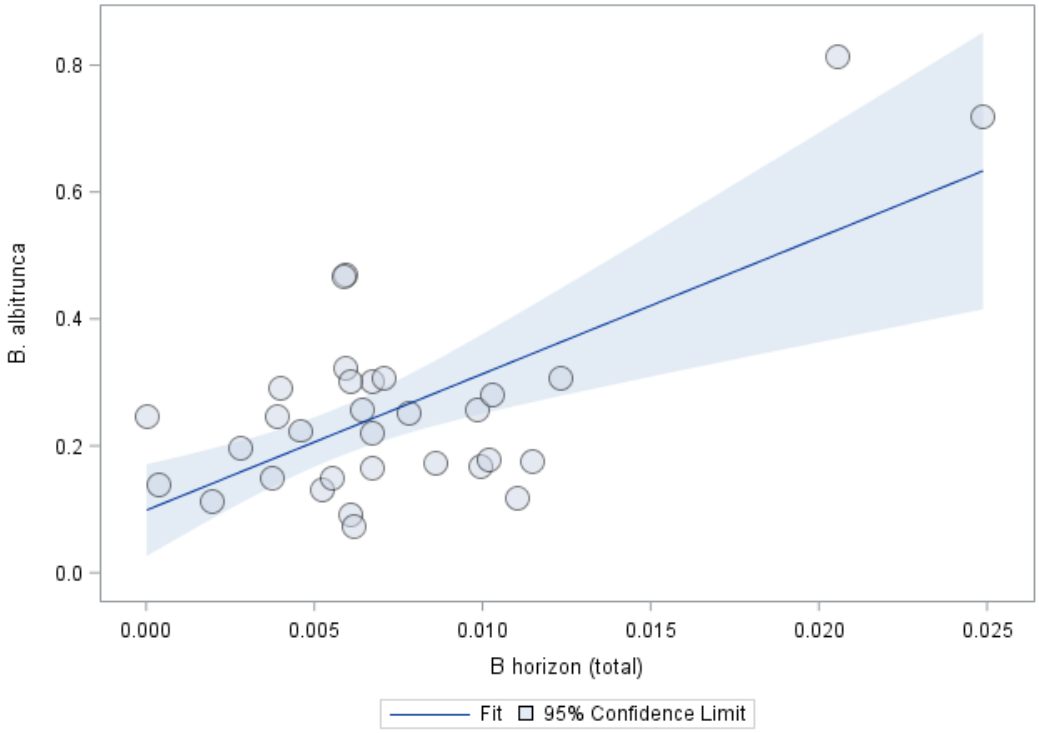

Figure A-5.1: Total Cd content in the B horizon versus Cd content in leaves of *B. albitrunca*.

The R^2 indicates that 44% of the variance in leaf Cd content can be predicted by model 1. A statistically significant relationship is also indicated in model 2, by regression coefficients of soluble B horizon content as well as pH (Table A-5.1; $p < 0.005$ and $p < 0.05$). Every 1 ppm increase in total [Cd] in the soil will result in a 22.94 ppm increase in leaf Cd content. Every

unit increase in pH will result in a 0.11 ppm decrease in [Cd] in the leaves of *B. albitrunca*. The contributing R^2 values (Table A-5.1) indicate that 44% of the variance in leaf content can be predicted from the [Cd] in the soil and 4.7% of the variance is attributed to the effect of pH. Therefore, model 2 can be used to predict 48.7% of the variance in leaf Cd content.

The regression coefficient of soluble B horizon content indicated a statistically significant relationship in model 1 (Table A-5.1; $p < 0.05$). However, Cd concentrations for most of the soil samples were below the lowest detectable limit for ICP-MS and the correlation between soil content and concentrations in plant tissue was caused by only a few samples with detectable levels of Cd. Therefore, unreliable results were produced.

Table A-5.1: Regression analysis for Cd content in the leaves of *B. albitrunca*. Significant at $p < 0.05$; highly significant at $p < 0.005$.

Model	Independent variable	Intercept	Regression coefficient	t-value	p-value	R^2 (contributing)	Total R^2
1	A horizon (total)	0.176	9.680	1.20	0.239	0.111	0.111
2	A horizon (total)	0.948	12.540	1.37	0.180	0.111	0.164
	pH		-0.119	-2.27	**0.031**	0.053	
1	B horizon (total)	0.098	21.495	3.97	**0.001**	0.440	**0.440**
2	B horizon (total)	0.794	22.937	4.06	**<0.001**	0.440	**0.487**
	pH		-0.105	-2.69	**0.012**	0.047	
1	B horizon (soluble)	0.199	281.098	2.94	**0.007**	0.416	**0.416**
2	B horizon (soluble)	0.681	292.623	2.89	**0.008**	0.416	**0.439**
	pH		-0.072	-1.90	0.068	0.023	

Regression analysis was used to predict the dependent variable, [Cd] in *C. gratissimus* tissue, from the independent variables, soil concentrations and soil pH (Table A-5.2).

The regression coefficient of pH in model 2, for total A horizon content, indicated a statistically significant relationship (Table A-5.2; $p < 0.005$). Every unit increase in pH will result in a 0.009 ppm decrease in [Cd] in the leaves of *C. gratissimus*. The contributing R^2 (Table A-5.2) indicates that 15.7% of the variance in leaf content can be predicted from soil pH. Even though the unique contribution of total A horizon content was not significant, model 2 exhibited statistical significance and it can be used to predict 20.4% of the variance in leaf Cd content.

The regression coefficient of pH in model 2, for total B horizon content, indicated a statistically significant relationship (Table A-5.2; $p < 0.005$). Every unit increase in pH will result in a 0.009 ppm decrease in [Cd] in the leaves of *C. gratissimus*. The contributing R^2 (Table A-5.2) indicates that 20.5% of the variance in leaf content can be predicted from soil

pH. Even though the unique contribution of total B horizon content was not significant, model 2 exhibited statistical significance and it can be used to predict 20.5% of the variance leaf Cd content.

The regression coefficient of pH in model 2, for soluble B horizon content, indicated a statistically significant relationship (Table A-5.2; $p < 0.005$). Every unit increase in pH will result in a 0.008 ppm decrease in [Cd] in the leaves of *C. gratissimus*. The contributing R^2 (Table A-5.2) indicates that 18.3% of the variance in leaf content can be predicted from soil pH. Even though the unique contribution of soluble B horizon content was not significant, model 2 exhibited statistical significance and it can be used to predict 18.6% of the variance leaf Cd content.

Table A-5.2: Regression analysis for Cd content in the leaves of *C. gratissimus*. Significant at $p < 0.05$; highly significant at $p < 0.005$.

Model	Independent variable	Intercept	Regression coefficient	t-value	p-value	R^2 (contributing)	Total R^2
1	A horizon (total)	0.012	-0.410	-1.74	0.095	0.047	0.047
2	A horizon (total)	0.068	0.092	0.29	0.776	0.047	0.204
	pH		-0.009	-3.19	**0.004**	0.157	
1	B horizon (total)	0.009	-0.052	-0.14	0.894	<0.001	<0.001
2	B horizon (total)	0.068	0.268	0.53	0.601	<0.001	0.205
	pH		-0.009	-3.94	**0.001**	0.205	
1	B horizon (soluble)	0.009	-14.421	-0.87	0.395	0.002	0.002
2	B horizon (soluble)	0.065	-27.426	-1.71	0.103	0.002	0.186
	pH		-0.008	-4.00	**0.001**	0.183	

Regression analysis was used to predict the dependent variable, [Cd] in *G. bicolor* tissue, from the independent variables, soil concentrations and soil pH (Table A-5.3).

The regression coefficient of pH in model 2, for total A horizon content, indicated a statistically significant relationship (Table A-5.3; $p < 0.005$). Every unit increase in pH will result in a 0.007 ppm decrease in [Cd] in the leaves of *G. bicolor*. The contributing R^2 (Table A-5.3) indicates that 12.9% of the variance in leaf content can be predicted from soil pH. Even though the unique contribution of total A horizon content was not significant, model 2 exhibited statistical significance and it can be used to predict 16% of the variance leaf Cd content.

The regression coefficient of pH in model 2, for total B horizon content, indicated a statistically significant relationship (Table A-5.3; $p < 0.005$). Every unit increase in pH will result in a 0.007 ppm decrease in [Cd] in the leaves of *G. bicolor*. The contributing R^2 (Table

A-5.3) indicates that 12.9% of the variance in leaf content can be predicted from soil pH. Even though the unique contribution of total B horizon content was not significant, model 2 exhibited statistical significance and it can be used to predict 14.7% of the variance leaf Cd content.

The regression coefficient of pH in model 2, for soluble B horizon content, indicated a statistically significant relationship (Table A-5.3; $p < 0.005$). Every unit increase in pH will result in a 0.006 ppm decrease in [Cd] in the leaves of *G. bicolor*. The contributing R^2 (Table A-5.3) indicates that 13% of the variance in leaf content can be predicted from soil pH. Even though the unique contribution of soluble B horizon content was not significant, model 2 exhibited statistical significance and it can be used to predict 13.1% of the variance leaf Cd content.

Table A-5.3: Regression analysis for Cd content in the leaves of *G. bicolor*. Significant at p < 0.05; highly significant at p < 0.005.

Model	Independent variable	Intercept	Regression coefficient	t-value	p-value	R^2 (contributing)	Total R^2
1	A horizon (total)	0.010	-0.279	-1.74	0.091	0.031	0.031
2	A horizon (total)	0.056	0.046	0.26	0.794	0.031	0.160
	pH		-0.007	-3.79	**0.001**	0.129	
1	B horizon (total)	0.010	-0.234	-1.25	0.221	0.018	0.018
2	B horizon (total)	0.054	-0.021	-0.12	0.904	0.018	0.147
	pH		-0.007	-3.82	**0.001**	0.129	
1	B horizon (soluble)	0.007	0.986	0.52	0.607	0.001	0.001
2	B horizon (soluble)	0.050	1.504	0.67	0.511	0.001	0.131
	pH		-0.006	-3.36	**0.002**	0.130	

A-6 Chromium

Regression analysis results for Cr are displayed in Table A-6.1 to Table A-6.3. Regression analysis was used to predict the dependent variable, [Cr] in *B. albitrunca* tissue, from the independent variables, soil concentrations and soil pH (Table A-6.1).

None of the independent variables displayed a statistically significant correlation with Cr content in the leaves of *B. albitrunca*.

Table A-6.1: Regression analysis for Cr content in the leaves of *B. albitrunca*. Significant at p < 0.05; highly significant at p < 0.005.

Model	Independent variable	Intercept	Regression coefficient	t-value	p-value	R^2 (contributing)	Total R^2
1	A horizon (total)	2.472	-0.001	-1.77	0.094	0.037	0.037
2	A horizon (total)	2.361	-0.001	-1.98	0.063	0.037	0.037
	pH		0.017	0.05	0.962	<0.001	
1	B horizon (total)	2.190	<0.001	0.33	0.742	0.002	0.002
2	B horizon (total)	2.547	<0.001	0.36	0.725	0.002	0.002
	pH		-0.050	-0.16	0.877	<0.001	
1	B horizon (soluble)	2.265	0	-	-	0	0
2	B horizon (soluble)	2.867	0	-	-	0	0.001
	pH		-0.088	-0.24	0.813	0.001	

Regression analysis was used to predict the dependent variable, [Cr] in *C. gratissimus* tissue, from the independent variables, soil concentrations and soil pH (Table A-6.2).

The regression coefficient of pH in model 2, for total A horizon content, indicated a statistically significant relationship (Table A-6.2; $p < 0.005$). Every unit increase in pH will result in a 1.11 ppm decrease in [Cr] in the leaves of *C. gratissimus*. The contributing R^2 (Table A-6.2) indicates that 35.1% of the variance in leaf content can be predicted from soil pH. Even though the unique contribution of total A horizon content was not significant, model 2 exhibited statistical significance and it can be used to predict 35.3% of the variance leaf Cr content.

The regression coefficient of pH in model 2, for total B horizon content, indicated a statistically significant relationship (Table A-6.2; $p < 0.005$). Every unit increase in pH will result in a 1.07 ppm decrease in [Cr] in the leaves of *C. gratissimus*. The contributing R^2 (Table A-6.2) indicates that 32% of the variance in leaf content can be predicted from soil pH. Even though the unique contribution of total B horizon content was not significant, model 2 exhibited statistical significance and it can be used to predict 38.5% of the variance leaf Cr content.

The regression coefficient of pH in model 2, for soluble B horizon content, indicated a statistically significant relationship (Table A-6.2; $p < 0.005$). Every unit increase in pH will result in a 1.13 ppm decrease in [Cr] in the leaves of *C. gratissimus*. The contributing R^2 (Table A-6.2) indicates that 35.8% of the variance in leaf content can be predicted from soil pH. The total R^2 of 35.8% indicates that soil pH contributes almost all the prediction value of model 2.

Table A-6.2: Regression analysis for Cr content in the leaves of *C. gratissimus*. Significant at p < 0.05; highly significant at p < 0.005.

Model	Independent variable	Intercept	Regression coefficient	t-value	p-value	R^2 (contributing)	Total R^2
1	A horizon (total)	2.234	<0.001	0.20	0.845	0.003	0.003
2	A horizon (total)	10.065	<0.001	0.26	0.796	0.003	0.353
	pH		-1.108	-6.11	**<0.001**	0.351	
1	B horizon (total)	1.922	0.002	1.16	0.266	0.065	0.065
2	B horizon (total)	9.588	0.001	0.90	0.385	0.065	0.385
	pH		-1.068	-5.75	**<0.001**	0.320	
1	B horizon (soluble)	2.415	1.664	0.60	0.557	0.001	0.001
2	B horizon (soluble)	10.410	-5.021	-1.52	0.152	0.001	0.358
	pH		-1.132	-5.93	**<0.001**	0.358	

Regression analysis was used to predict the dependent variable, [Cr] in *G. bicolor* tissue, from the independent variables, soil concentrations and soil pH (Table A-6.3).

The regression coefficient of pH in model 2, for total A horizon content, indicated a statistically significant relationship (Table A-6.3; $p < 0.05$). Every unit increase in pH will result in a 0.74 ppm decrease in [Cr] in the leaves of *G. bicolor*. The contributing R^2 (Table A-6.3) indicates that 17.2% of the variance in leaf content can be predicted from soil pH. The total R^2 of 17.2% indicates that soil pH contributes almost all the prediction value of model 2.

Table A-6.3: Regression analysis for Cr content in the leaves of *G. bicolor*. Significant at p < 0.05; highly significant at p < 0.005.

Model	Independent variable	Intercept	Regression coefficient	t-value	p-value	R^2 (contributing)	Total R^2
1	A horizon (total)	2.307	<0.001	-0.03	0.980	<0.001	<0.001
2	A horizon (total)	7.487	<0.001	-0.14	0.891	<0.001	0.172
	pH		-0.735	-2.72	**0.013**	0.172	
1	B horizon (total)	2.512	-0.001	-0.49	0.633	0.011	0.011
2	B horizon (total)	9.317	-0.001	-1.20	0.244	0.011	**0.264**
	pH		-0.940	-3.71	**0.001**	0.253	
1	B horizon (soluble)	2.340	0	-	-	0	0
2	B horizon (soluble)	8.121	0	-	-	0	0.213
	pH		-0.828	-3.24	**0.004**	0.213	

The regression coefficient of pH in model 2, for total B horizon content, indicated a statistically significant relationship (Table A-6.3; $p < 0.005$). Every unit increase in pH will result in a 0.94 ppm decrease in [Cr] in the leaves of *G. bicolor*. The large contributing R^2 (Table A-6.3), indicates that 25.3% of the variance in leaf content can be predicted from soil

pH. Even though the unique contribution of total B horizon content was not significant, model 2 exhibited statistical significance and it can be used to predict 26.4% of the variance leaf Cr content.

The regression coefficient of pH in model 2, for soluble B horizon content, indicated a statistically significant contribution (Table A-6.3; $p < 0.005$). However, model 2 did not exhibit statistical significance and can therefore not be used to predict Cr concentrations in *G. bicolor* tissue.

A-7 Cobalt

Regression analysis results for Co are displayed in Table A-7.1 to Table A-7.3. Regression analysis was used to predict the dependent variable, [Co] in *B. albitrunca* tissue, from the independent variables, soil concentrations and soil pH (Table A-7.1).

The regression coefficient of total A horizon content indicated a statistically significant relationship in model 1 (Table A-7.1; $p < 0.005$). Every 1 ppm increase in total [Co] in the soil will result in a 0.001 ppm increase in leaf Co content (Figure A-7.1).

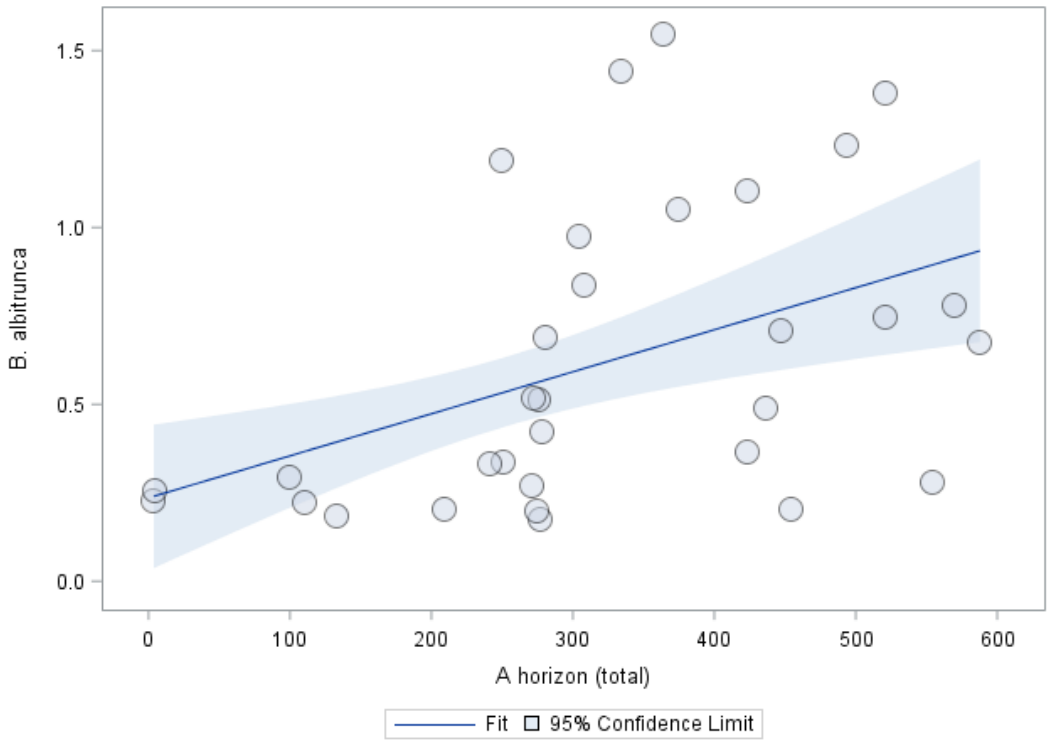

Figure A-7.1: Total Co content in the A horizon versus Co content in leaves of *B. albitrunca*.

The R^2 indicates that 19.2% of the variance in leaf Co content can be predicted by model 1. In model 2, the regression coefficient of pH is significant. Every unit increase in pH will result in a 0.62 ppm decrease in [Co] in the leaves of *B. albitrunca*. Even though the unique contribution of total A horizon content was not significant, model 2 exhibited statistical significance and it can be used to predict 40.8% of the variance leaf Co content.

The regression coefficient of pH in model 2, for total B horizon content, indicated a statistically significant relationship (Table A-7.1; $p < 0.005$). Every unit increase in pH will result in a 0.73 ppm decrease in [Co] in the leaves of *B. albitrunca*. The contributing R^2 (Table A-7.1) indicates that 35.6% of the variance in leaf content can be predicted from soil pH. Even though the unique contribution of total B horizon content was not significant, model 2 exhibited statistical significance and it can be used to predict 37.1% of the variance leaf Co content.

The regression coefficient of pH in model 2, for soluble B horizon content, indicated a statistically significant relationship (Table A-7.1; $p < 0.005$). Every unit increase in pH will result in a 0.76 ppm decrease in [Co] in the leaves of *B. albitrunca*. The contributing R^2 (Table A-7.1) indicates that 35.5% of the variance in leaf content can be predicted from soil pH. Even though the unique contribution of soluble B horizon content was not significant, model 2 exhibited statistical significance and it can be used to predict 36.5% of the variance leaf Co content.

Table A-7.1: Regression analysis for Co content in the leaves of *B. albitrunca*. Significant at $p < 0.05$; highly significant at $p < 0.005$.

Model	Independent variable	Intercept	Regression coefficient	t-value	p-value	R^2 (contributing)	Total R^2
1	A horizon (total)	0.236	0.001	3.42	**0.002**	0.192	0.192
2	A horizon (total)	4.553	0.001	1.76	0.089	0.192	**0.408**
	pH		-0.619	-3.64	**0.001**	0.216	
1	B horizon (total)	0.678	<0.001	-0.70	0.489	0.015	0.015
2	B horizon (total)	5.574	<0.001	-0.80	0.430	0.015	**0.371**
	pH		-0.732	-4.85	**<0.001**	0.356	
1	B horizon (soluble)	0.575	<0.001	0.52	0.605	0.010	0.010
2	B horizon (soluble)	5.743	<0.001	-0.21	0.837	0.010	**0.365**
	pH		-0.762	-4.68	**<0.001**	0.355	

Regression analysis was used to predict the dependent variable, [Co] in *C. gratissimus* tissue, from the independent variables, soil concentrations and soil pH (Table A-7.2).

The regression coefficient of pH in model 2, for total A horizon content, indicated a statistically significant relationship (Table A-7.2; $p < 0.005$). Every unit increase in pH will result in a 0.03 ppm decrease in [Co] in the leaves of *C. gratissimus*. The contributing R^2 (Table A-7.2) indicates that 34% of the variance in leaf content can be predicted from soil pH. The total R^2 of 34% indicates that soil pH contributes almost all the prediction value of model 2.

The regression coefficient of pH in model 2, for total B horizon content, indicated a statistically significant relationship (Table A-7.2; $p < 0.005$). Every unit increase in pH will result in a 0.03 ppm decrease in [Co] in the leaves of *C. gratissimus*. The contributing R^2 (Table A-7.2) indicates that 31.3% of the variance in leaf content can be predicted from soil pH. Even though the unique contribution of total B horizon content was not significant, model 2 exhibited statistical significance and it can be used to predict 34% of the variance leaf Co content.

The regression coefficient of pH in model 2, for soluble B horizon content, indicated a statistically significant relationship (Table A-7.2; $p < 0.005$). Every unit increase in pH will result in a 0.028 ppm decrease in [Co] in the leaves of *C. gratissimus*. The contributing R^2 (Table A-7.2) indicates that 28.7% of the variance in leaf content can be predicted from soil pH. Even though the unique contribution of soluble B horizon content was not significant, model 2 exhibited statistical significance and it can be used to predict 29.8% of the variance leaf Co content.

Table A-7.2: Regression analysis for Co content in the leaves of *C. gratissimus*. Significant at $p < 0.05$; highly significant at $p < 0.005$.

Model	Independent variable	Intercept	Regression coefficient	t-value	p-value	R^2 (contributing)	Total R^2
1	A horizon (total)	0.092	<0.001	-0.08	0.935	<0.001	<0.001
2	A horizon (total)	0.327	<0.001	-1.95	0.064	<0.001	**0.340**
	pH		-0.032	-5.50	**<0.001**	0.340	
1	B horizon (total)	0.099	<0.001	-0.81	0.425	0.027	0.027
2	B horizon (total)	0.307	<0.001	-1.34	0.194	0.027	**0.340**
	pH		-0.030	-3.73	**0.001**	0.313	
1	B horizon (soluble)	0.095	<0.001	-0.48	0.637	0.011	0.011
2	B horizon (soluble)	0.291	<0.001	-0.87	0.394	0.011	**0.298**
	pH		-0.028	-3.29	**0.004**	0.287	

Regression analysis was used to predict the dependent variable, [Co] in *G. bicolor* tissue, from the independent variables, soil concentrations and soil pH (Table A-7.3).

The regression coefficient of total A horizon content indicated a statistically significant relationship in model 1 (Table A-7.3; $p < 0.05$). Every 1 ppm increase in total [Co] in the soil will result in an 0.0001 ppm increase in leaf Co content (Figure A-7.2). The R^2 indicates that 17.4% of the variance in leaf Co content can be predicted by model 1. A statistically significant relationship is also indicated in model 2, by regression coefficients of total A horizon content as well as pH (Table A-7.3; $p < 0.05$ and $p < 0.005$). Every 1 ppm increase in total [Co] in the soil will result in a 0.0001 ppm increase in leaf Co content. Every unit increase in pH will result in a 0.035 ppm decrease in [Co] in the leaves of *G. bicolor*. The contributing R^2 values (Table A-7.3) indicate that 17.4% of the variance in leaf content can be predicted from the [Co] in the soil and 16.5% of the variance is attributed to the effect of pH. Therefore, model 2 can be used to predict 33.9% of the variance in leaf Co content.

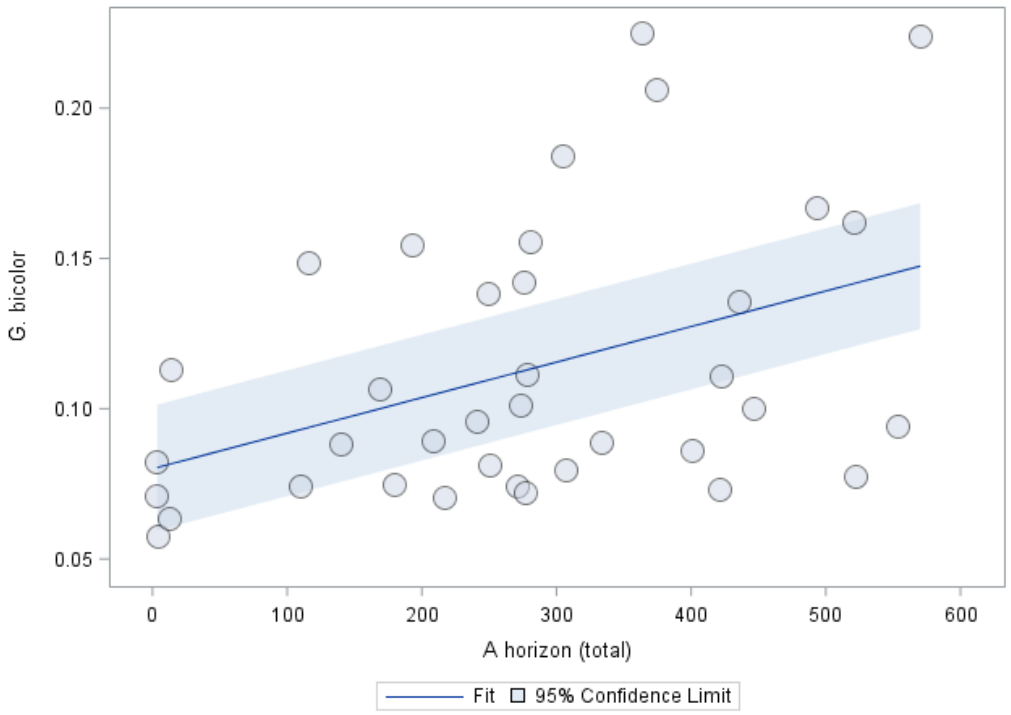

Figure A-7.2: Total Co content in the A horizon versus Co content in leaves of *G. bicolor*.

The regression coefficient of pH in model 2 (for total B horizon content), indicated a statistically significant relationship (Table A-7.3; $p < 0.005$). Every unit increase in pH will result in a 0.04 ppm decrease in [Co] in the leaves of *G. bicolor*. The contributing R^2 (Table A-7.3) indicates that 23.9% of the variance in leaf content can be predicted from soil pH. Even though the unique contribution of total B horizon content was not significant, model 2 exhibited statistical significance and it can be used to predict 24.7% of the variance leaf Co content.

The regression coefficient of pH in model 2, for soluble B horizon content, indicated a statistically significant relationship (Table A-7.3; $p < 0.005$). Every unit increase in pH will result in a 0.035 ppm decrease in [Co] in the leaves of *G. bicolor*. The contributing R^2 (Table A-7.3) indicates that 18.3% of the variance in leaf content can be predicted from soil pH. Even though the unique contribution of soluble B horizon content was not significant, model 2 exhibited statistical significance and it can be used to predict 27% of the variance leaf Co content.

Table A-7.3: Regression analysis for Co content in the leaves of *G. bicolor*. Significant at p < 0.05; highly significant at p < 0.005.

Model	Independent variable	Intercept	Regression coefficient	t-value	p-value	R^2 (contributing)	Total R^2
1	A horizon (total)	0.080	0.001	2.99	**0.005**	0.174	0.174
2	A horizon (total)	0.327	0.0001	2.12	**0.042**	0.174	**0.339**
	pH		-0.035	-4.21	**<0.001**	0.165	
1	B horizon (total)	0.111	<0.001	0.47	0.644	0.008	0.008
2	B horizon (total)	0.390	<0.001	0.06	0.954	0.008	0.247
	pH		-0.040	-4.30	**<0.001**	0.239	
1	B horizon (soluble)	0.103	<0.001	1.42	0.166	0.087	0.087
2	B horizon (soluble)	0.350	<0.001	1.00	0.328	0.087	**0.270**
	pH		<0.001	-4.17	**<0.001**	0.183	

A-8 Copper

Regression analysis results for Cu are displayed in Table A-8.1 to Table A-8.4. Regression analysis was used to predict the dependent variable, soil Cu concentrations and pH, from the independent variable, ore Cu content (Table A-8.1).

None of the dependent variables displayed a statistically significant correlation with Cu concentrations in the ore body.

Table A-8.1: Regression analysis for ore Cu content. Significant at p < 0.05; highly significant at p < 0.005.

Model	Dependent variable	Intercept	Regression coefficient	t-value	p-value	R^2 (contributing)	Total R^2
1	A horizon (total)	4.903	<0.001	0.06	0.954	<0.001	<0.001
1	B horizon (total)	6.149	<0.001	-0.83	0.420	0.038	0.038
1	B horizon (soluble)	0.059	<0.001	-1.14	0.274	0.087	0.087
1	pH A horizon	6.795	<0.001	0.24	0.814	0.001	0.001
1	pH B horizon	6.530	<0.001	0.73	0.478	0.016	0.016

Regression analysis was used to predict the dependent variable, [Cu] in *B. albitrunca* tissue, from the independent variables, soil concentrations and soil pH (Table A-8.2).

None of the independent variables displayed a statistically significant correlation with Cu content in the leaves of *B. albitrunca*.

Table A-8.2: Regression analysis for Cu content in the leaves of *B. albitrunca*. Significant at p < 0.05; highly significant at p < 0.005.

Model	Independent variable	Intercept	Regression coefficient	t-value	p-value	R^2 (contributing)	Total R^2
1	A horizon (total)	1.703	0.090	1.79	0.085	0.093	0.093
2	A horizon (total)	6.299	0.108	1.94	0.063	0.093	0.180
	pH		-0.700	-1.74	0.094	0.087	
1	B horizon (total)	1.568	0.101	1.85	0.075	0.091	0.091
2	B horizon (total)	5.416	0.107	1.99	0.057	0.091	0.153
	pH		-0.580	-1.54	0.136	0.062	
1	B horizon (soluble)	1.656	9.772	0.74	0.463	0.037	0.037
2	B horizon (soluble)	4.210	7.736	0.63	0.535	0.037	0.061
	pH		-0.367	-1.13	0.270	0.024	

Regression analysis was used to predict the dependent variable, [Cu] in *C. gratissimus* tissue, from the independent variables, soil concentrations and soil pH (Table A-8.3).

Table A-8.3: Regression analysis for Cu content in the leaves of *C. gratissimus*. Significant at p < 0.05; highly significant at p < 0.005.

Model	Independent variable	Intercept	Regression coefficient	t-value	p-value	R^2 (contributing)	Total R^2
1	A horizon (total)	5.626	0.199	2.33	**0.029**	0.124	0.124
2	A horizon (total)	7.560	0.223	1.97	0.061	0.124	0.131
	pH		-0.304	-0.44	0.666	0.007	
1	B horizon (total)	5.628	0.167	1.32	0.201	0.063	0.063
2	B horizon (total)	5.468	0.166	1.28	0.214	0.063	0.063
	pH		0.024	0.04	0.972	<0.001	
1	B horizon (soluble)	6.125	5.321	0.29	0.773	0.004	0.004
2	B horizon (soluble)	4.513	3.762	0.19	0.853	0.004	0.011
	pH		0.249	0.37	0.718	0.008	

The regression coefficient of total A horizon content indicated a statistically significant relationship in model 1 (Table A-8.3; $p < 0.05$). Every 1 ppm increase in total [Cu] in the soil will result in a 0.199 ppm increase in [Cu] in the leaves of *C. gratissimus* (Figure A-8.1).

Model 2 did not exhibit statistical significance and can therefore not be used to predict Cu concentrations in *C. gratissimus* tissue.

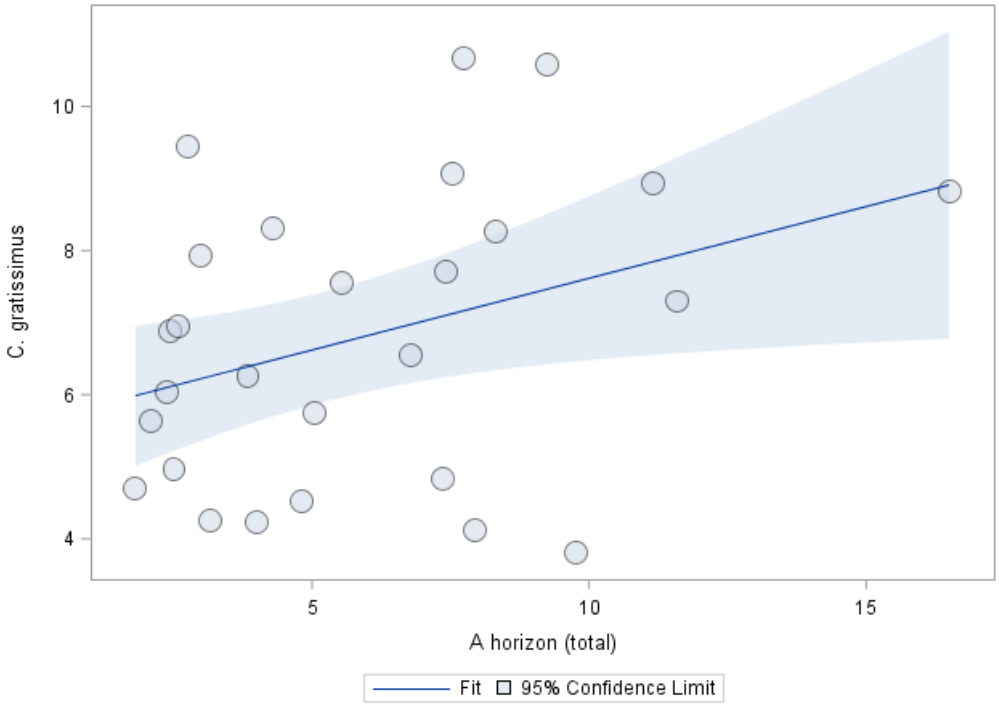

Figure A-8.1: Total Cu content in the A horizon versus Cu content in leaves of *C. gratissimus*.

Regression analysis was used to predict the dependent variable, [Cu] in *G. bicolor* tissue, from the independent variables, soil concentrations and soil pH (Table A-8.4).

The regression coefficient of total A horizon content indicated a statistically significant relationship in model 2 (Table A-8.4; $p < 0.05$). Every 1 ppm increase in total [Cu] in the soil will result in a 0.26 ppm increase in leaf Cu content. The regression coefficient for pH also indicated a statistically significant relationship (Table A-8.4; $p < 0.05$). Every unit increase in pH will result in a 1.93 ppm decrease in [Cu] in the leaves of *G. bicolor*. The contributing R^2 values indicate that 2.1% of the variance in leaf content can be predicted from total [Cu] in the soil and 12% of the variance is attributed to the effect of pH. Therefore, model 2 can be used to predict 14% of the variance in leaf Ba content.

The regression coefficient of pH in model 2, for total B horizon content, indicated a statistically significant relationship (Table A-8.4; $p < 0.05$). Every unit increase in pH will result in a 1.51 ppm decrease in [Cu] in the leaves of *G. bicolor*. The contributing R^2 (Table A-8.4) indicates that 8.5% of the variance in leaf content can be predicted from soil pH. Even

though the unique contribution of total B horizon content was not significant, model 2 exhibited statistical significance and it can be used to predict 15.1% of the variance leaf Cu content.

Table A-8.4: Regression analysis for Cu content in the leaves of *G. bicolor*. Significant at p < 0.05; highly significant at p < 0.005.

Model	Independent variable	Intercept	Regression coefficient	t-value	p-value	R^2 (contributing)	Total R^2
1	A horizon (total)	6.145	0.115	1.01	0.319	0.021	0.021
2	A horizon (total)	18.524	0.263	2.20	**0.035**	0.021	0.140
	pH		-1.928	-2.65	**0.013**	0.120	
1	B horizon (total)	5.217	0.266	1.56	0.129	0.065	0.065
2	B horizon (total)	15.218	0.320	2.00	0.055	0.065	0.151
	pH		-1.510	-2.36	**0.025**	0.085	
1	B horizon (soluble)	7.296	-17.174	-0.61	0.544	0.017	0.017
2	B horizon (soluble)	13.848	-12.902	-0.43	0.669	0.017	0.063
	pH		-0.989	-1.44	0.160	0.046	

A-9 Iron

Regression analysis results for Fe are displayed in Table A-9.1 to Table A-9.3. Regression analysis was used to predict the dependent variable, [Fe] in *B. albitrunca* tissue, from the independent variables, soil concentrations and soil pH (Table A-9.1).

Table A-9.1: Regression analysis for Fe content in the leaves of *B. albitrunca*. Significant at p < 0.05; highly significant at p < 0.005.

Model	Independent variable	Intercept	Regression coefficient	t-value	p-value	R^2 (contributing)	Total R^2
1	A horizon (total)	69.461	0.001	0.33	0.747	0.004	0.004
2	A horizon (total)	91.820	0.001	0.57	0.576	0.004	0.011
	pH		-3.511	-0.74	0.466	0.007	
1	B horizon (total)	56.320	0.004	1.76	0.096	0.097	0.097
2	B horizon (total)	93.344	0.004	2.12	**0.048**	0.097	0.121
	pH		-5.809	-1.30	0.209	0.024	
1	B horizon (soluble)	74.222	-3.743	-0.63	0.539	0.017	0.017
2	B horizon (soluble)	55.552	-5.368	-0.54	0.597	0.017	0.020
	pH		2.912	0.33	0.743	0.004	

The regression coefficient of total B horizon content indicated a statistically significant contribution in model 2 (Table A-9.1; $p < 0.05$). However, model 2 did not exhibit statistical

significance and can therefore not be used to predict Fe concentrations in *B. albitrunca* tissue.

Regression analysis was used to predict the dependent variable, [Fe] in *C. gratissimus* tissue, from the independent variables, soil concentrations and soil pH (Table A-9.2).

None of the independent variables displayed a statistically significant correlation with Fe content in the leaves of *C*. *gratissimus*.

Table A-9.2: Regression analysis for Fe content in the leaves of *C. gratissimus*. Significant at p < 0.05; highly significant at p < 0.005.

Model	Independent variable	Intercept	Regression coefficient	t-value	p-value	R^2 (contributing)	Total R^2
1	A horizon (total)	62.145	0.002	0.73	0.479	0.024	0.024
2	A horizon (total)	105.360	0.004	1.31	0.210	0.024	0.049
	pH		-6.986	-0.72	0.483	0.025	
1	B horizon (total)	74.453	-0.002	-0.49	0.631	0.019	0.019
2	B horizon (total)	69.722	-0.003	-0.50	0.622	0.019	0.019
	pH		0.761	0.12	0.904	<0.001	
1	B horizon (soluble)	56.777	11.386	1.45	0.171	0.142	0.142
2	B horizon (soluble)	187.119	25.489	1.62	0.129	0.142	0.343
	pH		-20.208	-1.30	0.217	0.201	

Regression analysis was used to predict the dependent variable, [Fe] in *G. bicolor* tissue, from the independent variables, soil concentrations and soil pH (Table A-9.3).

Table A-9.3: Regression analysis for Fe content in the leaves of *G. bicolor*. Significant at p < 0.05; highly significant at p < 0.005.

Model	Independent variable	Intercept	Regression coefficient	t-value	p-value	R^2 (contributing)	Total R^2
1	A horizon (total)	164.901	-0.010	-0.87	0.395	0.058	0.058
2	A horizon (total)	94.914	-0.013	-0.89	0.381	0.058	0.065
	pH		11.338	0.82	0.419	0.007	
1	B horizon (total)	201.700	-0.017	-1.05	0.306	0.113	0.113
2	B horizon (total)	202.057	-0.017	-1.03	0.316	0.113	0.113
	pH		-0.055	-0.01	0.995	<0.001	
1	B horizon (soluble)	146.103	-22.995	-0.82	0.420	0.038	0.038
2	B horizon (soluble)	30.065	-37.766	-0.78	0.444	0.038	0.049
	pH		18.390	0.68	0.507	0.011	

None of the independent variables displayed a statistically significant correlation with Fe content in the leaves of *G. bicolor*.

A-10 Lead

Regression analysis results for Pb are displayed in Table A-10.1 to Table A-10.4. Regression analysis was used to predict the dependent variable, soil Pb concentrations and pH, from the independent variable, ore Pb content (Table A-10.1).

None of the dependent variables displayed a statistically significant correlation with Pb concentrations in the ore body.

Table A-10.1: Regression analysis for ore Pb content. Significant at p < 0.05; highly significant at p < 0.005.

Model	Dependent variable	Intercept	Regression coefficient	t-value	p-value	R^2 (contributing)	Total R^2
1	A horizon (total)	1.766	<0.001	-1.53	0.153	0.058	0.058
1	B horizon (total)	1.999	<0.001	-2.05	0.063	0.165	0.165
1	B horizon (soluble)	3.9E-04	<0.001	-1.37	0.197	0.016	0.016
1	pH A horizon	6.765	<0.001	-1.17	0.265	0.084	0.084
1	pH B horizon	6.586	<0.001	-0.42	0.679	0.007	0.007

Regression analysis was used to predict the dependent variable, [Pb] in *B. albitrunca* tissue, from the independent variables, soil concentrations and soil pH (Table A-10.2).

The regression coefficient of pH in model 2, for total A horizon content, indicated a statistically significant relationship (Table A-10.2; $p < 0.05$). Every unit increase in pH will result in a 0.16 ppm decrease in [Pb] in the leaves of *B. albitrunca*. The contributing R^2 (Table A-10.2) indicates that 13% of the variance in leaf content can be predicted from soil pH. Even though the unique contribution of total A horizon content was not significant, model 2 exhibited statistical significance and it can be used to predict 14.4% of the variance leaf Pb content.

The regression coefficient of pH in model 2, for total B horizon content, indicated a statistically significant relationship (Table A-10.2; $p < 0.05$). Every unit increase in pH will result in a 0.16 ppm decrease in [Pb] in the leaves of *B. albitrunca*. The contributing R^2 (Table A-10.2) indicates that 13.3% of the variance in leaf content can be predicted from soil pH. Even though the unique contribution of total B horizon content was not significant, model 2 exhibited statistical significance and it can be used to predict 15.3% of the variance leaf Cu content.

Table A-10.2: Regression analysis for Pb content in the leaves of *B. albitrunca*. Significant at p < 0.05; highly significant at p < 0.005.

Model	Independent variable	Intercept	Regression coefficient	t-value	p-value	R^2 (contributing)	Total R^2
1	A horizon (total)	0.120	-0.032	-0.68	0.501	0.014	0.014
2	A horizon (total)	1.152	-0.021	-0.58	0.566	0.014	0.144
	pH		-0.157	-2.26	**0.032**	0.130	
1	B horizon (total)	0.133	-0.038	-0.80	0.429	0.020	0.020
2	B horizon (total)	1.179	-0.032	-0.84	0.410	0.020	0.153
	pH		-0.158	-2.20	**0.036**	0.133	
1	B horizon (soluble)	0.064	0.627	0.05	0.958	<0.001	<0.001
2	B horizon (soluble)	1.122	2.073	0.21	0.836	<0.001	0.131
	pH		-0.158	-1.98	0.058	0.131	

Regression analysis was used to predict the dependent variable, [Pb] in *C. gratissimus* tissue, from the independent variables, soil concentrations and soil pH (Table A-10.3).

The regression coefficient of total A horizon content indicated a statistically significant relationship in model 1 (Table A-10.3; $p < 0.05$). However, Pb concentrations for many of the plant samples were below the lowest detectable limit for ICP-MS. Therefore, unreliable results were produced. The regression coefficient of pH in model 2 also indicated a statistically significant relationship (Table A-10.3; $p < 0.005$). Every unit increase in pH will result in a 0.054 ppm decrease in [Pb] in the leaves of *C. gratissimus*. The contributing R^2 (Table A-10.3) indicates that 21.3% of the variance in leaf content can be predicted from soil pH. Even though the unique contribution of total A horizon content was not significant, model 2 exhibited statistical significance and it can be used to predict 27.9% of the variance leaf Pb content.

The regression coefficient of pH in model 2, for total B horizon content, indicated a statistically significant relationship (Table A-10.3; $p < 0.005$). Every unit increase in pH will result in a 0.049 ppm decrease in [Pb] in the leaves of *C. gratissimus*. The contributing R^2 (Table A-10.3) indicates that 21% of the variance in leaf content can be predicted from soil pH. Even though the unique contribution of total B horizon content was not significant, model 2 exhibited statistical significance and it can be used to predict 25.4% of the variance in leaf Pb content.

The regression coefficient of soluble B horizon content indicated a statistically significant relationship in model 1 (Table A-10.3; $p < 0.005$). However, Pb concentrations for the

majority of soil as well as plant samples were below the lowest detectable limit for ICP-MS. Therefore, unreliable results were produced.

Table A-10.3: Regression analysis for Pb content in the leaves of *C. gratissimus*. Significant at p < 0.05; highly significant at p < 0.005.

Model	Independent variable	Intercept	Regression coefficient	t-value	p-value	R^2 (contributing)	Total R^2
1	A horizon (total)	0.069	-0.016	-2.20	**0.038**	0.065	0.065
2	A horizon (total)	0.385	0.012	1.02	0.316	0.065	**0.279**
	pH		-0.054	-4.06	**0.001**	0.213	
1	B horizon (total)	0.074	-0.017	-1.23	0.232	0.044	0.044
2	B horizon (total)	0.354	0.011	0.66	0.519	0.044	**0.254**
	pH		-0.049	-3.81	**0.001**	0.210	
1	B horizon (soluble)	0.044	-10.105	-3.49	**0.002**	0.055	0.055
2	B horizon (soluble)	0.290	-6.703	-2.10	**0.049**	0.055	0.249
	pH		-0.036	-5.17	**<0.001**	0.194	

Regression analysis was used to predict the dependent variable, [Pb] in *G. bicolor* tissue, from the independent variables, soil concentrations and soil pH (Table A-10.4).

The regression coefficient of pH in model 2, for total A horizon content, indicated a statistically significant relationship (Table A-10.4; $p < 0.05$). Every unit increase in pH will result in a 0.12 ppm decrease in [Pb] in the leaves of *G. bicolor*. The contributing R^2 (Table A-10.4) indicates that 4.5% of the variance in leaf content can be predicted from soil pH. Even though the unique contribution of total A horizon content was not significant, model 2 exhibited statistical significance and it can be used to predict 10% of the variance leaf Pb content.

The regression coefficient of pH in model 2, for total B horizon content, indicated a statistically significant relationship (Table A-10.4; $p < 0.05$). Every unit increase in pH will result in a 0.118 ppm decrease in [Pb] in the leaves of *G. bicolor*. The contributing R^2 (Table A-10.4) indicates that 4.5% of the variance in leaf content can be predicted from soil pH. Even though the unique contribution of total B horizon content was not significant, model 2 exhibited statistical significance and it can be used to predict 9.8% of the variance leaf Pb content.

The regression coefficient of pH in model 2, for soluble B horizon content, indicated a statistically significant contribution (Table A-10.4; $p < 0.05$). However, model 2 did not exhibit statistical significance and can therefore not be used to predict Pb concentrations in *G. bicolor* tissue.

Table A-10.4: Regression analysis for Pb content in the leaves of *G. bicolor*. Significant at p < 0.05; highly significant at p < 0.005.

Model	Independent variable	Intercept	Regression coefficient	t-value	p-value	R^2 (contributing)	Total R^2
1	A horizon (total)	0.234	-0.068	-1.70	0.099	0.056	0.056
2	A horizon (total)	0.971	-0.012	-0.35	0.727	0.056	0.100
	pH		-0.124	-2.86	**0.007**	0.045	
1	B horizon (total)	0.264	-0.082	-1.46	0.154	0.053	0.053
2	B horizon (total)	0.961	-0.025	-0.50	0.624	0.053	0.098
	pH		-0.118	-2.72	**0.011**	0.045	
1	B horizon (soluble)	0.112	-38.114	-1.46	0.154	0.009	0.009
2	B horizon (soluble)	0.996	1.722	0.09	0.927	0.009	0.085
	pH		-0.131	-2.17	**0.039**	0.076	

A-11 Manganese

Regression analysis results for Mn are displayed in Table A-11.1 to Table A-11.3. Regression analysis was used to predict the dependent variable, [Mn] in *B. albitrunca* tissue, from the independent variables, soil concentrations and soil pH (Table A-11.1).

The regression coefficient of total A horizon content indicated a statistically significant relationship in model 1 (Table A-11.1; p < 0.005). Every 1 ppm increase in total [Mn] in the soil will result in a 1.36 ppm decrease in leaf Mn content (Figure A-11.1).

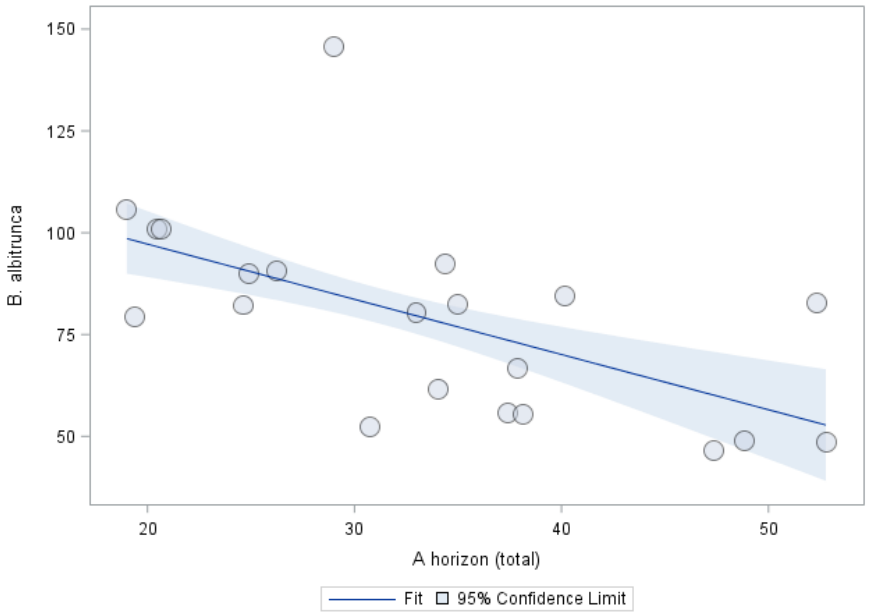

Figure A-11.1: Total Mn content in the A horizon versus Mn content in leaves of *B. albitrunca*.

The decreasing concentrations in leaf content is an unexpected trend. It is suspected that some other factor, such as pH, plant physiology or antagonistic interactions with other elements, may have caused this tendency. The R^2 indicates that 34.9% of the variance in leaf Mn content can be predicted by model 1. Even though the unique contribution of pH is not significant in model 2, the model exhibited statistical significance and it can be used to predict 36.9% of the variance in leaf Mn content.

The regression coefficient of total B horizon content indicated a statistically significant relationship in model 1 (Table A-11.1; $p < 0.005$). Every 1 ppm increase in total [Mn] in the soil will result in a 0.89 ppm decrease in leaf Mn content (Figure A-11.2). The same unexpected trend as for the A horizon is exhibited. The same factors may also have played a role. The R^2 indicates that 18.1% of the variance in leaf Mn content can be predicted by model 1. Even though the unique contribution of pH is not significant in model 2, the model exhibited statistical significance and it can be used to predict 19.2% of the variance in leaf Mn content.

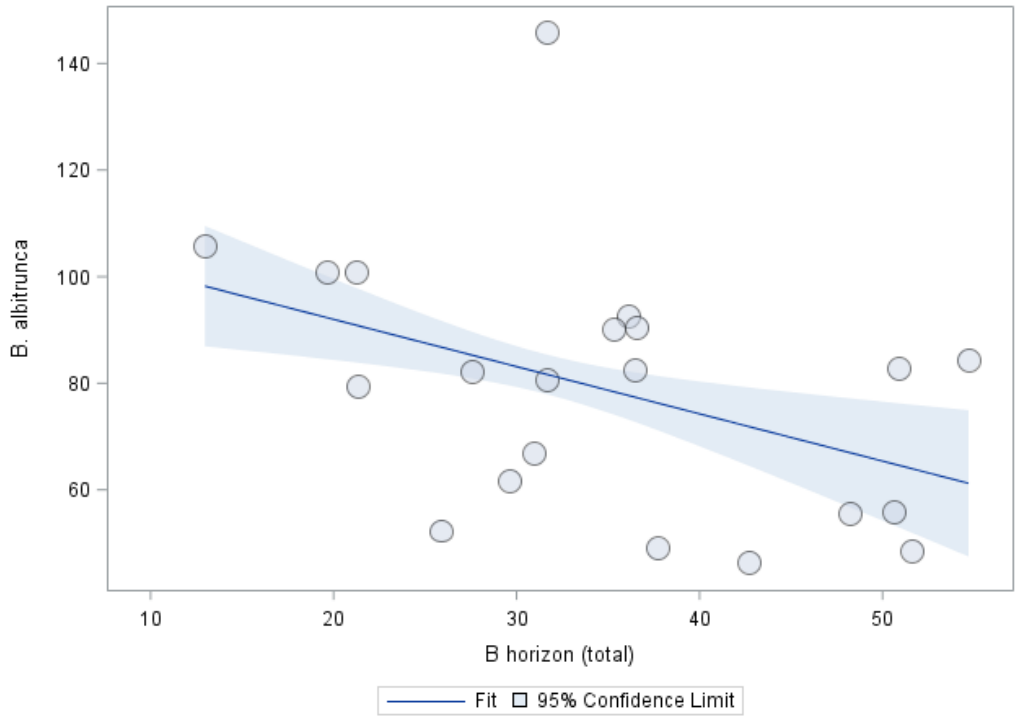

Figure A-11.2: Total Mn content in the B horizon versus Mn content in leaves of *B. albitrunca*.

The regression coefficient of pH in model 2, for soluble B horizon content, indicated a statistically significant contribution (Table A-11.1; $p < 0.05$). However, model 2 did not exhibit

statistical significance and can therefore not be used to predict Mn concentrations in *G. bicolor* tissue.

Table A-11.1: Regression analysis for Mn content in the leaves of *B. albitrunca*. Significant at p < 0.05; highly significant at p < 0.005.

Model	Independent variable	Intercept	Regression coefficient	t-value	p-value	R^2 (contributing)	Total R^2
1	A horizon (total)	124.320	-1.356	-4.71	**<0.001**	0.349	**0.349**
2	A horizon (total)	34.049	-1.700	-8.08	**<0.001**	0.349	**0.369**
	pH		14.940	1.51	0.148	0.020	
1	B horizon (total)	109.707	-0.886	-3.26	**0.004**	0.181	0.181
2	B horizon (total)	167.442	-0.730	-2.33	**0.031**	0.181	0.192
	pH		-9.272	-0.89	0.385	0.011	
1	B horizon (soluble)	85.365	-1.084	-0.46	0.654	0.010	0.010
2	B horizon (soluble)	247.814	-0.922	-0.65	0.527	0.010	0.119
	pH		-23.975	-2.50	**0.022**	0.109	

Regression analysis was used to predict the dependent variable, [Mn] in *C. gratissimus* tissue, from the independent variables, soil concentrations and soil pH (Table A-11.2).

The regression coefficient of total A horizon content indicated a statistically significant relationship in model 1 (Table A-11.2; $p < 0.05$). Every 1 ppm increase in total [Mn] in the soil will result in a 0.483 ppm decrease in leaf Mn content (Figure A-11.3).

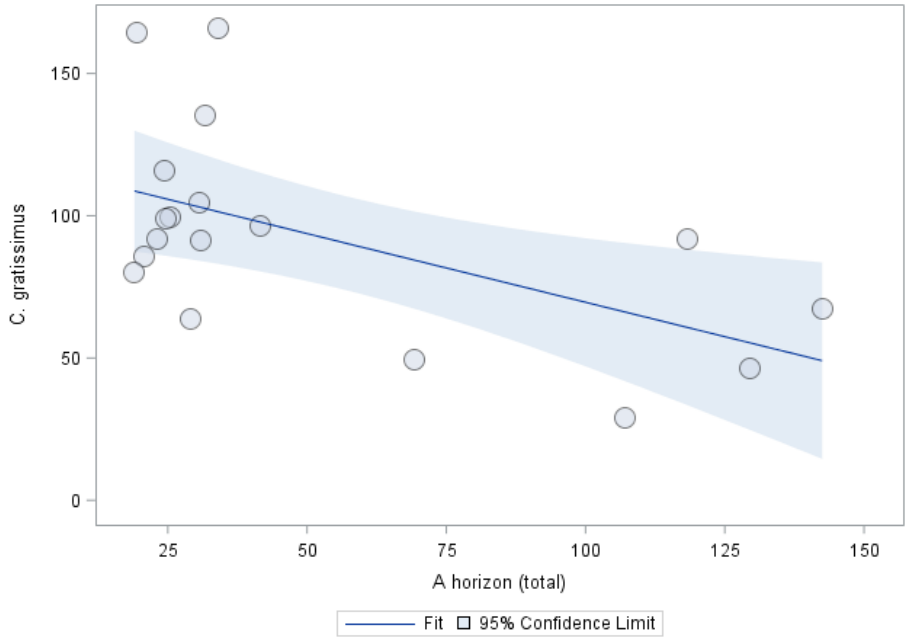

Figure A-11.3: Total Mn content in the A horizon versus Mn content in leaves of *C. gratissimus*.

The decreasing concentrations in leaf content is an unexpected trend. It is suspected that some other factor, such as pH, plant physiology or antagonistic interactions with other elements, may have caused this tendency. The R^2 indicates that 31% of the variance in leaf Mn content can be predicted by model 1. In model 2, the p-value for pH indicates significance. Every unit increase in pH will result in a 32.87 ppm decrease in [Mn] in the leaves of *C. gratissimus*. The contributing R^2 (Table A-11.2) indicates that 15.8% of the variance in leaf content can be predicted from soil pH. Even though the unique contribution of total A horizon content was not significant, model 2 exhibited statistical significance and it can be used to predict 46.8% of the variance leaf Mn content.

Total B horizon content exhibited a p-value of < 0.05 in model 1 (Table A-11.2), indicating that the regression coefficient is statistically significant. Every 1 ppm increase in total [Mn] in the soil will result in a 1.002 ppm decrease in leaf Mn content (Figure A-11.4).

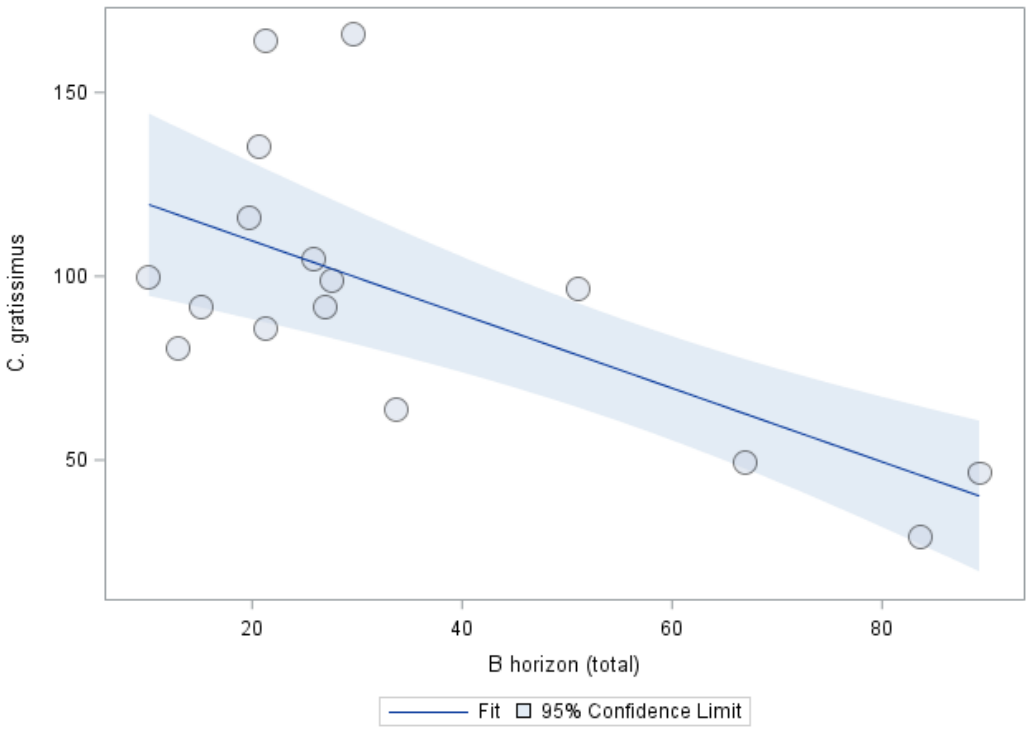

Figure A-11.4: Total Mn content in the B horizon versus Mn content in leaves of *C. gratissimus*.

The same unexpected trend as for the A horizon is exhibited. The same factors may also have played a role. The R^2 indicates that 41.5% of the variance in leaf Mn content can be predicted by model 1. The regression coefficient of pH in model 2 also indicated a statistically significant relationship (Table A-11.2; $p < 0.05$). Every unit increase in pH will result in a 24.32 ppm decrease in [Mn] in the leaves of *C. gratissimus*. The contributing R^2

(Table A-11.2) indicates that 6.4% of the variance in leaf content can be predicted from soil pH. Even though the unique contribution of total B horizon content was not significant, model 2 exhibited statistical significance and it can be used to predict 47.9% of the variance leaf Mn content.

The regression coefficient of pH in model 2, for soluble B horizon content, indicated a statistically significant relationship (Table A-11.2; $p < 0.005$). Every unit increase in pH will result in a 40.02 ppm decrease in [Mn] in the leaves of *C. gratissimus*. The contributing R^2 (Table A-11.2) indicates that 47.3% of the variance in leaf content can be predicted from soil pH. Even though the unique contribution of soluble B horizon content was not significant, model 2 exhibited statistical significance and it can be used to predict 48% of the variance leaf Mn content.

Table A-11.2: Regression analysis for Mn content in the leaves of *C. gratissimus*. Significant at $p < 0.05$; highly significant at $p < 0.005$.

Model	Independent variable	Intercept	Regression coefficient	t-value	p-value	R^2 (contributing)	Total R^2
1	A horizon (total)	117.848	-0.483	-2.91	**0.011**	0.310	**0.310**
2	A horizon (total)	331.192	-0.110	-0.89	0.387	0.310	**0.468**
	pH		-32.870	-3.84	**0.002**	0.158	
1	B horizon (total)	129.681	-1.002	-4.84	**<0.001**	0.415	**0.415**
2	B horizon (total)	282.476	-0.475	-2.07	0.059	0.415	**0.479**
	pH		-24.321	-2.56	**0.024**	0.064	
1	B horizon (soluble)	101.257	-1.170	-0.44	0.671	0.007	0.007
2	B horizon (soluble)	390.712	-2.616	-1.20	0.253	0.007	**0.480**
	pH		-40.018	5.25	**<0.001**	0.473	

Regression analysis was used to predict the dependent variable, [Mn] in *G. bicolor* tissue, from the independent variables, soil concentrations and soil pH (Table A-11.3).

The regression coefficient of total A horizon content indicated a statistically significant relationship in model 1(Table A-11.3; $p < 0.005$). Every 1 ppm increase in total [Mn] in the soil will result in a 0.21 ppm decrease in leaf Mn content (Figure A-11.5). The decreasing concentrations in leaf content is an unexpected trend. It is suspected that some other factor, such as pH, plant physiology or antagonistic interactions with other elements, may have caused this tendency. The R^2 indicates that 28.8% of the variance in leaf Mn content can be predicted by model 1. The regression coefficient of pH also indicated a statistically significant relationship (Table A-11.3; $p < 0.005$). Every unit increase in pH will result in a 14.06 ppm decrease in [Mn] in the leaves of *G. bicolor*. The contributing R^2 (Table A-11.3) indicates that

14.4% of the variance in leaf content can be predicted from soil pH. Even though the unique contribution of total A horizon content was not significant, model 2 exhibited statistical significance and it can be used to predict 43.1% of the variance leaf Mn content.

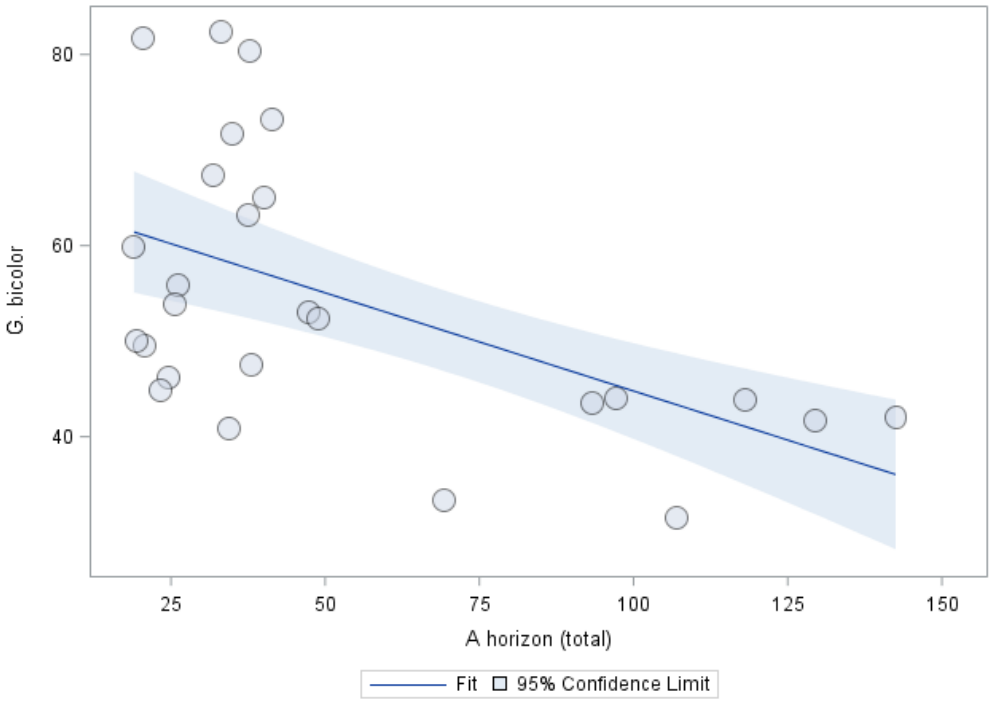

Figure A-11.5: Total Mn content in the A horizon versus Mn content in leaves of *G. bicolor*.

The regression coefficient of total B horizon content indicated a statistically significant relationship in model 1 (Table A-11.3; $p < 0.005$). Every 1 ppm increase in total [Mn] in the soil will result in a 0.26 ppm decrease in leaf Mn content (Figure A-11.6). The same unexpected trend as for the A horizon is exhibited. The same factors may also have played a role. The R^2 indicates that 20.2% of the variance in leaf Mn content can be predicted by model 1. The regression coefficient for pH also indicated a statistically significant relationship in model 2 (Table A-11.3; $p < 0.005$). Every unit increase in pH will result in a 16.39 ppm decrease in [Mn] in the leaves of *G. bicolor*. The contributing R^2 (Table A-11.3) indicates that 22.3% of the variance in leaf content can be predicted from soil pH. Even though the unique contribution of total B horizon content was not significant, model 2 exhibited statistical significance and it can be used to predict 42.5% of the variance leaf Mn content.

The regression coefficient of pH in model 2, for soluble B horizon content, indicated a statistically significant relationship (Table A-11.3; $p < 0.005$). Every unit increase in pH will result in a 15.51 ppm decrease in [Mn] in the leaves of *G. bicolor*. The contributing R^2 (Table

A-11.3) indicates that 41% of the variance in leaf content can be predicted from soil pH. Even though the unique contribution of soluble B horizon content was not significant, model 2 exhibited statistical significance and it can be used to predict 47% of the variance leaf Mn content.

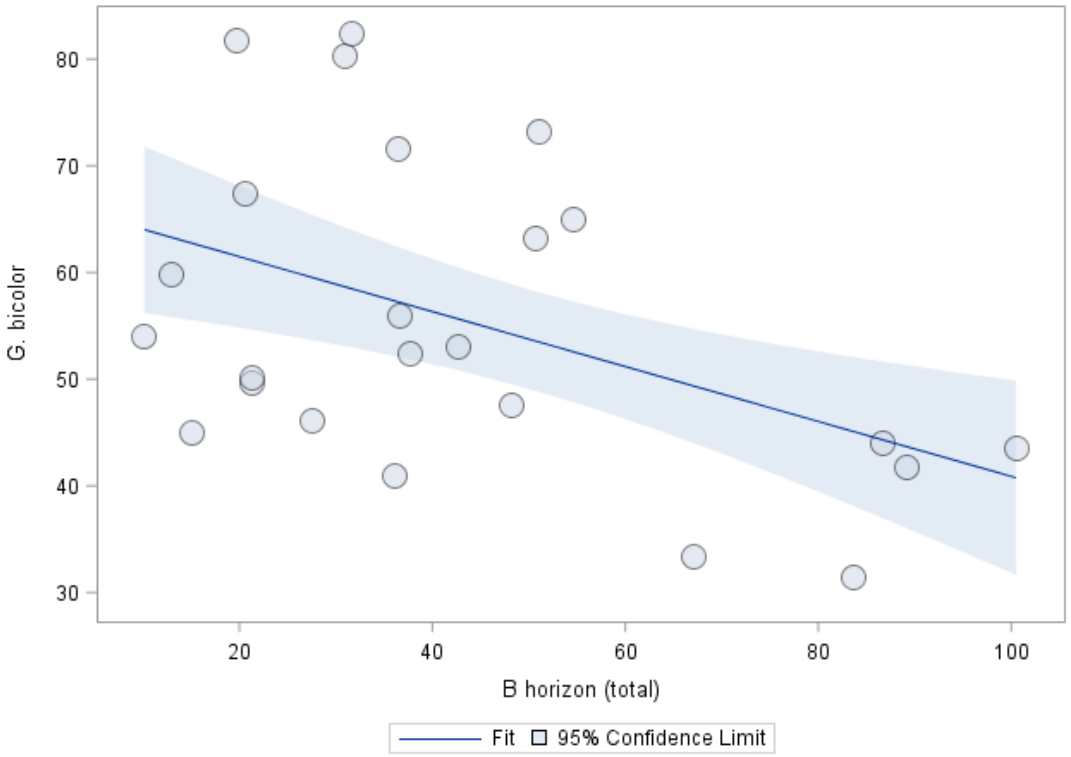

Figure A-11.6: Total Mn content in the B horizon versus Mn content in leaves of *G. bicolor*.

Table A-11.3: Regression analysis for Mn content in the leaves of *G. bicolor*. Significant at p < 0.05; highly significant at p < 0.005.

Model	Independent variable	Intercept	Regression coefficient	t-value	p-value	R^2 (contributing)	Total R^2
1	A horizon (total)	65.332	-0.205	-4.65	**<0.001**	0.288	**0.288**
2	A horizon (total)	155.259	-0.039	-0.61	0.547	0.288	**0.431**
	pH		-14.064	-3.85	**0.001**	0.144	
1	B horizon (total)	66.620	-0.257	-3.45	**0.003**	0.202	0.202
2	B horizon (total)	169.423	0.014	0.14	0.886	0.202	**0.425**
	pH		-16.391	-4.42	**<0.001**	0.223	
1	B horizon (soluble)	47.711	1.397	1.09	0.290	0.059	0.059
2	B horizon (soluble)	157.277	1.172	1.26	0.222	0.059	**0.470**
	pH		-15.505	-4.45	**<0.001**	0.410	

A-12 Mercury

Regression analysis results for Hg are displayed in Table A-12.1 to Table A-12.3. Regression analysis was used to predict the dependent variable, [Hg] in *B. albitrunca* tissue, from the independent variables, soil concentrations and soil pH (Table A-12.1).

None of the independent variables displayed a statistically significant correlation with Hg content in the leaves of *B. albitrunca*.

Table A-12.1: Regression analysis for Hg content in the leaves of *B. albitrunca*. Significant at p < 0.05; highly significant at p < 0.005.

Model	Independent variable	Intercept	Regression coefficient	t-value	p-value	R^2 (contributing)	Total R^2
1	A horizon (total)	0.031	-0.002	-0.25	0.806	0.002	0.002
2	A horizon (total)	0.188	0.000	-0.02	0.985	0.002	0.030
	pH		-0.024	-1.43	0.163	0.028	
1	B horizon (total)	0.022	0.006	0.83	0.412	0.023	0.023
2	B horizon (total)	0.200	0.007	1.00	0.327	0.023	0.060
	pH		-0.027	-1.68	0.104	0.037	
1	B horizon (soluble)	0.028	0.019	0.18	0.861	0.001	0.001
2	B horizon (soluble)	0.263	0.099	0.72	0.477	0.001	0.050
	pH		-0.035	-1.33	0.196	0.049	

Regression analysis was used to predict the dependent variable, [Hg] in *C. gratissimus* tissue, from the independent variables, soil concentrations and soil pH (Table A-12.2).

The regression coefficient of total A horizon content indicated a statistically significant relationship in model 2 (Table A-12.2; $p < 0.05$). Every 1 ppm increase in total [Hg] in the soil will result in a 0.01 ppm increase in leaf Hg content. The regression coefficient for pH also indicated a statistically significant relationship (Table A-12.2; $p < 0.05$). Every unit increase in pH will result in a 0.03 ppm decrease in [Hg] in the leaves of *C. gratissimus*. The contributing R^2 values indicate that 5.8% of the variance in leaf content can be predicted from total [Hg] in the soil and 19.3% of the variance is attributed to the effect of pH. Therefore, model 2 can be used to predict 25.1% of the variance in leaf Hg content.

The regression coefficient of pH in model 2, for total B horizon content, indicated a statistically significant relationship (Table A-12.2; $p < 0.05$). Every unit increase in pH will result in a 0.02 ppm decrease in [Hg] in the leaves of *C. gratissimus*. The contributing R^2 (Table A-12.2) indicates that 16.4% of the variance in leaf content can be predicted from soil pH. Even though the unique contribution of total B horizon content was not significant, model

2 exhibited statistical significance and it can be used to predict 23.9% of the variance leaf Hg content.

The regression coefficient of soluble B horizon content indicated a statistically significant relationship in model 1 (Table A-12.2; $p < 0.05$). However, Mo concentrations for the majority of soil as well as plant samples were below the lowest detectable limit for ICP-MS. Therefore, unreliable results were produced. The regression coefficient for pH indicated a statistically significant relationship in model 2 (Table A-12.2; $p < 0.05$). Every unit increase in pH will result in a 0.02 ppm decrease in [Hg] in the leaves of *C. gratissimus*. The contributing R^2 (Table A-12.2) indicates that 14.6% of the variance in leaf content can be predicted from soil pH. Even though the unique contribution of soluble B horizon content was not significant, model 2 exhibited statistical significance and it can be used to predict 19% of the variance leaf Hg content.

Table A-12.2: Regression analysis for Hg content in the leaves of *C. gratissimus*. Significant at $p < 0.05$; highly significant at $p < 0.005$.

Model	Independent variable	Intercept	Regression coefficient	t-value	p-value	R^2 (contributing)	Total R^2
1	A horizon (total)	0.009	0.008	1.86	0.076	0.058	0.058
2	A horizon (total)	0.177	0.009	2.50	**0.021**	0.058	**0.251**
	pH		-0.025	-2.77	**0.011**	0.193	
1	B horizon (total)	0.009	0.010	1.64	0.116	0.074	0.074
2	B horizon (total)	0.171	0.009	1.68	0.108	0.074	0.239
	pH		-0.024	-2.95	**0.008**	0.164	
1	B horizon (soluble)	0.023	-0.126	-2.45	**0.024**	0.044	0.044
2	B horizon (soluble)	0.179	-0.055	-0.72	0.481	0.044	0.190
	pH		-0.023	-2.95	**0.008**	0.146	

Regression analysis was used to predict the dependent variable, [Hg] in *G. bicolor* tissue, from the independent variables, soil concentrations and soil pH (Table A-12.3).

None of the independent variables displayed a statistically significant correlation with Hg content in the leaves of *G. bicolor*.

Table A-12.3: Regression analysis for Hg content in the leaves of *G. bicolor*. Significant at p < 0.05; highly significant at p < 0.005.

Model	Independent variable	Intercept	Regression coefficient	t-value	p-value	R^2 (contributing)	Total R^2
1	A horizon (total)	0.046	0.016	0.61	0.547	0.003	0.003
2	A horizon (total)	0.927	0.022	1.03	0.309	0.003	0.070
	pH		-0.129	-1.31	0.201	0.067	
1	B horizon (total)	0.018	0.065	1.39	0.175	0.067	0.067
2	B horizon (total)	0.861	0.062	1.45	0.159	0.067	0.123
	pH		-0.123	-1.26	0.218	0.056	
1	B horizon (soluble)	0.080	-0.388	-1.36	0.186	0.004	0.004
2	B horizon (soluble)	0.956	0.029	0.07	0.944	0.004	0.062
	pH		-0.130	-1.27	0.216	0.057	

A-13 Molybdenum

Regression analysis results for Mo are displayed in Table A-13.1 to Table A-13.4. Regression analysis was used to predict the dependent variable, soil Mo concentrations and pH, from the independent variable, ore Mo content (Table A-13.1).

None of the dependent variables displayed a statistically significant correlation with Mo concentrations in the ore body.

Table A-13.1: Regression analysis for ore Mo content. Significant at p < 0.05; highly significant at p < 0.005.

Model	Dependent variable	Intercept	Regression coefficient	t-value	p-value	R^2 (contributing)	Total R^2
1	A horizon (total)	3.671	-0.029	-1.49	0.163	0.146	0.146
1	B horizon (total)	4.596	-0.026	-1.14	0.278	0.092	0.092
1	B horizon (soluble)	0.002	<0.001	-1.04	0.320	0.082	0.082
1	pH A horizon	6.617	0.001	0.71	0.492	0.044	0.044
1	pH B horizon	6.415	0.002	0.67	0.515	0.047	0.047

Regression analysis was used to predict the dependent variable, [Mo] in *B. albitrunca* tissue, from the independent variables, soil concentrations and soil pH (Table A-13.2).

The regression coefficient of pH in model 2, for total A horizon content, indicated a statistically significant relationship (Table A-13.2; $p < 0.005$). Every unit increase in pH will result in a 0.74 ppm increase in [Mo] in the leaves of *B. albitrunca*. This trend was not

expected, since an increase in pH is usually anticipated to cause precipitation of elements, rendering them unavailable for plant uptake. However, it is possible that Mo becomes more soluble at higher pH levels so that higher concentrations can be absorbed by plant roots. The contributing R^2 (Table A-13.2) indicates that 24% of the variance in leaf content can be predicted from soil pH. Even though the unique contribution of total A horizon content was not significant, model 2 exhibited statistical significance and it can be used to predict 27.4% of the variance leaf Mo content.

The regression coefficient of pH in model 2, for total B horizon content, indicated a statistically significant relationship (Table A-13.2; $p < 0.05$). Every unit increase in pH will result in a 0.86 ppm increase in [Mo] in the leaves of *B. albitrunca*. The same unexpected trend as for the A horizon is exhibited. The same factors may therefore also have played a role. The contributing R^2 (Table A-13.2) indicates that 27.3% of the variance in leaf content can be predicted from soil pH. Even though the unique contribution of total B horizon content was not significant, model 2 exhibited statistical significance and it can be used to predict 27.6% of the variance leaf Mo content.

Table A-13.2: Regression analysis for Mo content in the leaves of *B. albitrunca*. Significant at $p < 0.05$; highly significant at $p < 0.005$.

Model	Independent variable	Intercept	Regression coefficient	t-value	p-value	R^2 (contributing)	Total R^2
1	A horizon (total)	0.629	-0.044	-1.43	0.168	0.034	0.034
2	A horizon (total)	-4.381	-0.038	-1.40	0.176	0.034	**0.274**
	pH		0.741	3.41	**0.003**	0.240	
1	B horizon (total)	0.593	-0.012	-0.17	0.866	0.003	0.003
2	B horizon (total)	-5.368	0.041	0.60	0.554	0.003	**0.276**
	pH		0.861	3.00	**0.007**	0.273	
1	B horizon (soluble)	0.569	-0.233	-3.11	**0.005**	0.009	0.009
2	B horizon (soluble)	-4.496	-0.199	-2.73	**0.012**	0.009	**0.256**
	pH		0.751	3.60	**0.002**	0.247	

The regression coefficient of soluble B horizon content indicated a statistically significant relationship in model 1 (Table A-13.2; $p < 0.05$). However, Mo concentrations for most of the soil samples were below the lowest detectable limit for ICP-MS and the correlation between soil content and concentrations in plant tissue was caused by a single outlier with detectable levels of soil soluble Mo. Therefore, unreliable results were produced. The regression coefficient of pH indicated a statistically significant relationship in model 2 (Table A-13.2; $p < 0.005$). Every unit increase in pH will result in a 0.75 ppm increase in [Mo] in the leaves of *B. albitrunca*. Although a negative correlation between pH and leaf element content is

expected, it is possible that Mo becomes more soluble at higher pH levels so that higher concentrations can be absorbed by plant roots. The contributing R^2 values (Table A-13.2) indicates that 0.9% of the variance in leaf content can be predicted from the [Mo] in the soil and 24.7% of the variance is attributed to the effect of pH. Therefore, model 2 can be used to predict 25.6% of the variance in leaf Mo content.

Regression analysis was used to predict the dependent variable, [Mo] in *C. gratissimus* tissue, from the independent variables, soil concentrations and soil pH (Table A-13.3).

The regression coefficient of pH in model 2, for total A horizon content, indicated a statistically significant relationship (Table A-13.3; $p < 0.005$). Every unit increase in pH will result in a 0.13 ppm increase in [Mo] in the leaves of *C. gratissimus*. Although a negative correlation between pH and leaf element content is expected, it is possible that Mo becomes more soluble at higher pH levels so that higher concentrations can be absorbed by plant roots. The contributing R^2 (Table A-13.3) indicates that 17% of the variance in leaf content can be predicted from soil pH. Even though the unique contribution of total A horizon content was not significant, model 2 exhibited statistical significance and it can be used to predict 18% of the variance leaf Mo content.

The regression coefficient of pH in model 2, for total B horizon content, indicated a statistically significant relationship (Table A-13.3; $p < 0.005$). Every unit increase in pH will result in a 0.15 ppm increase in [Mo] in the leaves of *C. gratissimus*. The same unexpected trend as for the A horizon is exhibited. The same factors may also have played a role. The contributing R^2 (Table A-13.3) indicates that 21.1% of the variance in leaf content can be predicted from soil pH. Even though the unique contribution of total B horizon content was not significant, model 2 exhibited statistical significance and it can be used to predict 21.2% of the variance leaf Mo content.

The regression coefficient of soluble B horizon content indicated a statistically significant relationship in model 1 (Table A-13.3; $p < 0.05$). However, Mo concentrations for most of the soil samples were below the lowest detectable limit for ICP-MS and the correlation between soil content and concentrations in plant tissue was caused by only a few samples with detectable levels of Mo. Therefore, unreliable results were produced. The regression coefficient for pH indicated a statistically significant relationship in model 2 (Table A-13.3; $p < 0.05$). Every unit increase in pH will result in a 0.11 ppm increase in [Mo] in the leaves of *C. gratissimus*. The contributing R^2 (Table A-13.3) indicates that 10.3% of the variance in leaf content can be predicted from soil pH. Even though the unique contribution of soluble B

horizon content was not significant, model 2 exhibited statistical significance and it can be used to predict 24.1% of the variance leaf Sb content.

Table A-13.3: Regression analysis for Mo content in the leaves of *C. gratissimus*. Significant at p < 0.05; highly significant at p < 0.005.

Model	Independent variable	Intercept	Regression coefficient	t-value	p-value	R^2 (contributing)	Total R^2
1	A horizon (total)	0.197	-0.006	-0.57	0.577	0.010	0.010
2	A horizon (total)	-0.696	-0.001	-0.09	0.933	0.010	0.180
	pH		0.127	4.50	**<0.001**	0.170	
1	B horizon (total)	1.677	0.002	0.18	0.858	0.001	0.001
2	B horizon (total)	-0.884	0.009	1.13	0.273	0.001	0.212
	pH		0.149	5.43	**<0.001**	0.211	
1	B horizon (soluble)	0.142	22.000	2.13	**0.048**	0.138	0.138
2	B horizon (soluble)	-0.572	15.158	1.85	0.082	0.138	0.241
	pH		0.105	3.00	**0.008**	0.103	

Regression analysis was used to predict the dependent variable, [Mo] in *G. bicolor* tissue, from the independent variables, soil concentrations and soil pH (Table A-13.4).

None of the independent variables displayed a statistically significant correlation with Mo content in the leaves of *G. bicolor*.

Table A-13.4: Regression analysis for Mo content in the leaves of *G. bicolor*. Significant at p < 0.05; highly significant at p < 0.005.

Model	Independent variable	Intercept	Regression coefficient	t-value	p-value	R^2 (contributing)	Total R^2
1	A horizon (total)	428924.36	-73872.31	-0.92	0.368	0.016	0.016
2	A horizon (total)	4592798.36	-96513.78	-0.96	0.344	0.016	0.058
	pH		-594787.50	-1.00	0.327	0.041	
1	B horizon (total)	383826.26	-26895.00	-1.07	0.295	0.003	0.003
2	B horizon (total)	4731131.18	-58476.18	-1.07	0.293	0.003	0.042
	pH		-616181.08	-1.00	0.328	0.039	
1	B horizon (soluble)	322893.81	-317472.39	-0.98	0.335	0.001	0.001
2	B horizon (soluble)	3931134.57	-408663.28	-0.96	0.346	0.001	0.032
	pH		-523136.86	-0.95	0.350	0.031	

A-14 Nickel

Regression analysis results for Ni are displayed in Table A-14.1 to Table A-14.3. Regression analysis was used to predict the dependent variable, [Ni] in *B. albitrunca* tissue, from the independent variables, soil concentrations and soil pH (Table A-14.1).

The regression coefficient of pH in model 2, for total A horizon content, indicated a statistically significant relationship (Table A-14.1; $p < 0.05$). Every unit increase in pH will result in a 1.56 ppm decrease in [Ni] in the leaves of *B. albitrunca*. The contributing R^2 (Table A-14.1) indicates that 15.5% of the variance in leaf content can be predicted from soil pH. Even though the unique contribution of total A horizon content was not significant, model 2 exhibited statistical significance and it can be used to predict 21.3% of the variance in leaf Ni content.

The regression coefficient of total B horizon content indicated a statistically significant relationship in model 1 (Table A-14.1; $p < 0.005$). Every 1 ppm increase in total [Ni] in the soil will result in a 0.001 ppm increase in leaf Ni content (Figure A-14.1).

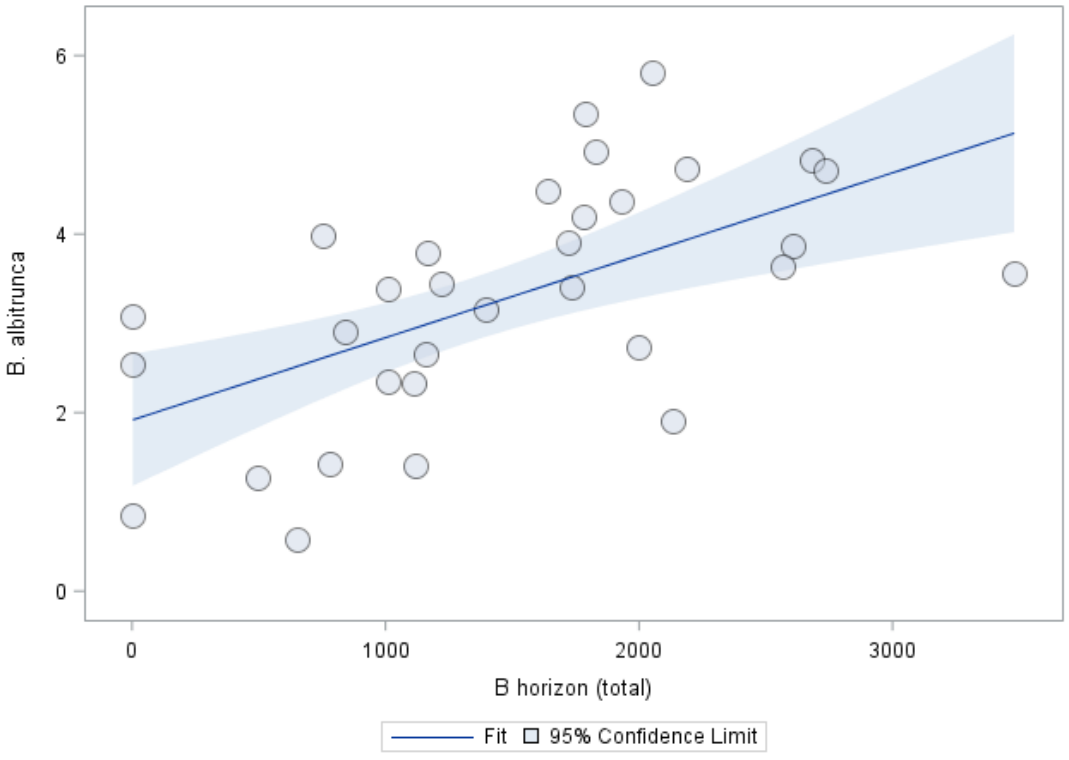

Figure A-14.1: Total Ni content in the B horizon versus Ni content in leaves of *B. albitrunca*.

The R^2 indicates that 34.9% of the variance in leaf Ni content can be predicted by model 1. Regression coefficients of total B horizon content as well as pH indicate a statistically significant contribution in model 2 (Table A-14.1; $p < 0.005$ and $p < 0.05$). Every unit increase in pH will result in a 1.11 ppm decrease in [Ni] in the leaves of *B. albitrunca*. The contributing R^2 values (Table A-14.1) indicates that 34.9% of the variance in leaf content can be predicted from the [Ni] in the soil and 7.6% of the variance is attributed to the effect of pH. Therefore, model 2 can be used to predict 42.5% of the variance in leaf Ni content.

The regression coefficient of soluble B horizon content indicated a statistically significant relationship in model 1 (Table A-14.1; $p < 0.005$). Every 1 ppm increase in soluble [Ni] in the soil will result in a 0.01 ppm increase in leaf Ni content (Figure A-14.2). The R^2 indicates that 31.4% of the variance in leaf Ni content can be predicted by model 1. The regression coefficient of soluble B horizon content indicated a statistically significant relationship in model 2 (Table A-14.1; $p < 0.05$). Even though the unique contribution of pH was not significant in model 2, the model exhibited statistical significance and it can be used to predict 37.2% of the variance in leaf Ni content.

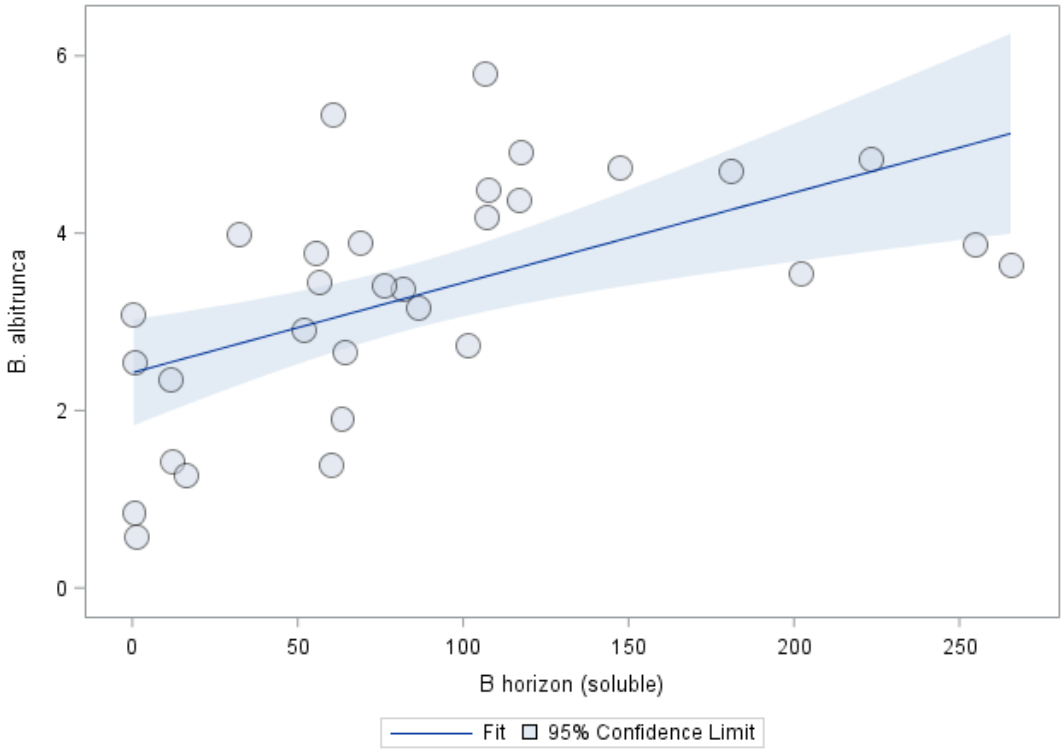

Figure A-14.2: Soluble Ni content in the B horizon versus Ni content in leaves of *B. albitrunca*.

Table A-14.1: Regression analysis for Ni content in the leaves of *B. albitrunca*. Significant at p < 0.05; highly significant at p < 0.005.

Model	Independent variable	Intercept	Regression coefficient	t-value	p-value	R^2 (contributing)	Total R^2
1	A horizon (total)	3.702	<0.001	-1.29	0.208	0.058	0.058
2	A horizon (total)	13.975	<0.001	-0.80	0.431	0.058	0.213
	pH		-1.555	-2.77	**0.010**	0.155	
1	B horizon (total)	1.916	0.001	3.87	**0.001**	0.349	**0.349**
2	B horizon (total)	9.563	0.001	3.23	**0.003**	0.349	**0.425**
	pH		-1.114	-2.17	**0.039**	0.076	
1	B horizon (soluble)	2.427	0.010	3.59	**0.001**	0.314	**0.314**
2	B horizon (soluble)	9.701	0.008	2.80	**0.009**	0.314	**0.372**
	pH		-1.056	-1.98	0.059	0.058	

Regression analysis was used to predict the dependent variable, [Ni] in *C. gratissimus* tissue, from the independent variables, soil concentrations and soil pH (Table A-14.2).

The regression coefficient of pH in model 2, for total A horizon content, indicated a statistically significant relationship (Table A-14.2; $p < 0.005$). Every unit increase in pH will result in a 0.52 ppm decrease in [Ni] in the leaves of *C. gratissimus*. The contributing R^2 (Table A-14.2) indicates that 50.1% of the variance in leaf content can be predicted from soil pH. Even though the unique contribution of total A horizon content was not significant, model 2 exhibited statistical significance and it can be used to predict 52.1% of the variance in leaf Ni content.

The regression coefficient of pH in model 2, for total B horizon content, indicated a statistically significant relationship (Table A-14.2; $p < 0.005$). Every unit increase in pH will result in a 0.51 ppm decrease in [Ni] in the leaves of *C. gratissimus*. The contributing R^2 (Table A-14.2) indicates that 47% of the variance in leaf content can be predicted from soil pH. Even though the unique contribution of total B horizon content was not significant, model 2 exhibited statistical significance and it can be used to predict 47.2% of the variance leaf Ni content.

The regression coefficient of pH in model 2, for soluble B horizon content, indicated a statistically significant relationship (Table A-14.2; $p < 0.005$). Every unit increase in pH will result in a 0.48 ppm decrease in [Ni] in the leaves of *C. gratissimus*. The contributing R^2 (Table A-14.2) indicates that 40.9% of the variance in leaf content can be predicted from soil pH. Even though the unique contribution of soluble B horizon content was not significant,

model 2 exhibited statistical significance and it can be used to predict 47.4% of the variance in leaf Ni content.

Table A-14.2: Regression analysis for Ni content in the leaves of *C. gratissimus*. Significant at p < 0.05; highly significant at p < 0.005.

Model	Independent variable	Intercept	Regression coefficient	t-value	p-value	R^2 (contributing)	Total R^2
1	A horizon (total)	1.050	7.5E-05	0.64	0.526	0.020	0.020
2	A horizon (total)	4.624	6.8E-05	0.93	0.364	0.020	0.521
	pH		-0.521	-6.46	**<0.001**	0.501	
1	B horizon (total)	1.124	2.2E-05	0.26	0.800	0.002	0.002
2	B horizon (total)	4.717	-5.2E-05	-0.64	0.527	0.002	0.472
	pH		-0.512	-6.73	**<0.001**	0.470	
1	B horizon (soluble)	1.018	0.001	1.19	0.249	0.065	0.065
2	B horizon (soluble)	4.378	-2.2E-04	-0.35	0.733	0.065	0.474
	pH		-0.475	-6.00	**<0.001**	0.409	

Regression analysis was used to predict the dependent variable, [Ni] in *G. bicolor* tissue, from the independent variables, soil concentrations and soil pH (Table A-14.3).

The regression coefficient of pH in model 2, for total A horizon content, indicated a statistically significant relationship (Table A-14.3; $p < 0.005$). Every unit increase in pH will result in a 0.36 ppm decrease in [Ni] in the leaves of *G. bicolor*. The large contributing R^2 (Table A-14.3), indicates that 47.7% of the variance in leaf content can be predicted from soil pH. Even though the unique contribution of total A horizon content was not significant, model 2exhibited statistical significance and it can be used to predict 47.8% of the variance in leaf Ni content.

The regression coefficient of pH in model 2, for total B horizon content, indicated a statistically significant relationship (Table A-14.3; $p < 0.005$). Every unit increase in pH will result in a 0.34 ppm decrease in [Ni] in the leaves of *G. bicolor*. The contributing R^2 (Table A-14.3) indicates that 40.3% of the variance in leaf content can be predicted from soil pH. Even though the unique contribution of total B horizon content was not significant, model 2 exhibited statistical significance and it can be used to predict 45.9% of the variance leaf Ni content.

The regression coefficient of soluble B horizon content indicated a statistically significant relationship in model 1 (Table A-14.3; $p < 0.05$). Every 1 ppm increase in soluble [Ni] in the soil will result in a 0.001 ppm increase in leaf Ni content (Figure A-14.3). The R^2 indicates that 12% of the variance in leaf Ni content can be predicted by model 1. The regression

coefficient of pH in model 2, for soluble B horizon content, indicated a statistically significant relationship (Table A-14.3; $p < 0.005$). Every unit increase in pH will result in a 0.33 ppm decrease in [Ni] in the leaves of *G. bicolor*. The contributing R^2 (Table A-14.3) indicates that 31.6% of the variance in leaf content can be predicted from soil pH. Even though the unique contribution of soluble B horizon content was not significant, model 2 exhibited statistical significance and it can be used to predict 43.6% of the variance leaf Ni content.

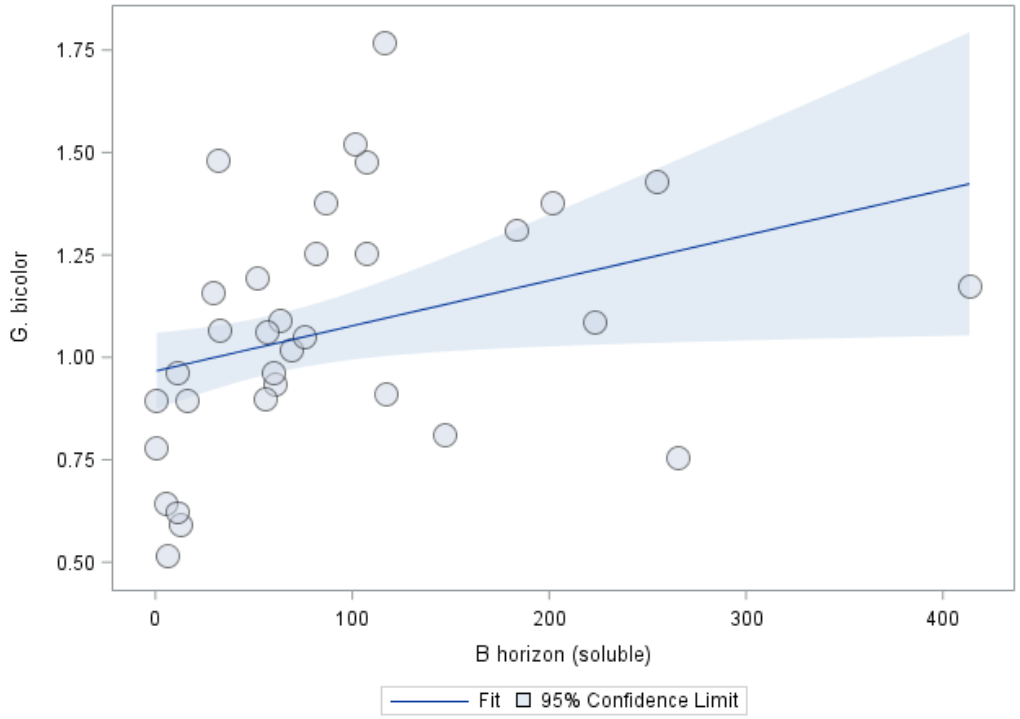

Figure A-14.3: Soluble Ni content in the B horizon versus Ni content in leaves of *G. bicolor*.

Table A-14.3: Regression analysis for Ni content in the leaves of *G. bicolor*. Significant at $p < 0.05$; highly significant at $p < 0.005$.

Model	Independent variable	Intercept	Regression coefficient	t-value	p-value	R^2 (contributing)	Total R^2
1	A horizon (total)	1.064	<0.001	-0.15	0.885	0.001	0.001
2	A horizon (total)	3.566	<0.001	-0.31	0.762	0.001	**0.478**
	pH		-0.364	-7.94	**<0.001**	0.477	
1	B horizon (total)	0.950	<0.001	1.92	0.064	0.056	0.056
2	B horizon (total)	3.369	<0.001	0.99	0.332	0.056	**0.459**
	pH		-0.344	-7.13	**<0.001**	0.403	
1	B horizon (soluble)	0.967	0.001	2.21	**0.035**	0.120	0.120
2	B horizon (soluble)	3.313	<0.001	0.40	0.692	0.120	**0.436**
	pH		-0.331	-5.93	**<0.001**	0.316	

A-15 Selenium

Regression analysis results for Se are displayed in Table A-15.1 to Table A-15.3. Regression analysis was used to predict the dependent variable, [Se] in *B. albitrunca* tissue, from the independent variables, soil concentrations and soil pH (Table A-15.1).

The regression coefficient of total A horizon content indicated a statistically significant relationship in model 1 (Table A-15.1; $p < 0.05$). Every 1 ppm increase in total [Se] in the soil will result in a 14.34 ppm increase in leaf Se content (Figure A-15.1).

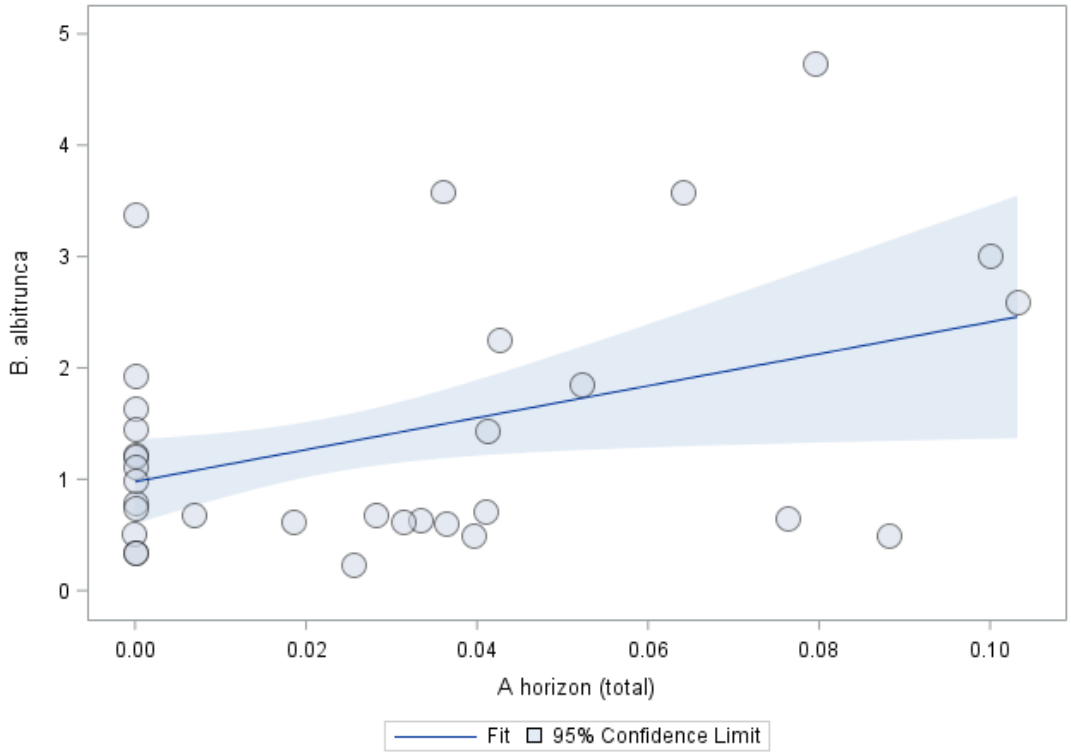

Figure A-15.1: Total Se content in the A horizon versus Se content in leaves of *B. albitrunca*.

This is a significant anomaly; and extremely high potential for hyperaccumulation of Se in *B. albitrunca* exists. The R^2 indicates that 16.3% of the variance in leaf Se content can be predicted by model 1. The regression coefficient of pH indicated a statistically significant relationship in model 2 (Table A-15.1; $p < 0.005$). Every unit increase in pH will result in a 2.056 ppm increase in [Se] in the leaves of *B. albitrunca*. This trend was not expected, since an increase in pH is usually anticipated to cause precipitation of elements, rendering them unavailable for plant uptake. However, it is possible that Se becomes more soluble at higher pH levels so that higher concentrations can be absorbed by plant roots. The contributing R^2 (Table A-15.1) indicates that 30.2% of the variance in leaf content can be predicted from soil

pH. Even though the unique contribution of total A horizon content was not significant, model 2 exhibited statistical significance and it can be used to predict 46.5% of the variance in leaf Se content.

The regression coefficient of pH in model 2, for total B horizon content, indicated a statistically significant relationship (Table A-15.1; $p < 0.005$). Every unit increase in pH will result in a 2.28 ppm increase in [Se] in the leaves of *B. albitrunca*. The same unexpected trend as for the A horizon is exhibited. The same factors may also have played a role. The contributing R^2 (Table A-15.1) indicates that 45.2% of the variance in leaf content can be predicted from soil pH. Even though the unique contribution of total B horizon content was not significant, model 2 exhibited statistical significance and it can be used to predict 45.4% of the variance in leaf Se content.

Soluble Se content for all B horizon soil samples were below the lowest detectable limits for ICP-MS. Therefore, no definitive regression results were produced.

Table A-15.1: Regression analysis for Se content in the leaves of *B. albitrunca*. Significant at $p < 0.05$; highly significant at $p < 0.005$.

Model	Independent variable	Intercept	Regression coefficient	t-value	p-value	R^2 (contributing)	Total R^2
1	A horizon (total)	0.978	14.343	2.25	**0.033**	0.163	0.163
2	A horizon (total)	-12.507	5.100	1.01	0.319	0.163	**0.465**
	pH		2.056	5.06	**<0.001**	0.302	
1	B horizon (total)	1.357	2.501	0.26	0.795	0.002	0.002
2	B horizon (total)	-13.907	4.198	0.71	0.485	0.002	**0.454**
	pH		2.276	5.19	**<0.001**	0.452	
1	B horizon (soluble)	1.429	0	-	-	0	0
2	B horizon (soluble)	-13.725	0	-	-	0	**0.439**
	pH		2.260	5.38	**<0.001**	0.439	

Regression analysis was used to predict the dependent variable, [Se] in *C. gratissimus* tissue, from the independent variables, soil concentrations and soil pH (Table A-15.2).

The regression coefficient of total A horizon content indicated a statistically significant relationship in model 1 (Table A-15.2; $p < 0.005$). Every 1 ppm increase in total [Se] in the soil will result in a 0.995 ppm increase in leaf Se content (Figure A-15.2). The R^2 indicates that 34.5% of the variance in leaf Se content can be predicted by model 1. Regression coefficients of total A horizon content as well as pH indicate a statistically significant relationship in model 2 (Table A-15.2; $p < 0.05$). Every unit increase in pH will result in a 0.059 ppm decrease in [Se] in the leaves of *C. gratissimus*. The contributing R^2 values

(Table A-15.2) indicate that 34.5% of the variance in leaf content can be predicted from the [Se] in the soil and 30.6% of the variance is attributed to the effect of pH. Therefore, model 2 can be used to predict 65.1% of the variance in leaf Se content.

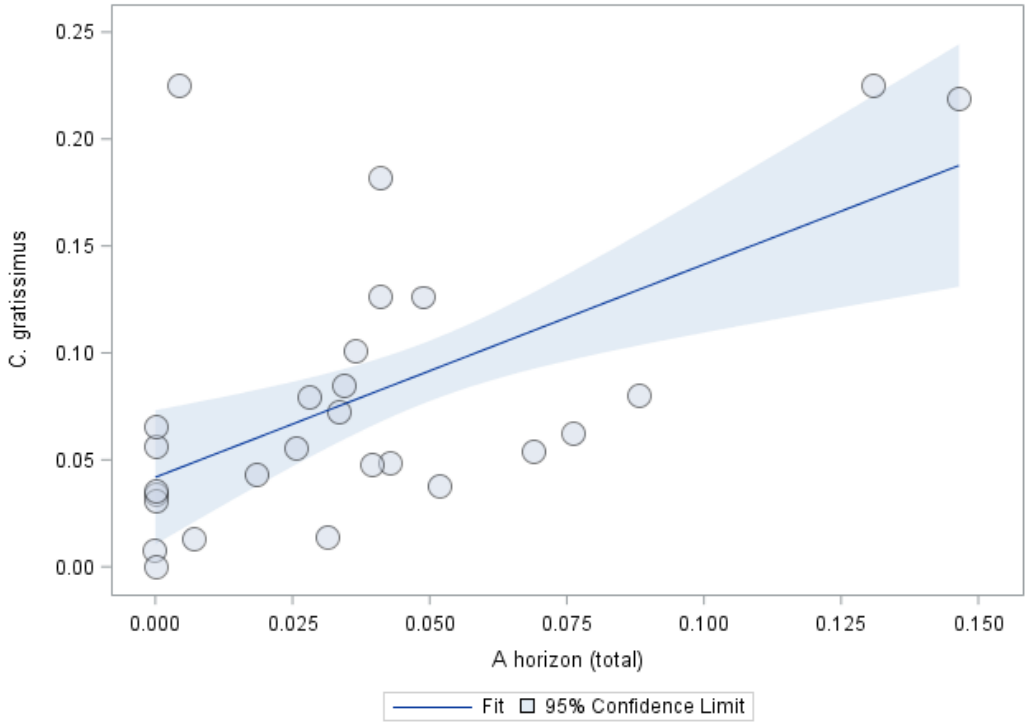

Figure A-15.2: Total Se content in the A horizon versus Se content in leaves of *C. gratissimus*.

The regression coefficient of pH in model 2, for total B horizon content, indicated a statistically significant relationship (Table A-15.2; $p < 0.005$). Every unit increase in pH will result in a 0.062 ppm increase in [Se] in the leaves of *C. gratissimus*. Although a negative correlation between pH and leaf element content is expected, it is possible that Se becomes more soluble at higher pH levels so that higher concentrations can be absorbed by plant roots. The contributing R^2 (Table A-15.2) indicates that 53.6% of the variance in leaf content can be predicted from soil pH. Even though the unique contribution of total B horizon content was not significant, model 2 exhibited statistical significance and it can be used to predict 54.3% of the variance leaf Se content.

Soluble Se content for all B horizon soil samples were below the lowest detectable limits for ICP-MS. Therefore, no definitive regression results were produced.

Table A-15.2: Regression analysis for Se content in the leaves of *C. gratissimus*. Significant at p < 0.05; highly significant at p < 0.005.

Model	Independent variable	Intercept	Regression coefficient	t-value	p-value	R^2 (contributing)	Total R^2
1	A horizon (total)	0.042	0.995	3.64	**0.001**	0.345	**0.345**
2	A horizon (total)	-0.355	0.754	2.73	**0.012**	0.345	**0.651**
	pH		0.059	2.94	**0.007**	0.306	
1	B horizon (total)	0.062	0.187	0.57	0.575	0.006	0.006
2	B horizon (total)	-0.361	0.267	0.97	0.344	0.006	**0.543**
	pH		0.062	3.40	**0.003**	0.536	
1	B horizon (soluble)	0.066	0	-	-	0	0
2	B horizon (soluble)	-0.375	0	-	-	0	**0.583**
	pH		0.065	3.81	**0.001**	0.583	

Regression analysis was used to predict the dependent variable, [Se] in *G. bicolor* tissue, from the independent variables, soil concentrations and soil pH (Table A-15.3).

The regression coefficient of total A horizon content indicated a statistically significant relationship in model 1 (Table A-15.3; p < 0.05). Every 1 ppm increase in total [Se] in the soil will result in a 0.4 ppm increase in leaf Se content (Figure A-15.3).

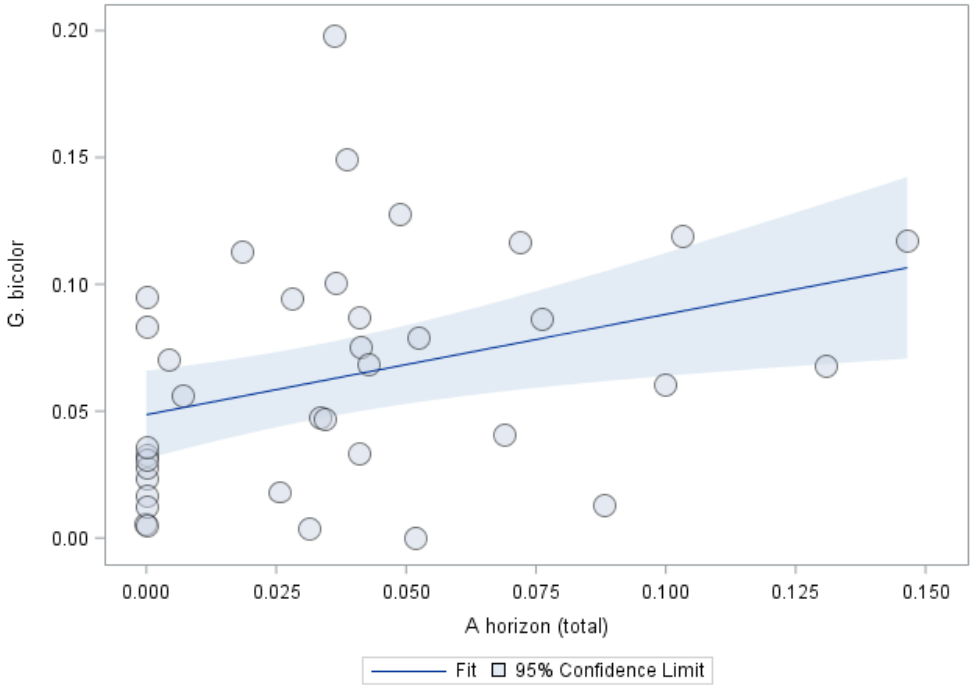

Figure A-15.3: Total Se content in the A horizon versus Se content in leaves of *G. bicolor*.

The R^2 indicates that 10.9% of the variance in leaf Se content can be predicted by model 1. The regression coefficient of total A horizon content also indicated a statistically significant relationship in model 2. Even though the unique contribution of pH is not significant in model 2, the model exhibited statistical significance and it can be used to predict 21.1% of the variance in leaf Se content.

The regression coefficient of total B horizon content indicated a statistically significant relationship in model 1 and model 2 (Table A-15.3; $p < 0.05$). However, the correlation between soil content and concentrations in plant tissue was caused by a single outlier. Therefore, unreliable results were produced.

Soluble Se content for all B horizon soil samples were below the lowest detectable limits for ICP-MS. Therefore, no definitive regression results were produced.

Table A-15.3: Regression analysis for Se content in the leaves of *G. bicolor*. Significant at p < 0.05; highly significant at p < 0.005.

Model	Independent variable	Intercept	Regression coefficient	t-value	p-value	R^2 (contributing)	Total R^2
1	A horizon (total)	0.049	0.396	2.81	**0.008**	0.109	0.109
2	A horizon (total)	-0.133	0.292	2.15	**0.039**	0.109	0.211
	pH		0.027	2.01	0.053	0.102	
1	B horizon (total)	0.054	0.290	2.85	**0.008**	0.062	0.062
2	B horizon (total)	-0.138	0.248	2.89	**0.007**	0.062	0.175
	pH		0.028	2.02	0.052	0.113	
1	B horizon (soluble)	0.059	0	-	-	0	0
2	B horizon (soluble)	-0.156	0	-	-	0	0.147
	pH		0.031	2.13	**0.042**	0.147	

The results and statistical analyses show that Se increase if in high concentrations available in both the A and B horizon for more than one species. The increase of Se in plant tissue with increase in pH is not well understood, since a decrease of Se content is expected with increase in pH. This phenomenon should therefore be investigated further. The results remain positive with respect to high pH calcrete which is not able to screen the Se values between the soluble and total element environment. It is also significant from a biogeochemical exploration point of view for a couple of species, such as *B. albitrunca* and *C. gratissimus*.

A-16 Silver

Regression analysis results for Ag are displayed in Table A-16.1 to Table A-16.4. Regression analysis was used to predict the dependent variable, soil Ag concentrations and pH, from the independent variable, ore Ag content (Table A-16.1).

None of the dependent variables displayed a statistically significant correlation with Ag concentrations in the ore body.

Table A-16.1: Regression analysis for ore Ag content. Significant at p < 0.05; highly significant at p < 0.005.

Model	Dependent variable	Intercept	Regression coefficient	t-value	p-value	R^2 (contributing)	Total R^2
1	A horizon (total)	0.128	-0.007	-1.63	0.125	0.133	0.133
1	B horizon (total)	0.074	-0.002	-1.13	0.278	0.068	0.068
1	B horizon (soluble)	0.001	<0.001	-0.76	0.463	0.015	0.015
1	pH A horizon	6.686	0.018	0.89	0.388	0.039	0.039
1	pH B horizon	6.506	0.023	0.88	0.396	0.039	0.039

Regression analysis was used to predict the dependent variable, [Ag] in *B. albitrunca* tissue, from the independent variables, soil concentrations and soil pH (Table A-16.2).

Table A-16.2: Regression analysis for Ag content in the leaves of *B. albitrunca*. Significant at p < 0.05; highly significant at p < 0.005.

Model	Independent variable	Intercept	Regression coefficient	t-value	p-value	R^2 (contributing)	Total R^2
1	A horizon (total)	0.025	0.064	1.00	0.324	0.036	0.036
2	A horizon (total)	0.105	0.060	0.92	0.366	0.036	0.048
	pH		-0.012	-0.96	0.345	0.012	
1	B horizon (total)	0.012	0.330	2.42	**0.022**	0.154	0.154
2	B horizon (total)	0.066	0.321	2.36	**0.026**	0.154	0.160
	pH		-0.008	-0.77	0.448	0.005	
1	B horizon (soluble)	0.030	-1.194	-0.24	0.814	0.002	0.002
2	B horizon (soluble)	0.143	-0.280	-0.05	0.959	0.002	0.024
	pH		-0.017	-1.11	0.276	0.022	

The regression coefficient of total B horizon content indicated a statistically significant relationship in model 1 (Table A-16.2; $p < 0.05$). Every 1 ppm increase in total [Ag] in the soil will result in a 0.33 ppm increase in leaf Ag content (Figure A-16.1). The R^2 indicates that 15.4% of the variance in leaf Ag content can be predicted by model 1. The regression coefficient of total B horizon content also indicated a statistically significant relationship in

model 2 (Table A-16.2; $p < 0.05$). Even though the unique contribution of pH is not significant in model 2, the model exhibited statistical significance and it can be used to predict 16% of the variance in leaf Ag content.

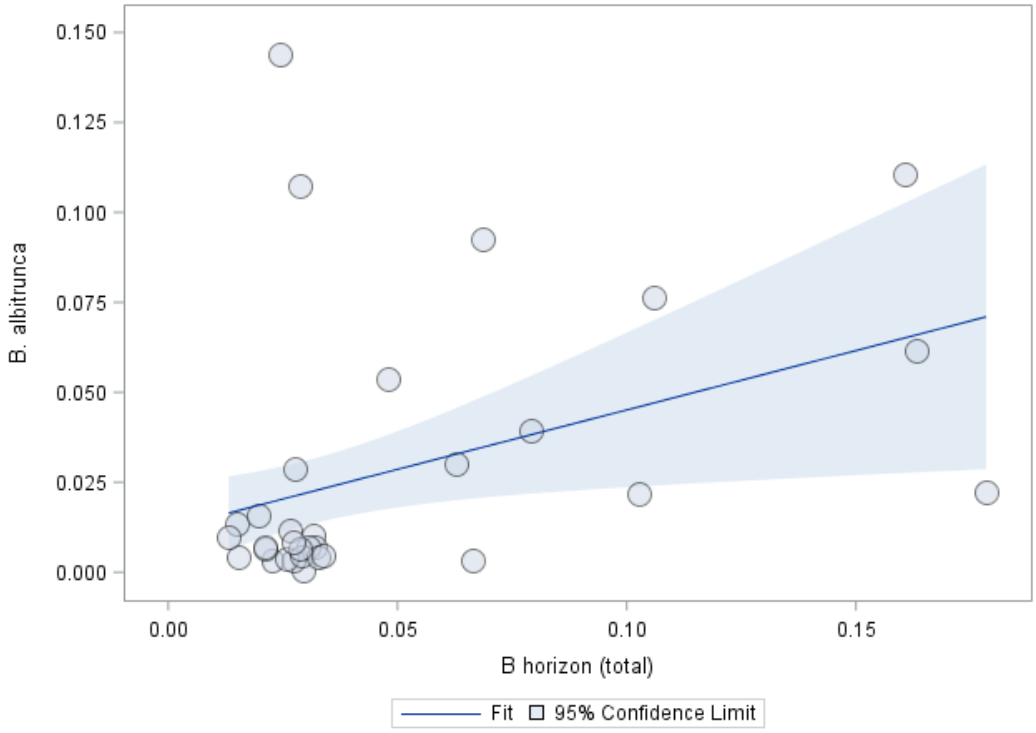

Figure A-16.1: Total Ag content in the B horizon versus Ag content in leaves of *B. albitrunca*.

Regression analysis was used to predict the dependent variable, [Ag] in *C. gratissimus* tissue, from the independent variables, soil concentrations and soil pH (Table A-16.3).

The unique contributions of the independent variables in model 2, for total A horizon content and pH, were not statistically significant. However, model 2 exhibited statistical significance and it can therefore be used to predict 5.6% of the variance in leaf Ag content.

The regression coefficient of soluble B horizon content indicated a statistically significant relationship in model 1 and model 2 (Table A-16.3; $p < 0.005$). However, Ag concentrations for most soil samples were below the lowest detectable limit for ICP-MS and the correlation between soil content and concentrations in plant tissue was caused by only a few samples with detectable levels of Ag. Therefore, unreliable results were produced.

Table A-16.3: Regression analysis for Ag content in the leaves of *C. gratissimus*. Significant at p < 0.05; highly significant at p < 0.005.

Model	Independent variable	Intercept	Regression coefficient	t-value	p-value	R^2 (contributing)	Total R^2
1	A horizon (total)	0.089	0.095	2.02	0.055	0.026	0.026
2	A horizon (total)	0.257	0.084	1.55	0.135	0.026	0.056
	pH		-0.024	-1.48	0.153	0.030	
1	B horizon (total)	0.072	0.398	1.30	0.208	0.059	0.059
2	B horizon (total)	0.245	0.374	1.16	0.258	0.059	0.089
	pH		-0.025	-1.45	0.162	0.029	
1	B horizon (soluble)	0.079	77.807	4.38	**<0.001**	0.226	0.226
2	B horizon (soluble)	0.362	83.703	8.15	**<0.001**	0.226	0.306
	pH		-0.042	-1.93	0.067	0.080	

Regression analysis was used to predict the dependent variable, [Ag] in *G. bicolor* tissue, from the independent variables, soil concentrations and soil pH (Table A-16.4).

The regression coefficient of total A horizon content indicated a statistically significant relationship in model 1 (Table A-16.4; p < 0.05). Every 1 ppm increase in total [Ag] in the soil will result in a 0.14 ppm increase in [Ag] in the leaves of G. bicolor (Figure A-16.2).

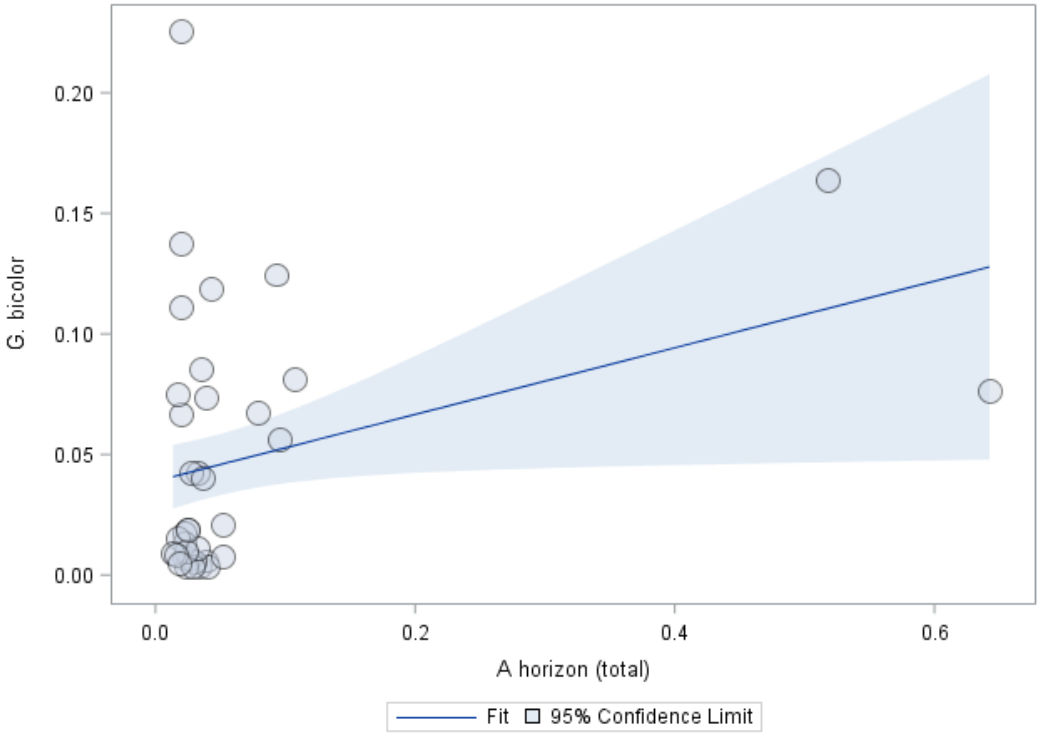

Figure A-16.2: Total Ag content in the A horizon versus Ag content in leaves of *G. bicolor.*

The R^2 indicates that 10.9% of the variance in leaf Ag content can be predicted by model 1. Model 2 did not exhibit statistical significance and can therefore not be used to predict Ag concentrations in *G. bicolor* tissue.

The unique contributions of the independent variables in model 2, for soluble B horizon content and pH, were not statistically significant. However, model 2 did exhibit statistical significance and it can therefore be used to predict 7.3% of the variance in leaf Ag content.

Table A-16.4: Regression analysis for Ag content in the leaves of *G. bicolor*. Significant at p < 0.05; highly significant at p < 0.005.

Model	Independent variable	Intercept	Regression coefficient	t-value	p-value	R^2 (contributing)	Total R^2
1	A horizon (total)	0.039	0.138	2.14	**0.040**	0.109	0.109
2	A horizon (total)	0.159	0.129	1.91	0.066	0.109	0.142
	pH		-0.017	-1.25	0.219	0.034	
1	B horizon (total)	0.029	0.384	1.82	0.078	0.115	0.115
2	B horizon (total)	0.147	0.365	1.70	0.099	0.115	0.145
	pH		-0.017	-1.19	0.245	0.030	
1	B horizon (soluble)	0.054	-10.339	-1.47	0.154	0.022	0.022
2	B horizon (soluble)	0.205	-8.439	-1.08	0.290	0.022	0.073
	pH		-0.022	-1.62	0.117	0.051	

A-17 Vanadium

Regression analysis results for V are displayed in Table A-17.1 to Table A-17.3. Regression analysis was used to predict the dependent variable, [V] in *B. albitrunca* tissue, from the independent variables, soil concentrations and soil pH (Table A-17.1).

None of the independent variables displayed a statistically significant correlation with V content in the leaves of *B. albitrunca*.

Table A-17.1: Regression analysis for V content in the leaves of *B. albitrunca*. Significant at p < 0.05; highly significant at p < 0.005.

Model	Independent variable	Intercept	Regression coefficient	t-value	p-value	R^2 (contributing)	Total R^2
1	A horizon (total)	0.157	-0.004	-0.67	0.512	0.005	0.005
2	A horizon (total)	0.489	<0.001	0.03	0.975	0.005	0.038
	pH		-0.052	-1.40	0.177	0.034	
1	B horizon (total)	0.102	0.004	0.57	0.573	0.010	0.010
2	B horizon (total)	0.501	0.006	0.94	0.358	0.010	0.060
	pH		-0.061	-1.69	0.109	0.050	
1	B horizon (soluble)	0.133	0.553	0.68	0.507	<0.001	<0.001
2	B horizon (soluble)	0.733	7.749	1.69	0.108	<0.001	0.069
	pH		-0.089	-1.56	0.136	0.069	

Regression analysis was used to predict the dependent variable, [V] in *C. gratissimus* tissue, from the independent variables, soil concentrations and soil pH (Table A-17.2).

The regression coefficient of pH in model 2, for total A horizon content, indicated a statistically significant relationship (Table A-17.2; $p < 0.005$). Every unit increase in pH will result in a 0.03 ppm decrease in [V] in the leaves of *C. gratissimus*. The contributing R^2 (Table A-17.2) indicates that 10.5% of the variance in leaf content can be predicted from soil pH. Even though the unique contribution of total A horizon content was not significant, model 2 exhibited statistical significance and it can be used to predict 24.5% of the variance leaf V content.

The regression coefficient of pH in model 2, for total B horizon content, indicated a statistically significant relationship (Table A-17.2; $p < 0.005$). Every unit increase in pH will result in a 0.04 ppm decrease in [V] in the leaves of *C. gratissimus*. The contributing R^2 (Table A-17.2) indicates that 21.7% of the variance in leaf content can be predicted from soil pH. Even though the unique contribution of total B horizon content was not significant, model 2 exhibited statistical significance and it can be used to predict 37.9% of the variance leaf V content.

The regression coefficient of pH in model 2, for soluble B horizon content, indicated a statistically significant contribution (Table A-17.2; $p < 0.05$). However, model 2 did not exhibit statistical significance and can therefore not be used to predict V concentrations in *C. gratissimus* tissue.

Table A-17.2: Regression analysis for V content in the leaves of *C. gratissimus*. Significant at p < 0.05; highly significant at p < 0.005.

Model	Independent variable	Intercept	Regression coefficient	t-value	p-value	R^2 (contributing)	Total R^2
1	A horizon (total)	0.169	-0.009	-1.67	0.115	0.140	0.140
2	A horizon (total)	0.346	-0.005	-0.98	0.342	0.140	0.245
	pH		-0.029	-4.14	**0.001**	0.105	
1	B horizon (total)	0.191	-0.011	-1.37	0.195	0.162	0.162
2	B horizon (total)	0.449	-0.011	-1.49	0.160	0.162	**0.379**
	pH		-0.037	-4.21	**0.001**	0.217	
1	B horizon (soluble)	0.121	-4.358	-0.56	0.583	0.015	0.015
2	B horizon (soluble)	0.434	6.026	0.71	0.490	0.015	**0.254**
	pH		-0.045	-2.23	**0.044**	0.239	

Regression analysis was used to predict the dependent variable, [V] in *G. bicolor* tissue, from the independent variables, soil concentrations and soil pH (Table A-17.3).

The regression coefficient of soluble B horizon content indicated a statistically significant relationship in model 1 (Table A-17.3; $p < 0.05$). However, V concentrations for most of the soil samples were below the lowest detectable limit for ICP-MS. Therefore, unreliable results were produced.

Table A-17.3: Regression analysis for V content in the leaves of *G. bicolor*. Significant at p < 0.05; highly significant at p < 0.005.

Model	Independent variable	Intercept	Regression coefficient	t-value	p-value	R^2 (contributing)	Total R^2
1	A horizon (total)	0.313	-0.016	-1.44	0.163	0.087	0.087
2	A horizon (total)	0.676	-0.011	-1.26	0.222	0.087	0.187
	pH		-0.057	-1.88	0.073	0.100	
1	B horizon (total)	0.277	-0.008	-0.80	0.433	0.034	0.034
2	B horizon (total)	0.810	-0.010	-1.07	0.298	0.034	0.206
	pH		-0.074	-1.93	0.068	0.173	
1	B horizon (soluble)	0.219	-18.421	-2.49	**0.022**	0.056	0.056
2	B horizon (soluble)	0.682	-0.707	-0.07	0.946	0.056	0.152
	pH		-0.067	-1.40	0.177	0.096	

A-18 Zinc

Regression analysis results for Zn are displayed in Table A-18.1 to Table A-18.4. Regression analysis was used to predict the dependent variable, soil Zn concentrations and pH, from the independent variable, ore Zn content (Table A-18.1).

None of the dependent variables displayed a statistically significant correlation with Zn concentrations in the ore body.

Table A-18.1: Regression analysis for ore Zn content. Significant at p < 0.05; highly significant at p < 0.005.

Model	Dependent variable	Intercept	Regression coefficient	t-value	p-value	R^2 (contributing)	Total R^2
1	A horizon (total)	3.397	0.001	1.31	0.215	0.131	0.131
1	B horizon (total)	3.722	<0.001	0.46	0.657	0.008	0.008
1	B horizon (soluble)	0.066	<0.001	-0.13	0.902	0.001	0.001
1	pH A horizon	6.605	<0.001	0.98	0.346	0.081	0.081
1	pH B horizon	6.490	<0.001	0.60	0.560	0.012	0.012

Regression analysis was used to predict the dependent variable, [Zn] in *B. albitrunca* tissue, from the independent variables, soil concentrations and soil pH (Table A-18.2).

None of the independent variables displayed a statistically significant correlation with Zn content in the leaves of *B. albitrunca*.

Table A-18.2: Regression analysis for Zn content in the leaves of *B. albitrunca*. Significant at p < 0.05; highly significant at p < 0.005.

Model	Independent variable	Intercept	Regression coefficient	t-value	p-value	R^2 (contributing)	Total R^2
1	A horizon (total)	9.782	-0.354	-0.82	0.417	0.009	0.009
2	A horizon (total)	11.209	-0.326	-0.77	0.449	0.009	0.009
	pH		-0.230	-0.14	0.888	<0.001	
1	B horizon (total)	10.505	-0.522	-1.77	0.087	0.036	0.036
2	B horizon (total)	1.738	-0.715	-1.74	0.092	0.036	0.044
	pH		1.430	0.70	0.493	0.008	
1	B horizon (soluble)	5.158	50.809	1.24	0.227	0.171	0.171
2	B horizon (soluble)	3.055	51.336	1.19	0.245	0.171	0.172
	pH		0.309	0.18	0.858	0.001	

Regression analysis was used to predict the dependent variable, [Zn] in *C. gratissimus* tissue, from the independent variables, soil concentrations and soil pH (Table A-18.3).

The regression coefficient of total A horizon content indicated a statistically significant relationship in model 1 (Table A-18.3; $p < 0.05$. Every 1 ppm increase in total [Zn] in the soil will result in a 0.54 ppm increase in [Zn] in the leaves of *C. gratissimus* (Figure A-18.1). The R^2 indicates that 20.2% of the variance in leaf Zn content can be predicted by model 1. Model 2 did not exhibit statistical significance and can therefore not be used to predict Zn concentrations in *C. gratissimus* tissue.

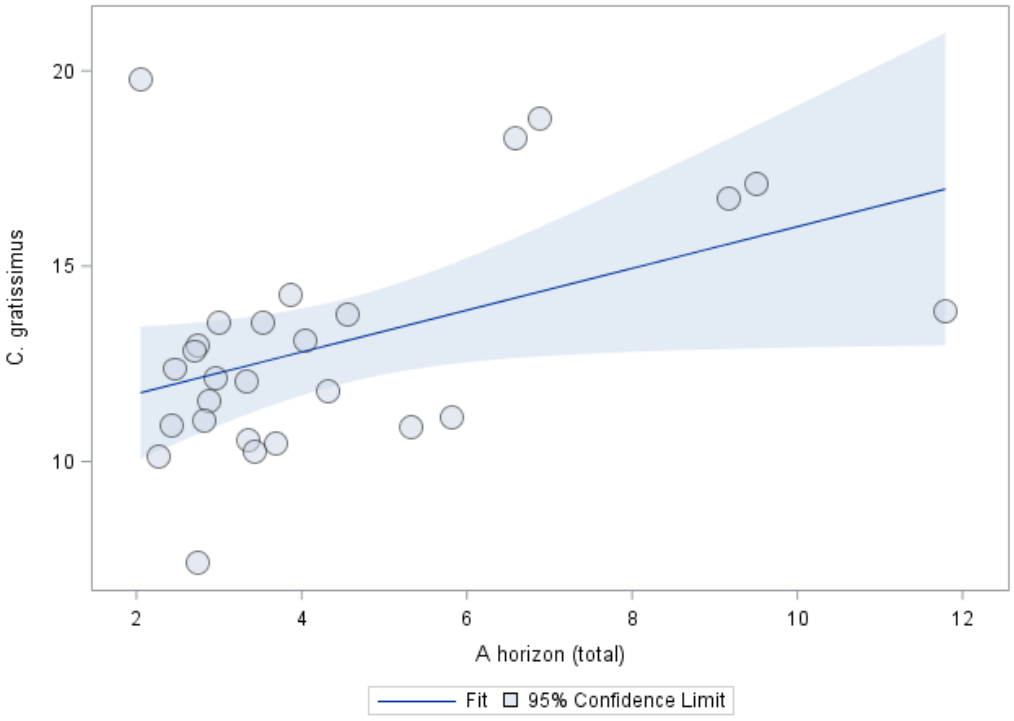

Figure A-18.1: Total Zn content in the A horizon versus Zn content in leaves of *C. gratissimus.*

Table A-18.3: Regression analysis for Zn content in the leaves of *C. gratissimus*. Significant at $p < 0.05$; highly significant at $p < 0.005$.

Model	Independent variable	Intercept	Regression coefficient	t-value	p-value	R^2 (contributing)	Total R^2
1	A horizon (total)	10.664	0.535	2.09	**0.048**	0.202	0.202
2	A horizon (total)	5.524	0.366	1.01	0.323	0.202	0.216
	pH		0.859	0.71	0.485	0.014	
1	B horizon (total)	10.256	0.617	1.75	0.094	0.141	0.141
2	B horizon (total)	3.843	0.307	0.73	0.476	0.141	0.173
	pH		1.118	1.15	0.261	0.032	
1	B horizon (soluble)	13.183	-8.359	-0.39	0.698	0.013	0.013
2	B horizon (soluble)	0.999	-8.089	-0.51	0.618	0.013	0.183
	pH		1.783	1.80	0.087	0.170	

Regression analysis was used to predict the dependent variable, [Zn] in *G. bicolor* tissue, from the independent variables, soil concentrations and soil pH (Table A-18.4).

The regression coefficient of total A horizon content indicated a statistically significant relationship in model 1 (Table A-18.4; $p < 0.005$). Every 1 ppm increase in total [Zn] in the soil will result in a 0.37 ppm decrease in [Zn] in the leaves of *G. bicolor* (Figure A-18.2). The decreasing concentrations in leaf content is an unexpected trend. It is suspected that some other factor, such as pH, plant physiology or antagonistic interactions with other elements, may have caused this tendency. The R^2 indicates that 13.6% of the variance in leaf Zn content can be predicted by model 1. The unique contributions of the independent variables in model 2 were not statistically significant. However, model 2 did exhibit statistical significance and it can therefore be used to predict 19% of the variance in leaf Zn content.

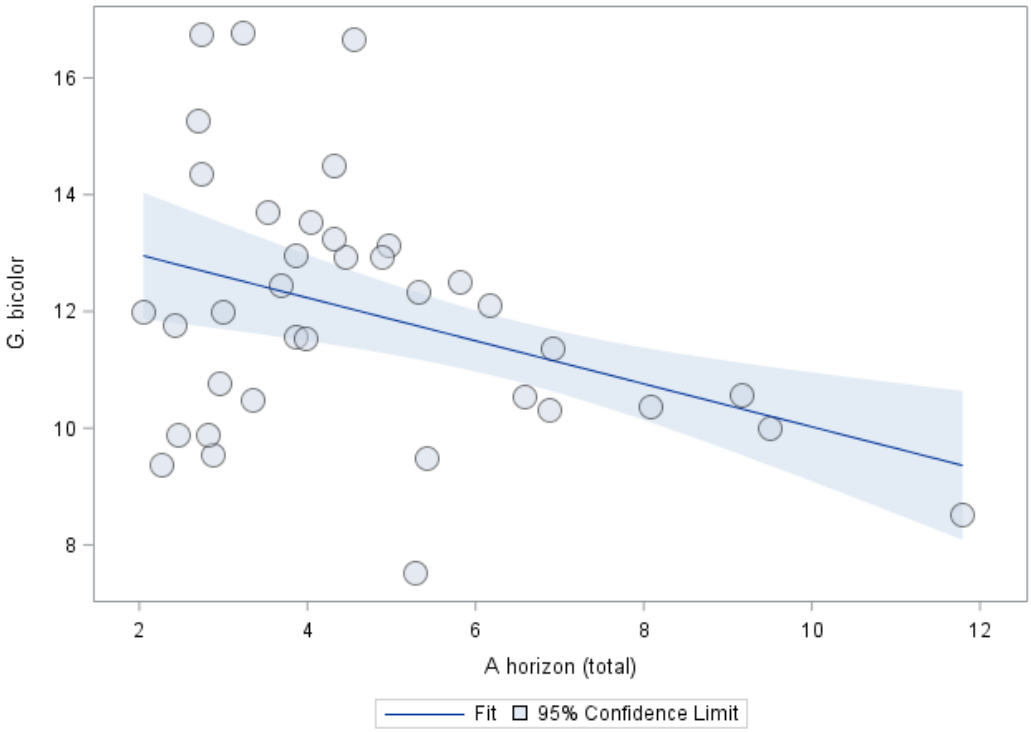

Figure A-18.2: Total Zn content in the A horizon versus Zn content in leaves of *G. bicolor.*

The regression coefficient of pH in model 2, for total B horizon content, indicated a statistically significant relationship (Table A-18.4; $p < 0.05$). Every unit increase in pH will result in a 1.68 ppm decrease in [Zn] in the leaves of *G. bicolor*. The contributing R^2 (Table A-18.4) indicates that 10.3% of the variance in leaf content can be predicted from soil pH. Even though the unique contribution of total B horizon content was not significant, model 2

exhibited statistical significance and it can be used to predict 17.7% of the variance leaf Zn content.

The regression coefficient of pH in model 2, for soluble B horizon content, indicated a statistically significant relationship (Table A-18.4; $p < 0.005$). Every unit increase in pH will result in a 1.74 ppm decrease in [Zn] in the leaves of *G. bicolor*. The contributing R^2 (Table A-18.4) indicates that 18% of the variance in leaf content can be predicted from soil pH. Even though the unique contribution of soluble B horizon content was not significant, model 2 exhibited statistical significance and it can be used to predict 19% of the variance leaf Zn content.

Table A-18.4: Regression analysis for Zn content in the leaves of *G. bicolor*. Significant at p < 0.05; highly significant at p < 0.005.

Model	Independent variable	Intercept	Regression coefficient	t-value	p-value	R^2 (contributing)	Total R^2
1	A horizon (total)	13.707	-0.369	-3.46	**0.002**	0.136	0.136
2	A horizon (total)	22.076	-0.097	-0.46	0.645	0.136	0.190
	pH		-1.405	-1.60	0.120	0.054	
1	B horizon (total)	13.490	-0.314	-1.83	0.077	0.075	0.075
2	B horizon (total)	23.593	-0.007	-0.03	0.973	0.075	0.177
	pH		-1.682	-2.70	**0.011**	0.103	
1	B horizon (soluble)	11.699	6.470	0.55	0.588	0.010	0.010
2	B horizon (soluble)	23.560	6.536	0.57	0.576	0.010	0.190
	pH		-1.735	-3.52	**0.002**	0.180	

APPENDIX B

Element concentrations in *B. albitrunca* were evaluated in terms of its relationship to content in the underlying ore. The regression coefficient of Cu content indicated a statistically significant relationship (Table B-1; $p < 0.005$). Every 1 ppm increase in Cu in the leaves of *B. albitrunca* is related to a 3626.02 ppm/m increase in ore content (Figure B-1). The large R^2 value (Table B-1) indicates that 35% of the variance in ore content can be predicted from [Cu] in the plant tissue.

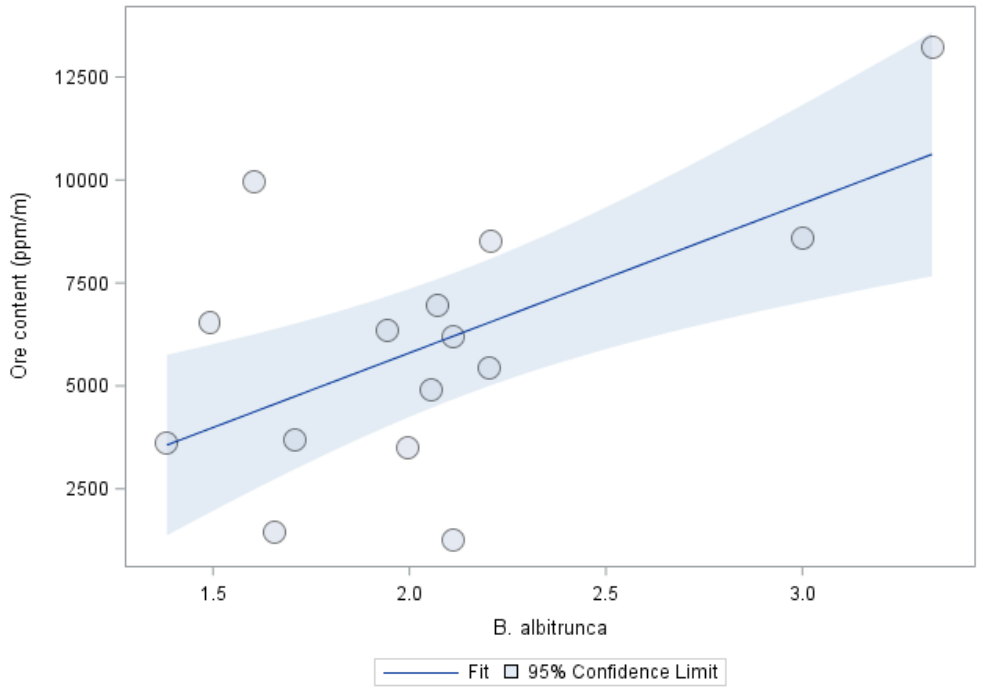

Figure B-1: Cu content in the ore versus Cu content in leaves of *B. albitrunca.*

Table B-1: Regression analysis for the main ore trace elements as it relates to concentrations in the leaves of *B. albitrunca*. Significant at $p < 0.05$; highly significant at $p < 0.005$.

Element	Intercept	Regression coefficient	t-value	p-value	Total R^2
Cu	-1449.22	3626.02	3.75	**0.003**	**0.350**
Pb	544.28	-585.53	-0.20	0.848	0.003
Mo	52.98	18.72	64.00	0.540	0.022
Ag	7.24	17.10	0.49	0.631	0.008
Zn	859.69	-17.75	-2.63	**0.023**	0.030

The regression coefficient of Zn content also exhibited a significant relationship (Table B-1; $p < 0.05$). Every 1 ppm increase in Zn in the leaves of *B. albitrunca* is related to a 17.75

ppm/m decrease in ore content. The small R^2 value (Table B-1), however, indicates that only 3% of the variance in ore content can be predicted from [Zn] in the plant tissue.

Where element concentrations in *C. gratissimus* were evaluated in terms of its relationship to content in the underlying ore, the regression coefficient of Ag content indicated a statistically significant relationship (Table B-2; $p < 0.05$). Every 1 ppm increase in Ag in the leaves of *C. gratissimus* is related to a 63.76 ppm/m decrease in ore content (Figure B-2). The large R^2 value (Table B-2) indicates that 31.9% of the variance in ore content can be predicted from [Ag] in the plant tissue.

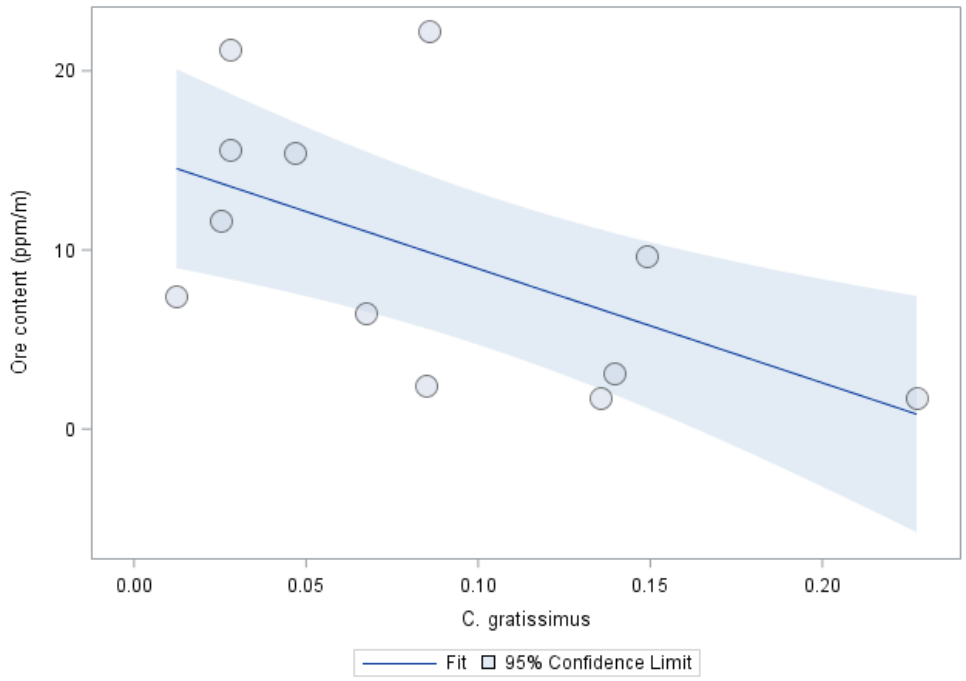

Figure B-2: Ag content in the ore versus Ag content in leaves of *C. gratissimus.*

Table B-2: Regression analysis for the main ore trace elements as it relates to concentrations in the leaves of *C. gratissimus*. Significant at $p < 0.05$; highly significant at $p < 0.005$.

Element	Intercept	Regression coefficient	t-value	p-value	Total R^2
Cu	1741.01	557.87	1.11	0.298	0.082
Pb	442.60	1331.36	0.21	0.841	0.007
Mo	61.37	-28.75	-0.32	0.763	0.021
Ag	15.33	-63.76	-3.66	**0.006**	**0.319**
Zn	1908.38	-113.88	-1.74	0.133	0.053

Where element concentrations in *G. bicolor* were evaluated in terms of its relationship to content in the underlying ore, the regression coefficient of Mo content indicated a statistically significant relationship (Table B-3; $p < 0.05$). However, Mo concentrations in leaves of G. bicolor were mostly below the lowest limit of detection for ICP-MS and the large R^2 was caused by a single outlier that had detectable levels of Mo.

Table B-3: Regression analysis for the main ore trace elements as it relates to concentrations in the leaves of *G. bicolor*. Significant at $p < 0.05$; highly significant at $p < 0.005$.

Element	Intercept	Regression coefficient	t-value	p-value	Total R^2
Cu	5598.24	87.87	0.29	0.779	0.008
Pb	544.21	32.63	0.02	0.988	<0.001
Mo	48.86	<0.001	6.37	**<0.001**	**0.257**
Ag	9.10	-3.52	-0.09	0.930	0.001
Zn	654.03	-11.07	-0.35	0.733	0.004